รายงานวิจัยฉบับสมบูรณ์

โครงการ “การหาสารออกฤทธิ์ต้านการติดเชื้อและฤทธิ์ต้านมะเร็งจากจุลินทรีย์”

โดย ดร. ปัทมา พิทยขจรวุฒิ

31 มีนาคม 2562

สัญญาเลขที่ RSA5980001

รายงานวิจัยฉบับสมบูรณ์

โครงการ “การหาสารออกฤทธิ์ต้านการติดเชื้อและฤทธิ์ต้านมะเร็งจากจุลินทรีย์”

ดร. ปัทมา พิทยขจรวุฒิ
ศูนย์พันธุวิศวกรรมและเทคโนโลยีชีวภาพแห่งชาติ

สนับสนุนโดยสำนักงานกองทุนสนับสนุนการวิจัย และศูนย์พันธุวิศวกรรมและเทคโนโลยีชีวภาพแห่งชาติ
(ความเห็นในรายงานนี้เป็นของผู้วิจัย สกว.และต้นสังกัดไม่จำเป็นต้องเห็นด้วยเสมอไป)

บทคัดย่อ

รหัสโครงการ : RSA5980001

ชื่อโครงการ : การหาสารออกฤทธิ์ต้านการติดเชื้อและฤทธิ์ต้านมะเร็งจากจุลินทรีย์

ชื่อนักวิจัย :ดร.ปัทมา พิทยขจรวุฒิ ศูนย์พันธุวิศวกรรมและเทคโนโลยีชีวภาพแห่งชาติ
สำนักงานพัฒนาวิทยาศาสตร์และเทคโนโลยีแห่งชาติ

E-mail Address : pattamap@biotec.or.th

ระยะเวลาโครงการ : 3 ปี (16 มิถุนายน 2559 – 31 มีนาคม 2562)

สารบริสุทธิ์จำนวน 84 ตัว สามารถแยกได้จากจุลินทรีย์ 6 สายพันธุ์ ประกอบด้วยเชื้อเห็ดรา 2 สายพันธุ์ คือ *Garnoderma* sp. BCC73587 และ *Cyathus subglopbisporus* BCC44381 เชื้อราไม้ *Hypoxylon fendleri* BCC32408 เชื้อราเอนโดไฟท์ *Gloeostereum incarnatum* BCC41461 เชื้อราแยกจากขยะชานอ้อย *Curvularia* sp. BCC52426 และเชื้อแอคติโนมัยซีท *Actinomadura* sp. BCC47066 โดยโครงสร้างของสารบริสุทธิ์ที่แยกได้นี้สามารถยืนยันด้วยข้อมูลทางสปกโตรสโกปี อันประกอบด้วย 1D / 2D NMR IR Mass และ UV-Visible และจากการศึกษาสารบริสุทธิ์ที่แยกได้เหล่านี้พบว่า สารบริสุทธิ์จำนวน 39 ตัวเป็นสารใหม่ที่พบเป็นครั้งแรก และสารบริสุทธิ์จำนวน 32 ตัวมีฤทธิ์ทางชีวภาพที่อยู่ในความสนใจในการศึกษาครั้งนี้ อันประกอบด้วยฤทธิ์ต้านมาลาเรีย ฤทธิ์ยับยั้งวัณโรค ฤทธิ์ยับยั้งแบคทีเรีย ทั้งแกรมบวก คือ *Bacillus cereus*, *Enterococcus faecium*, *Staphylococcus aureus* และแกรมลบ คือ *Escherichia coli*, *Acinetobacter baumannii*, *Klebsiella pneumoniae*, *Pseudomonas aeruginosa* ฤทธิ์ต้านเชื้อรา ประกอบด้วย *Candida albicans*, *Colletotrichum capsici*, *Colletotrichum gloeosporioides*, *Alternaria brassicicola* และ *Magnaporthe grisea* ฤทธิ์ต้านไวรัสโรคเริม สายพันธุ์ที่ 1 (HSV-1) และ ฤทธิ์ต้านมะเร็ง 3 ชนิดคือ มะเร็งเต้านม (MCF-7) มะเร็งช่องปาก (KB) มะเร็งปอด (NCI-H187) นอกจากนั้นสารบริสุทธิ์ที่แยกได้ทั้งหมดยังนำไปทดสอบเพื่อดูความเป็นพิษต่อเซลล์ปกติจากไตของลิง (Vero) อีกด้วย

คำหลัก : จุลินทรีย์, สารออกฤทธิ์ทางชีวภาพ ฤทธิ์ต้านจุลชีพ ฤทธิ์ต้านมาลาเรีย ฤทธิ์ยับยั้งมะเร็ง ความเป็นพิษ

Abstract

Project Code : RSA5980001

Project Title : Anti-infective and anticancer substances from microorganisms

Investigator : Dr. Pattama Pittayakhajonwut, National Center for Genetic Engineering and Biotechnology, National Science and Technology Development Agency

E-mail Address : pattamap@biotec.or.th

Project Period : 3 years (16 June 2016 - 31 March 2019)

Total of 84 compounds were isolated from six chosen microorganisms including two mushrooms (*Garnoderma* sp. BCC73587 and *Cyathus subglobisporus* BCC44381), one wood fungus (*Hypoxylon fendleri* BCC32408), one endophytic fungus (*Gloeostereum incaratum* BCC41461), one agricultural waste fungus (*Curvularia* sp. BCC52426), and one actinomycete (*Actinomadura* sp. BCC47066). All isolated compounds were identified based on spectroscopic methods such as 1D/2D NMR, IR, Mass, and UV-Visible spectroscopy. Half of the isolated compounds were new and 32 compounds possessed biological activity of interest such as antimalarial (against *Plasmodium falciparum*), anti-TB (against *Mycobacterium tuberculosis*), antibacterial both Gram-positive (*Bacillus cereus*, *Enterococcus faecium*, and *Staphylococcus aureus*) and Gram-negative (*Escherichia coli*, *Acinetobacter baumannii*, *Klebsiella pneumoniae*, and *Pseudomonas aeruginosa*), antifungal (against *Candida albicans*, *Colletotrichum capsici*, *Colletotrichum gloeosporioides*, *Alternaria brassicicola*, and *Magnaporthe grisea*), anti-Herpes-Simplex virus type 1 (HSV-1), and anticancer (against human breast cancer, MCF-7; human oral epidermoid carcinoma KB; human small-cell lung cancer, NCI-H187) activities. Cytotoxicity against African green monkey kidney fibroblasts (Vero) cell was also evaluated.

Keywords: microorganisms, bioactive compounds, antimicrobial, antimalarial, anticancer, cytotoxicity

บทสรุปสำหรับผู้บริหาร (Executive Summary)

รหัสโครงการ : RSA5980001

ชื่อโครงการ : การหาสารออกฤทธิ์ต้านการติดเชื้อและฤทธิ์ต้านมะเร็งจากจุลินทรีย์

ชื่อนักวิจัย : ดร.ปัทมา พิทยขจรวุฒิ ศูนย์พันธุวิศวกรรมและเทคโนโลยีชีวภาพแห่งชาติ
สำนักงานพัฒนาวิทยาศาสตร์และเทคโนโลยีแห่งชาติ

E-mail Address : pattamap@biotec.or.th

ระยะเวลาโครงการ : 3 ปี (16 มิถุนายน 2559 – 31 มีนาคม 2562)

รายละเอียดผลการดำเนินงานของโครงการ

โครงการนี้มุ่งเน้นการแยกและพิสูจน์เอกลักษณ์ขององค์ประกอบทางเคมี รวมทั้งการตรวจสอบฤทธิ์ทางชีวภาพของสารบริสุทธิ์ที่แยกได้จากเชื้อจุลินทรีย์จำนวน 6 สายพันธุ์ ประกอบด้วยเชื้อเห็ดรา 2 สายพันธุ์ คือ *Garnoderma* sp. BCC73587 และ *Cyathus subglopbisporus* BCC44381 เชื้อราไม้ *Hypoxylon fendleri* BCC32408 เชื้อราเอนโดไฟท์ *Gloeostereum incarnatum* BCC41461 เชื้อราแยกจากขยะชานอ้อย *Curvularia* sp. BCC52426 และเชื้อแอคติโนมัยซีท *Actinomadura* sp. BCC47066 โดยสามารถแยกสารบริสุทธิ์ได้จำนวน 84 ตัว ซึ่งโครงสร้างของสารบริสุทธิ์ที่แยกได้เหล่านี้สามารถยืนยันด้วยข้อมูลทางสปกโตรสโกปี อันประกอบด้วย 1D / 2D NMR IR Mass และ UV-Visible และจากการศึกษาสารบริสุทธิ์ที่แยกได้เหล่านี้พบว่า สารบริสุทธิ์จำนวน 39 ตัวเป็นสารใหม่ที่พบเป็นครั้งแรก และสารบริสุทธิ์จำนวน 32 ตัวมีฤทธิ์ทางชีวภาพที่อยู่ในความสนใจในการศึกษาครั้งนี้ อันประกอบด้วย ฤทธิ์ต้านมาลาเรีย ฤทธิ์ยับยั้งวัณโรค ฤทธิ์ยับยั้งแบคทีเรีย ทั้งแกรมบวก คือ *Bacillus cereus*, *Enterococcus faecium*, *Staphylococcus aureus* และแกรมลบ คือ *Escherichia coli*, *Acinetobacter baumannii*, *Klebsiella pneumoniae*, *Pseudomonas aeruginosa* ฤทธิ์ต้านเชื้อรา ประกอบด้วย *Candida albicans*, *Colletotrichum capsici*, *Colletotrichum gloeosporioides*, *Alternaria brassicicola* และ *Magnaporthe grisea* ฤทธิ์ต้านไวรัสโรคเริม สายพันธุ์ที่ 1 (HSV-1) และ ฤทธิ์ต้านมะเร็ง 3 ชนิด คือ มะเร็งเต้านม (MCF-7) มะเร็งช่องปาก (KB) มะเร็งปอด (NCI-H187) นอกจากนั้นสารบริสุทธิ์เหล่านี้ยังถูกนำไปทดสอบเพื่อดูความเป็นพิษต่อเซลล์ปกติจากไตของลิง (Vero) อีกด้วย

คำหลัก : จุลินทรีย์, สารออกฤทธิ์ทางชีวภาพ ฤทธิ์ต้านจุลชีพ ฤทธิ์ต้านมาลาเรีย ฤทธิ์ยับยั้งมะเร็ง ความเป็นพิษ

รายละเอียดผลการดำเนินงานของโครงการ

1. บทนำ

1.1 ความสำคัญและที่มาของปัญหาที่ทำการวิจัย

สืบเนื่องมาจากการค้นพบเพนิซิลินจากเชื้อ *Penicillium notatum* ในปี 1928 ทำให้มีการค้นหายาปฏิชีวนะอย่างกว้างขวางจากเชื้อจุลินทรีย์ อันนำไปสู่การค้นพบยาปฏิชีวนะหลายตัว เช่น streptomycin (จากเชื้อ *Streptomyces griseus* ในปี 1940) tetracycline (จากเชื้อ *Streptomyces* sp. ในปี 1945) chloramphenicol (จากเชื้อ *Streptomyces venezuelae* ในปี 1949) gentamicin (จากเชื้อ *Micromonospora purpurea* ในปี 1963) lovastatin (จากเชื้อ *Aspergillus terreus* ในปี 1978) เป็นต้น การค้นพบสารเหล่านี้ทำให้จุลินทรีย์เข้ามามีบทบาทและความสำคัญในการเป็นแหล่งของการค้นหายาตัวใหม่ๆ ปัจจุบันมีการค้นพบสารที่มีฤทธิ์ทางชีวภาพมากกว่า 22,500 ตัวจากจุลินทรีย์หลายชนิด ซึ่งในจำนวนนี้ได้มาจากแอคติโนมัยซีทประมาณ 45% ได้มาจากเชื้อรา ประมาณ 38% และได้มาจากแบคทีเรียเซลล์เดียว ประมาณ 17% (Berdy, 2005) ในระยะเวลา 30 ปี (ตั้งแต่ปี 1981 – 2010) หนึ่งในสามของสารที่มีการรายงานฤทธิ์ทางชีวภาพอันได้มาจากธรรมชาติ หรือเป็นอนุพันธ์ของสารที่ได้จากธรรมชาติ พบว่าส่วนใหญ่เป็นสารที่มีฤทธิ์ยับยั้งการติดเชื้อจากแบคทีเรีย เชื้อรา เชื้อปรสิต เชื้อไวรัส และฤทธิ์ต้านมะเร็ง (Newman and Cragg, 2012) จากข้อมูลเหล่านี้จะเห็นได้ว่าสารที่มีฤทธิ์ยับยั้งการติดเชื้อ และ ฤทธิ์ต้านมะเร็ง เป็นสารกลุ่มที่มีความสำคัญในการค้นหาและพัฒนาเป็นยา นอกจากนี้การอุบัติของเชื้อที่ดื้อยา และการติดเชื้อที่มาจากโรคต่างๆ เช่น โรควัณโรค โรคเอดส์ เป็นสาเหตุสำคัญที่ทำให้ต้องมีการค้นหายาตัวใหม่ๆในการรักษา เพื่อลดอัตราการตายอันเกิดจากการติดเชื้อ

การเก็บจุลินทรีย์ที่มาจากแหล่งที่มีสิ่งแวดล้อมที่แตกต่างกัน จะเป็นการเพิ่มโอกาสในการหาสารใหม่ๆที่มีความหลากหลายทั้งในแง่ของโครงสร้างทางเคมี และฤทธิ์ทางชีวภาพ ในการศึกษาครั้งนี้จะมุ่งเน้นไปที่การคัดหาสารที่มีฤทธิ์ยับยั้งเชื้อแบคทีเรีย เชื้อมาลาเรีย เชื้อวัณโรค และฤทธิ์มะเร็ง (KB, MCF-7, NCI-H187) จากเชื้อจุลินทรีย์ที่เก็บมาจากหลายแหล่ง โดยในที่นี้จะทำการศึกษาเชื้อจุลินทรีย์ 6 ตัว คือ เชื้อเห็ดรา 2 สายพันธุ์ คือ *Garnoderma* sp. BCC73587 และ *Cyathus subglopbisporus* BCC44381 เชื้อราไม้ *Hypoxylon fendleri* BCC32408 เชื้อราเอนโดไฟท์ *Gloeostereum incarnatum* BCC41461 เชื้อราแยกจากขยะชานอ้อย *Curvularia* sp. BCC52426 และเชื้อแอคติโนมัยซีท *Actinomadura* sp. BCC47066 โดยคัดเลือกจากฤทธิ์ทางชีวภาพ (ตารางที่ 1) และการวิเคราะห์องค์ประกอบทางเคมีขั้นต้นด้วย HPLC เพื่อที่จะลดการซ้ำซ้อนในการแยกสารเดิมๆ การคัดกรองทางเคมี โดยใช้ HPLC เข้ามาช่วยในการตรวจสอบสารที่ได้มีการค้นพบแล้ว จะเพิ่มความรวดเร็วในการค้นหาสารที่ฤทธิ์ทางชีวภาพใหม่ๆ

1.2 งานวิจัยที่เกี่ยวข้อง

ได้มีการรายงานของสารทุติยภูมิมากมายหลายชนิดจากเชื้อจุลินทรีย์ที่คัดมาศึกษาในโครงการนี้ ดังยกตัวอย่างพอสังเขปดังนี้

สาร botryanes **1** – **3** แยกได้จากน้ำเลี้ยงเชื้อ *Hypoxylon rickii* ที่เก็บมาจากเกาะมาร์ตีนิก ที่อยู่แถบตะวันออกของทะเลแคริบเบียน สารเหล่านี้ไม่แสดงฤทธิ์ต่อเชื้อแบคทีเรียแกรมบวก และแกรมลบ แต่แสดงความเป็นพิษต่อเซลล์เนื้อเยื่อไฟโบรบลาสต์ของหนูและเซลล์มะเร็งปากมดลูกที่ความเข้มข้น 8.5 – 28 μg/mL (Kuhnert et al., 2015)

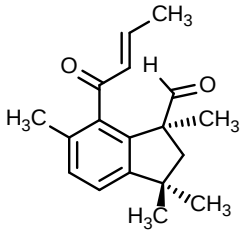

1

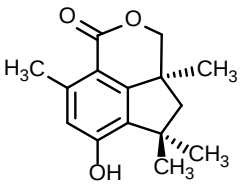

2

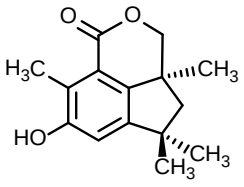

3

สารอนุพันธ์ของ benzo[j]fluoranthene ชื่อ Hypoxylonols C – F (**4** – **7**) แยกได้จาก *Hypoxylon truncatum* สารเหล่านี้แสดงฤทธิ์ต้านการเพิ่มจำนวนของเซลล์ผนังหลอดเลือดดำและเซลล์หลอดเลือดดำของสายสะดือ มีค่า IC_{50} 6.9 – 21 และ 4.1 – 16 μM (Fukai et al., 2012)

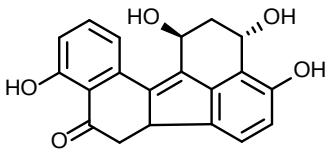

4

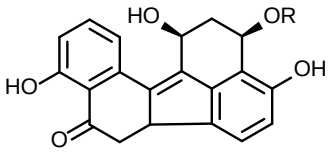

5 R = CH_2CH_3

6 R = CH_3

7 R = H

สารอนุพันธ์ของ azaphilone ชื่อ rubiginosins A – C (**8** – **10**) แยกได้จาก *Hypoxylon rubiginosum* สารกลุ่มนี้ใช้เป็นตัวบ่งชี้ทางเคมีในกลุ่ม Xylariaceae และยังไม่มีการรายงานฤทธิ์ทางชีวภาพ (Quang et al., 2004)

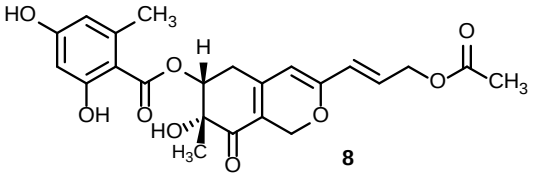

8

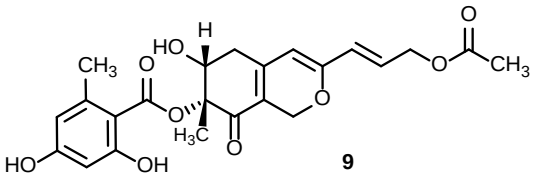

9

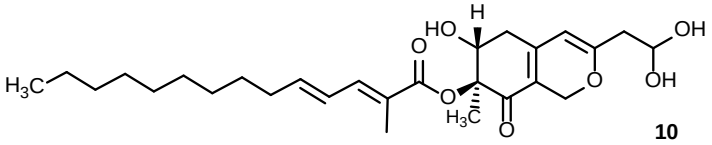

10

สารอนุพันธ์ของ depsidone ชื่อ excelsional (**11**) และสารอนุพันธ์ของ decaline เช่น 9-hydroxyphomopsidin (**12**) alternariol (**13**) alternariol-5-*O*-methyl ether (**14**) 5′-hydroxyalternariol (**15**) และ alternusin (**16**) พบได้จากเชื้อราเอนโดไฟต์ *Phomopsis* sp. CAFT69 สาร **11** และ **12** ที่ความเข้มข้น 1 – 10 μg/mL สามารถแสดงฤทธิ์ยับยั้งการเจริญเติบโตของเชื้อ *Plasmopara viticola* ที่ก่อโรคราน้ำค้างในไร่องุ่น

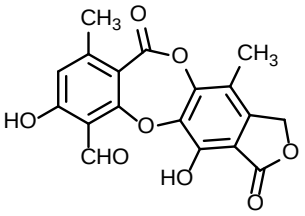

11

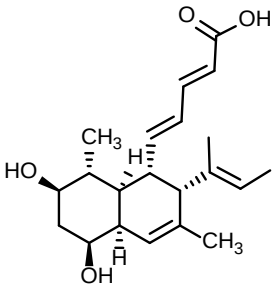

12

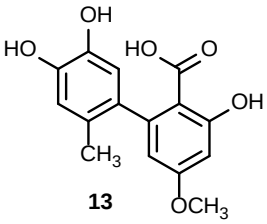

13

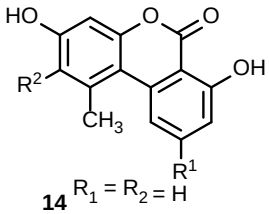

14 $R_1 = R_2 = H$

15 $R_1 = CH_3$, $R_2 = H$

16 $R_1 = R_2 = OH$

สารจำนวน 7 ตัว คือสาร **17** – **23** พบได้จากเชื้อรา 5 สายพันธุ์ที่แยกมาจากต้นสน (*Pinus strobus*) ซึ่งมีต้นกำเนิดในรัฐโนวาสโกเชีย ตั้งอยู่ทางชายฝั่งตะวันออกเฉียงใต้ของแคนาดา สาร **17** **18** และ **21** แสดงฤทธิ์ต้านเชื้อรา *Saccharomyces cerevisae* และ *Microbotryum violaceum* (มีความใกล้เคียงทางชีวภาพ กับโรคราสนิม) (Sumarah et al., 2011)

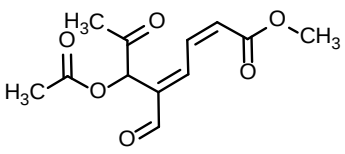

17

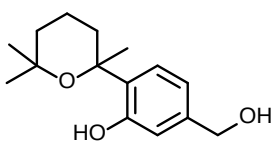

18

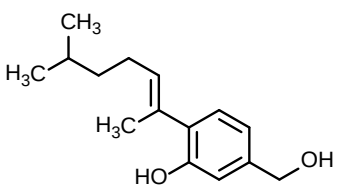

19

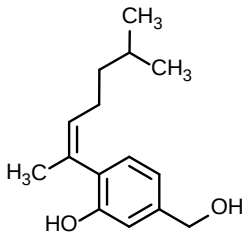

20

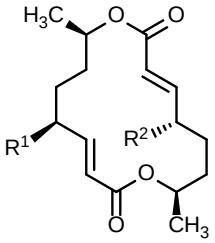

21 $R_1 = R_2 = OH$

22 $R_1 = OH, R_2 = =O$

23 $R_1 = R_2 = =O$

คันพบสารที่เป็นอนุพันธ์ของ tremulane sesquiterpene เช่น ceriponols A – K (**24** – **34**) tremulenediol A (**35**) 11, 12-dihydroxy-1-tremulen-5-one (**36**) และ conocenol B (**37**) จากเชื้อราเอนโดไฟต์ *Ceriporia lacerate* ที่อยู่ในกิ่งของพืชสมุนไพรแป๊ะก๊วย (*Huperzia serrata*) มีเพียงสาร ceriponols F (**29**) และ K (**34**) แสดงความเป็นพิษในระดับปานกลางกับเซลล์มะเร็ง 3 ชนิด คือ HeLa HepG2 และ SGC 7901 ด้วยค่า IC_{50} 32.3 – 173.2 μM (Ying et al., 2013)

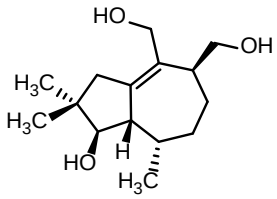

24

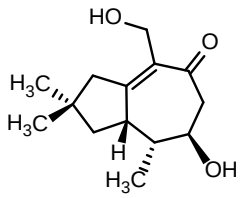

25

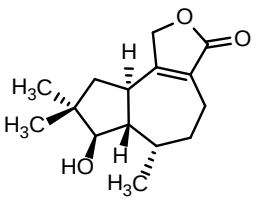

26

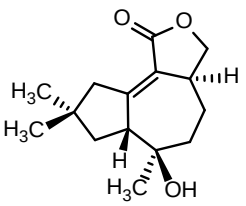

27

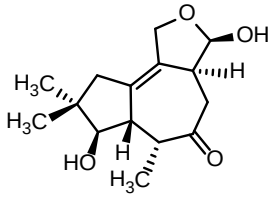

28

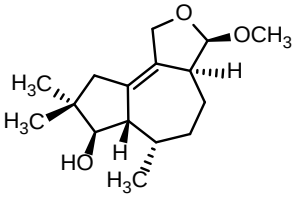

29

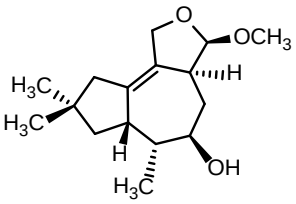

30

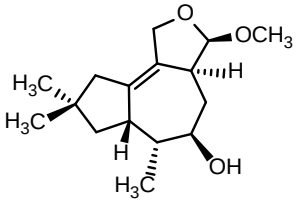

31

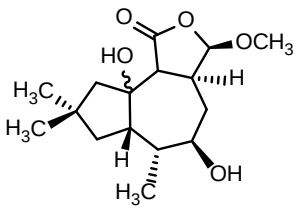

32

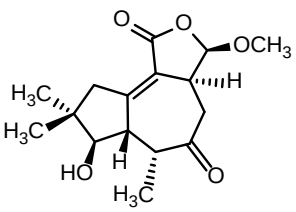

33

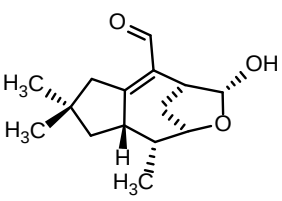

34

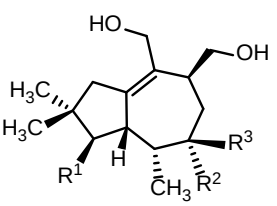

35 $R^1 = R_2 = R_3 = H$

36 $R^1 = H, R_2 + R_3 = O$

37 $R^1 = R_3 = H, R_2 = OH$

พบสารในกลุ่ม α-Pyrone ชื่อ miaolienone (**38**) และ สารในกลุ่ม butanolide ชื่อ miaolinolide (**39**) จากเชื้อแอคติโนมัยซีท *Actinomadura miaoliensis* BCRC16873 และยังพบว่าสารทั้งสองตัวนี้ ในระดับหลอดทดลอง มีฤทธิ์ยับยั้งการผลิตปัจจัยที่ก่อเนื้อร้ายในมนุษย์ (TNF-α) ที่เกิดจาก lipopolysaccharide (LPS) โดยแสดงค่า IC_{50} 0.59 และ 0.79 μM ตามลำดับ (Tseng et al., 2013)

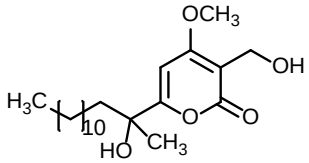

38

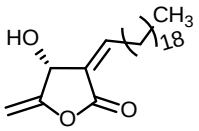

39

ค้นพบสารอนุพันธ์ของ indocarbazole คือ AT2433-A3 A4 A5 และ B3 (**40** – **43**) จาก *Acitnomadura melliaura* ATCC 39691 ซึ่งเก็บมาจากดินในเมืองบริสตอลโคฟ รัฐแคลิฟอเนีย มีการค้นพบว่าสารในกลุ่มนี้ที่มีคลอรีนเป็นองค์ประกอบจะมีฤทธิ์ยับยั้งเชื้อรา ยับยั้งเชื้อวัณโรค และ ยับยั้งเชื้อแบคทีเรียแกรมบวก ดังนั้นสารที่แยกได้จากเชื้อแอคติโนมัยซีทนี้จึงได้นำไปทดสอบฤทธิ์ยับยั้งแบคทีเรียแกรมบวก 5 สายพันธุ์ด้วยกัน คือ *Staphylococcus aureus* ATCC 6538 *Micrococcus luteus* NRRL B-287 *Mycobacterium smegmatis* ATCC 14468 *Salmonella enterica* ATCC 10708 และ *Escherichia coli* NRRL B-3708 นอกจากนั้นยังได้ทดสอบฤทธิ์ต้านเชื้อรา *Saccharomyces cerevisiae* ATCC 204508 และฤทธิ์ต้านมะเร็ง 3 ชนิด คือ เซลล์มะเร็งต่อมลูกหมาก (PC-3) เซลล์มะเร็งปอด (A549) และเซลล์มะเร็งสมอง (U118) พบว่า สาร **40** และ **43** มีฤทธิ์ยับยั้งเชื้อแบคทีเรีย *Staphylococcus aureus* ATCC6538 (MIC 4.0 – 5.0 μg/mL) และ *Micrococcus leteus* NRRL B-287 (MIC 5.0 – 7.7 μg/mL) ส่วนสาร **40** ยังแสดงฤทธิ์ยับยั้งเชื้อแบคทีเรีย *Mycobacterium smegmatis* ATCC 14468 (MIC 80 μg/mL) อีกด้วย (Shaaban et al., 2015)

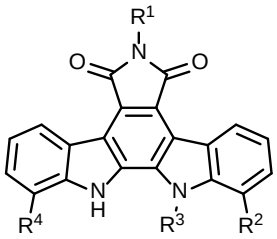

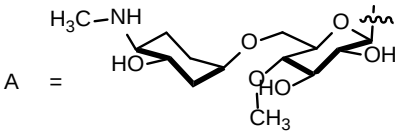

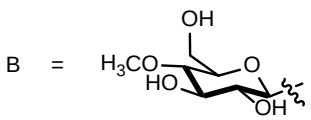

40 $R_1 = R_4 = H$, $R_2 = Cl$, $R_3 = A$; AT2433-A3

41 $R_1 = CH_3$, $R_4 = H$, $R_2 = Cl$, $R_3 = B$; AT2433-A4

42 $R_1 = R_3 = R_4 = H$, $R_2 = Cl$; AT2433-A5

43 $R_1 = CH_3$, $R_2 = R_4 = H$, $R_3 = B$; AT2433-B3

มีการค้นพบสารในกลุ่ม Triterpenoids steroids และ polysaccharides โดยทั่วไปจากเชื้อเห็ดราในกลุ่ม *Ganoderma* spp. และยังได้มีการรายงานฤทธิ์ทางชีวภาพของสารที่ค้นพบในกลุ่มนี้หลายชนิดด้วยกัน เช่น ฤทธิ์ต้านมะเร็ง ฤทธิ์ต้านไวรัสโรคเริม ชนิดที่ 1 ฤทธิ์ยับยั้งความดันโลหิต ฤทธิ์ยับยั้งการสร้างหลอดเลือดเลี้ยงเซลล์มะเร็ง ฤทธิ์การสร้างภูมิคุ้มกัน ฤทธิ์ต้านแอนโดรเจน ฤทธิ์ยับยั้งไวรัสตับอักเสบบี ฤทธิ์ต้านการอักเสบ ฤทธิ์ต้านอนุมูลอิสระ ฤทธิ์ต้านจุลชีพ และผลของการลดไขมันในเลือด (Chairul et al., 1990; Gonzalez et al., 2002; Komoda et al., 1989; Lin et al., 2003; Min et al., 2000; Rios et al., 2012; Sonoda et al., 1988; You et al., 2013) เชื้อในกลุ่ม *Ganoderma* จัดอยู่ในจำพวกเห็ดราที่มีฤทธิ์ทางยา เห็ดราที่เป็นที่รู้จักกันดีในกลุ่มนี้ คือ เห็ดหลินจือ สารเป็นจำนวนมากรายงานมาจากเชื้อ *G. lucidum* (Baby et al., 2015) สารที่ค้นพบในกลุ่มนี้ส่วนใหญ่เป็น triterpenes ชื่อ lanostane ซึ่งการเชื่อมต่อระหว่างวง A/B B/C และ C/D เป็น *trans*- และมี methyl ที่ตำแหน่ง 10 และ 13 อยู่ในแบบ β และมี methyl ที่ตำแหน่ง 14 อยู่ในแบบ α ส่วน side chain ที่ตำแหน่ง 17 อยู่ในแบบ β และที่ตำแหน่ง 20 มีการจัด configuration เป็น *R*

สาร ganoderic acids A (**44**) และ B (**45**) จัดเป็นสารในกลุ่ม C30 lanostanes ซึ่งค้นพบเป็นครั้งแรกจาก fruiting bodies ของ *G. lucidum* (Kubota et al., 1982)

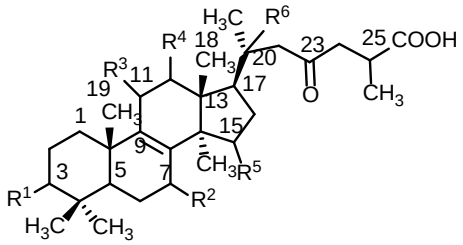

44 $R_1 = O, R_2 = \beta\text{-OH}, R_3 = O, R_4 = H, R_5 = \alpha\text{-OH}, R_6 = H$

45 $R_1 = \beta\text{-OH}, R_2 = \beta\text{-OH}, R_3 = O, R_4 = H, R_5 = O, R_6 = H$

มาจนกระทั่งปัจจุบันนี้ สารในกลุ่ม C30 lanostanes หรือ อนุพันธ์ของ ganoderic acid มีจำนวนอย่างน้อย 284 สาร ซึ่งมี side-chains แตกต่างกันไป เช่น มีกลุ่มของ keto furano acetyl และ ethylene เข้ามาเป็นองค์ประกอบควบไปกับการมีกลุ่ม carboxylic acid สารที่จัดว่าเป็นสารที่หายากในกลุ่มนี้จะประกอบด้วย β-hydroxy ที่ตำแหน่ง 11 คือสาร ganoderic acid Df (**46**) ซึ่งแยกได้จาก fruiting bodies ของ *Ganoderma lucidum* และพบว่าสารนี้มีฤทธิ์ยับยั้งเอนไซม์ aldose reductase (Fatmawati et al., 2010)

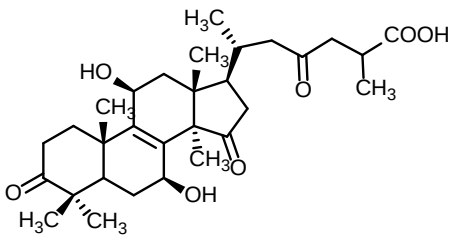

46

ในปี 2010 สามารถแยกสาร 7-*O*-ethyl ganoderic acid O (**47**) ซึ่งมีกลุ่ม ethoxyl ที่ตำแหน่งที่ 7 ถือว่าเป็นสารที่พบได้ยาก จาก *G. lucidum* โดยกลุ่มของ Wang et al. (Wang et al., 2010) และในปี 2012 กลุ่มของ Yang et al. ได้รายงานอนุพันธ์ของ lanostane ที่มีกลุ่ม acetal ที่ตำแหน่งที่ 7 และ 15 โดยจัดวางตัวเป็น 7-membered 1,3-dioxepane คือสาร ganodermacetal (**48**) ว่าเป็นสารจากธรรมชาติที่แยกได้จาก *G. amboinense* (Yang et al., 2012) ซึ่งโดยก่อนหน้านี้มีผู้รายงานว่าสารที่คล้ายคลึงกับสาร **48** (**49**) เป็นสารที่ไม่ได้เกิดเองตามธรรมชาติ (Lee et al., 2011)

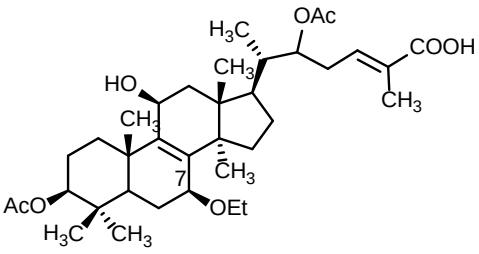

47

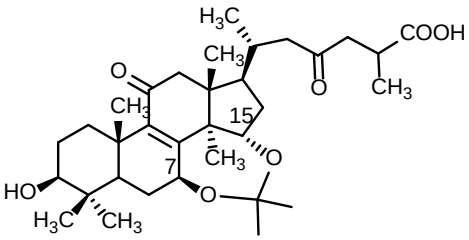

48

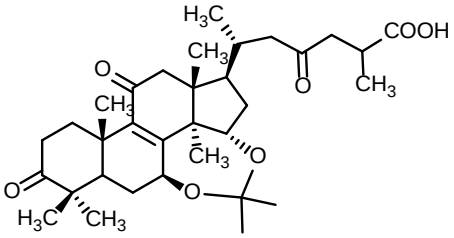

49

กลุ่มของ Sato et al. ได้รายงานว่าภายใต้สภาวะที่ไม่รุนแรง กลุ่ม triterpene-farnesyl hydroquinone conjugates สามารถพบได้ เช่น สาร ganosinensins A – C (**50** – **52**) ซึ่งแยกได้จาก *G. sinense* (Sato et al., 2009)

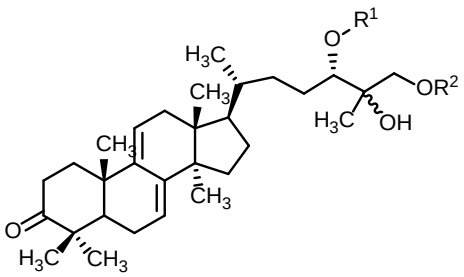

50 R_1 = H, R_2 =

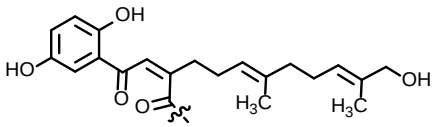

51 R_1 =

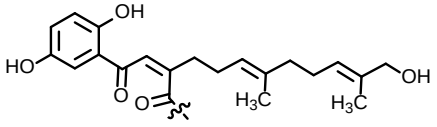

, R_2 = H

52 R_1 =

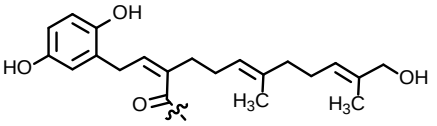

, R_2 = H

สารกลุ่มอื่นที่นอกเหนือไปจาก terpenes ที่แยกได้จาก *Ganoderma* เช่น alkaloids prenyl hydraquinones benzofurans และ benzopyranones อัลคาลอยด์ตัวแรกๆที่แยกมาจาก fruiting bodies ของ *G. capense* คือ ganoderma alkaloids A (**53**) และ B (**54**) แยกได้ในปี 1989 (Yang and Yu, 1989) ส่วนสาร sinensines B – E (**55** – **58**) และ sinensine (**59**) แยกได้จาก fruiting bodies ของ *G. sinense* ในปี 2011 (Liu et al., 2011)

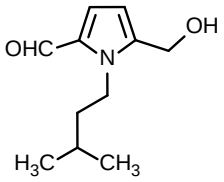

53

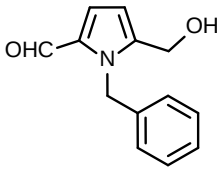

54

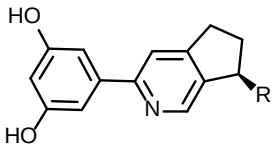

55 R = H
56 R = OH

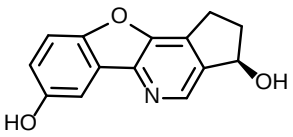

57

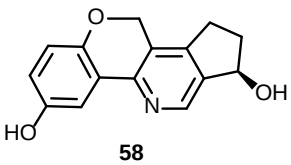

58

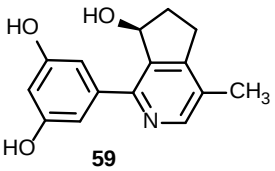

59

สารในกลุ่ม diterpenes ชื่อ cyathins J – P (**60** – **66**) สามารถแยกได้จากเชื้อเห็ดรา *Cyathus gansuensis* โดยพบว่า สาร cyathin J แสดงฤทธิ์ที่ดีในการยับยั้งการสร้างไนตริกออกไซด์ (NO) จาก แมกโครเฟจ ซึ่งเป็นเซลล์ของระบบภูมิคุ้มกันที่มีผลต่อการสร้าง lipopolysaccharide ที่ระดับ IC_{50} 42 $\pm$ 2 μM ส่วนสาร **61** และ **63** แสดงฤทธิ์ปานกลางในการยับยั้งการสร้างไนตริกออกไซด์ (NO) จาก แมกโครเฟจ ที่ระดับ IC_{50} 78 $\pm$ 4 μM และ IC_{50} 80 $\pm$ 2 μM ตามลำดับ (Wang et al., 2014)

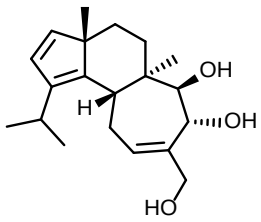

60

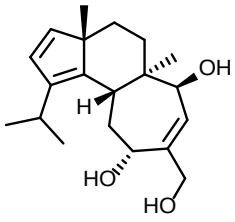

61

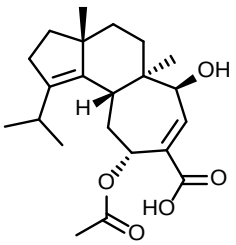

62

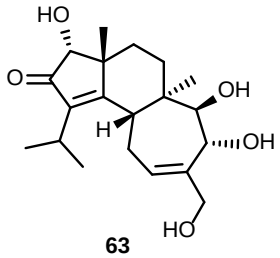

63

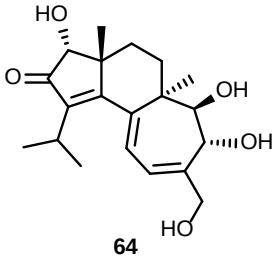

64

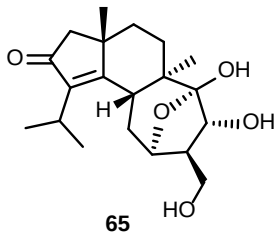

65

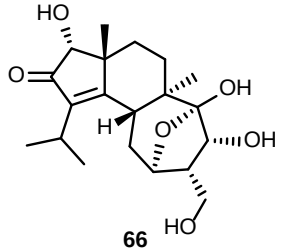

66

สารในกลุ่มของ cyathane diterpenoid-xyloside ชื่อ streatoids A – F (**67** – **72**) สามารถแยกได้จากเชื้อเห็ดรา Cyathus striatus และยังพบว่าสารเหล่านี้แสดงฤทธิ์ต่อการเพิ่มแขนงประสาทของหนู pheochromocytoma (PC-12 cells) (Bai et al., 2015)

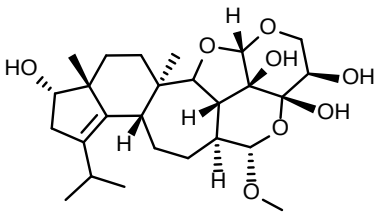

67

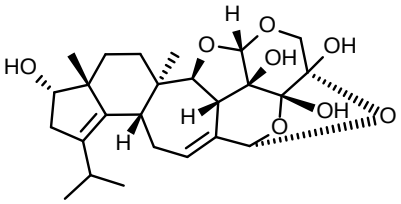

68

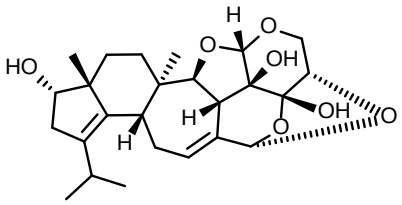

69

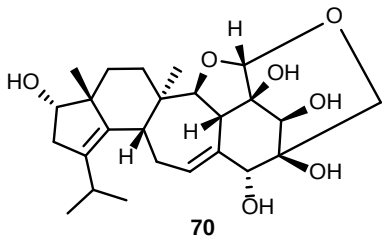

70

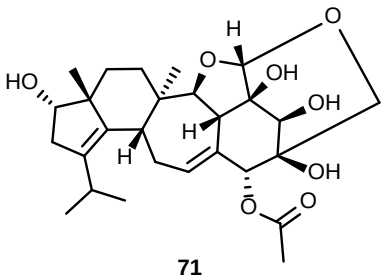

71

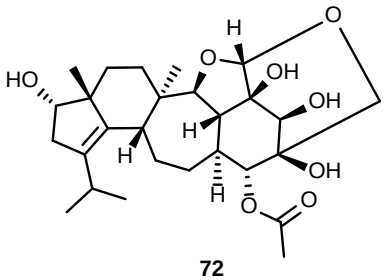

72

สารใหม่ในกลุ่มของ pyrino-cyathane diterpenoids ชื่อ pyristriatins A (**73**) และ B (**74**) สามารถแยกได้จากเชื้อเห็ดรา *Cyathus* cf. *striatus* โดยสารทั้งสองนี้แสดงฤทธิ์ต้านจุลชีพ ทั้งต่อเชื้อรา และแบคทีเรีย (Richter et al., 2016)

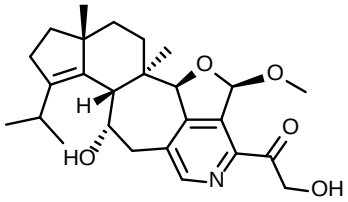

73

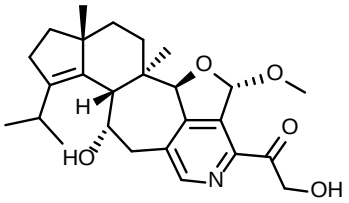

74

2. วัตถุประสงค์

2.1) เพื่อหาองค์ประกอบทางเคมี จากเชื้อราที่ได้คัดเลือกมาทั้ง 6 ตัว โดยวิธีทางโครมาโทกราฟี

2.2) เพื่อหาโครงสร้างทางเคมีของสารที่แยกได้โดยใช้วิธีทางสเปกโทรสโกปี

2.3) ทดสอบฤทธิ์ทางชีวภาพของสารที่แยกได้

2.4) ศึกษาเพิ่มเติม ในการเพิ่มศักยภาพในการพัฒนาในการเป็นยาของสารที่แยกได้บางตัวที่มีฤทธิ์ที่น่าสนใจ โดยการทำอนุพันธ์ของสารนั้น ทั้งนี้เพื่อให้สารดังกล่าวมีฤทธิ์ที่ดียิ่งขึ้น โดยอนุพันธ์ที่ทำขึ้นจะถูกนำไปทดสอบฤทธิ์ทางชีวภาพด้วย เพื่อนำมาเปรียบเทียบฤทธิ์ทางชีวภาพกับสารเดิม

3. วิธีการทดลอง

3.1 การเตรียมสารสกัดหยาบจากเชื้อราและทดสอบฤทธิ์ทางชีวภาพเบื้องต้น

เชื้อทั้ง 6 ชนิดที่ถูกคัดเลือก จะนำมาผลิตเพื่อเพิ่มจำนวนในระดับปริมาณมากขนาด 10–20 ลิตร (large scale production) หลักจากนั้นกรองแยกระหว่างเซลล์ (mycelium) และน้ำเลี้ยงเชื้อรา (broth) ในส่วนของน้ำเลี้ยงเชื้อราให้นำมาสกัดด้วยตัวทำละลาย EtOAc แล้วระเหยตัวทำละลายออก จะได้สารสกัดหยาบในส่วนของน้ำเลี้ยงเชื้อรา ส่วนเซลล์ของเชื้อรา ให้นำมาแช่ใน MeOH และ CH_2Cl_2 ตามลำดับ เป็นเวลาอย่างน้อย 3 วัน แล้วนำตัวทำละลายทั้งสองนี้มารวมกันแล้วระเหยตัวทำละลายออกไปบางส่วน จากนั้นเติมน้ำ 100–200 มิลลิลิตร แล้วนำมาสกัดด้วย *n*-hexane 2–3 ครั้ง จากนั้นสกัดด้วย EtOAc จำนวน 3 ครั้ง เมื่อระเหย *n*-hexane และ EtOAc ออกไป ก็จะได้สารสกัดหยาบในส่วนของ *n*-hexane และ EtOAc ตามลำดับ โดยสารสกัดหยาบทั้งสามนี้ จะนำไปทดสอบฤทธิ์ทางชีวภาพ และ วิเคราะห์ chemical profiles อีกครั้งหนึ่งว่ามีการผลิตในระดับ large scale ได้ผลเหมือนเดิมหรือไม่ ถ้าได้ผลเหมือนเดิม จึงจะนำสารสกัดหยาบเหล่านี้ไปทำการแยกให้บริสุทธิ์ต่อไป

3.2 การแยกสารและพิสูจน์เอกลักษณ์ขององค์ประกอบทางเคมีของสารสกัดหยาบ

การแยกสารให้บริสุทธิ์จากสารสกัดหยาบที่ได้นี้ จะใช้เทคนิคทางโครมาโทกราฟี เช่น คอลัมน์โครมาโทกราฟี, โครมาโทกราฟีของเหลวสมรรถนะสูง (high performance liquid chromatography, HPLC), preparative thin-layer chromatography (PLC) รวมไปถึงการตกผลึก หลังจากได้สารบริสุทธิ์แล้วจะนำสารบริสุทธิ์ที่ได้ไปทำวิเคราะห์หาโครงสร้างทางเคมี โดยใช้ข้อมูลทางสเปกโทรสโกปี เช่น NMR, IR, Mass, UV-visible, CD (Circular Dichroism) และ X-ray เป็นต้น

3.3 การตรวจหาฤทธิ์ทางชีวภาพของสารบริสุทธิ์ที่แยกได้

สารบริสุทธิ์ที่แยกได้ที่มีปริมาณที่มากพอจะถูกส่งตรวจหาฤทธิ์ทางชีวภาพที่ห้องปฏิบัติการตรวจหาสารออกฤทธิ์ทางชีวภาพ โดยการตรวจหาฤทธิ์ทางชีวภาพดังกล่าวจะสอดคล้องกับฤทธิ์ทางชีวภาพของสารสกัดหยาบ เช่น ฤทธิ์ยับยั้งเชื้อมาลาเรีย (*Plasmodium falciparum*, K1), ฤทธิ์ยับยั้งเชื้อวัณโรค (*Mycobacterium tuberculosis*, H37Ra), ฤทธิ์ยับยั้งเชื้อแบคทีเรียทั้งแกรมบวก (*Bacillus cereus*, *Enterococcus faecium*, *Staphylococcus aureus*) และแกรมลบ(*Acinetobacter baumannii, Escherichia coli*, *Klebsiella pneumoniae*, *Pseudomonas aeruginosa*), ฤทธิ์ยับยั้งการเจริญของเชื้อโรคพืช (*Alternaria brassicicola*, *Colletotrichum acutatum*, *C. capsici*, *C. gloeosporioides*, *Curvularia lunata* และ *Magnaporthe grisea*), ฤทธิ์ยับยั้งเซลล์มะเร็ง (ประกอบด้วย MCF-7, เซลล์มะเร็งเต้านม; NCI-H187, เซลล์มะเร็งปอด; KB, เซลล์มะเร็งช่องปาก) และทดสอบความเป็นพิษต่อเซลล์ปกติ (Vero, เซลล์ปกติจากไตของลิง)

3.4 บทสรุปของงานวิจัย

รายละเอียดขององค์ประกอบทางเคมี และฤทธิ์ทางชีวภาพของสารบริสุทธิ์ที่แยกได้ ได้ถูกรายงานไว้ในรายงานฉบับสมบูรณ์ และผลงานเหล่านี้บางส่วนได้ตีพิมพ์ในวารสารต่างประเทศ

4. ผลการทดลองและวิจารณ์ผลการทดลอง

4.1 ผลของฤทธิ์ทางชีวภาพที่ได้จากสารสกัดหยาบในระดับ large scale ของเชื้อที่ได้ทำการคัดเลือกมา 6 ตัว

ตารางที่ 1. ตารางแสดงฤทธิ์ทางชีวภาพของสารสกัดหยาบ

ชื่อเชื้อจุลินทรีย์	**ผลของฤทธิ์ทางชีวภาพจากสารสกัดหยาบ ***
1) เชื้อ *Ganoderma* sp. BCC73587	Antimalaria (IC_{50} 4.22 μg/mL) Anti-TB (MIC 12.5 μg/mL) Anti-NCI-H187 (IC_{50} 48.90 μg/mL)
2) เชื้อ *Cyathus subglopbisporus* BCC44381	Antimalaria (IC_{50} 0.22-1.21 μg/mL) Anti-TB (MIC 25-50 μg/mL) Anti-*Colletotrichum gloeosporioides* (MIC 12.5-25 μg/mL) Anti-*Colletotrichum capsici* (MIC 12.5-25 μg/mL) Anti-MCF-7 (IC_{50} 1.06-9.31 μg/mL) Anti-KB (IC_{50} 0.29-1.87 μg/mL) Anti-NCI-H187 (IC_{50} 0.80-2.07 μg/mL)
3) เชื้อ *Hypoxylon* sp. BCC32408	Antimalaria (IC_{50} 3.31 μg/mL) Anti-*Bacillus cereus* (MIC 6.25 μg/mL) Anti-MCF-7 (IC_{50} 11.58 μg/mL) Anti-KB (IC_{50} 8.26 μg/mL) Anti-NCI-H187 (IC_{50} 21.79 μg/mL)
4) เชื้อราเอนโดไฟท์ BCC41461	Anti-TB (MIC 50.0 μg/mL) Anti-*Bacillus cereus* (MIC 25.0 μg/mL)
5) เชื้อ *Curvularia* sp. BCC52426	Anti-*Acinetobacter baumannii* (MIC 25.0 μg/mL) Antifungal against *Aspergillus* sp. BCC51998
6) เชื้อ *Actinomadura* sp. BCC47066	Anti-*Bacillus cereus* (MIC 25.0 μg/mL)

*แสดงเฉพาะส่วนที่แสดงฤทธิ์ทางชีวภาพเท่านั้น

4.2 การแยกและพิสูจน์เอกลักษณ์ขององค์ประกอบทางเคมี และฤทธิ์ทางชีวภาพของสารบริสุทธิ์ที่แยกได้

ก) เชื้อเห็ดรา *Ganoderma* sp. BCC73587

นำส่วนสกัดหยาบจากทั้งน้ำเลี้ยงเชื้อรา (1.6 กรัม) และ เซลล์ (0.95 กรัม) มาทำการแยกหาองค์ประกอบทางเคมีโดยใช้เทคนิคทางโครมาโทกราฟี และพิสูจน์เอกลักษณ์ของสารบริสุทธิ์ที่แยกได้ พบสารบริสุทธิ์จำนวนทั้งหมด 12 ตัว (รูปที่ 1) และสารบริสุทธิ์ที่แยกได้มีการรายงานฤทธิ์ทางชีวภาพแล้ว ดังแสดงในตารางที่ 2

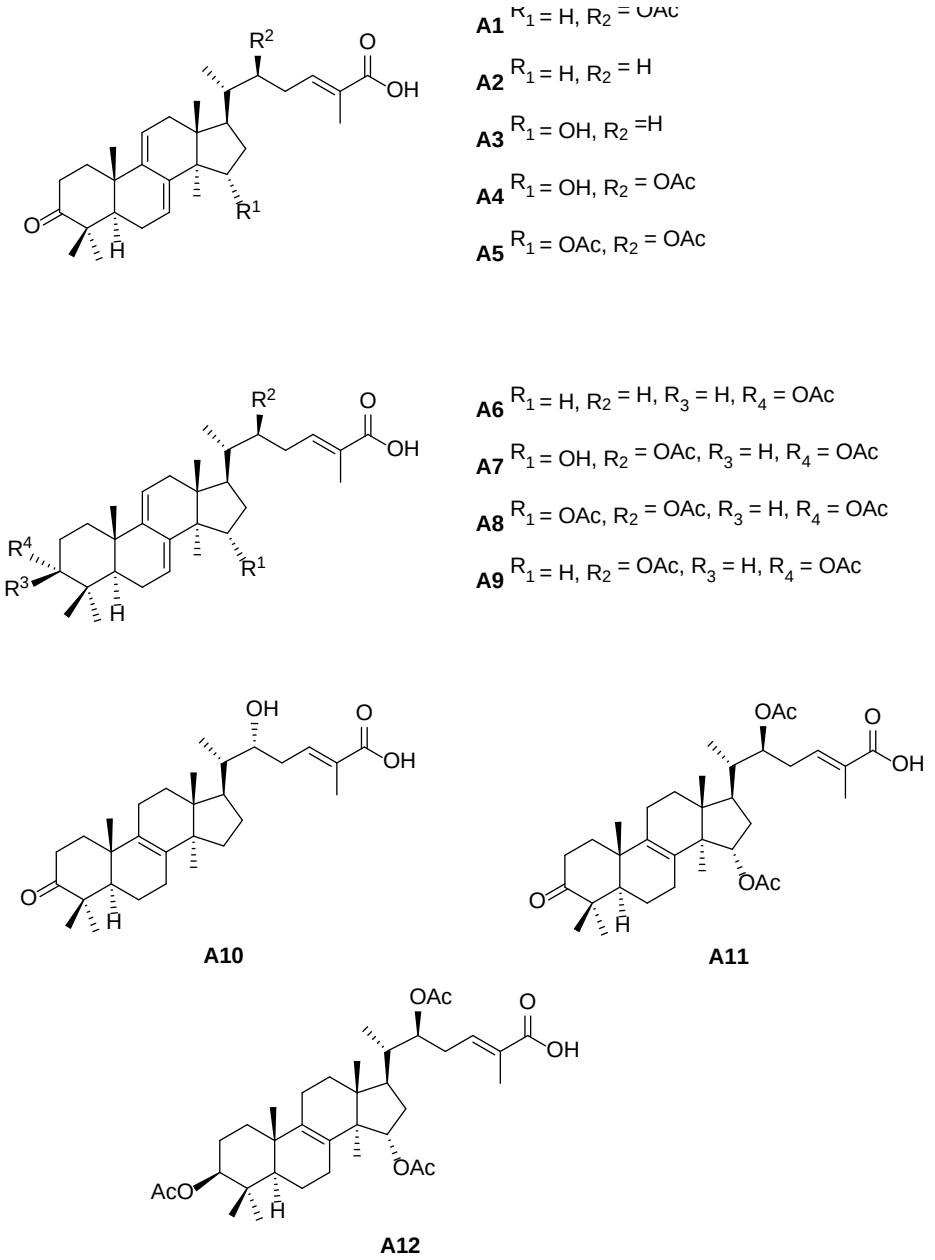

รูปที่ 1 องค์ประกอบทางเคมีจากเชื้อเห็ดรา *Ganoderma* sp. BCC73587

ตารางที่ 2. ฤทธิ์ทางชีวภาพของสารบริสุทธิ์ที่แยกได้

สารประกอบ	ฤทธิ์ทางชีวภาพ	เอกสารอ้างอิง
A1	Antimalarial IC_{50} > 20 μM Anti-TB MIC > 98 μM NCI-H187 IC_{50}= 65 μM MCF-7 IC_{50} > 98 μM KB IC_{50} = 65 μM Vero IC_{50} = 35 μM	Phytochem., 2013, **87**, 133 - 139
A2	Antimalarial IC_{50} 11 μM	J Nat Prod., 2010, **73** (5), 897 - 900
A3	Antimalarial IC_{50} 20 μM Anti-TB MIC = 50 μg/mL Vero IC_{50} > 107 μM	J Nat Prod., 2010, **73** (5), 897 - 900 J Nat Prod., 2016, **79** (1), 161 - 169
A4	Antimalarial IC_{50} > 19 μM Anti-TB MIC > 95 μM NCI-H187 IC_{50} = 34 μM MCF-7 IC_{50} > 95 μM KB IC_{50} > 95 μM Vero IC_{50} >95 μM	Phytochem., 2013, **87**, 133 - 139
A5[a]	Antimalarial IC_{50} = 8.55 μg/mL Anti-TB MIC = 25 μg/mL Vero IC_{50} = 48.04 μg/mL	Phytochem., 2013, **87**, 133 - 139
A6[a]	Antimalarial IC_{50} > 10 μg/mL Anti-TB MIC > 50 μg/mL Vero IC_{50} = 28.57 μg/mL	J Nat Prod., 2016, **79** (1), 161 - 169
A7[a]	Antimalarial IC_{50} > 10 μg/mL Anti-TB MIC > 50 μg/mL Vero IC_{50} = 23.95 μg/mL	Agric Biol Chem., 1987, **57** (4), 1149 - 1153
A8	Antimalarial IC_{50} = 5.5 μM Anti-TB MIC = 10 μM NCI-H187 IC_{50} = 15 μM MCF-7 IC_{50} = 78 μM KB IC_{50} = 18 μM Vero IC_{50} > 95 μM	Phytochem., 2013, **87**, 133 - 139
A9	ไม่มีรายงานฤทธิ์ทางชีวภาพ	Phytochem., 2013, **87**, 133 - 139
A10	Anti-TB MIC 25 μg/mL NCI-H187 IC_{50} = 48.35 μg/mL MCF-7 IC_{50} > 50 μg/mL KB IC_{50} = 19.99 μg/mL Anti-*Enterococcus faecium* MIC 25 μg/mL NCI-H187 IC_{50} > 50 μg/mL MCF-7 IC_{50} > 50 μg/mL KB IC_{50} > 50 μg/mL Vero IC_{50} = 48 μg/mL	J Agric Food Chem., 2012, **60**, 2834 - 2841 Tetrahedron, 2016, **72**, 3288 - 3295
A11	Anti-TB MIC >50 μg/mL Vero IC_{50} = 18.81 μg/mL	J Nat Prod., 2016, **79** (1), 161 - 169
A12	Anti-TB MIC >50 μg/mL Vero IC_{50} = 50 μg/mL	J Nat Prod., 2016, **79** (1), 161 - 169

[a] รายงานของฤทธิ์ทางชีวภาพเป็นครั้งแรก

ข) เชื้อราจากไม้ *Hypoxylon fendleri* BCC32408

นำสารสกัดหยาบส่วนน้ำเลี้ยงเชื้อรา (2.20 g) มาทำการแยกหาองค์ประกอบทางเคมีโดยใช้เทคนิคทางโครมาโทกราฟี และพิสูจน์เอกลักษณ์ของสารบริสุทธิ์ที่แยกได้ สามารถพบสารบริสุทธิ์ทั้งหมด 17 ตัว (รูปที่ 2) โดยเป็นสารใหม่จำนวน 10 ตัว และสารที่มีการรายงานไว้แล้ว จำนวน 7 ตัว และได้นำไปทดสอบฤทธิ์ทางชีวภาพดังแสดงในตารางที่ 3

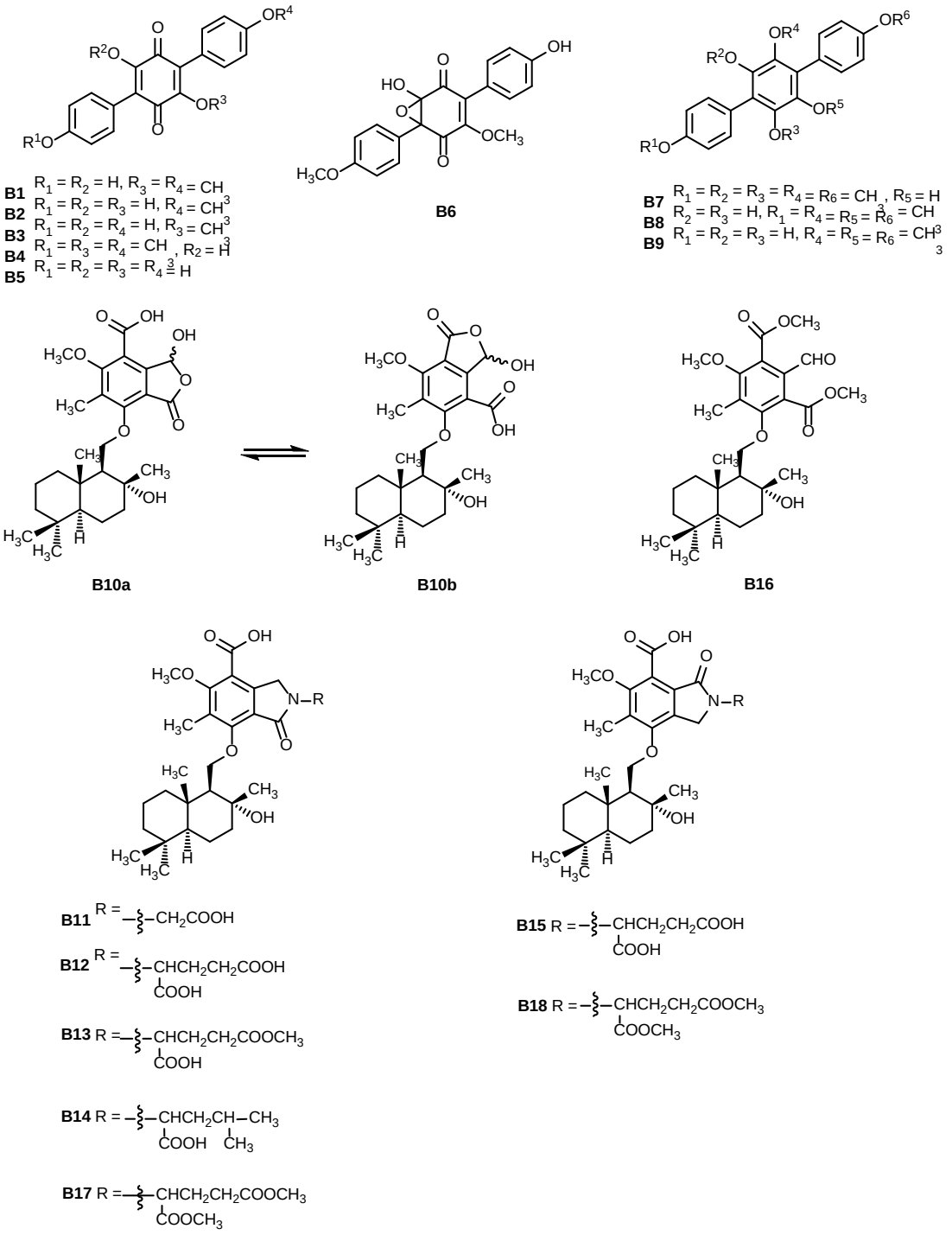

รูปที่ 2 องค์ประกอบทางเคมีจากเชื้อรา *Hypoxylon fendleri* BCC32408

ตารางที่ 3. ผลการทดสอบฤทธิ์ทางชีวภาพของสารบริสุทธิ์ที่แยกได้

Compound	Anti-malarial (IC_{50}, µg/mL)	Anti-*C. albicans* (IC_{50}, µg/mL)	Anti-*B. cereus* (MIC, µg/mL)	Cytotoxicity (IC_{50}, µg/mL)			
				KB	MCF-7	NCI-H187	Vero
B1	>10	nt	>25	>50	>50	48.10	48.96
B4	>10	nt	>25	>50	>50	41.97	49.09
B5	>10	>50	>25	>50	>50	>50	>50
B6	>10	nt	>25	>50	>50	>50	>50
B7	>10	>50	>25	>50	>50	>50	>50
B8	>10	>50	>25	>50	>50	>50	>50
B9	>10	>50	>25	>50	>50	>50	>50
B10	>10	>50	>25	>50	>50	>50	>50
B12	>10	nt	>25	>50	>50	>50	>50
B13	>10	nt	>25	>50	>50	>50	>50
B14	>10	nt	>25	>50	>50	>50	>50
B15	>10	nt	>25	>50	>50	>50	>50
B16	>10	>50	>25	>50	>50	11.77	35.25
dihydroartemisinin	7.00×10^{-4}	nt	nt	nt	nt	nt	nt
mefloquine	0.0097	nt	nt	nt	nt	nt	nt
ellipticine	nt	nt	nt	3.42	nt	2.80	1.26
doxorubicin	nt	nt	nt	1.70	14.92	0.073	nt
tamoxifen	nt	nt	nt	nt	9.83	nt	nt
amphotericin B	nt	0.11	nt	nt	nt	nt	nt
vancomycin	nt	nt	2.0	nt	nt	nt	nt

nt = not being tested

ค) เชื้อราเอนโดไฟท์ *Gloeostereum incarnatum* BCC41461

นำสารสกัดหยาบส่วนน้ำเลี้ยงเชื้อรา (9.66 g) มาทำการแยกหาองค์ประกอบทางเคมีโดยใช้เทคนิคทางโครมาโทกราฟี และพิสูจน์เอกลักษณ์ของสารบริสุทธิ์ที่แยกได้ พบว่าได้สารบริสุทธิ์จำนวนทั้งหมด 13 ตัว (รูปที่ 3) โดยเป็นสารใหม่จำนวน 11 ตัว และสารที่มีการรายงานไว้แล้วจำนวน 2 ตัว และได้นำไปทดสอบฤทธิ์ทางชีวภาพ ดังแสดงในตารางที่ 4

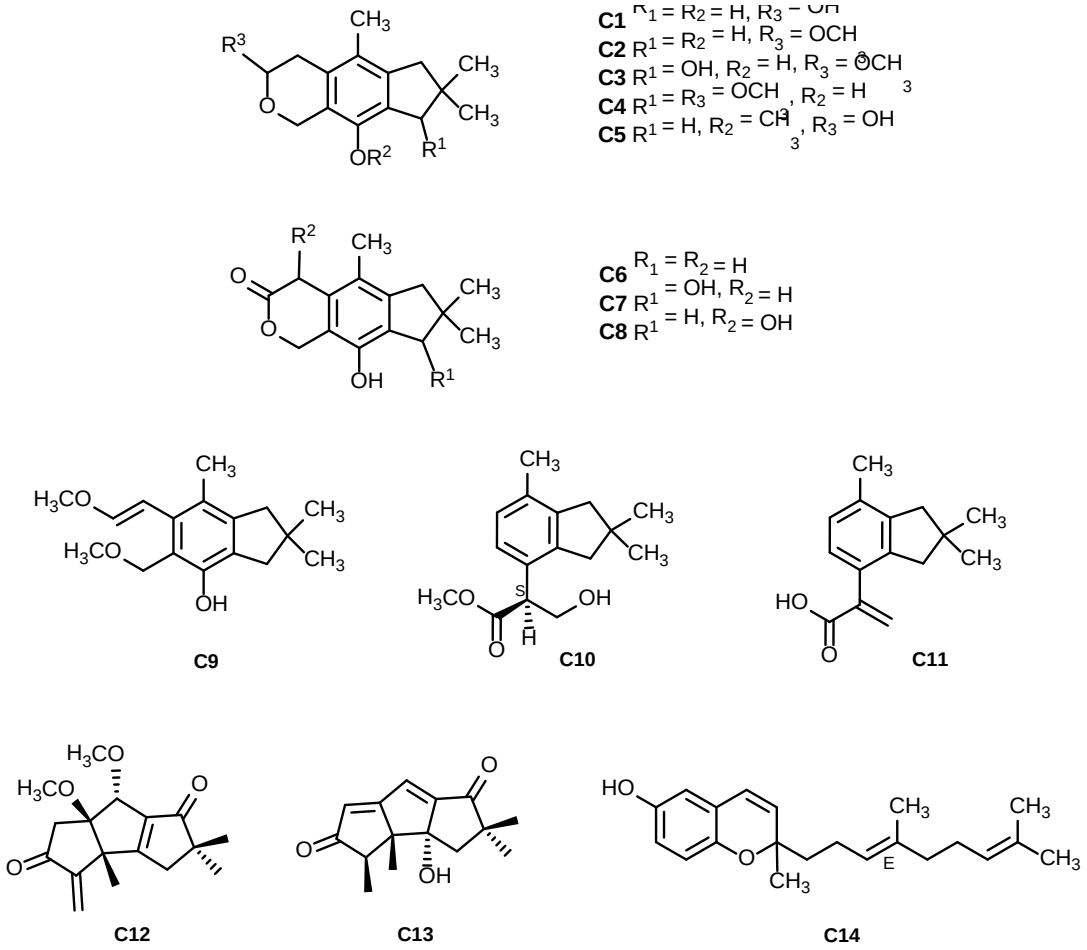

รูปที่ 3 องค์ประกอบทางเคมีจากเชื้อราเอนโดไฟท์ *Gloeostereum incarnatum* BCC41461

ตารางที่ 4. ผลการทดสอบฤทธิ์ทางชีวภาพของสารบริสุทธิ์ที่แยกได้

Compound	Antimalarial (IC_{50}, µg/mL)	Anti-TB (MIC, µg/mL)	Anti *B. cereus* (MIC, µg/mL)	Cytotoxicity (IC_{50}, µg/mL)			
				MCF-7	KB	NCI-H187	Vero
C1	9.80	>50	>25	>50	>50	>50	>50
C2	3.93	50.0	>25	29.76	28.15	22.97	18.86
C3	>10	>50	>25	>50	>50	>50	>50
C6	>10	>50	>25	>50	>50	>50	>50
C8	>10	>50	25.0	>50	37.97	47.25	47.52
C10	>10	50.0	25.0	15.15	11.79	7.27	2.99
C13	3.10	12.5	25.0	4.98	2.05	0.63	0.65
C14	>10	12.5	1.56	17.09	5.62	35.05	9.34
dihydroartemisinin	8.8×10^{-4}	-	-	-	-	-	-
mefloquine	0.025	-	-	-	-	-	-
rifampicin	-	0.025	-	-	-	-	-
ofloxacin	-	0.391	-	-	-	-	-
streptomycin	-	0.313	-	-	-	-	-
isoniazid	-	0.047	-	-	-	-	-
ethambutol	-	0.469	-	-	-	-	-
ellipticine	-	-	-	-	3.19	2.95	1.52
doxorubicin	-	-	-	9.56	0.68	0.13	-
tamoxifen	-	-	-	7.45	-	-	-
vancomycin	-	-	2.0	-	-	-	-

ง) เชื้อแอคติโนมัยซีท *Actinomadura* sp. BCC47066

นำสารสกัดหยาบรวมของส่วนน้ำเลี้ยงเชื้อ และ ส่วนเซลล์ (9.16 กรัม) มาทำการแยกหาองค์ประกอบทางเคมีโดยใช้เทคนิคทางโครมาโทกราฟี และพิสูจน์เอกลักษณ์ของสารบริสุทธิ์ที่แยกได้ ได้สารจำนวนทั้งสิ้น 16 ตัว (รูปที่ 4) โดยเป็นสารใหม่จำนวน 8 ตัว และสารที่มีผู้รายงานแล้วจำนวน 8 ตัว และได้นำไปทดสอบฤทธิ์ทางชีวภาพ ดังแสดงไว้ในตารางที่ 5

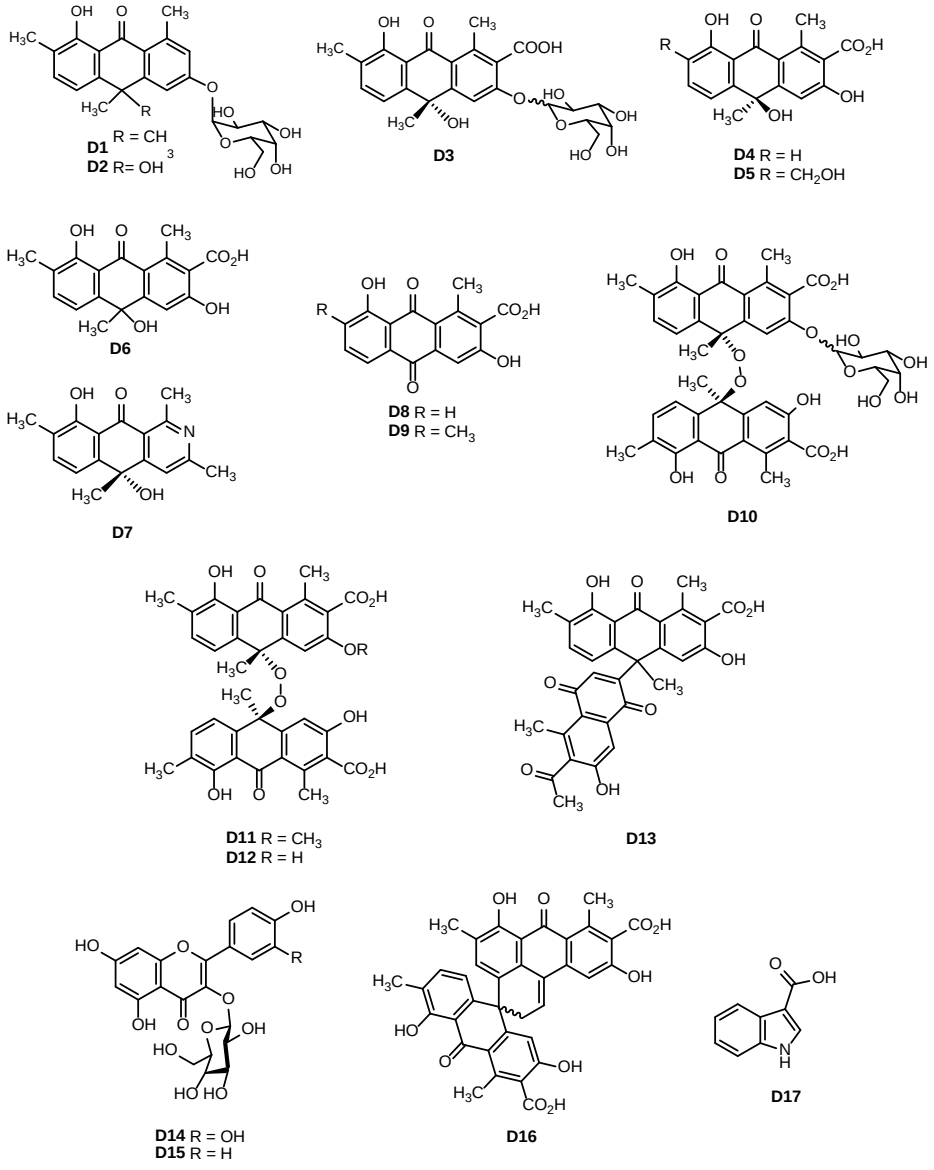

รูปที่ 4 องค์ประกอบทางเคมีจากเชื้อแอคติโนมัยซีท *Actinomadura* sp. BCC47066

ตารางที่ 5. ผลการทดสอบฤทธิ์ทางชีวภาพของสารบริสุทธิ์ที่แยกได้

Compound	Anti *B. cereus*[a]	Anti-HSV-1[b]	Anti-*C. capsici*[a]	Anti-*C. gloeosporioides*[a]	Anti-*A. brassicicola*[b]	Anti-*M. grisea*[b]	Cytotoxicity[b] (IC_{50}, μg/mL)			
	(MIC, μg/mL)	(IC_{50}, μg/mL)	(MIC, μg/mL)	(MIC, μg/mL)	(MIC, μg/mL)	(MIC, μg/mL)	MCF-7	KB	NCI-H187	Vero
D1	>25	2.33	>25	>25	>50	>50	>50	>50	>50	>50
D2	>25	>50	>25	>25	>50	>50	>50	>50	>50	>50
D6	>25	>50	>25	>25	>50	>50	>50	>50	>50	>50
D8	>25	>50	>25	>25	>50	>50	>50	>50	>50	>50
D9	>25	20.86	>25	>25	>50	>50	>50	31.72	33.19	>50
D10	3.13	10.32	6.25	6.25	>50	>50	>50	30.13	>50	>50
D12	1.56	>50	6.25	6.25	50.0	25.0	>50	>50	>50	27.64
D16	12.50	>50	>25	>25	50.0	>50	>50	>50	>50	>50
vancomycin	2.0	-	-	-	-	-	-	-	-	-
acyclovir	-	4.99	-	-	-	-	-	-	-	-
amphotericin B	-	-	1.56-3.13	1.56-3.13	1.56	3.13	-	-	-	-
ellipticine	-	-	-	-	-	-	-	2.60	1.94	1.53
doxorubicin	-	-	-	-	-	-	8.59	0.353	0.079	-
tamoxifen	-	-	-	-	-	-	8.17	-	-	-

[a] = ความเข้มข้นสูงสุดที่ใช้ในการทดสอบ คือ 25 μg/mL

[b] = ความเข้มข้นสูงสุดที่ใช้ในการทดสอบ คือ 50 μg/mL

จ) เชื้อรา *Curvularia* sp. BCC52426 ที่แสดงฤทธิ์ยับยั้งเชื้อ *Aspergillus* sp. BCC51998

นำสารสกัดหยาบจากการสกัดน้ำเลี้ยงเชื้อ (0.81 g) และ สารสกัดหยาบจากการสกัดส่วนเซลล์ (4.7 g) มาทำให้บริสุทธิ์โดยวิธีโครมาโตกราฟี และได้ทำการพิสูจน์เอกลักษณ์ของสารบริสุทธิ์ที่แยกได้ ได้สารจำนวนทั้งสิ้น 8 ตัว (รูปที่ 5) โดยเป็นสารใหม่จำนวน 4 ตัว และสารที่มีผู้รายงานแล้วจำนวน 4 ตัว และได้นำสารที่แยกได้เหล่านี้ไปทดสอบฤทธิ์ทางชีวภาพ ดังแสดงไว้ในตารางที่ 6

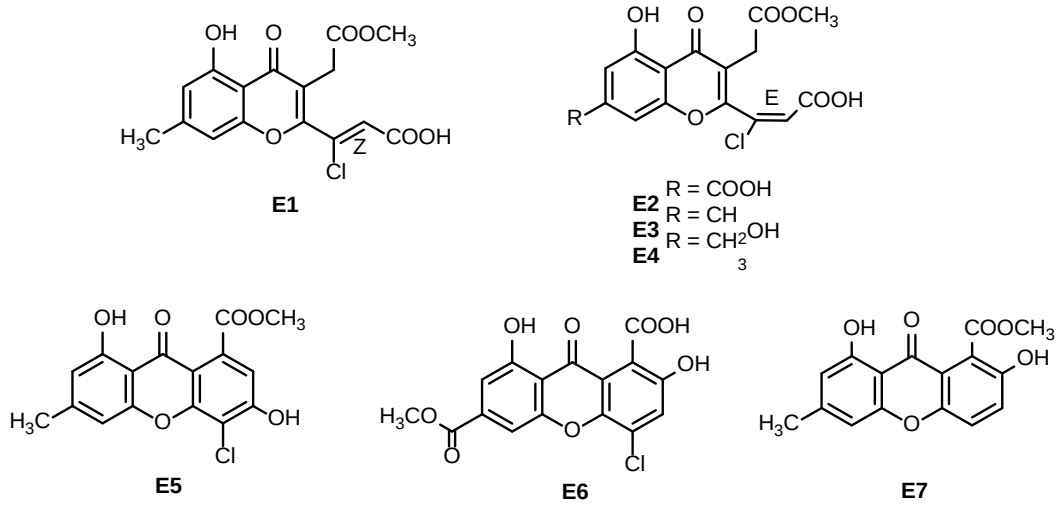

รูปที่ 5 องค์ประกอบทางเคมีจากเชื้อรา *Curvularia* sp. BCC52426

ตารางที่ 6. ผลการทดสอบฤทธิ์ทางชีวภาพของสารบริสุทธิ์ที่แยกได้

Compound	Antimalarial (IC_{50}, µg/mL)	Anti-TB (MIC, µg/mL)	Anti *B. cereus* (MIC, µg/mL)	Cytotoxicity (IC_{50}, µg/mL)			
				MCF-7	KB	NCI-H187	Vero
E1	>10	50	>25	>50	>50	49.58	26.29
E2	>10	>50	>25	>50	>50	>50	>50
E4	>10	>50	>25	>50	>50	>50	>50
E5	>10	>50	25.0	12.62	20.34	>50	34.19
E7	>10	>50	>25	>50	>50	>50	>50
dihydroartemisinin	8.1×10^{-4}	-	-	-	-	-	-
mefloquine	0.024	-	-	-	-	-	-
rifampicin	-	0.025	-	-	-	-	-
ofloxacin	-	0.391	-	-	-	-	-
streptomycin	-	0.313	-	-	-	-	-
isoniazid	-	0.047	-	-	-	-	-
ethambutol	-	0.469	-	-	-	-	-
ellipticine	-	-	-	-	3.19	3.46	1.59
doxorubicin	-	-	-	9.56	0.68	0.21	-
tamoxifen	-	-	-	7.45	-	-	-
vancomycin	-	-	2.0	-	-	-	-

ฉ) เชื้อเห็ดรา *Cyathus subglobisporus* BCC44381

นำสารสกัดหยาบส่วนน้ำเลี้ยงเชื้อรา (9.4 g) มาแยกด้วยเทคนิคทางโครมาโตกราฟี และพิสูจน์เอกลักษณ์ทางเคมีโดยใช้เทคนิคสเปกโทรสโกปี พบว่าได้สารบริสุทธิ์จำนวนทั้งสิ้น 12 ตัว (รูปที่ 6) โดยเป็นสารใหม่จำนวน 6 ตัว และสารที่มีผู้รายงานแล้วจำนวน 6 ตัว และได้นำสารบริสุทธิ์ที่แยกได้ไปทดสอบฤทธิ์ทางชีวภาพ ดังแสดงในตารางที่ 7 และ 8 ตามลำดับ

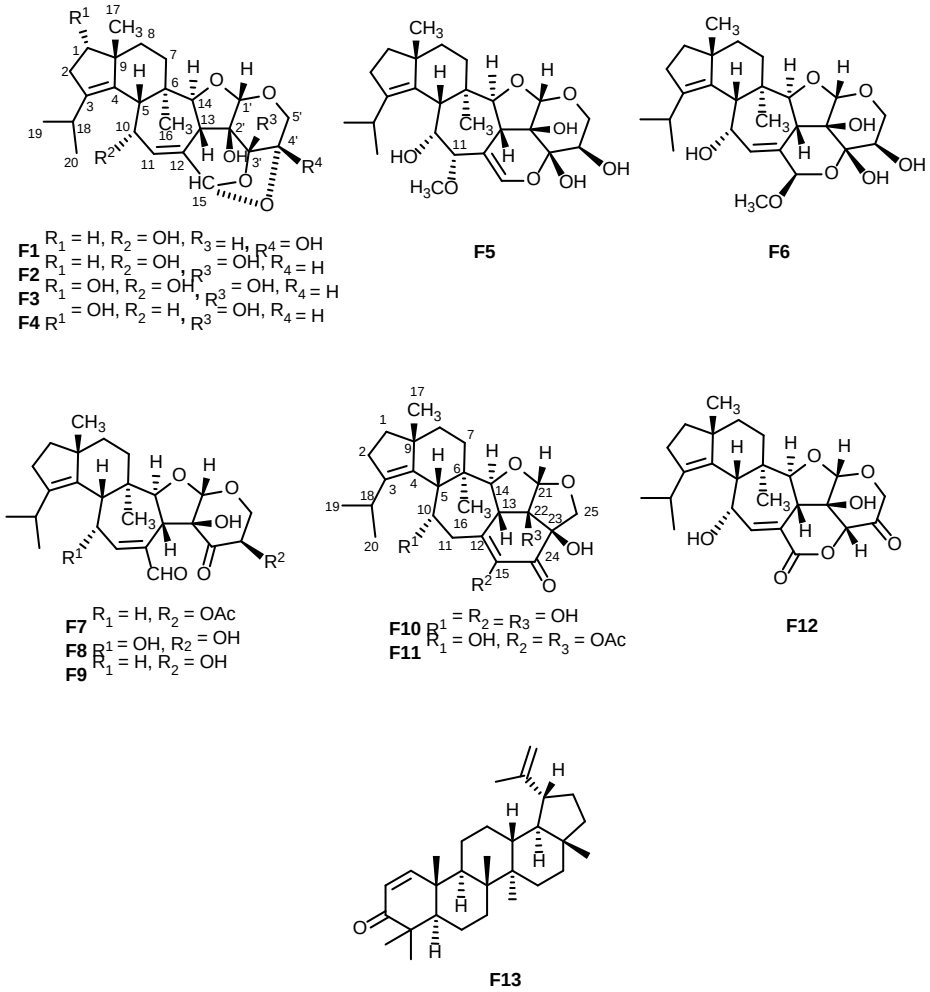

รูปที่ 6 องค์ประกอบทางเคมีจากเชื้อเห็ดรา *Cyathus subglobisporus* BCC44381

ตารางที่ 7. ผลการทดสอบฤทธิ์ทางชีวภาพของสารบริสุทธิ์ที่แยกได้

Compound	Anti-*P. falciparum* (IC_{50}, μM)	Anti-*C. albicans* (IC_{50}, μM)	Antibacterial activity (MIC, μg/mL)						
			M. tuberculosis	*B. cereus*	*E. faecium*	*E. coli* +PAβN	*P. aeruginosa* + PAβN	*A. baumannii* +PAβN	*K. pneumoniae* +PAβN
F1	7.51	inactive	50.0	25.0	50.0	25.0	inactive	nt	inactive
F3	inactive	inactive	inactive	inactive	inactive	inactive	inactive	inactive	inactive
F4	7.33	inactive	inactive	12.5	inactive	50.0	inactive	12.5	inactive
F5	2.13	80.3	50.0	3.13	50.0	12.5	inactive	6.25	inactive
F6	1.40	75.8	50.0	1.56	25.0	6.25	inactive	3.13	50.0
F7	1.03	72.3	50.0	1.56	25.0	6.25	inactive	12.5	50.0
F8	0.88	8.6	25.0	0.78	6.25	3.13	inactive	6.25	25.0
F9	2.12	inactive	inactive	6.25	50.0	50.0	inactive	nt	inactive
F10	inactive	inactive	inactive	inactive	inactive	inactive	inactive	inactive	inactive
F11	inactive	inactive	inactive	inactive	inactive	inactive	inactive	inactive	inactive
F12	inactive	inactive	inactive	25.0	inactive	inactive	inactive	inactive	inactive
dihydroartemisinine	0.0029	-	-	-	-	-	-	-	-
mefloquine	0.043	-	-	-	-	-	-	-	-
amphotericin B	-	0.08	-	-	-	-	-	-	-
vancomycin	-	-	-	2.0	-	-	-	-	-
rifampicin	-	-	0.013	-	1.56	0.05	-	0.10	0.20
streptomycin	-	-	0.63	-	-	-	-	-	-
isoniazid	-	-	0.047	-	-	-	-	-	-
ofloxacin	-	-	0.78	-	-	-	-	-	-
ethambutol	-	-	0.94	-	-	-	-	-	-
tetracycline HCl	-	-	-	-	0.10-0.20	-	-	-	-
erythromycin	-	-	-	-	-	0.78	>32	0.78	6.25

ตารางที่ 8. ผลการทดสอบฤทธิ์ต้านมะเร็ง และความเป็นพิษต่อเซลล์ปกติ

Compound	Cytotoxicity[a] (IC_{50}, μM)			
	MCF-7	**KB**	**NCI-H187**	**Vero**
F1	28.32	12.85	8.48	6.93
F3	inactive	inactive	inactive	inactive
F4	18.14	2.94	20.85	1.69
F5	3.87	0.48	0.44	0.13
F6	3.58	0.36	4.02	0.15
F7	1.41	0.6	3.97	0.20
F8	6.91	0.84	6.21	0.51
F9	inactive	inactive	17.73	3.62
F10	inactive	inactive	inactive	91.50
F11	inactive	inactive	inactive	inactive
F12	inactive	39.17	109.37	13.11
tamoxifen	19.22	-	-	-
doxorubicin	12.14	1.06	0.36	-
ellipticine	-	5.81	5.40	4.38

เอกสารอ้างอิง

Baby, S., Johnson, A. J., Govindan, B., 2015. Secondary metabolites from *Ganoderma*. Phytochem 114, 66-101.

Bai, R., Zhang, C.-C., Yin, X., Wei, J., Gao, J.-M., 2015. Striatoids A–F, Cyathane diterpenoids with neurotrophic cctivity from cultures of the fungus *Cyathus striatus*. J Nat Prod 78, 783-788.

Chairul, Tokuyama, T., Nishizawa, M., Shiro, M., Tokuda, H., Hayashiji, Y., 1990. Malonate half-esters of homolanostanoid from an asian *Ganoderma* fungus. Phytochem 29, 923-928.

Fatmawati, S., Shimizu, K., Kondo, R., 2010. Ganoderic acid Df, a new triterpenoid with aldose reductase inhibitory activity from the fruiting body of *Ganoderma lucidum*. Fitoterapia 81, 1033-1036.

Fukai, M., Tsukada, M., Miki, K., Suzuki, T., Sugita, T., Kinoshita, K., Takahashi, K., Shiro, M., Koyama, K., 2012. Hypoxylonols C-F, benzo[j]fluoranthenes from *Hypoxylon truncatum*. J Nat Prod 75, 22-25.

Gonzalez, A. G., Leon, F., Rivera, A., Padron, J. I., Gonzalez-Plata, J., Zuluaga, J. C., Quintana, J., Estevez, F., Bermejo, J., 2002. New lanostanoids from the fungus *Ganoderma concinna*. J Nat Prod 65, 417-421.

Komoda, Y., Shimizu, M., Sonoda, Y., Sato, Y., 1989. Ganoderic acid and its derivatives as cholesterol synthesis inhibitors Chem pharm bull 37, 531-533.

Kubota, T., Asaka, Y., Miura, I., Mori, H., 1982. Structures of Ganoderic Acid A and B, Two New Lanostane Type Bitter Triterpenes from *Ganoderma lucidum* (FR.) KARST. Helv Chim Acta 65, 611-619.

Kuhnert, E., Surup, F., Wiebach, V., Bernecker, S., Stadler, M., 2015. Botryane, noreudesmane and abietane terpenoids from the ascomycete *Hypoxylon rickii*. Phytochemistry 117, 116-122.

Lee, S. Y., Kim, J. S., Lee, S., Kang, S. S., 2011. Polyoxygenated ergostane-type sterols from the liquid culture of *Ganoderma applanatum*. Nat Prod Res 25, 1304-1311.

Lin, S. B., Li, C. H., Lee, S. S., Kan, L. S., 2003. Triterpene-enriched extracts from *Ganoderma lucidum* inhibit growth of hepatoma cells via suppressing protein kinase C, activating mitogen-activated protein kinases and G2-phase cell cycle arrest. Life Sci 72, 2381-2390.

Liu, J.-Q., Wang, C.-F., Peng, X.-R., Qiu, M.-H., 2011. New alkaloids from the fruiting bodies of *Ganoderma sinense*. Nat Prod Bioprospect 1, 93-96.

Min, B.-S., Gao, J.-J., Nakamura, N., Hattori, M., 2000. Triterpenes from the Spores of *Ganoderma lucidum* and Their Cytotoxicity against Meth-A and LLC Tumor Cells. Chem Pharm Bull 48, 1026-1033.

Quang, D. N., Hashimoto, T., Stadler, M., Asakawa, Y., 2004. New azaphilones from the inedible mushroom *Hypoxylon rubiginosum*. J Nat Prod 67, 1152-1155.

Richter, C., Helaly, S. E., Thongbai, B., Hyde, K. D., Stadler, M., 2016. Pyristriatins A and B: Pyridino-cyathane antibiotics from the Basidiomycete *Cyathus* cf. *striatus*. J Nat Prod 79, 1684-1688.

Rios, J. L., Andujar, I., Recio, M. C., Giner, R. M., 2012. Lanostanoids from fungi: a group of potential anticancer compounds. J Nat Prod 75, 2016-2044.

Sato, N., Ma, C. M., Komatsu, K., Hattori, M., 2009. Triterpene-farnesyl hydroquinone conjugates from *Ganoderma sinense*. J Nat Prod 72, 958-961.

Shaaban, K. A., Elshahawi, S. I., Wang, X., Horn, J., Kharel, M. K., Leggas, M., Thorson, J. S., 2015. Cytotoxic Indolocarbazoles from *Actinomadura melliaura* ATCC 39691. J Nat Prod, *in press*.

Sonoda, Y., Sekigawa, Y., Sato, Y., 1988. *In vitro* effects of oxygenated lanosterol derivatives on cholesterol biosynthesis from 24, 25-dihydrolanosterol. Chem Pharm Bull 36, 966-973.

Sumarah, M. W., Kesting, J. R., Sørensen, D., Miller, J. D., 2011. Antifungal metabolites from fungal endophytes of *Pinus strobus*. Phytochem 72, 1833-1837.

Tseng, M., Su, Y.-S., Cheng, M.-J., Liu, T.-W., Chen, I.-S., Wu, M.-D., Chang, H.-S., Yuan, G.-F., 2013. Chemical constituents from a soil-derived actinomycete, *Actinomadura miaoliensis*

BCRC 16873, and their inhibitory activities on lipopolysaccharide-induced tumor necrosis factor production. Chem Biodivers 10, 303-312.

Wang, B., Han, J., Xu, W., Chen, Y., Liu, H., 2014. Production of bioactive cyathane diterpenes by a bird's nest fungus Cyathus gansuensis growing on cooked rice. Food Chem 152, 169-176.

Wang, J. L., Li, Y. B., Liu, R. M., Zhong, J. J., 2010. A new ganoderic acid from *Ganoderma lucidum* mycelia. J Asian Nat Prod Res 12, 727-730.

Yang, J., Yu, D., 1989. [Synthesis of ganoderma alkaloid A and B]. Acta pharm Sin 25, 555-559.

Yang, S.-X., Yu, Z.-C., Lu, Q.-Q., Shi, W.-Q., Laatsch, H., Gao, J.-M., 2012. Toxic lanostane triterpenes from the basidiomycete *Ganoderma amboinense*. Phytochem Lett 5, 576-580.

Ying, Y.-M., Shan, W.-G., Zhang, L.-W., Zhan, Z.-J., 2013. Ceriponols A–K, tremulane sesquitepenes from *Ceriporia lacerate* HS-ZJUT-C13A, a fungal endophyte of *Huperzia serrata*. Phytochem 95, 360-367.

You, B. J., Lee, M. H., Tien, N., Lee, M. S., Hsieh, H. C., Tseng, L. H., Chung, Y. L., Lee, H. Z., 2013. A novel approach to enhancing ganoderic acid production by *Ganoderma lucidum* using apoptosis induction. PLoS One 8, e53616.

Output จากโครงการวิจัยที่ได้รับทุนจาก สกว.

1. ผลงานตีพิมพ์ในวารสารวิชาการนานาชาติ ดังต่อไปนี้

1.1) เรื่อง “Terphenyl derivatives and drimane – Phthalide / isoindolinones from *Hypoxylon fendleri* BCC32408” ใน วารสาร “Phytochemistry” ปี 2017 เล่มที่ 139 หน้า 8-17

C. Intaraudom, N. Bunbamrung, A. Dramae, N. Boonyuen, P. Kongsaeree, K. Srichomthong, S. Supothina, **P. Pittayakhajonwut**, Terphenyl derivatives and drimane - Phthalide/isoindolinones from *Hypoxylon fendleri* BCC32408, *Phytochemistry* (2017), **139**, 8-17.

1.2) เรื่อง “Antimicrobial activity of illudalane and alliacane sesquiterpenes from the mushroom *Gloeostereum incarnatum* BCC41461” ใน วารสาร “Phytochemistry Letters” ปี 2017 เล่มที่ 20 หน้า 274-281

N. Bunbamrung, C. Intaraudom, A. Dramae, N. Boonyuen, S. Veeranondha, P. Rachtawee, **P. Pittayakhajonwut**, Antimicrobial activity of illudalane and alliacane sesquiterpenes from the mushroom *Gloeostereum incarnatum* BCC41461, *Phytochemistry Letters* (2017), **20**, 274-281.

1.3) เรื่อง “Anthrone derivatives from the terrestrial actinomycete, *Actinomadura* sp. BCC47066” ใน วารสาร “Phytochemistry Letters” ปี 2018 เล่มที่ 25 หน้า 109-117

N. Bunbamrung, K. Supong, C. Intaraudom, A. Dramae, P. Auncharoen, **P. Pittayakhajonwut**, Anthrone derivatives from the terrestrial actinomycete, *Actinomadura* sp. BCC47066, *Phytochemistry Letters* (2018), **25**, 109-117.

1.4) เรื่อง “Antagonistic metabolites produced by the fungus *Curvularia* sp. BCC52426 against *Aspergillus* sp. BCC51998” ใน วารสาร “Phytochemistry Letters” ปี 2018 เล่มที่ 26 หน้า 33-37

N. Bunbamrung, C. Intaraudom, A. Dramae, N. Boonyuen, R. Chanthaket, P. Rachtawee, **P. Pittayakhajonwut**, Antagonistic metabolites produced by the fungus *Curvularia* sp. BCC52426 against *Aspergillus* sp. BCC51998, *Phytochemistry Letters* (2018**)**, **26**, 33-37.

1.5) เรื่อง “Antimicrobial activity of cyathane derivatives from *Cyathus subglobisporus* BCC44381” ใน วารสาร “Tetrahedron” ปี 2018 เล่มที่ 74 หน้า 6907-6916

S. Nitthithanasilp, C. Intaraudom, N. Boonyuen, R. Suvannakad, **P. Pittayakhajonwut**, Antimicrobial activity of cyathane derivatives from *Cyathus subglobisporus* BCC44381, *Tetrahedron* (2018), **74**, 6907-6916.

2. สิทธิบัตร

นำผลงานวิจัยที่ได้ ไปจดสิทธิบัตรในประเทศ เรื่อง “สารประกอบเฟนเลอรัล และองค์ประกอบทางเภสัชกรรมของสารดังกล่าว” เมื่อวันที่ 23 กันยายน 2559 เลขที่คำขอ 1601005549

ผลงานวิจัยนี้เป็นงานวิจัยที่ได้รับการสนับสนุนทุนวิจัยจากสำนักงานกองทุนสนับสนุนการวิจัย รหัสโครงการ RSA5980001

ภาคผนวก

Phytochemistry 139 (2017) 8–17

Contents lists available at ScienceDirect

Phytochemistry

journal homepage: www.elsevier.com/locate/phytochem

Terphenyl derivatives and drimane – Phathalide/isoindolinones from *Hypoxylon fendleri* BCC32408

Chakapong Intaraudom [a], Nantiya Bunbamrung [a], Aibrohim Dramae [a], Nattawut Boonyuen [a], Palangpon Kongsaeree [b, c], Kitlada Srichomthong [a], Sumalee Supothina [a], Pattama Pittayakhajonwut [a, *]

[a] National Center for Genetic Engineering and Biotechnology (BIOTEC), National Science and Technology Development Agency (NSTDA), Thailand Science Park, Paholyothin Road, Klong Luang, Pathumthani, 12120, Thailand
[b] Department of Chemistry, Center of Excellence for Innovation in Chemistry, Faculty of Science, Mahidol University, Rama 6 Road, Bangkok, 10400, Thailand
[c] Center for Excellence in Protein Structure and Function, Faculty of Science, Mahidol University, Rama 6 Road, Bangkok, 10400, Thailand

ARTICLE INFO

Article history:
Received 22 November 2016
Received in revised form
1 March 2017
Accepted 29 March 2017

Keywords:
Hypoxylon fendleri
Xylariaceae
Antimicrobial
Cytotoxicity
Fendleryls
Fendlerinines

ABSTRACT

The genus *Hypoxylon*, a member of the family Xylariaceae, has been known to produce significant secondary metabolites in terms of chemical diversity. Moreover, the compounds isolated can also be used as chemotaxonomic characters for differentiation among the two sections, which are sect. *Annulata* and sect. *Hypoxylon*. In our continuing chemical screening programme for novel compounds, the crude extracts of *H. fendleri* BCC32408 gave significant chemical profiles in HPLC analyses. Thus, the chemical investigation of these crude extracts was then carried out. The investigation led to the isolation of ten previously undescribed compounds including three terphenylquinones (fendleryls A – C), one terphenyl (fendleryl D), and six novel drimane – phthalide-type lactone/isoindolinones derivatives (fendlerinines A – F) along with seven known compounds (2-*O*-methylatromentin, rickenyl E, atromentin, rickenyls C – D, (+)-ramulosin, and *O*-hydroxyphenyl acetic acid). The chemical structures were determined on the basis of spectroscopic analyses, including 1D, 2D NMR and high-resolution mass spectrometry, as well as chemical transformations. In addition, these isolated compounds were assessed for antimicrobial activity including antimalarial (against *Plasmodium falciparum*, K-1 strain), antifungal (against *Candida albicans*), antibacterial (against *Bacillus cereus*) activities. Cytotoxicity against both cancerous (KB, MCF-7, NCI-H187) and non-cancerous (Vero) cells of these compounds were also evaluated.

1. Introduction

Xylariaceae has been known to produce many diverse secondary metabolites with several unique chemical structures. The well-known genera in term of secondary metabolites production are *Biscogniauxia*, *Daldinia*, *Hypoxylon*, *Nemania*, *Poronia*, *Rosellinia*, and *Xylaria* (Whalley and Edwards, 1995). The genus "*Hypoxylon*" is categorized into two sections, which are *Annulata* and *Hypoxylon*. These two sections were primarily differentiated by its morphological characters (the presence or absence of a layer of carbonaceous stromatal tissue enclosing perithecia and the physical characteristics of the perispore) (Hsieh et al., 2005) and secondary metabolites produced either in stromata or in cultures (Whalley and Edwards, 1995). So far, the prominent compounds used as fingerprint in differentiated sections among *Hypoxylon* spp. are binaphthalenetetrol (BNT) or binaphyls, orsellinic acid, mitorubrin-type azaphilones, macrocarpones (Kuhnert et al., 2015c; Mühlbauer et al., 2002). *H. fendleri* is a member in the sect. *Hypoxylon* and to our knowledge, only few species in this section have been reported of their secondary metabolites. For examples, polyketides (carneic acids A and B) were isolated from *H. carneum* and exhibited antimicrobial activity against various filamentous fungi, yeast *Yarrowia lipolytica* and bacteria *Bacillus cereus* (Quang et al., 2006); Lepraic acid was isolated from *H. aeruginosum* and possessed anti-Gram positive bacterial activity (Læssøe et al., 2010); the guaiane sesquiterpenes (hypoxylonol, hypoxylonol A, and investienol) were isolated from the endophytic *H. investiens* BCRC 10F0115 and were inactive for nitric oxide (NO) inhibitory test (Chang et al., 2014); sporothriolide derivatives were isolated from *H. monticulosim*

* Corresponding author.
E-mail address: pattamap@biotec.or.th (P. Pittayakhajonwut).

http://dx.doi.org/10.1016/j.phytochem.2017.03.008
0031-9422/

(MUCL 54604) and were inactive for antibacterial (both Gram-negative and Gram-positive) activity and no cytotoxicity against HCT-116, CHO-K1, and U-2 OS cell lines (Surup et al., 2014) but only sporothriolide had anti-phytopathogenic activity against *Rhizoctonia solani*, *Sclerotinia sclerotiorum*, and *Magnaporthe oryzae* (Cao et al., 2016). Recently, sesquiterpene botryanes, diterpenoid with abietane-type backbone (rickitin A) were isolated from *H. rickii* and were inactive for antimicrobial tests such as antibacterial both Gram-positive and Gram-negative, antimalarial, and antifungal activities (Kuhnert et al., 2015d). Moreover, other metabolites of silphiperfolene-type sesquiterpenoids including 13-hydroxysilphiperfol-6-ene and rickinic acids A − C were later reported from the same *H. rickii*. Only rickinic acid A showed weak antimicrobial activity against the yeast *Saccharomyces cerevisiae* and the bacteria *Bacillus subtilis* without cytotoxicity (Surup et al., 2015).

In our continuing chemical screening programme based on HPLC analyses, the chemical profiles of the crude extracts obtained from *H. fendleri* showed the production of various metabolites. Therefore, we investigated the chemical constituents of *H. fendleri*. In addition, biological activity for antimicrobial activity and cytotoxic activity of compounds isolated were also evaluated.

2. Results and discussion

2.1. Structure determination

H. fendleri BCC32408 was cultivated in malt extract medium under static condition. The broth was separated from the mycelium by simple filtration and then extracted with EtOAc. The crude extract was subjected to reverse-phase preparative HPLC to give ten new compounds, named fendleryls A − D (terphenyl derivatives) and fendlerinines A − F (drimane − phthalide-type lactone/isoindolinones) and seven known compounds. The chemical structures were elucidated by spectroscopic information including 1D, 2D NMR, UV−Vis, IR spectral data, and HRESIMS data together with chemical means.

Compound **1** was obtained as a brown solid and had the molecular formula of $C_{20}H_{16}O_6$, which was determined by the sodium-adduct precursor ion peak at *m/z* 375.0837 $[M+Na]^+$ in the HRESIMS spectrum, indicating thirteen degrees of unsaturation. The ^1H NMR spectrum of compound **1** showed two sets of *para*-substituted phenyl ring system [at δ_H 6.78 (2H, d, J = 8.5 Hz), 7.21 (2H, d, J = 8.5 Hz); and δ_H 6.99 (2H, d, J = 8.6 Hz), 7.27 (2H, d, J = 8.6 Hz)] and two methoxy signals resonating at δ_H 3.80. The ^{13}C NMR spectrum gave twenty carbons including two methoxy (at δ_C 51.8 and 62.0), eight aromatic methine [at δ_C 113.9 (× 2), 115.1 (× 2), 132.4 (× 2), and 132.6 (× 2)], and ten quaternary (δ_C 118.3, 121.9, 123.0, 125.6, 152.5, 156.1, 157.5, 159.8, 183.4, and 184.2) carbons. The HMBC spectrum showed correlations from H-2/H-6 to C-4 and C-1′; from H-3/H-5 to C-1; from H-2″/H-6″ to C-4′ and C-4″; and from H-3″/H-5″ to C-1″. The methoxy group (δ_H 3.80) was placed at C-4 (δ_C 159.8) and C-6′ (δ_C 156.1) according to the evidence from HMBC correlations as well as NOESY correlation between 6′−OCH_3 and H-2/H-4. The three remaining quaternary carbons resonating at δ_C 152.5 (C-3′), 183.4 (C-2′) and 184.1 (C-5′) indicated a carbon attached to oxygen and a presence of carbonyl carbons of *p*-benzoquinone system, respectively. Therefore, compound **1** was depicted as shown in Fig. 1 and was given a trivial name fendleryl A. Compound **1** was similar to rickenyl E, isolated from the fungus *H. rickii* (Kuhnert et al., 2015a).

Compound **2** was obtained as a brown solid. The ^1H NMR spectrum was similar to that of compound **1**, except the absence of a methoxy signal. HRESIMS data revealed 14 mass units less than that of **1**, confirming the molecular formula $C_{19}H_{12}O_6$ (*m/z* 337.0720, $[M-H]^-$). In the ^{13}C NMR spectrum, a broad carbonyl resonating at δ_C 169.0 was similar to those of quinone carbonyls of atromentin (**5**) (Ye et al., 2010), indicating hydroxyl substituents at C-3′ and C-6′. The HMBC spectrum confirmed the position of methoxy group at C-4 by showing correlation from H-2/H-6 (δ_H 7.35) and a methoxy (δ_H 3.78) signals to C-4. Thus, compound **2** had the chemical structure as shown in Fig. 1 and fendleryl B is given as its trivial name.

Compound **6** was obtained as a yellow solid. The ^1H NMR spectrum was similar to that of **1**, except that two methoxy signals were not superimposed as in **1**. The ^{13}C NMR spectrum showed an extra sp^3 quaternary carbon attached to an oxygen at δ_C 66.1 and the absence of one sp^2 quaternary carbon attached to oxygen. The evidence from the ^{13}C NMR spectral data suggested the replacement of a double bond with an epoxide. In addition, the HMBC spectrum showed correlations from H-2″/H-6″ to C-4′ (δ_C 66.1) and C-4″; from two methoxy signals at δ_H 3.68 and 3.74 to two quaternary carbons at C-6′ and C-4″, respectively. Therefore, based on spectroscopic evidence, epoxide was placed at C-3′ and C-4′ and HRESIMS spectral data confirmed the chemical structure of compound **6**. In addition, H-2/H-6 (resonating at δ_H 8.06) of compound **6**, resonating at lower field than those of compounds **1**–**4** (δ_H 7.3−7.4), was caused by a steric hindrance of a methoxyl at C-6′, which affected a twist of the phenyl group substituted at C-1′ and resulted in a deshielding effect from an epoxide. However, compound **6** did not provide the CD spectrum in order to compare with the similar compound 3-hydroxy-1,4-diphenyl-7-oxabicyclo[4.1.0] hept-3-ene-2-2,5-dione (Colson et al., 1985), therefore this compound could be racemic. Compound **6** (Fig. 1) is given a trivial name fendleryl C.

Compound **7** was obtained as a brown solid and HRESIMS data gave the mass ion peak at *m/z* 397.1644 $[M+H]^+$, establishing the molecular formula $C_{23}H_{25}O_6$. The ^1H and ^{13}C NMR spectra of compound **7** were similar to that of rickenyl C (**8**) (Kuhnert et al., 2015b), except the presence of an additional methoxy signal. In the ^1H NMR spectrum, there were five methoxy signals and two sets of *para*-substituted phenyl ring system [at δ_H 6.98 (2H, d, J = 8.8 Hz), 7.39 (2H, d, J = 8.8 Hz); and δ_H 7.02 (2H, d, J = 8.8 Hz), 7.42 (2H, d, J = 8.8 Hz)]. The HMBC spectrum showed correlations from H-2/H-6 to C-4 and C-1′; from H-3/H-5 to C-1; from H-2″/H-6″ to C-4′ and C-4″; from H-3″/H-5″ to C-1″ and C-4″. Moreover, two methoxy signals at δ_H 3.84 and 3.86 correlated respectively to C-4″ and C-4 in HMBC spectrum. Three remaining methoxy groups (δ_H 3.30, 3.48, 3.53) could now be placed in the central ring of terphenyl system and correlated to the carbons at δ_C 141.2, 143.8, and 148.0, respectively. In addition, NOESY spectrum showed cross-peak correlation between two methoxyl groups at δ_H 3.48 and 3.53, indicating these two methoxyls were at C-2′ and C-3′. Thus, compound **7** could be depicted as shown in Fig. 1 and given a trivial name fendleryl D.

Compound **10** was obtained as a pale brown solid. The ^{13}C NMR spectrum showed complex signals indicating an isomeric mixture, which was inseparable by various chromatographic means. After methylation with CH_3I/K_2CO_3 in dried acetone, the only given product was compound **16**, whose molecular formula was determined to be $C_{28}H_{40}O_8$ by the HRESIMS data, giving the sodium-adduct precursor ion peak at *m/z* 527.2623 $[M+Na]^+$. The ^{13}C NMR spectrum of the derivative (Table 2) gave twenty-eight signals, which was differentiated by DEPT-135 spectrum, consisting of five methyl, three methoxy, six methylene, two sp^3 methine, one aldehydic, and eleven quaternary carbons. The methine carbon resonating at δ_C 187.8 (C-11′) indicated an aldehyde. The IR spectrum also showed absorption of carbonyl ester at ν_{max} 1770 cm^{-1} and of aldehyde at ν_{max} 1736 cm^{-1}. The ^1H NMR spectrum (Table 3) showed five singlet methyl (resonating at δ_H 0.81, 0.83, 0.90, 1.28, and 2.34), three methoxy [resonating at δ_H 3.83, 3.96(1), and 3.96(3)], five sets

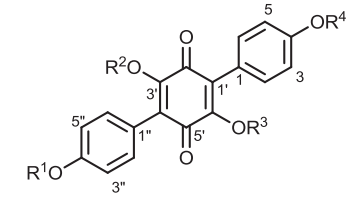

1 $R^1 = R^2 = H$, $R^3 = R^4 = CH_3$
2 $R^1 = R^2 = R^3 = H$, $R^4 = CH_3$
3 $R^1 = R^2 = R^4 = H$, $R^3 = CH_3$
4 $R^1 = R^3 = R^4 = CH_3$, $R^2 = H$
5 $R^1 = R^2 = R^3 = R^4 = H$

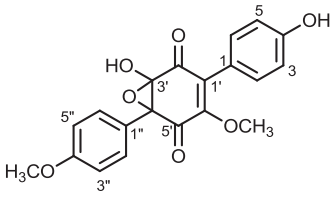

6

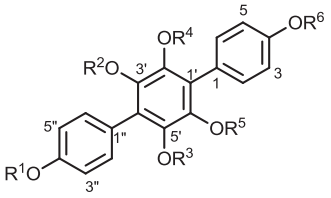

7 $R^1 = R^2 = R^3 = R^4 = R^6 = CH_3$, $R^5 = H$
8 $R^2 = R^3 = H$, $R^1 = R^4 = R^5 = R^6 = CH_3$
9 $R^1 = R^2 = R^3 = H$, $R^4 = R^5 = R^6 = CH_3$

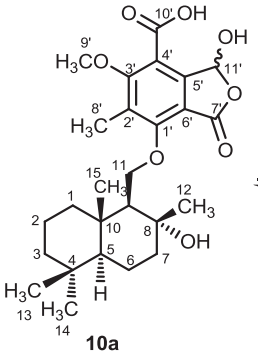

10a

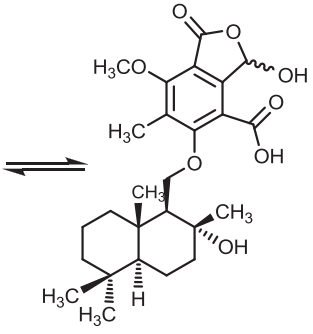

10b

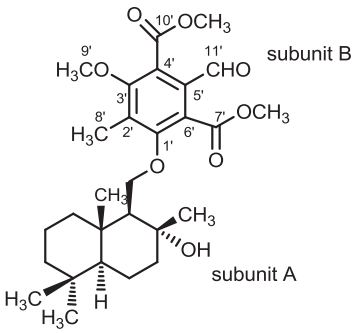

16

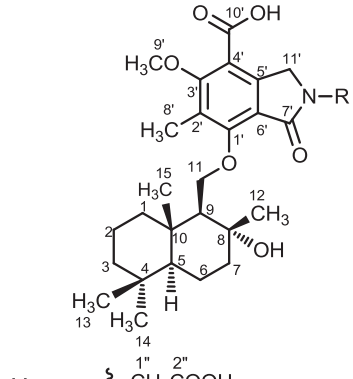

11 R = $-CH_2COOH$

12 R = $-CHCH_2CH_2COOH$ (COOH at 5")

13 R = $-CHCH_2CH_2COOCH_3$ (COOH at 5")

14 R = $-CHCH_2CH(CH_3)-CH_3$ (COOH at 5")

17 R = $-CHCH_2CH_2COOCH_3$ (COOCH$_3$ at 5")

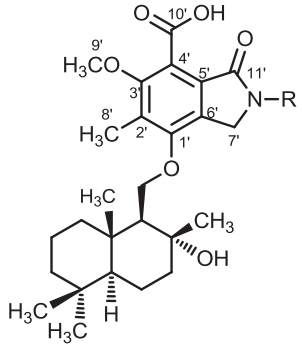

15 R = $-CHCH_2CH_2COOH$ (COOH at 5")

18 R = $-CHCH_2CH_2COOCH_3$ (COOCH$_3$ at 5")

Fig. 1. Chemical structures of secondary metabolites isolated from *Hypoxylon fendleri* BCC32408.

of methylene (resonating at δ_H 1.24/1.40, 1.42–1.52, 1.56/1.92, 1.69–1.73, and 1.65–1.69/1.73–1.76), one oxymethylene (resonating at δ_H 4.11/4.23), two sp^3 methine (resonating at δ_H 1.02 and 1.82), and an aldehydic proton (resonating at δ_H 9.86). The COSY spectrum showed three spin systems, which were H-1–H-3, H-5–H-7, and H-9/H_2-11. The HMBC spectrum showed correlations from H_3-13 and

H_3-14 to C-3, C-4, and C-5; from H_3-15 to C-1, C-5, C-9, and C-10; from H_2-11 to C-8, C-9 and C-10; from H_3-12 to C-7, C-8, and C-9; from H-9 to C-8, C-11, C-12, and C-15; from H_2-7 to C-5 and C-8; from H_3-8′ to C-1′, C-2′, and C-3′; from H_3-9′ to C-3′; from H-11′ (CHO) to C-4′, C-5′, and C-6′; from 10′–OCH_3 to C-10′; and from 7′–OCH_3 to C-7′. The spectral information disclosed two subunits, A and B (Fig. 1). Subunit A was drimane-type structure and its relative stereochemistry was indicated by the NOESY spectrum, showing cross-peak correlations from H-5 to H-9; H_2-11 to H_3-15 and H_3-12; and from H_3-15 to H_3-13. These subunits must be joined together with oxygen, confirming by the HRESIMS spectrum. Therefore, compound **16** could now be drawn as shown in Fig. 1. The positive specific rotation of compound **16** ($[\alpha]_D^{25}$+7.83 in MeOH or $[\alpha]_D^{25}$+23.68 in $CHCl_3$), resulting from the drimane part, confirmed its absolute configuration by comparing with that of synthesized (+)-driman-8,11-diol ($[\alpha]_D^{26}$+3.5, $CHCl_3$), one of the starting materials for (+)-ambrein (Fujiwara et al., 2006). Therefore, the absolute configuration at C-5, C-8, C-9, and C-10 of substructure A were assigned as *S*, *R*, *S*, and *S*, respectively.

Preparation of compound **16** suggested that compounds **10** existed in tautomeric forms, **10a** and **10b**. Moreover, each form had isomeric mixtures at C-11′, whose ^{13}C NMR spectrum indicated at least three oxymethine signals resonating at δ_C 95–97. As a result, the chemical transformation by using CH_3I provided a dicarboxylic aldehyde intermediate, proposed in Scheme 1. In addition, the phthalide-type lactone, a partial structure of compound **10**, was earlier reported an existence in a tautomeric mixture (Tsantrizos et al., 1992b). IR spectrum of compound **10** also confirmed the presence of carboxylic acid and a phthalide-type lactone by showing absorption peaks at ν_{max} 1721 and 1750 cm^{-1}, respectively. HRESIMS spectrum of compound **10** confirmed the molecular formula $C_{26}H_{36}O_8$ by showing the sodium-adduct precursor ion peak at *m/z* 499.2282 $[M+Na]^+$. Compound **10** is given a trivial name fendlerinine A.

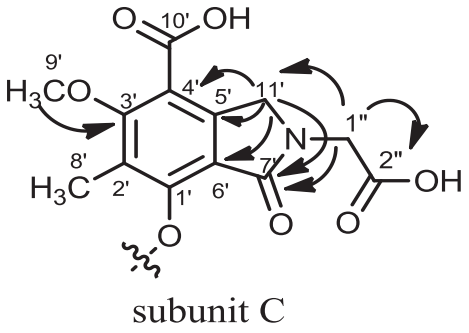

Fig. 2. Subunit C with selected HMBC correlations.

Compound **11** was obtained as a pale yellow solid and gave the sodium-adduct precursor ion peak at *m/z* 540.2560 $[M+Na]^+$, indicating a nitrogen atom present in the molecule. The molecular formula of $C_{28}H_{39}NO_8$ was revealed and indicated ten degrees of unsaturation. The ^{13}C NMR spectrum showed twenty-eight carbons, consisting of five methyl, one methoxy, eight methylene, two sp^3 methine, three sp^3 quaternary, and nine sp^2 quaternary carbons. The ^{1}H NMR spectrum displayed a pattern of drimane sesquiterpene moiety, similar to that of compound **10**. The drimane part (subunit A) was assured by 2D (COSY, HSQC, HMBC, and NOESY) spectral analyses. The rest of the molecule was also determined by HMBC spectral data, showing the correlations from H_3-8′ to C-1′, C-2′, and C-3′; from H_3-9′ (OCH_3) to C-3′; from H_2-11′ to C-4′, C-5′, C-6′, and C-7′; and from H-1″ to C-7′, C-11′, and C-2″. Moreover, IR spectrum showed the presence of acid by displaying broad absorption peak at 3600–3000 cm^{-1}. The spectroscopic information revealed the substructure C (Fig. 2), which was the phthalimidine structure of duricaulic acid isolated from *Aspergillus duricaulis* (Achenbach et al., 1985), and implied that these two

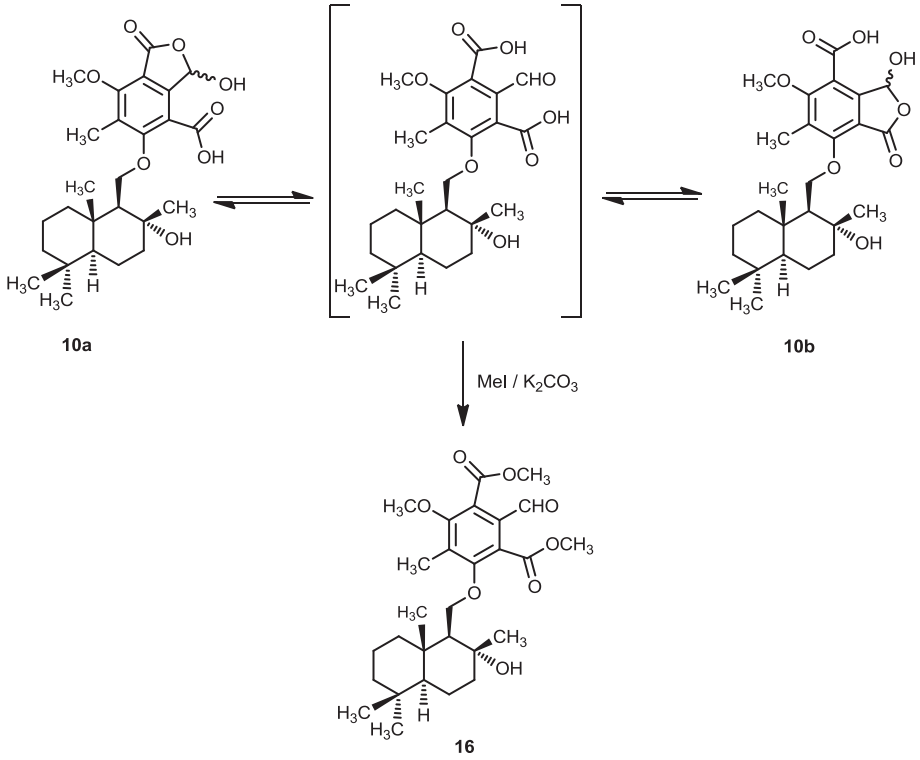

Scheme 1. The chemical transformation of compound **10.**

subunits (A and C) must be linked with oxygen. The same correlations provided by the NOESY spectrum as that of compound **10** and the positive optical rotation ($[\alpha]_D$ +21.71 in MeOH) indicated the same absolute configuration of drimane moiety. Furthermore, compound **11** should derive from the same biosynthesis as that of compound **10**. The evidences led to the chemical structure of compound **11** (Fig. 1). Fendlerinine B is a trivial name given for compound **11**.

The ^{1}H NMR spectrum of compound **12** was similar to that of compound **11**, except that the presence of non-equivalent methylene (resonating at δ_H 4.66 and 4.77), a low field shift of the methine (resonating at δ_H 5.06), and additional multiplet methylene (resonating at δ_H 2.40–2.47) and the absence of two singlet methylene signals at H_2-1″ and H_2-11′, observed for compound **11**. The ^{13}C NMR spectrum showed four additional signals (one sp^3 methine, two methylene, and one quaternary carbons) and the absence of one methylene attached to nitrogen. The spectroscopic information suggested a different alkyl substituent in the molecule (Fig. 1). The COSY spectrum showed cross-peak correlations from the methine at δ_H 5.06 (H-1″) to δ_H 2.20–2.32 and 2.40–2.47 (H_2-2″ and H_2-3″) and the HMBC spectrum showed correlations from a non-equivalent methylene at δ_H 4.66 and 4.77 (H_2-11′) to C-4′, C-5′, C-6′, and C-7′; from H-1″ to C-7′ and C-5″; from H_2-2″ to C-1″and C-4″; and from H_2-3″ to C-1″, C-2″, and C-4″. The spectral data indicated “R” group as “glutamine” unit, confirmed by the HRESIMS data which gave the sodium-adduct precursor ion peak at *m/z* 612.2770 $[M+Na]^+$. Fendlerinine C is a trivial name given for compound **12**. In addition, the attempts to cleave drimane and phthalimidine units by using NaI/Zn (Fujimoto and Tatsuno, 1976) and to reduce C-N bond by using catalytic hydrogenolysis (Martinelli et al., 1990) were unsuccessful. Therefore, the configuration at C-1″ cannot be determined at this stage.

Compound **13** was obtained as a pale yellow solid and its ^{1}H NMR spectrum was almost identical to that of compound **12**, apart from the additional methoxy group at δ_H 3.56. The HRESIMS data of **13** showed 14 mass units higher than that of compound **12**, confirming an extra methoxy group. The HMBC spectrum showed that the additional methoxy group was attached to C-4″, to which H_2-2″ and H_2-3″ were also correlated. Unfortunately the configuration at C-1″ of **13** cannot be identified. Thus, compound **13** was elucidated as shown in Fig. 1 and fendlerinine D is given as its trivial name. In addition, compound **17** could be obtained from the reaction of both compounds **12** and **13** with diazomethane in dioxane. The ^{1}H, ^{13}C NMR, HRESIMS spectra, and the specific rotations of compound **17**, obtained from both compounds, were identical. The ^{1}H and ^{13}C NMR spectral data of the methylated compound (**17**) were also provided in Tables 2 and 3.

The ^{1}H NMR spectrum of compound **14** was similar to that of compound **13**, apart from two additional doublet methyl groups (resonating at δ_H 0.96 and 0.97) and the absence of one methylene (resonating at δ_H 2.40–2.50, H_2-3″). Moreover, the ^{13}C NMR spectrum showed three additional signals, which were two methyl (at δ_C 20.6 and 22.6) and one sp^3 methine (at δ_C 24.6) carbons, and the absence of one carbonyl of acid. The spectroscopic evidence suggested the replacement of “glutamine” unit in compound **13** with “leucine” unit without determination of the configuration at C-1″. The chemical structure was reassured by 2D NMR spectral data, including COSY, HMQC, HMBC, and NOESY together with HRESIMS data, giving the sodium-adduct precursor ion peak at *m/z* 596.3197 $[M+Na]^+$. Fendlerinine E is a trivial name given for compound **14**.

Compound **15** was obtained as a pale brown solid and HRESIMS data indicated the same molecular formula as that of compound **12**. Compound **15** was more polar than compound **12** in the same solvent system. The ^{1}H NMR spectrum of compound **15** was almost identical to that of compound **12**, except an upfield shift of methyl signal at H_3-12 (δ_H 1.11), a downfield shift of the methyl at H_3-15 (δ_H 0.96), and a downfield shift of one non-equivalent methylene proton (δ_H 4.88). The HMBC spectrum showed key correlations from H_2-7′ to C-1′, C-6′, and C-11′; H_3-8′ to C-1′, C-2′, and C-3′; H_3-9′ (OCH_3) to C-3′; from H-1″ to C-7′ and C-5″; from H_2-2″ and H_2-3″ to C-4″. Moreover, the NOESY spectrum showed additional cross-peak correlations from H_2-11 to H_3-8′ and H_2-7′. Thus, the chemical structure of compound **15** could be depicted without the configuration at C-1″ as shown in Fig. 1. Due to the lack of conjugation to a carbonyl at C-11′ in compound **15** caused a slight hypsochromic shift in UV–Vis spectrum (λ_{max} 222), compared with that of compound **12** observed at λ_{max} 226. Compound **15** was given a trivial name fendlerinine E. Reaction with diazomethane afforded compound **18**, which was more polar than compound **17** in the same solvent system. Also, the ^{1}H and ^{13}C NMR spectral data of the methylated compound (**18**) were provided in Tables 2 and 3.

The ^{1}H and ^{13}C NMR spectral data of the known compounds including 2-*O*-methylatromentin (**3**), atromentin (**5**), rickenyls C (**8**), D (**9**), and E (**4**), (+)-ramulosin were compared with those reported in the literature (Islam et al., 2007; Kuhnert et al., 2015a; Ye et al., 2010). Pigments **3** and **5** were commonly found in the fruit bodies of the edible mushrooms *Thelephora gunbajun* (Hu et al., 2001) and *T. Aurantiotincta* (Ngoc Quang et al., 2003; Quang et al., 2003) and rickenyls C (**8**), D (**9**), and E (**4**) were earlier isolated from the fungus *H. Rickii* (Kuhnert et al., 2015a). (+)-Ramulosin was originally isolated from the fungus *Pestolatia ramulosa* (Stodola et al., 1964) and later from *Truncatella hartigii*, *H. Howeianum* (Turner and Aldridge, 1983), *Botrytis* sp. (Stierle et al., 1998), and the endophytic *Pezicula* sp. (Wang et al., 2014), respectively.

Terphenyls are described for compounds having a chain of three benzene rings and classified into three types depending on the substitution position (either *ortho*-, *meta*-, or *para*-) of the terminal rings on the middle aromatic ring. Terphenyls and terphenylquinones have frequently isolated from various sources and had a broad range of biological activity such as anti-insectan and antibacterial activities of 3,3″-dihydroxy-6′-desmethylterphenyllin isolated from the sclerotia of *Penicillium raistrickii* (Belofsky et al., 1998), prolyl oligopeptidase (POP) inhibitory activity of kanapcin-12 isolated from the mushroom *Polyozellus multiplex* (Lee et al., 2000), DPPH radical scavenging effect of ganbajunin C and aurantiotinin A isolated from three mushrooms *Thelephora ganbajun, T. aurantiotincta,* and *Boletopsis grisea* (Liu et al., 2004), antimicrobial and phosphodiesterase (PDE) inhibitory activities of BTH-II0204-207:A isolated from the fungus in the order Chaetothyiales (MSX 47445) (El-Elimat et al., 2013), and anti-*Candida albicans* activity of flovicolin C isolated from the endolichenic fungus *Floricola striata* (Li et al., 2016).

Drimane sesquiterpenes have mostly been isolated from the plants in the family Cannellaceae and Polygonaceae, from the liverwort in the genus *Porella*, and the marine sponges of the genera *Dysidea*, *Doriopsilla*, and *Dendrodoris* (Jansen and de Groot, 2004). Fungi that produced drimanes included *Aspergillus* spp., *Kuehneromyces* sp., *Trichopezizella barbata*, *Mniopetalum* sp., *Lactarius uvidus, Cryptoporous volvatus*, *Penicillium* spp., *Polyporus* spp., the endophytic *Pestalotiopsis* spp. etc (Jansen and de Groot, 2004). They also exhibited a wide range of biological activities such as antifeedant, anti-insecticidal, antimicrobial, piscicidal, molluscicidal, anthelmintal, phytotoxic, cytotoxic activities, and plant-growth regulation (Jansen and de Groot, 2004). Due to the limitation of its occurrence in nature, drimane sesquiterpenoids can also be used as chemosystematic markers.

Phthalide derivatives were isolated from a few fungi with broad biological activity such as herbicidal activity against *Corzvolvulus arvensis* (field bindweed) of convolvulanic acids A and B isolated from *Phomopsis convolvulus* (Tsantrizos et al., 1992a) and moderate

antifungal activity against *Microsporum gypseum* SH-MU-4 and *Cryptococcus neoformans* of microsphaerophthalides A and E isolated from *Microsphaeropsis arundinis* PSU-G18 (Sommart et al., 2012). Apart from duricaulic acid (Achenbach et al., 1985), compounds having related isoindolinone (phthalimidine) in the molecule were reported from several fungi including selective inhibition for enzyme causing obesity in human of sterenins A and C (Hu et al., 2000; Shinohara et al., 1996) isolated from the basidiomycetes *Stereum* sp. SANK 21205 (Ito-Kobayashi et al., 2008), human leukocyte elastase (HLE) inhibition of mariline A from the sponge-associated fungus *Stachylidium* sp. (Almeida et al., 2012), and anti-HIV-1 activity of chartarutines B, G, and H from the fungus *S. chartarum* (Li et al., 2014).

2.2. Biological activity

All compounds, except compounds **2**, **3**, **11**, **17**, and **18**, were subjected for antimicrobial test including antimalarial, antifungal (against *C. albicans*), antibacterial (against *B. cereus*) activities and for cytotoxicity against cancerous (KB, MCF-7, NCI-H187) and non-cancerous (Vero) cells. However, compounds **1**, **4**, **6**, **12**–**15** were not tested for antifungal activity due to inadequate material. All tested compounds were inactive for antimicrobial activity at maximum test concentrations (10 μg/mL for antimalarial assay, 25 μg/mL for antibacterial assay, and 50 μg/mL for antifungal and cytotoxicity assays). Compounds **1**, **4**, and **16** displayed weak cytotoxicity against NCI-H187 (IC_{50} 48.10, 41.97, and 11.77 μg/mL, respectively) and Vero (IC_{50} 48.96, 49.09, and 35.25 μg/mL, respectively) cells. Significantly, this is the first report of drimane sesquiterpenes linked to either the phthalide lactone or isoindolinones, produced by the wood fungus *H. fendleri*. Although, all tested compounds were almost inactive to our biological assays, the biological results suggested that phthalide lactone or isoindolinone moiety may have a major effect in the biological activity. However, (+)-driman-8,11-diol (fendlerinines subunit) has not yet been reported of biological activity.

In addition, atromentin (**5**) was reported to inhibit the FabK (the enol-acetyl carrier protein reductase of *Streptococcus pneumoniae*) with IC_{50} value of 0.24 μM but did not inhibit the FabI (the enoyl-ACP reductase of either *Escherichia coli* or *Staphylococcus aureus*) at 200 μM, (Zheng et al., 2006) while rickenyls C – E (**8**–**9** and **4**) were also inactive for antibacterial [against several strains such as *Escherichia coli* DSM-1116, *E. coli* (TolC-deficient strain), *Pseudomonas aeruginosa* str. PA14, *Chromobacterium violaceum* DSM-30191, *Staphylococcus aureus* subsp. *aureus*, *B. subtilis* DSM-10, *Micrococcus luteus* SSM-1790, *Mycobacterium smegmatis* str. mc^2155 (ATCC 700084)] and for antifungal (against *Wickerhamomyces anomalus* DSM-6766, *C. albicans* DSM-1665 and *Mucor hiemalis* DSM-2656) activities (Kuhnert et al., 2015a). Compounds **4** and **5** also showed moderate antioxidant activity by measuring the relative amount of ROS in a present of menadione in U-2 OS cells (Kuhnert et al., 2015a).

3. Conclusion

Ten new compounds including three terphenylquinones (fendleryls A – C), one terphenyl (fendleryl D), and six novel drimane – phthalide-type lactone/isoindolinone derivatives (fendlerinines A – F) along with seven known compounds (2-*O*-methylatromentin, rickenyl E, atromentin, rickenyls C – D, (+)-ramulosin, and *O*-hydroxyphenyl acetic acid) were isolated from of *H. fendleri* BCC32408. Fendlerinines A – F might be specific to the species and could be used as chemotaxonomic character, while terphenyl derivatives might be distributed in the sect. *Hypoxylon* and suggested a close relationship between the two species (*rickii and fendleri*) in this section. Unfortunately, these compounds were inactive for antimicrobial activity and had no cytotoxic activity, except that compounds **1**, **4**, and **16** exhibited weak cytotoxicity against NCI-H187 and Vero cell lines.

4. Experimental

4.1. General experimental procedures

Melting points were determined on a melting point M-565 apparatus from Buchi. The optical rotations were measured on a JASCO P-1030 digital polarimeter. UV spectra were obtained in MeOH using a Spekol 1200 instrument, Analytic Jena. NMR experiments were recorded on a Bruker Avance 500 NMR spectrometer or Bruker Avance III 400. ^1H and ^{13}C chemical shifts were reported in ppm relative to an added internal standard such as $CDCl_3$ (δ_H 7.26, δ_C 77.2) or acetone-d_6 (δ_H 2.05, δ_C 29.3), or DMSO-d_6 (δ_H 2.50, δ_C 40.2). HRESIMS data were carried out on a Bruker MicrOTOF mass spectrometer. HPLC was performed on a Dionex – Ultimate 3000 series equipped with a binary pump, an autosampler, and diode array detector. A Sunfire C18 column from Waters (size 19 mm × 250 mm, particle size 10 μm at a flow rate 15 mL/min) and a Sunfire C18 column from Waters (size 19 mm × 150 mm, particle size 5 μm at a flow rate 9 mL/min) were used for preparative HPLC and semi-preparative HPLC, respectively.

4.2. Fungal material

The fungus was isolated from unidentified wood sample collected at Phu Sithan Wildlife Sanctuary, Kalasin province, Thailand. By the morphological data, the fungus was earlier identified in the genus *Hypoxylon* sp. and in order to affirm the genus and to identify its species, the analyses of the partial nuclear large subunits ribosomal DNA (nc28S), 5.8S-ITS rDNA, and β-tubulin gene of this fungus was conducted. The 28S rDNA (1298 bp; GenBank accession number KY173349) confirmed that the fungus was in the genus *Hypoxylon* (Sub-phylum Pezizomycotina; Class Sordariomycetes; Sub-class Xylariomycetidae, Order Xylariales and Family Xylariaceae) based on the data from NCBI, Mycobank, and CBS-KNAW Fungal Biodiversity Center. The ITS rDNA (586 bp; GenBank accession number KY173350) showed 99% similarity with *H. fendleri* (FM209440) and the β-tubulin sequence (397 bp; GenBank accession number KY173351) gave 96–97% similarity with *H. fendleri* (AY951718 and KF300547). The fungus was, therefore, identified on the basis of morphological and genetic evidences as *Hypoxylon fendleri* (Ascomycota; Pezizomycotina; Sordariomycetes; Xylariomycetidae; Xylariales; Xylariaceae), registered as BCC32408, and deposited at BIOTEC Culture Collection (BCC) at National Center for Genetic Engineering and Biotechnology (BIOTEC), Thailand.

4.3. Fermentation, extraction, and isolation

The fungus BCC32408 was grown on potato dextrose agar (PDA) plates at 25 °C and the cultures were cut into pieces. The pieces were transferred into 10 × 250 mL Erlenmeyer flasks, each containing 25 mL of potato dextrose broth (PDB). The cultures were grown on rotary shakers (200 rpm) at 25 °C for 5 days. Then they were transferred to 10 × 1 L Erlenmeyer flasks, each containing 250 mL of PDB and cultivated at 25 °C for 5 days on a rotary shaker (200 rpm). Every 25 mL of the seed cultures were transferred to 80 × 1 L Erlenmeyer flasks, each containing 250 mL of MEB medium (comprised (w/v): 0.6% malt extract, 0.18% maltose, 0.6% dextrose, 0.12% yeast extract in distilled water). The cultures were grown on static condition at 25 °C for 20 days. The cell was separated by simple filtration and the filtrate was extracted three times with

Table 1
The ^{13}C NMR and ^{1}H NMR assignments of compounds **1**, **2**, **6**, and **7**.

Position	1[a] in DMSO-d_6		2[b] in DMSO-d_6		6 [a] in DMSO-d_6		7[a] in acetone-d_6	
	δ_C, type	δ_H, mult. (*J* in Hz)	δ_C, type	δ_H, mult. (*J* in Hz)	δ_C, type	δ_H, mult. (*J* in Hz)	δ_C, type	δ_H, mult. (*J* in Hz)
1	123.0, C	–	124.0, C	–	120.8, C	–	126.2, C	–
2, 6	132.4, CH	7.27, d (8.6)	132.3, CH	7.35, d (8.7)	131.2, CH	8.06, d (8.8)	131.7, CH	7.42, d (8.8)
3, 5	113.9, CH	6.99, d (8.6)	113.7, CH	6.95, d (8.7)	116.0, CH	6.87, d (8.8)	113.4, CH	7.02, d (8.8)
4	159.8, C	–	159.0, C	–	159.2, C	–	159.2, C	–
1′	125.6, C	–	115.1, C	–	128.8, C	–	128.2, C	–
2′	183.4[c], C	–	169.0, C	–	193.9[d], C	–	148.0[e], C	–
3′	152.5, C	–	163.7, C	–	116.0, C	–	143.8[e], C	–
4′	118.3,C	–	115.6,C	–	66.1,C	–	122.4,C	–
5′	184.1[c], C	–	169.0, C	–	193.8[d], C	–	141.2, C	–
6′	156.1, C	–	163.7, C	–	168.0, C	–	144.0, C	–
1″	121.9, C	–	122.1, C	–	125.4, C	–	126.4, C	–
2″, 6″	132.6, CH	7.21, d (8.5)	132.3, CH	7.22, d (8.5)	129.9, CH	7.26, d (8.9)	132.0, CH	7.39, d (8.8)
3″, 5″	115.1, CH	6.78, d (8.5)	115.1, CH	6.77, d (8.5)	114.6, CH	6.95, d (8.9)	113.2, CH	6.98, d (8.8)
4″	157.5, C	–	157.3, C	–	159.8, C	–	159.0, C	–
4-OCH_3	51.8, CH_3	3.80, s	55.8, CH_3	3.78, s	–	–	54.8, CH_3	3.86, s
2′−OCH_3	–	–	–	–	54.0, CH_3	3.68, s	60.3, CH_3	3.48, s
3′−OCH_3	–	–	–	–	–	–	60.1, CH_3	3.53, s
5′−OCH_3	–	–	–	–	–	–	60.0, CH_3	3.30, s
6′−OCH_3	62.0, CH_3	3.80, s	–	–	–	–	–	–
4″−OCH_3	–	–	–	–	55.9, CH_3	3.74, s	54.8, CH_3	3.84, s

[a]Recorded at 400 MHz for ^{1}H NMR and 100 MHz for ^{13}C NMR.
[b]Recorded at 500 MHz for ^{1}H NMR and 125 MHz for ^{13}C NMR.
[c,d,e]Exchangeable.

equal volume of EtOAc. The EtOAc layers were combined, dried (Na_2SO_4), and evaporated to dryness to yield a brown gum (2.20 g).

The gum (2.20 g) was passed through a Sephadex column (4.5 cm × 40 cm), eluted with MeOH, to give 11 main fractions (F1 − F11). Three fractions including F3, F9, and F11 yielded compounds **7** (0.21 g), **2** (8.1 mg), and **5** (22.0 mg), respectively. The first fraction (F1, 0.91 g) was further purified by preparative HPLC, using a 35 min linear gradient of acetonitrile: water (30:70–80:20) at a flow rate of 15 mL/min to yield 4 subfractions (F1-1 − F1-4). Subfractions F1-1, F1-2, and F1-4 afforded compounds **15** (25.4 mg), **12** (23.7 mg), and **14** (10.0 mg), respectively. Subfraction F1-3 (25.5 mg) was further purified by preparative HPLC, using a 35 min linear gradient of acetonitrile: water (30:70–80:20) at a flow rate of 15 mL/min to yield compound **13** (12.0 mg). The second fraction (F2, 0.35 g) was subjected to preparative HPLC, using a 35 min linear gradient of acetonitrile: water (30:70–80:20) at a flow rate of 15 mL/min to afford (+)-ramulosin (34.7 mg), compounds **12** (32.0 mg), **11** (3.5 mg), and **10** (38.7 mg), respectively. The fourth (F4, 94.2 mg) and fifth (F5, 0.24 g) fractions were further purified by preparative HPLC, using a 20 min linear gradient of acetonitrile: water (5:95–65:35) at a flow rate of 15 mL/min to afford *O*-hydroxyphenyl acetic acid (8.7 mg), compounds **8** (9.2 mg) and **3** (10.4 mg), **6** (28.0 mg), and **1** (33.2 mg), respectively. The sixth fraction (F6, 0.10 g) was subjected to preparative HPLC, using a 20 min linear gradient acetonitrile: water (10:90–55:45) at a flow rate of 15 mL/min to obtain compounds **9** (7.2 mg) and **4** (14.8 mg), respectively. The seventh fraction (F7, 36.5 mg) was purified by preparative HPLC, using a 20 min linear gradient acetonitrile: water (5:95–55:45) at a flow rate of 15 mL/min to furnish compound **3** (15.7 mg). The eighth (F8, 18.0 mg) and tenth (F10, 12.0 mg) fractions were further purified by semi-preparative HPLC, using a 20 min linear gradient acetonitrile: water (5:95–60:40) at a flow rate of 9 mL/min to obtain compounds **2** (6.8 mg) and **5** (5.7 mg).

4.3.1. Fendleryl A (**1**)

A brown solid; UVλ_{max}^{MeOH} (nm) (log ε) 218 (4.37), 266 (4.53) nm; FTIR (ATR) ν_{max} 3322 (br), 1700, 1643, 1607, 1512, 1442, 1365, 1317, 1304, 1291, 1275, 1249, 1177, 1110, 1022, 833, 762, 751 cm^{-1}; ^{1}H (DMSO-d_6, 400 MHz) and ^{13}C NMR data (DMSO-d_6, 100 MHz), see Table 1; HRESIMS *m/z* 375.0837 $[M+Na]^+$ (calcd for $C_{20}H_{16}O_6Na$, 375.0839).

4.3.2. Fendleryl B (**2**)

A brown solid; UV λ_{max}^{MeOH} (nm) (log ε) 214 (4.15), 267 (4.40) nm; FTIR (ATR) ν_{max} 3313, 1606, 1513, 1319, 1308, 1275, 1258, 1177, 998, 830, 763, cm^{-1}; ^{1}H (DMSO-d_6, 500 MHz) and ^{13}C NMR data (DMSO-d_6, 125 MHz), see Table 1; HRESIMS *m/z* 337.0720 $[M-H]^-$ (calcd for $C_{19}H_{13}O_6$, 337.0718).

4.3.3. Fendleryl C (**6**)

A yellow solid, mp 129–131 °C; UV λ_{max}^{MeOH} (nm) (log ε) 217 (3.89), 228 (3.91), 267 (4.03), 370 (3.79) nm; FTIR (ATR) ν_{max} 3281 (br), 1750, 1724, 1681, 1606, 1513, 1379, 1251, 1182, 1157, 1017, 833, 759 cm^{-1}; ^{1}H (DMSO-d_6, 400 MHz) and ^{13}C NMR data (DMSO-d_6, 100 MHz), see Table 1; HRESIMS *m/z* 369.0965 $[M+H]^+$ (calcd for $C_{20}H_{17}O_7$, 369.0969).

4.3.4. Fendleryl D (**7**)

A brown solid; UV λ_{max}^{MeOH} (nm) (log ε) 218 (4.41), 229 (4.43), 267 (4.43) nm; FTIR (ATR) ν_{max} 3421 (br), 2932, 2837, 1609, 1519, 1458, 1420, 1395, 1287, 1245, 1176, 1115, 1048, 1004, 974, 829, 758 cm^{-1}; ^{1}H (acetone-d_6, 400 MHz) and ^{13}C NMR data (acetone-d_6, 100 MHz), see Table 1; HRESIMS *m/z* 397.1644 $[M+H]^+$ (calcd for $C_{23}H_{25}O_6$, 397.1646).

4.3.5. Fendlerinine A (**10**)

A pale brown solid; HRESIMS *m/z* 499.2282 $[M+Na]^+$ (calcd for $C_{26}H_{36}O_8Na$, 499.2302).

4.3.6. Fendlerinine B (**11**)

A pale yellow solid; $[\alpha]_D^{25}$ +21.71 (c 0.175, MeOH); UV λ_{max}^{MeOH} (nm) (log ε) 226 (4.15), 256 (3.94), 292 (3.45) nm; FTIR (ATR) ν_{max} 3000–3600 (br), 2925, 1675, 1589, 1461, 1390, 1305, 1219, 1125 cm^{-1}; ^{1}H (acetone-d_6, 400 MHz) and ^{13}C NMR data (acetone-d_6, 100 MHz), see Table 2; HRESIMS *m/z* 540.2560 $[M+Na]^+$ (calcd for $C_{28}H_{39}NO_8Na$, 540.2568).

Table 2
^{13}C NMR assignments of fendlerinines B – F (**11**–**15**) and their derivatives (**16**–**18**) in acetone-d_6.

Pos.	11[b]	12[a]	13[a]	14[b]	15[b]	16 in $CDCl_3$[a]	17[b]	18[b]
	δ_C, type	δ_C, type	δ_C, type	δ_C, type	δ_C, type	δ_C, type	δ_C, type	δ_C, type
1	40.6, CH_2	40.0, CH_2	40.0, CH_2	39.8, CH_2	41.1, CH_2	40.4, CH_2	41.2, CH_2	41.1, CH_2
2	19.2, CH_2	19.4, CH_2	18.6, CH_2	18.4, CH_2	19.1, CH_2	18.8, CH_2	19.5, CH_2	21.1, CH_2
3	42.7, CH_2	42.1, CH_2	42.0, CH_2	41.8, CH_2	42.6, CH_2	41.9, CH_2	43.1, CH_2	42.6, CH_2
4	33.9, C	32.3, C	33.3, C	33.0, C	33.8, C	33.5, C	34.1, C	33.8, C
5	56.8, CH	56.2, CH	56.2, CH	56.0, CH	56.6, CH	56.1, CH	57.2, CH	56.6, CH
6	20.9, CH_2	20.2, CH_2	20.2, CH_2	20.0, CH_2	21.1, CH_2	20.3, CH_2	21.3, CH_2	19.1, CH_2
7	44.3, CH_2	43.6, CH_2	43.7, CH_2	43.5, CH_2	45.0, CH_2	43.8, CH_2	44.9, CH_2	45.1, CH_2
8	72.2, C	71.8, C	71.7, C	71.4, C	72.1, C	73.0, C	72.6, C	72.1, C
9	63.2, CH	62.5, CH	62.5, CH	62.2, CH	63.3 CH	60.6, CH	63.5, CH	63.3, CH
10	38.8, C	38.1, C	38.2, C	37.9, C	38.7, C	38.1, C	39.2, C	38.7, C
11	73.8, CH_2	73.2, CH_2	73.1, CH_2	73.0, CH_2	71.3, CH_2	74.7, CH_2	74.3, CH_2	71.2, CH_2
12	25.4, CH_3	24.8, CH_3	24.8, CH_3	24.6, CH_3	25.0, CH_3	24.9, CH_3	25.7, CH_3	25.0, CH_3
13	21.8, CH_3	21.2, CH_3	21.2, CH_3	21.0, CH_3	21.9, CH_3	21.8, CH_3	22.1, CH_3	21.9, CH_3
14	33.8, CH_3	33.2, CH_3	33.8, CH_3	33.0, CH_3	33.8, CH_3	33.8, CH_3	34.0, CH_3	33.8, CH_3
15	16.4, CH_3	16.2, CH_3	16.2, CH_3	15.9, CH_3	16.5, CH_3	16.3, CH_3	17.0, CH_3	16.4, CH_3
1′	159.9, C	159.2, C	152.2, C	158.7, C	155.6, C	157.2, C	160.2, C	155.6, C
2′	126.9, C	126.3, C	126.3, C	126.0, C	128.8, C	133.6, C	127.2, C	128.7[e],C
3′	163.6, C	163.0, C	163.0, C	162.6, C	158.2, C	153.2, C	164.0, C	157.0, C
4′	116.6, C	116.1, C	116.1, C	116.5, C	129.4[c], C	126.1[d], C	117.1, C	120.7, C
5′	146.0, C	145.4, C	145.3, C	144.9, C	130.5, C	130.3, C	145.5, C	129.2, C
6′	120.8, C	120.1, C	120.1, C	120.0, C	129.5[c], C	126.4[d], C	120.5, C	128.8[e], C
7′	167.1, C	167.1, C	167.0, C	166.6, C	46.5, CH_2	166.6, C	167.7, C	43.4, CH_2
8′	10.1, CH_3	9.5, CH_3	9.5, CH_3	9.2, CH_3	10.7, CH_3	11.1, CH_3	10.3, CH_3	10.6, CH_3
9′	62.4, CH_3	61.8, CH_3	61.8, CH_3	61.5, CH_3	62.3, CH_3	62.5, CH_3	62.4, CH_3	62.3, CH_3
10′	165.9, C	165.4, C	165.4, C	165.5, C	166.4, C	167.2, C	166.2, C	167.0[f], C
11′	52.0, CH_2	48.2, CH_2	48.1, CH_2	47.7, CH_2	168.5, C	187.8, CH	48.8, CH_2	167.2[f], C
1″	43.8, CH_2	54.4, CH	53.8, CH	51.9, CH	54.3, CH		54.7, CH	54.1, CH
2″	170.6, C	24.9, CH_2	24.9, CH_2	38.2, CH_2	25.4, CH_2		25.9, CH_2	25.4, CH_2
3″		30.3, CH_2	30.5, CH_2	24.6, CH	30.8, CH_2		31.3, CH_2	30.9, CH_2
4″		173.2, C	172.7, C	22.6, CH_3	173.8, C		173.3, C	173.3, C
5″		171.1, C	171.6, C	172.6, C	172.3, C		171.9, C	171.7, C
3″–CH_3				20.6, CH_3				
4″–OCH_3			51.1, CH_3	51.1, CH_3			51.8, CH_3	51.7, CH_3
5″–OCH_3							52.7, CH_3	52.6, CH_3
7′–OCH_3						53.5, CH_3		
10′–OCH_3						53.2, CH_3	52.4, CH_3	52.5, CH_3

[a] Recorded at 100 MHz for ^{13}C NMR.
[b] Recorded at 125 MHz for ^{13}C NMR.
[c, d, e, f] Exchangeable.

4.3.7. Fendlerinine C (**12**)

A pale brown solid, mp 151–153 °C; $[\alpha]_D^{26}$ +9.14 (c 0.230, MeOH); UV λ_{max}^{MeOH} (nm) (log ε) 226 (4.21), 257 (4.00), 295 (3.41) nm; FTIR (ATR) ν_{max} 3600-3000 (br), 2930, 1709, 1673, 1589, 1446, 1390, 1365, 1299, 1221, 1192, 1123 cm^{-1}; ^{1}H (acetone-d_6, 400 MHz) and ^{13}C NMR data (acetone-d_6, 100 MHz), see Table 2; HRESIMS *m/z* 612.2770 $[M+Na]^+$ (calcd for $C_{31}H_{43}NO_{10}Na$, 612.2779).

4.3.8. Fendlerinine D (**13**)

A pale yellow solid, $[\alpha]_D^{26}$ +9.33 (c 0.575, MeOH); UV λ_{max}^{MeOH} (nm) (log ε) 226 (4.08), 256 (3.88), 294 (3.32) nm; FTIR (ATR) ν_{max} 3000–3600 (br), 2937, 1675, 1589, 1449, 1391, 1300, 1188, 1124 cm^{-1}; ^{1}H (acetone-d_6, 400 MHz) and ^{13}C NMR data (acetone-d_6, 100 MHz), see Table 2; HRESIMS *m/z* 626.2931 $[M+Na]^+$ (calcd for $C_{32}H_{45}NO_{10}Na$, 626.2936).

4.3.9. Fendlerinine E (**14**)

A pale yellow solid, $[\alpha]_D^{26}$ +10.84 (c 0.500, MeOH); UV λ_{max}^{MeOH} (nm) (log ε) 226 (4.26), 263 (4.17) nm; FTIR (ATR) ν_{max} 3500-3000 (br), 1710, 1672, 1589, 1454, 1389, 1367, 1300, 1218, 1190, 1117 cm^{-1}; ^{1}H (acetone-d_6, 500 MHz) and ^{13}C NMR data (acetone-d_6, 125 MHz), see Table 2; HRESIMS *m/z* 596.3197 $[M+Na]^+$ (calcd for $C_{32}H_{47}NO_8Na$, 596.3194).

4.3.10. Fendlerinine F (**15**)

A pale brown solid, $[\alpha]_D^{26}$ +2.48 (c 0.240, MeOH); UV λ_{max}^{MeOH} (nm) (log ε) 222 (3.99), 256 (3.82), 292 (3.39) nm; FTIR (ATR) ν_{max} 3600-300 (br), 2925, 2854, 1666, 1597, 1462, 1392, 1305, 1262, 1113 cm^{-1}; ^{1}H (acetone-d_6, 500 MHz) and ^{13}C NMR data (acetone-d_6, 125 MHz), see Table 2; HRESIMS *m/z* 612.2773 $[M+Na]^+$ (calcd for $C_{31}H_{43}NO_{10}Na$, 612.2779).

4.3.11. Compound **16**

A pale yellow solid, $[\alpha]_D^{26}$ +7.83 (c 0.115, MeOH); UV λ_{max}^{MeOH} (nm) (log ε) 230 (4.25), 256 (3.85), 294 (3.34) nm; FTIR (ATR) ν_{max} 3461, 2933, 1770, 1736, 1603, 1443, 1391, 1365, 1342, 1312, 1214, 1130, 1097, 1065, 952 cm^{-1}; ^{1}H ($CDCl_3$, 400 MHz) and ^{13}C NMR data ($CDCl_3$, 100 MHz), see Table 3; HRESIMS *m/z* 527.2623 $[M+Na]^+$ (calcd for $C_{28}H_{40}O_8Na$, 527.2615).

4.3.12. Compound **17**

A colorless solid, $[\alpha]_D^{25}$ +20.84 (c 0.095, MeOH); UV λ_{max}^{MeOH} (nm) (log ε) 232 (4.10), 258 (3.91), 292 (3.47) nm; FTIR (ATR) ν_{max} 3452, 2932, 1738, 1680, 1589, 1440, 1391, 1303, 1209, 1179, 1120, 983 cm^{-1}; ^{1}H (acetone-d_6, 500 MHz) and ^{13}C NMR data (acetone-d_6, 125 MHz), see Table 3; HRESIMS *m/z* 654.3251 $[M+Na]^+$ (calcd for $C_{34}H_{49}NO_{10}Na$, 654.3249).

4.3.13. Compound **18**

A colorless solid, $[\alpha]_D^{25}$ +1.86 (c 0.225, MeOH); UV λ_{max}^{MeOH} (nm) (log ε) 222 (4.17), 252 (4.04), 287 (3.60) nm; FTIR (ATR) ν_{max} 3417, 2929, 1738, 1698, 1681, 1434, 1392, 1334, 1306, 1206, 1200,

Table 3
^{1}H NMR assignments of fendlerinines B − F (**11**–**15**) and their derivatives (**16**–**18**) in acetone-d_6.

Pos.	11[c]	12 [b]	13 [b]	14 [c]	15 [c]	16 in $CDCl_3$[b]	17 [c]	18 [c]
	δ_H, mult. (J in Hz)	δ_H, mult. (J in Hz)	δ_H, mult. (J in Hz)	δ_H, mult. (J in Hz)	δ_H, mult. (J in Hz)	δ_H, mult. (J in Hz)	δ_H, mult. (J in Hz)	δ_H, mult. (J in Hz)
1	1.18–1.25, m	1.16–1.31, m	2.00–2.10[a]	1.16–1.30, m	1.25–1.32, m	1.65–1.69, m	1.20–1.25, m	1.25–13.2, m
	2.00–2.10[a]	2.00–2.10[a]		1.95–2.05, m	1.91, d (13.4)	1.73–1.76, m	2.00–2.08[a]	1.90, dm (13.3, <1)
2	1.62–1.73, m	1.43–1.53, m	1.18–1.30, m	1.62–1.74, m	1.47, dt (14.0, 3.2)	1.42–1.52, m	1.50, dd (13.1, 3.5)	1.30–1.40, m
					1.65–1.72, m		1.62–1.70, m	1.54–1.70, m
3	1.18–1.25, m	1.16–1.31, m	1.30–1.43, m	1.16–1.30, m	1.19–1.25, m	1.24, dt (12.9, 3.5)	1.24–1.32, m	1.22, dd (13.6, 3.5)
	1.34–1.43, m	1.31–1.43, m		1.36–1.43, m	1.42, d (13.6)	1.40, dt (12.9, <1)	1.38–1.41, m	1.41, dm (13.6, <1)
5	1.06, d (11.6)	1.06, d (11.0)	1.03–1.33, m	1.05, d (15.7)	1.08, d (12.3)	1.02, dd (12.1, <1)	1.05, dd (12.1, 1.9)	1.08 (dd, 12.1, <1)
6	1.34–1.43, m	1.63–1.73, m	1.30–1.43, m	1.32–1.37, m	1.30–1.45, m	1.69–1.73, m	1.35, dd (12.1, 2.7)	1.47, ddt (13.8, 12.1, 3.9)
	1.63–1.73, m		1.60–1.72, m	1.62–1.74, m	1.65–1.72, m		1.62–1.72, m	1.54–1.70, m
7	1.50–1.59, m	1.53–1.60, m	1.50–1.60, m	1.50–1.58, m	1.60, td (13.0, 3.5)	1.56, dt (12.9, 3.4)	1.54, dd (18.4, 3.0)	1.60, dt (13.1, 3.9)
	1.76–1.85, m	1.77–1.85, m	1.77–1.85, m	1.78–1.90, m	1.78–1.84, m	1.92, dt (12.9, 3.0)	1.79, dd (13.3, 3.5)	1.84, dt (13.1, 3.0)
9	1.76–1.85, m	1.77–1.85, m	1.77–1.85, m	1.78–1.90, m	1.78–1.84, m	1.82, dd (7.2, 4.2)	1.82, t (3.4)	1.78, dd (3.8, <1)
11	4.38, dd (9.6, 3.7)[d]	4.36, dd (9.6, 3.7)	4.36, dd (9.7, 3.9)	4.38, d (2.9)	4.32, dd (9.4, 5.6)	4.11, dd (9.6, 4.2)	4.35, dd (9.7, 3.8)	4.31, dd (9.4, 5.7)
	4.44, dd (9.6, 3.3)[d]	4.42, dd (9.6, 3.2)	4.44, dd (9.7, 3.6)		4.36, dd (9.4, 1.9)	4.23, dd (9.6, 7.2)	4.47, dd (9.7, 3.8)	4.37, dd (9.4, 2.0)
12	1.23, s	1.22, s	1.23, s	1.23, s	1.11, s	1.28, s	1.22, s	1.17, s
13	0.84, s	0.83, s	0.84, s	0.83, s	0.85, s	0.81, s	0.84, s	0.85, s
14	0.92, s	0.91, s	0.91, s	0.91, s	0.91, s	0.90, s	0.92, s	0.91, s
15	0.92, s	0.91, s	0.91, s	0.90, s	0.96, s	0.83, s	0.91, s	0.97, s
7′					4.73, d (17.0)			4.67, d (16.7)
					4.88, d (17.0)			4.81, d (16.7)
8′	2.29, s	2.28, s	2.28, s	2.28, s	2.30, s	2.34, s	2.27, s	2.29, s
9′	3.92, s	3.91, s	3.91, s	3.91, s	3.82, s	3.83, s	3.87, s	3.79, s
11′	4.73, s	4.66, d (18.6)	4.64, d (18.9)	4.58, d (18.7)		9.86, s	4.61, d (18.4)	
		4.77, d (18.6)	4.76, d (18.9)	4.83, d (18.7)			4.68, d (18.4)	
1″	4.41, s	5.06, dt (11.5, 4.4)	5.03, dd (10.5, 4.1)	5.07, dd (11.5, 4.0)	5.00, dd (11.6, 4.4)		5.05, dd (13.5, 4.4)	4.95, dd (11.0, 3.9)
2″		2.20–2.32, m	2.23–2.32, m	1.78–1.90, m	2.22–2.27, m		2.20–2.30, m	2.20–2.24, m
		2.40–2.47, m	2.42–2.48, m	1.95–2.00, m	2.41–2.47, m		2.39–2.45, m	2.36–2.45, m
3″		2.40–2.47, m	2.42–2.48, m	1.78–1.90, m	2.41–2.47, m		2.39–2.45, m	2.36–2.45, m
3″−CH_3				0.97, d (6.0)				
4″−OCH_3			3.56, s	3.56, s			3.57, s	3.56, s
5″−OCH_3							3.73, s	3.70, s
7′−OCH_3						3.96(3), s		
10′−OCH_3						3.96(1), s	3.91, s	3.86, s
8-OH							4.42, s	

[a] Signal overlapped with acetone-d_6 signal.
[b] Recorded at 400 MHz for ^{1}H NMR.
[c] Recorded at 500 MHz for ^{1}H NMR.
[d] Coupling constant values were clearly observed when recorded at 400 MHz.

1110 cm^{-1}; ^{1}H (acetone-d_6, 500 MHz) and ^{13}C NMR data (acetone-d_6, 125 MHz), see Table 3; HRESIMS m/z 654.3261 $[M+Na]^+$ (calcd for $C_{34}H_{49}NO_{10}Na$, 654.3249).

4.4. Preparation of compound **16**

To a solution of compound **10** (4.9 mg, 0.0103 mmol, 1.00 eq) in dried acetone (300 μL) was added K_2CO_3 (excess) and methyl iodide (4.0 μL, 0.0637 mmol, 6.18 eq) at room temperature overnight. The mixture was then filtered and evaporated to dryness to give compound **16** (5.0 mg, 96%) as a pale yellow solid.

4.5. Preparation of compounds **17** and **18**

To a solution of compound **12** (2.8 mg, 0.0048 mmol, 1.00 eq) in dried dioxane (300 μL) was added CH_2N_2 (excess) at 0 °C and then the solution was left room temperature overnight. The solution was evaporated to dryness to afford compound **17** (2.9 mg, 96%) as a colorless solid.

Compound **17** (2.0 mg, 83%) was also obtained from compound **13** (2.3 mg, 0.0038 mmol, 1.00 eq) with the same protocol as for compound **12**.

Compound **18** (4.5 mg, 95%) was prepared from compound **15** (4.4 mg, 0.0075 mmol, 1.00 eq) with the same protocol as for compound **17**.

4.6. Biological activity

Antimalarial activity against *P. falciparum* (K1-multidrug resistant strain) was evaluated by using the microculture radioisotope method (Desjardins et al., 1979). Dihydroartemisinin and mefloquine were used as standard references and showed IC_{50} values of 7.00×10^{-4} and 9.72×10^{-3} μg/mL, respectively. Antibacterial activity against *B. cereus* (ATCC 11778), antifungal activity against *C. albicans* (ATCC 90028), and cytotoxicity against cancerous cells including MCF-7 (human breast cancer, ATCC HTC-22), KB (human oral epidermoid carcinoma, ATCC CCL-17), and NCI-H187 (human small-cell lung cancer, ATCC CRL-5804) cells were done by using the resazuin microplate assay (REMA) (O'Brien et al., 2000; Sarker et al., 2007). Vancomycin and amphotericin B were used as standard references for anti-*B. cereus* and for anti-*C. albicans*, respectively and exhibited respective IC_{50} values of 2.00 and 0.11 μg/mL. Doxorubicin and tamoxifen were used as standard references for anti-MCF-7 and displayed IC_{50} values of 14.92 and 9.83 μg/mL, respectively. Doxorubicin and ellipticine were used as standard references for cytotoxicity against KB and NCI-H187 cells and displayed IC_{50} values of 3.42, 1.70 and 2.80, 0.073 μg/mL, respectively. Cytotoxicity against non-cancerous cells (Vero, African green monkey kidney fibroblasts, ATCC CCL-81) was performed by using the green fluorescent protein microplate assay (GFPMA) (Changsen et al., 2003) and ellipticine was used as a standard reference. Ellipticine showed IC_{50} value of 1.26 μg/mL. IC_{50} values represent 50

percent reduction of parasites or tested cell lines and were used for antimalarial activity and cytotoxicity. MIC values represent minimum inhibition concentration and were used for antibacterial, antifungal activities. 50 μg/mL was a maximum tested concentration for all tests, except those for *P. falciparum* and *B. cereus* were at 10 and 25 μg/mL, respectively.

Acknowledgements

Financial support from the Thailand Research Fund (TRF grant number: RSA5980001) and the National Center for Genetic Engineering and Biotechnology (BIOTEC grant number: P16-51093) are gratefully acknowledged.

Appendix A. Supplementary data

Supplementary data related to this article can be found at http://dx.doi.org/10.1016/j.phytochem.2017.03.008.

References

Achenbach, H., Mühlenfeld, A., Kohl, W., Brillinger, G.-U., 1985. Stoffwechselprodukte von Mikroorganismen, XXXI [1]. Duricaulinsäure, ein neuer Naturstoff vom Phthalimidin-Typ aus *Aspergillus duricaulis* Z. Naturforsch. B 40, 1219–1225.

Almeida, C., Hemberger, Y., Schmitt, S.M., Bouhired, S., Natesan, L., Kehraus, S., Dimas, K., Gutschow, M., Bringmann, G., Konig, G.M., 2012. Marilines A-C: novel phthalimidines from the sponge-derived fungus *Stachylidium* sp. Chem. (Weinheim der Bergstrasse, Ger. 18, 8827–8834.

Belofsky, G.N., Gloer, K.B., Gloer, J.B., Wicklow, D.T., Dowd, P.F., 1998. New *p*-terphenyl and polyketide metabolites from the sclerotia of *Penicillium raistrickii*. J. Nat. Prod. 61, 1115–1119.

Cao, L.-L., Zhang, Y.-Y., Liu, Y.-J., Yang, T.-T., Zhang, J.-L., Zhang, Z.-G., Shen, L., Liu, J.-Y., Ye, Y.-H., 2016. Anti-phytopathogenic activity of sporothriolide, a metabolite from endophyte *Nodulisporium* sp. A21 in *Ginkgo biloba*. Pest. Biochem. Physiol. 129, 7–13.

Chang, C.W., Chang, H.S., Cheng, M.J., Liu, T.W., Hsieh, S.Y., Yuan, G.F., Chen, I.S., 2014. Inhibitory effects of constituents of an endophytic fungus *Hypoxylon investiens* on nitric oxide and interleukin-6 production in RAW264.7 macrophages. Chem. Biodivers. 11, 949–961.

Changsen, C., Franzblau, S.G., Palittapongarnpim, P., 2003. Improved green fluorescent protein reporter gene-based microplate screening for antituberculosis compounds by utilizing an acetamidase promoter. Antimicrob. Agents Chemother. 47, 3682–3687.

Colson, K.L., Jackman, L.M., Jain, T., Simolike, G., Keeler, J., 1985. 3-Hydroxy-1,4-diphenyl-7-oxabicyclo[4.1.0]hept-3-ene-2,5-dione. A microbial product from *Streptomyces* species (AAA566). Tetrahedron Lett. 26, 4579–4582.

Desjardins, R.E., Canfield, C.J., Haynes, J.D., Chulay, J.D., 1979. Quantitative assessment of antimalarial activity in vitro by a semiautomated microdilution technique. Antimicrob. Agents Chemother. 16, 710–718.

El-Elimat, T., Figueroa, M., Raja, H.A., Graf, T.N., Adcock, A.F., Kroll, D.J., Day, C.S., Wani, M.C., Pearce, C.J., Oberlies, N.H., 2013. Benzoquinones and terphenyl compounds as phosphodiesterase-4B inhibitors from a fungus of the order Chaetothyriales (MSX 47445). J. Nat. Prod. 76, 382–387.

Fujimoto, Y., Tatsuno, T., 1976. A novel method for reductive removal of tosyloxy and mesyloxy groups. Tetrahedron Lett. 17, 3325–3326.

Fujiwara, N., Kinoshita, M., Akita, H., 2006. New total synthesis of (+)-ambrein. Tetrahedron Asymm. 17, 3037–3045.

Hsieh, H.M., Ju, Y.M., Rogers, J.D., 2005. Molecular phylogeny of Hypoxylon and closely related genera. Mycologia 97, 844–865.

Hu, L., Gao, J.-M., Liu, J.-K., 2001. Unusual poly(phenylacetyloxy)-substituted 1,10: 40,100-terphenyl derivativesfrom fruiting bodies of the Basidiomycete *Thelephora ganbajun*. Helv. Chim. Acta 84, 3342–3349.

Hu, W., Ohyama, S., Hasumi, K., 2000. Activation of fibrinolysis by SMTP-7 and -8, novel staplabin analogs with a pseudosymmetric structure. J. Antibiot. 53, 241–247.

Islam, M.S., Ishigami, K., Watanabe, H., 2007. Synthesis of (−)-mellein, (+)-ramulosin, and related natural products. Tetrahedron 63, 1074–1079.

Ito-Kobayashi, M., Aoyagi, A., Tanaka, I., Muramatsu, Y., Umetani, M., Takatsu, T., 2008. Sterenin A, B, C and D, novel 11beta-hydroxysteroid dehydrogenase type 1 inhibitors from *Stereum* sp. SANK 21205. J. Antibiot. 61, 128–135.

Jansen, B.J., de Groot, A., 2004. Occurrence, biological activity and synthesis of drimane sesquiterpenoids. Nat. Prod. Rep. 21, 449–477.

Kuhnert, E., Surup, F., Herrmann, J., Huch, V., Muller, R., Stadler, M., 2015a. Rickenyls A-E, antioxidative terphenyls from the fungus *Hypoxylon rickii* (Xylariaceae, Ascomycota). Phytochemistry 118, 68–73.

Kuhnert, E., Surup, F., Herrmann, J., Huch, V., Müller, R., Stadler, M., 2015b. Rickenyls A–E, antioxidative terphenyls from the fungus *Hypoxylon rickii* (Xylariaceae, Ascomycota). Phytochemistry 118, 68–73.

Kuhnert, E., Surup, F., Sir, E.B., Lambert, C., Hyde, K.D., Hladki, A.I., Romero, A.I., Stadler, M., 2015c. Lenormandins A—G, new azaphilones from *Hypoxylon lenormandii* and *Hypoxylon jaklitschii* sp. nov., recognised by chemotaxonomic data. Fungal Divers 71, 165–184.

Kuhnert, E., Surup, F., Wiebach, V., Bernecker, S., Stadler, M., 2015d. Botryane, noreudesmane and abietane terpenoids from the ascomycete *Hypoxylon rickii*. Phytochemistry 117, 116–122.

Læssøe, T., Srikitikulchai, P., Fournier, J., Köpcke, B., Stadler, M., 2010. Lepraric acid derivatives as chemotaxonomic markers in *Hypoxylon aeruginosum, Chlorostroma subcubisporum* and *C. cyaninum*, sp. nov. Fungal Biol. 114, 481–489.

Lee, H.J., Rhee, I.K., Lee, K.B., Yoo, I.D., Song, K.S., 2000. Kynapcin-12, a new p-terphenyl derivative from *Polyozellus multiplex*, inhibits prolyl endopeptidase. J. Antibiot. 53, 714–719.

Li, W., Gao, W., Zhang, M., Li, Y.-L., Li, L., Li, X.-B., Chang, W.-Q., Zhao, Z.-T., Lou, H.-X., 2016. *p*-Terphenyl derivatives from the endolichenic fungus *Floricola striata*. J. Nat. Prod. 79, 2188–2194.

Li, Y., Liu, D., Cen, S., Proksch, P., Lin, W., 2014. Isoindolinone-type alkaloids from the sponge-derived fungus *Stachybotrys chartarum*. Tetrahedron 70, 7010–7015.

Liu, J.-K., Hu, L., Dong, Z.-J., Hu, Q., 2004. DPPH radical scavenging activity of ten natural *p*-terphenyl derivatives obtained from three edible mushrooms indigenous to China. Chem. Biodiv. 1, 601–605.

Martinelli, M.J., Leanna, M.R., Varie, D.L., Peterson, B.C., Kress, T.J., Wepsiec, J.P., Khau, V.V., 1990. The synthesis of (+)- and (−)-1-benzoyl-1,2,2a,3,4,5-hexahydrobenz[cd]indol-4-amine, and preparation of LY228729. Tetrahedron Lett. 31, 7579–7582.

Mühlbauer, A., Triebel, D., Persoh, D., Wollweber, H., Seip, S., Stadler, M., 2002. Macrocarpones, novel metabolites from stromata of *Hypoxylon macrocarpum*, and new evidence on the chemotaxonomy of *Hypoxylon* species. Mycol. Prog. 1, 235–248.

Ngoc Quang, D., Hashimoto, T., Hitaka, Y., Tanaka, M., Nukada, M., Yamamoto, I., Asakawa, Y., 2003. Thelephantins D-H: five *p*-terphenyl derivatives from the inedible mushroom *Thelephora aurantiotincta*. Phytochemistry 63, 919–924.

O'Brien, J., Wilson, I., Orton, T., Pognan, F., 2000. Investigation of the Alamar Blue (resazurin) fluorescent dye for the assessment of mammalian cell cytotoxicity. Eur. J. Biochem. 267, 5421–5426.

Quang, D.N., Hashimoto, T., Nukada, M., Yamamoto, I., Hitaka, Y., Tanaka, M., Asakawa, Y., 2003. Thelephantins A, B and C: three benzoyl *p*-terphenyl derivatives from the inedible mushroom *Thelephora aurantiotincta*. Phytochemistry 62, 109–113.

Quang, D.N., Stadler, M., Fournier, J., Asakawa, Y., 2006. Carneic acids A and B, chemotaxonomically significant antimicrobial agents from the xylariaceous ascomycete *Hypoxylon carneum*. J. Nat. Prod. 69, 1198–1202.

Sarker, S.D., Nahar, L., Kumarasamy, Y., 2007. Microtitre plate-based antibacterial assay incorporating resazurin as an indicator of cell growth, and its application in the in vitro antibacterial screening of phytochemicals. Methods 42, 321–324.

Shinohara, C., Hasumi, K., Hatsumi, W., Endo, A., 1996. Staplabin, a novel fungal triprenyl phenol which stimulates the binding of plasminogen to fibrin and U937 cells. J. Antibiot. 49, 961–966.

Sommart, U., Rukachaisirikul, V., Tadpetch, K., Sukpondma, Y., Phongpaichit, S., Hutadilok-Towatana, N., Sakayaroj, J., 2012. Modiolin and phthalide derivatives from the endophytic fungus *Microsphaeropsis arundinis* PSU-G18. Tetrahedron 68, 10005–10010.

Stierle, D.B., Stierle, A.A., Kunz, A., 1998. Dihydroramulosin from *Botrytis* sp. J. Nat. Prod. 61, 1277–1278.

Stodola, F.H., Cabot, C., Benjamin, C.R., 1964. Structure of ramulosin, a metabolic product of the fungus *Pestalotia ramulosa*. Biochem. J. 93, 92–97.

Surup, F., Kuhnert, E., Lehmann, E., Heitkämper, S., Hyde, K.D., Fournier, J., Stadler, M., 2014. Sporothriolide derivatives as chemotaxonomic markers for *Hypoxylon monticulosum*. Mycology 5, 110–119.

Surup, F., Kuhnert, E., Liscinskij, E., Stadler, M., 2015. Silphiperfolene-type terpenoids and other metabolites from cultures of the tropical Ascomycete *Hypoxylon rickii* (Xylariaceae). Nat. Prod. Bioprospect. 5, 167–173.

Tsantrizos, Y.S., Ogilivie, K.K., Watson, A.K., 1992a. Phytotoxic metabolites of *Phomopsis convolvulus*, a host-specific pathogen of field bindweed. Can. J. Chem. 70, 2276–2284.

Tsantrizos, Y.S., Ogilvie, K.K., Watson, A.K., 1992b. Phytotoxic metabolites of *Phomopsis convolvulus*, a host-specific pathogen of field bindweed. Can. J. Chem. 70, 2276–2284.

Turner, W.B., Aldridge, D.C., 1983. Fungal Metabolites. Academic Press.

Wang, J., Wang, G., Zhang, Y., Zheng, B., Zhang, C., Wang, L., 2014. Isolation and identification of an endophytic fungus *Pezicula* sp. in *Forsythia viridissima* and its secondary metabolites. World J. Microbiol. Biotechnol. 30, 2639–2644.

Whalley, A.J.S., Edwards, R.L., 1995. Secondary metabolites and systematic arrangement within the Xylariaceae. Can. J. Bot. 73, 802–810.

Ye, Y.Q., Koshino, H., Abe, N., Nakamura, T., Hashizume, D., Takahashi, S., 2010. Synthesis of atromentin and its *O*-alkylated natural products. Biosci. Biotechnol. Biochem. 74, 2342–2344.

Zheng, C.J., Sohn, M.J., Kim, W.G., 2006. Atromentin and leucomelone, the first inhibitors specific to enoyl-ACP reductase (FabK) of *Streptococcus pneumoniae*. J. Antibiot. 59, 808–812.

Phytochemistry Letters 20 (2017) 274–281

Contents lists available at ScienceDirect

Phytochemistry Letters

journal homepage: www.elsevier.com/locate/phytol

Antimicrobial activity of illudalane and alliacane sesquiterpenes from the mushroom *Gloeostereum incarnatum* BCC41461

Nantiya Bunbamrung, Chakapong Intaraudom, Aibrohim Dramae, Nattawut Boonyuen, Sukitaya Veeranondha, Pranee Rachtawee, Pattama Pittayakhajonwut*

National Center for Genetic Engineering and Biotechnology (BIOTEC), Thailand Science Park, Paholyothin Road, Klong Luang, Pathumthani 12120, Thailand

ARTICLE INFO

Keywords:
Mushroom
Gloeostereum
Sesquiterpenes
Illudalane
Alliacane
Antimicrobial

ABSTRACT

Eleven previously undescribed sesquiterpenes **1**–**4** (named incarnatins A − D) and **6**–**12** (named incarnolactones A − C, incarnatin E, incarnate methyl ester, incarnetic acid, and incarnatenin), together with two known compounds, chondrosterin B (**13**) and (*E*)-dictyochromenol (**14**), were isolated from the mushroom *Gloeostereum incarnatum* BCC41461. The chemical structures were determined on the basis of 1D and 2D NMR spectroscopic information together with their specific rotation values for identification of the stereochemistry. Compounds were evaluated for antimicrobial activity, including antimalarial, antituberculosis, and anti-*Bacillus cereus*, along with cytotoxicity against both cancerous and non-cancerous cells. Compounds **1** and **8** exhibited antimalarial (IC_{50} 9.80 μg/mL) and anti-*B. cereus* (MIC 25 μg/mL) activities, respectively, with low cytotoxicity. In addition, incarnatin B (**2**) and chondrostenin B (**13**) displayed strong antimalarial activity with respective IC_{50} values of 3.93 and 3.10 μg/mL, while compound **14** showed anti-TB and anti-*B. cereus* with MIC 12.50 and 1.56 μg/mL, respectively.

1. Introduction

Many types of sesquiterpenoids have been isolated from various mushrooms, both edible and inedible, and possessed broad array of activities. For example, cadinane-type sesquiterpenes, strobilols A − D, were isolated from the edible mushroom *Strobilurus ohshimae* and were inactive for antimicrobial activity against *Candida albicans* ATCC 2019, *Staphylococcus aureus* NBRC 13276, and *Pseudomonas aeruginosa* ATCC 15442 (Hiramatsu et al., 2007); anthracophillic acid (spiro-sesquiterpene) and anthracophyllone (aristolane sesquiterpene) were isolated from *Anthracophyllum* sp. BCC18695 and showed cytotoxicity against KB, MCF-7, NCI-H187, and Vero cells (Intaraudom et al., 2013); Flammufuranones A − B and flammuspirones A − J (*seco*-cuparane sesquiterpenes) were isolated from *Flammulina velutipes* and flammuspirones A and C inhibited HMG-Co A reductase activity, while flammuspirones C, D, E, and H inhibited DPP-4 (dipeptidyl peptidase-4) activity (Tao et al., 2016); Russulanobilines A − C (lactarane sesquiterpenes) were isolated from *Russula nobilis* and postulated to involve in a chemical defense system against predators, parasites, and microorganisms (Malagòn et al., 2014); Atlanticones A − D (protoilludane sesquiterpenes) were isolated from *Lactarius atlanticus* and had a role in the taste of mushroom (Clericuzio et al., 2002).

As part of our continuing search for new antimicrobial substances, the crude extracts from the mushroom *Gloeostereum incarnatum* BCC41461 exhibited antimalarial (IC_{50} 3.12 μg/mL), anti-TB (MIC 12.5 μg/mL), anti-*B. cereus* (MIC 25.0 μg/mL) activities and provided the productive chemical profiles, therefore an investigation was conducted. Moreover, to the best of our knowledge, the chemical study of the genus *Gloeostereum* has not yet so far been investigated. The chemical investigation of the culture broth resulted in the isolation of eleven new sesquiterpenes (named incarnatins A − E, incarnolactones A − C, incarnate methyl ester, incarnetic acid, and incarnatenin), along with two known compounds, chondrosterin B (**13**) and (*E*)-dictyochromenol (**14**), whilst that of the cells provided compounds **2**, **6**, and **14**. The isolated compounds were further evaluated for antimicrobial activity and for cytotoxicity against both malignant (KB, MCF-7, NCI-H187) and non-malignant (Vero) cells.

2. Results and discussion

Compound **1** was obtained as a brown powder and gave a sodium-adduct precursor ion peak at *m/z* 271.1312 $[M+Na]^+$, establishing the molecular formula $C_{15}H_{20}O_3$. The ^{13}C NMR spectrum (Table 2) gave 15 signals, differentiated by DEPT-135 spectrum, including three methyl, four methylene, one sp^3 methine, and seven quaternary carbons. Signals in the ^1H NMR spectrum (Table 1), attributed by HMQC

* Corresponding author.
E-mail address: pattamap@biotec.or.th (P. Pittayakhajonwut).

http://dx.doi.org/10.1016/j.phytol.2017.05.017
Received 31 March 2017; Received in revised form 5 May 2017; Accepted 11 May 2017
Available online 19 May 2017

Table 1
^{1}H NMR assignment of incarnatins A − D (**1–4**) and incarnolactones A − C (**6–8**) in acetone-d_6.

position	incarnatin A (1)[a] δ_H, (mult., *J* in Hz)	incarnatin B (2)[a] δ_H, (mult., *J* in Hz)	incarnatin C (3)[a] δ_H, (mult., *J* in Hz)	incarnatin D (4)[a] δ_H, (mult., *J* in Hz)	incarnolactone A (6)[a] δ_H, (mult., *J* in Hz)	incarnolactone B (7)[b] δ_H, (mult., *J* in Hz)	incarnolactone C (8)[b] δ_H, (mult., *J* in Hz)
1	2.66 (s)	2.63 (s)	2.50 (d, 15.3) 2.64 (d,15.3)	2.52 (d, 15.3) 2.65 (d, 15.3)	2.68 (s)	2.57 (d, 15.6) 2.69 (d, 15.6)	2.69 (s)
5	2.52 (dd, 16.4, 5.3) 2.77 (d, 16.4)	2.54 (dd, 16.6, 3.3) 2.77 (dd, 16.6, 3.9)	2.54 (d, 16.8) 2.78 (dd, 16.8, < 1)	2.59 (d, 16.9) 2.78 (d, 16.9)	3.61 (s)	3.64 (s)	5.26 (s)
6	5.20 (m)	4.87 (t, 4.0)	4.88 (t, 3.8)/4.90 (t, 3.7)	4.88 (t, 3.8)/4.90 (t, 3.7)	–	–	–
7	4.62 (d, 15.2) 4.87 (d, 15.2)	4.63 (d, 15.5) 4.69 (d, 15.5)	4.62 (d, 15.1) 4.66 (d, 15.1)	4.63 (d, 15.1) 4.66 (d, 15.1)	5.33 (s)	5.30 (s)	5.42 (d, 13.9) 5.49 (d, 13.9)
11	2.63 (s)	2.66 (s)	4.97 (br s)	4.62(8) (s)/ 4.63(2) (s)	2.72 (s)	5.03 (s)	2.74 (s)
3-CH_3	1.99 (s)	1.97 (s)	1.96 (s)	1.96 (s)	2.10 (s)	2.09 (s)	2.21 (s)
2 × 12-CH_3	1.13 (s)	1.13(1) (s) 1.13(4) (s)	0.98 (s) 1.17 (s)/1.18 (s)	1.25 (s) 1.04 (s)/1.05 (s)	1.15 (s)	1.00 (s) 1.20 (s)	1.15 (s) 1.16 (s)
5-OH		–	–	–	–	–	7.87 (br s)
6-OH	5.43 (s)	–	–	–	–	–	–
6-OCH_3	–	3.42 (3H, s)	3.42(1) (s)/ 3.42(3) (s)	3.42 (s)	–	–	–
9-OH	7.26 (s)	–	7.54 (s)	7.28 (s)	7.78 (br s)	7.87 (s)	5.18 (s)
11-OH	–	–	4.78 (d, 5.6)/4.83 (d, 5.4)	–	–	4.93 (s)	–
11-OCH_3		–	–	3.51(6) (s)/3.52 (s)	–	–	–

[a] Recorded in 400 MHz.
[b] Recorded in 500 MHz.

spectral data, comprised three methyl [at δ_H 1.13 (×2) and 1.99], four sets of methylene (at δ_H 2.63, 2.66, 2.52/2.77, and 4.62/4.87), one singlet oxymethine (at δ_H 5.20), and two hydroxyl protons (at δ_H 5.43 and 7.26). The ^{1}H NMR spectral data and COSY spectrum showed correlation between H-5 and H-6. In addition, HMBC spectrum showed correlations from 12-CH_3 (×2) to C-1, C-11, and C-12; from 3-CH_3 to C-2, C-3 and C-4; from H_2-7 to C-4, C-6, C-8, and C-9; and from H_2-1 and H_2-11 to C-2, C-10, and 12-CH_3. In the ^{13}C NMR spectrum, the methylene at δ_C 60.2 (C-7) and the methine at δ_C 92.1 (C-6) indicated the attachment to one/two oxygen(s), respectively. The spectroscopic evidence indicated that compound **1** was illudalane-type structure, as shown in Fig. 1 and incarnatin A was given as its trivial name. Moreover, the reaction of compound **5** (named incarnatin F), derived from the reaction of compound **1** with MeI/K_2CO_3, with *R*– and *S* −MTPA gave an insignificant difference of surrounding chemical shifts together with low value of the specific rotation value ($[\alpha]_D^{25}$ − 3.34, $CHCl_3$), compared with that of the related compound, (*R*)-echinolactone B ($[\alpha]_D$ − 24.0, $CHCl_3$) (Suzuki et al., 2005), thus compound **1** was obtained as enantiomer mixture.

Compound **2** was obtained as a brown powder and HRESIMS spectrum showed 14 mass units higher than that of compound **1**, indicating the presence of an extra methyl group. The ^{1}H NMR spectrum displayed an additional methoxy signal resonating at δ_H 3.42 and an upfield shift of the methine signal at C-6 (δ_H 4.87). Moreover, the sp^3 methine at H-6 correlated in the HMBC spectrum to C-4, C-5, and C-7, and 6-OCH_3. The absolute configuration at C-6 of compound **2** could not be assigned due to a small value of its optical rotation ($[\alpha]_D^{25}$ −11.60, $CHCl_3$), compared with that of (*R*)-echinolactone B ($[\alpha]_D$ − 24.0, $CHCl_3$) (Suzuki et al., 2005). Therefore, compound **2** possessed the chemical structure as shown in Fig. 1 and a trivial

Table 2
^{13}C NMR assignment of incarnatins A − D (**1–4**) and incarnolactones A − C (**6–8**) in acetone-d_6.

position	incarnatin A (1)[a] δ_C, type	incarnatin B (2)[a] δ_C, type	incarnatin C (3)[a] δ_C, type	incarnatin D (4)[a] δ_C, type	incarnolactone A (6)[a] δ_C, type	incarnolactone B (7)[b] δ_C, type	incarnolactone C (8)[b] δ_C, type
1	43.9, CH_2	46.8, CH_2	45.0, CH_2	45.9, CH_2	46.9, CH_2	44.9, CH_2	46.8, CH_2
2	141.3, qC	141.3, qC	139.4(8)/139.5(3), qC	139.9, qC	144.1, qC	142.4, qC	144.5, qC
3	122.9, qC	122.7, qC	123.5, qC	123.7, qC	121.8, qC	122.6, qC	123.7, qC
4	129.5, qC	128.6, qC	131.2/131.3, qC	131.7/131.8, qC	129.3, qC	131.8, qC	132.1, qC
5	33.0, CH_2	31.2, CH_2	32.2, CH_2	32.2, CH_2	32.7, CH_2	33.8, CH_2	66.4, CH
6	92.3, CH	98.5, CH	99.3/99.4, CH	99.2/99.3, CH	170.6, qC	171.4, qC	170.7, qC
7	60.2, CH_2	58.9, CH_2	59.2, CH_2	59.3/59.4, CH_2	64.6, CH_2	64.9, CH_2	64.5, CH_2
8	119.7, qC	119.4, qC	120.0, qC	120.3, qC	117.2, qC	117.6, qC	118.6, qC
9	146.4, qC	146.4, qC	148.8, qC	148.8, qC	146.7, qC	149.0, qC	146.7, qC
10	125.3, qC	125.1, qC	125.8(7)/125.9(1), qC	124.9, qC	127.1, qC	127.5, qC	129.2, qC
11	46.9, CH_2	43.9, CH_2	83.5, CH	99.4, CH	44.0, CH_2	83.2, CH	44.1, CH_2
12	39.1, qC	39.1, qC	45.3/45.4, qC	45.2, qC	39.3, qC	45.5, qC	39.3, qC
3-CH_3	13.9, CH_3	13.5, CH_3	13.8, CH_3	13.9, CH_3	13.3, CH_3	13.7, CH_3	13.2, CH_3
2 × 12-CH_3	28.7, CH_3	28.6, CH_3	22.3, CH_3 26.8(5)/26.9, CH_3	22.2(9)/22.3(1), CH_3 28.6, CH_3	28.6, CH_3	22.2, CH_3 26.7, CH_3	28.4, CH_3 28.5, CH_3
6-OCH_3	–	54.3, CH_3	55.3, CH_3	55.3, CH_3	–	–	–
11-OCH_3	–	–	–	58.4, CH_3	–	–	–

[a] Recorded in 100 MHz.
[b] Recorded in 125 MHz.

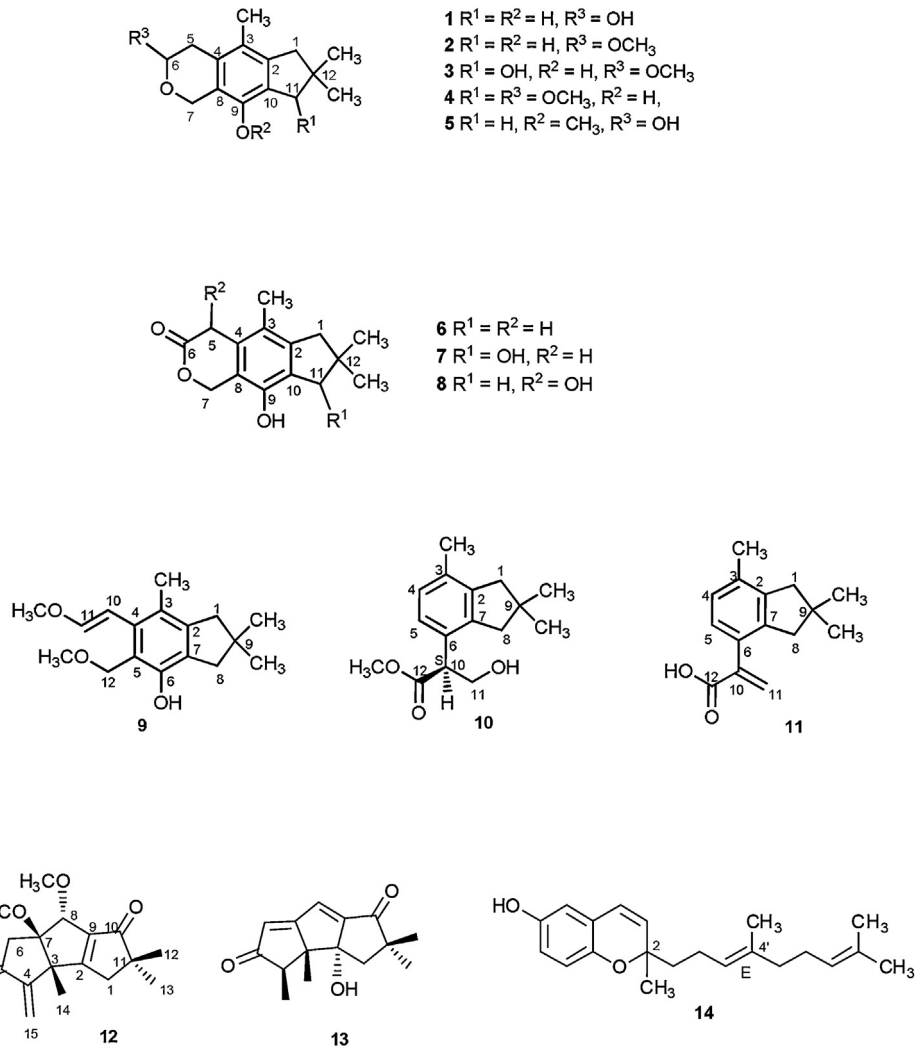

Fig. 1. Chemical structures of compounds **1- 14** isolated from the mushroom *Gloeostereum incarnatum* BCC41461.

name, incarnatin B, was given.

Compound **3** was obtained as a brown powder. The ^{13}C NMR spectrum displayed obviously doubled signals (Table 2), indicating an isomeric mixture. Also it showed the absence of a methylene signal and the presence of oxymethine signal (at δ_C 83.5), which bearing an oxymethine proton at δ_H 4.97, as attributed by the HMQC spectrum. Moreover, in the HMBC spectrum, the additional oxymethine correlated to C-2, C-9, C-10, and 12-CH_3, led to a hydroxyl substituent at C-11. HRESIMS spectrum confirmed the molecular formula of $C_{16}H_{22}O_4$ by giving the mass ion peak at *m/z* 277.1449 $[M - H]^-$. The molecule had two stereogenic centers (at C-6 and C-11) but no definite evidence could be pointed to which stereocenter(s) possessing a diastereomeric mixture, due to the insufficient amount for further investigation. Thus, the chemical structure of compound **3** could be provided as shown and incarnatin C was given as its informal name.

Compound **4** was obtained as a colourless gum. HRESIMS data indicated 14 mass units higher than that of compound **3**, revealing the sodium-adduct precursor ion peak at *m/z* 315.1582 $[M+Na]^+$. The ^1H and ^{13}C NMR spectra displayed doubled signals (Tables 1 and 2), indicating a diasteromeric mixture. The ^1H NMR spectrum (Table 1) showed doubled signals of additional methoxy at δ_H 3.52 and oxymethine methine at δ_H 4.63 (H-11) and 4.88/4.90 (H-6), compared with that of compound **3**. In HMBC spectrum, the extra methoxy signal correlated to the quaternary carbon at δ_C 99.4 (C-11) and H-11 (δ_H 4.63) correlated to δ_C 58.4 (11-OCH_3), C-10 (δ_C 124.9), and 12-CH_3. The spectroscopic evidence suggested the additional methoxy group situated at C-11. The rest of the molecule was also reassured by HMBC correlations. With the same reason given for compound **3**, thus compound **4** had the chemical structure as shown with a trivial name of incarnatin D.

Compound **6** was obtained as a brown powder. All signals in the ^1H NMR spectrum appeared as singlet and the methine carbon at C-9 in the ^{13}C NMR spectrum of compound **1** was replaced by a quaternary carbon at δ_C 170.6. Moreover, in the ^1H NMR spectrum the AB pattern of two non-equivalent methylene signals at H_2-5 and H_2-7 in compound **1** was replaced with two singlet methylene signals at δ_H 3.61 and 5.33. In HMBC spectrum, these signals correlated to the quaternary carbon at δ_C 170.6. The spectroscopic evidence suggested that the methine at H-6 in **1** was oxidized to carbonyl lactone, which showing an absorption peak at ν_{max} 1724 cm^{-1} in the FTIR spectrum. Thus, compound **6** possessed the chemical structure as shown in Fig. 1 and HRESIMS data confirmed its molecular formula $C_{15}H_{18}O_3$ by revealing the mass ion peak at *m/z* 245.1188 $[M-H]^-$. Incarnolactone A was given as its trivial name. Compound **6** was similar to lactonic acid, which obtained from an alkali treatment with the naturally isolated illudalic acid (Nair et al., 1969).

Compound **7**, isolated as a colourless solid, had the molecular formula $C_{15}H_{18}O_4$ as deduced by a sodium-adduct precursor ion peak at *m/z* 285.1095 $[M+Na]^+$. The mass spectral data showed 16 mass units higher than that of **6**, suggesting an additional hydroxyl group. The ^1H NMR spectral data was similar to that of **6**, except that two methyl

signals at C-12 appeared as two singlets (resonating at δ_H 1.00 and 1.20), the methylene at C-1 appeared as two doublets (resonating at δ_H 2.57 and 2.69), and an extra singlet oxymethine at δ_H 5.03 were observed. The non-equivalent methylene protons at C-1 indicated the presence of a hydroxyl group at C-11, which was confirmed by HMBC correlations from H-11 to C-2, C-9, C-10, and 12-CH_3 (×2). Unfortunately, Mosher modification with compound **7** cannot be done due to an inadequate amount. Although, compound **7** was similar to radulactone, isolated from the fungus *Radulomyces confluens*, the stereochemistry has not been identified (Fabian et al., 1998). Moreover, due to the low value of optical rotation ($[\alpha]_D^{24}$ + 8.80 in $CHCl_3$), compared with that of the similar compound, pterolacton A ($[\alpha]_D^{22}$ + 97.0 in $CHCl_3$) (Murakami et al., 1980), the absolute configuration at C-11 could not then be certainly assigned. Thus, the chemical structure of compound **7** was then depicted as shown in Fig. 1 and the name incarnolactone B was given.

Compound **8** was obtained as a brown gum. The ^{1}H NMR spectrum was similar to that of compound **6**, except that two methyl signals at C-12 appeared as two singlets (slightly different) and the methylene protons of H_2-7 appeared as two doublets (at δ_H 5.42 and 5.49). In addition, in the ^{13}C NMR spectrum differentiated by DEPT-135 spectrum, the methylene carbon at δ_C 32.7 in compound **6** was absence and instead an additional oxymethine at δ_C 66.4 was present in compound **8**. The evidence from the NOESY spectrum, showing a cross-peak correlation between H-5 and 3-CH_3, suggested that the oxymethine should be placed at C-5. HRESIMS data confirmed the molecular formula $C_{15}H_{18}O_4$, establishing the sodium-adduct precursor ion peak at *m/z* 285.1098 $[M+Na]^+$. The absolute configuration at C-5 could not be assigned due to low value of optical rotation ($[\alpha]_D^{26}$ − 6.76, $CHCl_3$), compared with that of the related compound, echinolactone B ($[\alpha]_D^{25}$ − 24, $CHCl_3$) (Suzuki et al., 2005). Therefore, the chemical structure of compound **8** was illustrated in Fig. 1 and incarnolactone C was given as its trivial name.

Compound **9** was obtained as a brown gum and HRESIMS spectrum showed the sodium-adduct precursor ion peak at *m/z* 299.1625 $[M+Na]^+$, suggesting the molecular formula $C_{17}H_{24}O_3$. In the ^{1}H NMR spectrum, apart from two *trans*- methine signals appeared as doublet at δ_H 5.71 (d, *J* = 13.1 Hz, H-10) and 6.49 (d, *J* = 13.1 Hz, H-11), there were all singlet signals of two methyls (at δ_H 1.14 and 2.00), three methylenes (δ_H 2.64, 2.67, and 4.58), two methoxyls (δ_H 3.35 and 3.69), and a hydroxyl proton (δ_H 7.50). HMBC spectrum showed correlations from 9-CH_3 to C-1, C-8, and C-9; from 3-CH_3 to C-2, C-3, and C-4; from H_2-12 to C-4, C-5, and C-6, and 12-OCH_3; from 12-OCH_3 to C-12; from H-11 to 11-OCH_3; and from 6-OH to C-5, C-6, and C-7. Moreover, the NOESY spectrum showing cross-peak correlation from 11-OCH_3 to H-10 confirmed *trans*-configuration of double bond at C-10 and C-11. The spectral information indicated the remaining signals of (*E*)-methoxyvinyl group being substituted at C-4. Therefore, compound **9** had the chemical structure as shown in Fig. 1 and should be derived from compound **2** (incarnatin B). The name incarnatin E was then given. Compound **9** was related to riparol B, formerly isolated from the mushrooms *Ripartites metrodii*, *R. tricholoma* (Weber et al., 2006), and recently from *Granulobasidium vellereum* (Kokubun et al., 2016).

Compound **10** was obtained as a brown gum. HRESIMS spectrum revealed the molecular formula $C_6H_{22}O_3$ by giving a sodium-adduct precursor ion peak at *m/z* 285.1470 $[M+Na]^+$. The ^{1}H NMR spectrum showed the signals of three methyls [at δ_H 1.14 (s), 1.16 (s), and 2.16 (s)], three methylenes [at δ_H 2.66 (s), 2.74 (d, *J* = 15.5 Hz)/2.80 (d, *J* = 15.5 Hz), and 3.65 (dd, *J* = 10.7, 5.6 Hz)/4.08 (dd, *J* = 10.7, 9.2 Hz)], one sp^3 methine [at δ_H 3.82 (dd, *J* = 9.2, 5.6)], two aromatic methines [at δ_H 6.90 (d, *J* = 7.8 Hz) and 6.97 (d, *J* = 7.8 Hz)]. In the ^{13}C NMR spectrum, the quaternary signal at δ_C 173.9 indicated a presence of an ester group, corresponding to an absorption peak in the FTIR spectrum at ν_{max} 1736 cm^{-1}. In addition, HMBC spectrum displayed the correlations from 9-CH_3 to C-1, C-8, and C-9; from H_2-1 to C-2, C-3, and C-8; from H_2-8 to C-2, C-6, and C-7; from 3-CH_3 to C-2, C-3 and C-4; from H-5 to C-3, C-7, and C-10; from H-4 to C-2 and C-6; from H-10 to C-6, C-7, C-11, and C-12; and from 12-OCH_3 to C-12. The spectral data led to methyl 3-hydroxy-2-(2,2,7-trimethyl-2,3-dihydro-1*H*-inden-4-yl)propanoate. The methylene protons of H_2-3 were resonated non-equivalently due to an effect from substituents on the chiral center at C-10. The absolute configuration of compound **10** was assigned as *S* by comparison of the specific rotation ($[\alpha]_D^{26}$ +18.51, MeOH) with the synthesized compound, methyl (*S*)-2-(7-hydroxy-2,3-dihydro-1*H*-inden-4-yl)propanoate ($[\alpha]_D^{25}$ + 44, $CHCl_3$) (Nakano and Lupton, 2016). Therefore, compound **10** had alliacane-type structure as shown in Fig. 1 with the name incarnate methyl ester.

Compound **11** was obtained as a brown gum. The ^{1}H NMR spectrum was similar to that of **10**, except an absence of signals in the area δ_H 3.5–4.2 and a presence of two additional methylene protons, which belonged to the vinylic methylene carbon at δ_C 126.9, which observed in the HMQC spectrum. In HMBC spectrum, these vinylic methylene protons correlated to C-6 and C-10. The spectroscopic evidence elaborated a loss of water in compound **10**. Moreover, the lack of a methoxy group and a presence of low field carbon at 167.9 indicated the replacement of methyl ester to a carboxylic acid, which characterized by FTIR absorption at 3000–3500 (br) and ν_{max} 1725 cm^{-1}. HRESIMS data gave a sodium-adduct precursor ion peak at *m/z* 253.1197 $[M+Na]^+$, confirming the molecular formula $C_{15}H_{18}O_2$. Therefore, compound **11** possessed the chemical structure as shown in Fig. 1 and incarnetic acid was given as the trivial name.

Compound **12** was obtained as a colourless gum and HRESIMS data established the molecular formula $C_{17}H_{22}O_4$, determined by the sodium-adduct precursor ion peak at *m/z* 313.1416 $[M+Na]^+$. The ^{1}H NMR spectrum gave signals of three methyl (at δ_H 1.07, 1.10, and 1.38), two methoxy (at δ_H 3.35 and 3.54), three sets of non-equivalent methylene (at δ_H 2.39/2.50, 2.65/2.76, and 5.53/6.02) and one oxymethine (at δ_H 4.54). In the ^{13}C NMR spectrum, seventeen signals differentiated by DEPT-135 spectrum included three methyl, two methoxy, three methylene, one oxymethine, and eight quaternary carbons. HMBC spectrum showed correlations from H_3-12 and H_3-13 to C-1, C-10, C-11, and C-13/C-12; from H_3-14 to C-2, C-3, C-4, and C-7; from H_2-1 to C-2 and C-9; from H_2-6 to C-4, C-5, and C-7; from H_2-15 to C-3, C-4, and C-5; from H-8 to C-7, C-9, and 8-OCH_3; from 8-OCH_3 to C-8; and from 7-OCH_3 to C-7. Moreover, the relative configuration could be assigned by the aid of the NOESY spectrum, by showing cross-peak correlations from H-8/7-OCH_3 and H_3-14, 7-OCH_3/H_3-14, and H_3-14/H_a-15 revealed the *cis*– relationship between H-8, 7-OCH_3, and 14-CH_3. Thus, the chemical structure of compound **12** was assigned with the relative configuration as shown in Fig. 1 with the name incarnatenin. Compound **12** was similar to the tricyclic sesquiterpene hirsutenol D, earlier isolated from the culture broth of the mushroom *Stereum hirsutum* (Yoo et al., 2006).

The ^{1}H, ^{13}C NMR spectrum and its physical properties of the known compounds (**13** and **14**) were in agreement with the documented data (Aoki et al., 2002; Li et al., 2012). Chondrosterin B (**13**) and (*E*)-dictyochromenol (**14**) were previously isolated from the soft coral-associated fungus *Chondrostereum* sp. (Li et al., 2012) and the brown alga *Dictyopteris undulate* Holmes, respectively (Dave et al., 1984). In addition, the specific rotation of the isolated compound **14** ($[\alpha]_D^{25}$ −6.70, c 0.18, $CHCl_3$) indicated its presence as a racemate, compared to those of synthesized *R/S*-(*E*)-dictyochromenol and *R/S*-(*Z*)-dictyochromenol (Aoki et al., 2002). Moreover, the methyl carbon substituted at C-4′ (δ_C 15.9) elaborated the *E*-configuration assignment of the double bond (Aoki et al., 2002), therefore compound **14** was obtained as enantiomeric mixture at C-2, typically isolated from the natural products (Bukuru et al., 2002; Dave et al., 1984).

The isolated compounds were assessed for antimicrobial activity, including antimalarial (*P. falciparum*, K-1 strain), anti-TB (*Mycobacterium tuberculosis* H37Ra), and anti-*B. cereus* activities, and for cytotoxicity against KB, MCF-7, NCI-H187, and Vero cells. Incarnatin B (**2**) and chondrosterin B (**13**) exhibited antimalarial (IC_{50}

Table 3
^{1}H and ^{13}C NMR assignments of compounds **9–11** in acetone-d_6.

position	incarnatin E (9)[a]		incarnate methyl ester (10)[b]		incarnetic acid (11)[b]	
	δ_H, (mult., *J* in Hz)	δ_C, type	δ_H, (mult., *J* in Hz)	δ_C, type	δ_H, (mult., *J* in Hz)	δ_C, type
1	2.64 (s)	48.0, CH_2	2.66 (s)	47.2[e], CH_2	2.66 (s)	47.3, CH_2
2		144.1, qC		143.2, qC		134.5, qC
3		124.2, qC		133.4, qC		143.3, qC
4		135.0[c], qC	6.90 (d, 7.8)	128.4, CH	6.94 (d, 8.5)	127.9[f], CH
5		121.0[c], qC	6.97 (d, 7.8)	125.7, CH	6.96 (d, 8.5)	128.0[f], CH
6		151.8, qC		131.0, qC		133.2, qC
7		127.4, qC		142.9, qC		142.5, qC
8	2.67 (s)	45.0, CH_2	2.74 (d, 15.5)[d] 2.80 (d, 15.5)[d]	47.3[e], CH_2	2.64 (s)	48.2, CH_2
9		40.0, qC		39.8, qC		40.2, qC
10	5.71 (d, 13.1)	101.5, CH	3.82 (dd, 9.2, 5.6)	52.6, CH		143.0, qC
11	6.49 (d, 13.1)	151.8, CH	3.65 (dd, 10.7, 5.6)[d] 4.08 (dd, 10.7, 9.2)	64.4, CH_2	5.73 (d, 1.2) 6.36 (d, 1.2)	126.9, CH_2
12	4.58 (s)	70.0, CH_2	–	173.9, qC	–	167.9, qC
2 × 9-CH_3	1.14 (s)	29.9, CH_3	1.14 (s) 1.16 (s)	29.2, CH_3	1.12 (s)	29.2, CH_3
3-CH_3	2.00 (s)	30.0, CH_3	2.16 (s)	18.8, CH_3	2.20 (s)	19.0, CH_3
6-OH	7.50 (s)	–	–	–	–	–
11-O**C**H_3	3.69 (s)	56.3, CH_3	–	–	–	–
12-O**C**H_3	3.35 (s)	57.8, CH_3	3.62 (s)	51.8, CH_3	–	–

[a] Recorded in 500 MHz for ^{1}H NMR and 125 MHz for ^{13}C NMR.
[b] Recorded in 400 MHz for ^{1}H NMR and 100 MHz for ^{13}C NMR.
[c] Observed in HMBC spectrum.
[d] Resolved from ^{1}H NMR spectral data recorded in CD_3OD.
[e] Exchangeable.
[f] Exchangeable.

3.93 and 3.10 μg/mL) and anti-TB (MIC 50.0 and 12.5 μg/mL) activities, while compound **13** also showed anti-*B. cereus* with MIC value of 25.0 μg/mL with strong cytotoxicity against both cancerous and non-cancerous cells (Table 4). In addition, compound **13** was earlier reported to be inactive (IC_{50} > 200 μM) against three cancer cell lines (human cancer cell A549, human nasopharyngeal carcinoma cell CNE2, and human colon cancer cell LoVo) (Li et al., 2012). Biological activity results of compounds **2** and **3** implied that a presence of hydroxyl group at C-11 resulted in a loss of antimicrobial activity (antimalarial and anti-TB) and cytotoxic activity. Incarnatin A (**1**), possessing antimalarial activity with IC_{50} value of 9.80 μg/mL without cytotoxic activity at maximum tested concentration (50 μg/mL), suggested the effect of hydroxyl substituent at C-6 for antimalarial activity, while incarnolactone C (**8**) indicated the effect of hydroxyl group at C-5 for anti-*B. cereus* activity. (*E*)-Dictyochromenol (**14**) displayed antimicrobial activity against *Mycobacterium tuberculosis* and *B. cereus* with MIC values of 12.50 and 1.56 μg/mL, respectively, and had cytotoxicity against cancerous (IC_{50} 5.62–35.05 μg/mL) and non-cancerous (Vero, IC_{50}

Table 4
Antimicrobial activity and cytotoxicity of the isolated compounds.

Compound	Antimalarial[a]	Anti-TB[b]	Anti *B. cereus*[c]	Cytotoxicity[d] (IC_{50}, μg/mL)			
	(IC_{50}, μg/mL)	(MIC, μg/mL)	(MIC, μg/mL)	MCF-7	KB	NCI-H187	Vero
1	9.80	> 50	> 25	> 50	> 50	> 50	> 50
2	3.93	50.0	> 25	29.76	28.15	22.97	18.86
3	> 10	> 50	> 25	> 50	> 50	> 50	> 50
6	> 10	> 50	> 25	> 50	> 50	> 50	> 50
8	> 10	> 50	25.0	> 50	37.97	47.25	47.52
10	> 10	50.0	25.0	15.15	11.79	7.27	2.99
13	3.10	12.5	25.0	4.98	2.05	0.63	0.65
14	> 10	12.5	1.56	17.09	5.62	35.05	9.34
dihydroartemisinin	8.8×10^{-4}	nt	nt	nt	nt	nt	nt
mefloquine	0.025	nt	nt	nt	nt	nt	nt
rifampicin	nt	0.025	nt	nt	nt	nt	nt
ofloxacin	nt	0.391	nt	nt	nt	nt	nt
streptomycin	nt	0.313	nt	nt	nt	nt	nt
isoniazid	nt	0.047	nt	nt	nt	nt	nt
ethambutol	nt	0.469	nt	nt	nt	nt	nt
ellipticine	nt	nt	nt	nt	3.19	2.95	1.52
doxorubicin	nt	nt	nt	9.56	0.68	0.13	nt
tamoxifen	nt	nt	nt	7.45	nt	nt	nt
vancomycin	nt	nt	2.0	nt	nt	nt	nt

nt = not being tested.
[a] Maximum tested concentration was done at 10 μg/mL.
[b] Maximum tested concentration was done at 50 μg/mL.
[c] Maximum tested concentration was done at 25 μg/mL.
[d] Maximum tested concentration was done at 50 μg/mL.

9.34 μg/mL) cells. Compound **14** was also reported earlier for having potent antifeedant activity (Dave et al., 1984). Furthermore, compounds **3** and **6** were inactive to all tests.

3. Experimental section

3.1. General procedures

Mps were recorded on a melting point MP90 apparatus from Mettler Toledo. UV spectra were done in MeOH, using a Spekol 1200, Analytik Jena AG. IR spectra were obtained by using a Bruker ALPHA FT-IR spectrometer. Optical rotations were taken in either $CHCl_3$ or MeOH on a JASCO P-1030 polarimeter. CD spectrum were done on a JASCO J-810 spectropolarimeter in MeOH. NMR spectra, including ^1H, ^{13}C, DEPT-135, COSY, NOESY, HMQC (or HSQC) and HMBC experiments, were recorded on either Bruker Avance 500 NMR spectrometer (at 500 MHz for ^1H and 125 MHz for ^{13}C) or Bruker Avance III 400 NMR spectrometer (at 400 MHz for ^1H and 100 MHz for ^{13}C), using either acetone-d_6 or $CHCl_3$ as internal standards. HR-ESI–MS data were determined on a Bruker MicrOTOF mass spectrometer. Preparative HPLC were performed using Dionex, Ultimate 3000 series model, which was equipped with a binary pump, an autosampler and a diode array detector. Preparative HPLC were assembled with a Waters Sunfire C18 OBD column (diam. 19 × 250 mm^2, particle size 10 μm) at a flow rate of 15 mL/min, respectively, unless otherwise mentioned.

3.2. Fungal material

The fungus was collected from an unidentified wood at Khao Nan National Park, Nakhon Si Thammarat province, Thailand. The fungal identification was done based on the partial nuclear large subunits ribosomal DNA (nc28S rDNA, 945 bps) and the internal transcribed spacer (ITS region, 639 bps). The combined nc28S rDNA and ITS sequences (1584 bps) indicated affinity with fungal taxa within Cyphellaceae, Agaricales, Agaricomycetidae, Agaricomycetes, Agaricomycotina, Basidiomycota and showed 97% similarity with *Gloeostereum incarnatum* AF141637 using BLAST (the Basic Local Alignment Search Tool) from GenBank and PSA (the Pairwise Sequence Alignment) from Mycobank. Thus, the fungus was identified as *Gloeostereum incarnatum* in Cyphellaceae, Agaricales, Agaricomycetidae, Agaricomycetes, Agaricomycotina, Basidiomycota, registered as BCC41461 at BIOTEC Culture Collection (BCC). The ITS and nc28S rDNA sequences were assigned with GenBank accession numbers KY614001 and KY614002, respectively.

3.3. Fermentation, extraction, and isolation

The fungus was grown on PDA (potato dextrose agar) at 25 °C for 19 days and then cut into small pieces (1 × 1 cm^2). Each piece was transferred into ten 1L Erlenmeyer flasks, which each contained 250 mL PDB (potato dextrose broth). The seed culture was grown at 25 °C on a rotary shaker at 200 rpm for 19 days and then every 25 mL of the seed culture was transferred into 1L Erlenmeyer flasks, which filled with 250 mL MEB (malt extract broth). The production culture (20L) was cultivated at 25 °C for 26 days at static condition. The broth and cell were then separated by simple filtration. The broth was extracted with equal volumn of EtOAC three times. The EtOAc was dried over Na_2SO_4 and then evaporated to dryness to yield a brown gum (9.7 g). The cell was macerated with MeOH for 3 days and followed by CH_2Cl_2 for 3 days. The organic solvents were then combined and concentrated by using rotary evaporator. Water (100 mL) was added and the mixture was then extracted with an equal volume of EtOAc three times. The EtOAc was dried over Na_2SO_4 and the evaporated to dryness to yield a brown gum (3.3 g).

A brown gum obtained from broth (9.7 g) was passed through a Sephadex LH20 column (4.5 cm × 40 cm), eluted with 100% MeOH, to give three main fractions. The first fraction (F1, 3.5 g) was re-chromatographed through a Sephadex LH20 column (4.5 cm × 40 cm), eluted with 100% MeOH, to afford 2 subfractions (F1-1 and F1-2). Subfraction F1-1 (2.5 g) was passed through another Sephadex LH20 column to give two fractions (F1-1-1 and F1-1-2) prior to purifying by a preparative HPLC, using a 45 min linear gradient of acetonitrile: water (20:80–65:35) monitored at 210 nm. Subfraction F1-1-1 (1.0 g) furnished compounds **12** (4.8 mg) and **10** (8.0 mg), while subfraction F1-1-2 (0.5 g) furnished compounds **13** (31.7 mg), **10** (4.1 mg), **2** (6.9 mg), and **9** (2.3 mg), respectively. Subfraction F1-2 (0.3 g) was purified by preparative HPLC, using a 45 min linear gradient of acetonitrile: water (20:80–65:35) monitored at 210 nm to yield compounds **13** (17.4 mg), **1** (8.0 mg), **14** (5.0 mg), and **2** (19.4 mg). The second fraction (F2, 3.5 g) was subjected to a Sephadex LH20 column (4.5 cm × 40 cm), eluted with 100% MeOH, to obtain 2 subfractions (F2-1 and F2-2). Subfraction F2-1 (2.9 g) was purified by preparative HPLC, using the same aforementioned system, to furnish compounds **13** (0.2 g), **6** (24.7 mg), **8** (1.8 mg), **2** (0.12 g), **3** (8.4 mg), **11** (3.7 mg), and **4** (6.3 mg), respectively. Subfraction F2-2 (0.5 g) was further purified by preparative HPLC using the previous condition to obtain compounds **7** (4.8 mg), **1** (39.6 mg), **2** (56.2 mg), and **5** (4.8 mg), respectively. The third fraction (F3, 0.1 g) was further purified by preparative HPLC, using a 40 min linear gradient of acetonitrile: water (20:80–70:30) monitored at 210 nm, to furnish compounds **7** (1.9 mg), **1** (11.9 mg), **6** (6.8 mg), and **2** (15.8 mg), respectively.

The crude from cell (3.3 g) was subjected to a Sephadex LH20 column (4.5 cm × 40 cm), eluted with 100% MeOH and followed by preparative HPLC, using a 55 min linear gradient of acetonitrile: water (20:80–65:35) monitored at 210 nm, to furnish compounds **6** (25.5 mg), **2** (42.4 mg), and **14** (0.1 g), respectively.

3.3.1. Incarnatin A (1)

Brown powder, mp 183–185 °C; $[\alpha]_D^{25}$ −3.34 (*c* 0.10, $CHCl_3$) and $[\alpha]_D^{25}$ − 8.84 (*c* 0.11, MeOH); UV (MeOH) λ_{max} (log ε) 230 (3.33), 272 (3.04), 327 (2.23), 424 (1.83) nm; FTIR (ATR) ν_{max} 3374, 2951, 2925, 2865, 2836, 1705, 1623 (w), 1596, 1455, 1382, 1364, 1347 (w), 1287, 1237, 1222, 1128, 1080, 1039, 1027, 1000, 989, 895, 873 cm^{-1}; ^1H NMR (400 MHz, acetone-d_6) and ^{13}C NMR (100 MHz, acetone-d_6) data, see Tables 1 and 2; HRESIMS *m/z* 271.1312 $[M+Na]^+$ (calcd for $C_{15}H_{20}O_3Na$, 271.1305).

3.3.2. Incarnatin B (2)

Brown powder, mp 82–84 °C; $[\alpha]_D^{25}$ −11.60 (*c* 0.12, $CHCl_3$) and $[\alpha]_D^{25}$ − 6.82 (*c* 0.11, MeOH); UV (MeOH) λ_{max} (log ε) 230 (3.39), 277 (3.15), 328 (2.75), 424 (2.65) nm; FTIR (ATR) ν_{max} 3390, 2951, 2926, 2864, 2835, 1705, 1623, 1598, 1455, 1384, 1364, 1286, 1222, 1189, 1137, 1082, 1057, 1039, 989, 861 cm^{-1}; ^1H NMR (400 MHz, acetone-d_6) and ^{13}C NMR (100 MHz, acetone-d_6) data, see Tables 1 and 2; HRESIMS *m/z* 261.1492 $[M-H]^-$ (calcd for $C_{16}H_{21}O_3$, 261.1496).

3.3.3. Incarnatin C (3)

Brown powder; UV (MeOH) λ_{max} (log ε) 232 (3.29), 279 (3.12), 326 (2.24), 423 (1.94) nm; FTIR (ATR) ν_{max} 3395, 2596, 2926, 2861, 1738, 1714, 1631, 1603, 1456, 1383, 1364, 1301, 1251, 1189, 1137, 1085, 1058, 1041, 986, 860 cm^{-1}; ^1H NMR (400 MHz, acetone-d_6) and ^{13}C NMR (100 MHz, acetone-d_6) data, see Tables 1 and 2; HRESIMS *m/z* 277.1449 $[M-H]^-$ (calcd for $C_{16}H_{21}O_4$, 277.1445).

3.3.4. Incarnatin D (4)

Colourless gum; UV (MeOH) λ_{max} (log ε) 230 (3.71), 268 (3.74), 424 (2.88) nm; FTIR (ATR) ν_{max} 3425, 2956, 2925, 2854, 1737, 1632, 1605, 1459, 1384, 1365, 1356, 1313, 1256, 1228, 1189, 1137, 1110, 1085, 1061, 997, 859 cm^{-1}; ^1H NMR (400 MHz, acetone-d_6) and ^{13}C NMR (100 MHz, acetone-d_6) data, see Tables 1 and 2; HRESIMS *m/z* 315.1582 $[M+Na]^+$ (calcd for $C_{17}H_{24}O_4Na$, 315.1567).

*3.3.5. Incarnatin F (**5**)*

Brown gum; $[\alpha]_D^{25}$ − 7.84 (*c* 0.16, MeOH); ^{1}H NMR (400 MHz, acetone-d_6) 1.14 (6H, s, 2 × 12-CH_3), 2.02 (3H, s, 3-CH_3), 2.53 (1H, dd, *J* = 16.3, 5.0 Hz, 5-H_a), 2.64 (2H, s, 1-H_2), 2.76 (2H, s, 11-H_2), 2.78 (1H, dd, *J* = 16.3, 3.2 Hz, 5-H_b), 3.71 (3H, s, 9-OC***H*₃**), 4.63 (1H, d, *J* = 15.3 Hz, 7-H_a), 4.86 (1H, d, *J* = 15.3 Hz, 7-H_b), 5.21 (1H, t, *J* = 4.38 Hz, 6-H); HRESIMS *m/z* 285.1467 $[M+Na]^+$ (calcd for $C_{16}H_{22}O_3Na$, 285.1461).

*3.3.6. Incarnolactone A (**6**)*

Brown powder, mp 182–184 °C; UV (MeOH) λ_{max} (log ε) 230 (3.54), 282 (3.25), 327 (2.75), 426 (2.67) nm; FTIR (ATR) ν_{max} 3386, 2953, 2926, 2861, 1724, 1601, 1464, 1386, 1365, 1299, 1247, 1221, 1105, 1093, 1033, 1006 cm^{-1}; ^{1}H NMR (400 MHz, acetone-d_6) and ^{13}C NMR (100 MHz, acetone-d_6) data, see Tables 1 and 2; HRESIMS *m/z* 245.1188 $[M-H]^-$ (calcd for $C_{15}H_{17}O_3$, 245.1183).

*3.3.7. Incarnolactone B (**7**)*

Colourless solid; $[\alpha]_D^{24}$ +8.80 (*c* 0.09, $CHCl_3$); UV (MeOH) λ_{max} (log ε) 232 (3.44), 284 (3.26), 318 (2.68), 424 (2.26) nm; FTIR (ATR) ν_{max} 3385, 2955, 2925, 2854, 1727, 1608, 1466, 1384, 1366, 1305, 1291, 1244, 1219, 1163, 1110, 1081, 1034, 997 cm^{-1}; ^{1}H NMR (500 MHz, acetone-d_6) and ^{13}C NMR (125 MHz, acetone-d_6) data, see Tables 1 and 2; HRESIMS *m/z* 285.1095 $[M+Na]^+$ (calcd for $C_{15}H_{18}O_4Na$, 285.1097).

*3.3.8. Incarnolactone C (**8**)*

Brown gum; $[\alpha]_D^{26}$ − 6.76 (*c* 0.18, $CHCl_3$); UV (MeOH) λ_{max} (log ε) 223 (3.68), 286 (3.36), 424 (2.93) nm; FTIR (ATR) ν_{max} 3396, 2953, 2926, 2864, 1728, 1601, 1463, 1383, 1365, 1343, 1267, 1231, 1218, 1134, 1091, 1029, 1000 cm^{-1}; ^{1}H NMR (500 MHz, acetone-d_6) and ^{13}C NMR (125 MHz, acetone-d_6) data, see Tables 1 and 2; HRESIMS *m/z* 285.1098 $[M+Na]^+$ (calcd for $C_{15}H_{18}O_4Na$, 285.1097).

*3.3.9. Incarnatin E (**9**)*

Brown gum; UV (MeOH) λ_{max} (log ε) 230 (3.60), 283 (3.25), 424 (2.09) nm; FTIR (ATR) ν_{max} 3385, 2952, 2928, 2866, 1707, 1639, 1460, 1383, 1365, 1208, 1157, 1133, 1091, 1040, 1002, 940 cm^{-1}; ^{1}H NMR (500 MHz, acetone-d_6) and ^{13}C NMR (125 MHz, acetone-d_6) data, see Table 3; HRESIMS *m/z* 299.1625 $[M+Na]^+$ (calcd for $C_{17}H_{24}O_3Na$, 299.1618).

*3.3.10. Incarnate methyl ester (**10**)*

Brown gum;$[\alpha]_D^{26}$ +3.36 (*c* 0.14, $CHCl_3$) and $[\alpha]_D^{26}$ +18.51 (0.20, MeOH); CD (MeOH, *c* 0.016 g/L) Δε (nm): +2.2 (221), +0.4 (357); UV (MeOH) λ_{max} (log ε) 232 (3.58), 265 (3.47), 423 (2.74) nm; FTIR (ATR) ν_{max} 3393, 2952, 2927, 2864, 1736, 1462, 1435, 1379, 1365, 1229, 1217, 1205, 1159, 1081, 1039 cm^{-1}; ^{1}H NMR (400 MHz, acetone-d_6) and ^{13}C NMR (100 MHz, acetone-d_6) data, see Table 3; HRESIMS *m/z* 285.1470 $[M+Na]^+$ (calcd for $C_{16}H_{22}O_3Na$, 285.1461).

*3.3.11. Incarnetic acid (**11**)*

Brown gum; UV (MeOH) λ_{max} (log ε) 235 (3.48), 262 (3.36), 424 (2.61) nm; FTIR (ATR) ν_{max} 3385 (br), 2952, 2926, 2865, 1737, 1725, 1619, 1460, 1378, 1365, 1227, 1217, 1095, 1038 cm^{-1}; ^{1}H NMR (400 MHz, acetone-d_6) and ^{13}C NMR (100 MHz, acetone-d_6) data, see Table 3; HRESIMS *m/z* 253.1197 $[M+Na]^+$ (calcd for $C_{15}H_{18}O_2Na$, 253.1199).

*3.3.12. Incarnatenin (**12**)*

Colourless gum; $[\alpha]_D^{26}$ +18.71 (0.24, MeOH); UV (MeOH) λ_{max} (log ε) 238 (3.45), 324 (2.38), 424 (1.78) nm; FTIR (ATR) ν_{max} 2957, 2925, 2854, 1729, 1703, 1633, 1462, 1380, 1360, 1278, 1237, 1196, 1161, 1119, 1090, 1079 cm^{-1}; ^{1}H NMR (400 MHz, acetone-d_6) 1.07 (3H, s, 13-CH_3), 1.10 (3H, s, 12-CH_3), 1.38 (3H, s, 14-CH_3), 2.39 (1H, dd, *J* = 18.8, 1.5 Hz, 1-H_a), 2.50 (1H, dd, *J* = 18.8, 2.8 Hz, 1-H_b), 2.65 (1H, d, *J* = 18.9, 2.8 Hz, 6-H_a), 2.76 (1H, d, *J* = 18.9 Hz, 6-H_b), 3.35 (3H, s, 7-OCH_3), 3.54 (3H, s, 8-OCH_3), 4.54 (1H, t, *J* = 2.1 Hz, 8-H), 5.53 (1H, s, 15-H_a), 6.02 (1H, s, 15-H_b); ^{13}C NMR (100 MHz, acetone-d_6) 19.3 (14-**C**H_3), 25.3[a] (12-**C**H_3), 25.6[a] (13-**C**H_3), 39.4 (1-**C**H_2), 42.0 (6-**C**H_2), 49.7 (11-C), 52.7 (7-O**C**H_3), 58.1 (3-C), 58.9 (8-O**C**H_3), 83.9 (8-CH), 96.0 (7-C), 118.2 (15-**C**H_2), 142.9 (9-C), 150.3 (4-C), 185.3 (2-C), 202.2 (5-C), 207.7 (10-C); HRESIMS *m/z* 313.1416 $[M+Na]^+$ (calcd for $C_{17}H_{22}O_4Na$, 313.1410). [a] = exchangeable

3.4. Biological assays

All isolated compounds except **4**, **5**, **7**, **9**, **11**, and **12** were evaluated for antimicrobial activity against malaria parasite *P. falciparum* (K1-multidrug resistant strain), bacteria *Mycobacterium tuberculosis* H37Ra (TB) and *Bacillus cereus* (ATCC 11778) and for cytotoxicity against both cancerous (KB, MCF-7, NCI-H187) and non-cancerous (Vero) cells. The microculture radio isotope technique was used to study antimalarial activity against the multidrug–resistant *Plasmodium falciparum*, K1 strain(Desjardins et al., 1979). The green fluorescent protein microplate assay (GFPMA) was performed to evaluate the growth inhibitory activity against *Mycobacterium tuberculosis* H37Ra and cytotoxicity against Vero cells (African green monkey kidney fibroblasts, ATCC CCL-81) (Changsen et al., 2003). The resazurin microplate assay (REMA) was employed to evaluate anti-*Bacillus cereus* and cytotoxicity against KB (human epidermoid carcinoma, ATCC CCL-17), MCF-7 (human breast cancer, ATCC HTC-22) and NCI-H187 (human small lung cancer, ATCC CRL-5804) cells (O'Brien et al., 2000). Dihydroartemisinine and mefloquine were used as positive controls for antimalarial activity and showed IC_{50} values of 8.76×10^{-4} and 0.025 μg/mL, respectively. Rifampicin, ofloxacin, streptomycin, isoniazid and ethambutol were used as positive controls for anti-TB activity and displayed MIC values of 0.025, 0.391, 0.313, 0.047, 0.47 μg/mL, respectively. Vancomycin was used as a positive control for anti-*B. cereus* and exhibited MIC value of 2.00 μg/mL. Tamoxifen and doxorubicin were used as positive controls for anti-MCF-7 activity and showed IC_{50} values of 7.45 and 9.56 μg/mL. Doxorubicin and ellipticine were used as positive controls for anti-KB and anti-NCI-H187 activities and showed IC_{50} values of 0.68, 3.19 and 0.13, 2.95 μg/mL, respectively. Ellipticine was used as a positive control for cytotoxicity against Vero cell and displayed IC_{50} value of 1.52 μg/mL. Maximum tested concentration was done at 50 μg/mL, except for anti-*B. cereus* and antimalarial activities were done at 25 and 10 μg/mL, respectively.

Acknowledgements

Financial support from the Thailand Research Fund (TRF grant number: RSA5980001) and the National Center for Genetic Engineering and Biotechnology (BIOTEC grant number: P16-51093) are gratefully acknowledged.

Appendix A. Supplementary data

Supplementary data associated with this article can be found, in the online version, at 10.1016/j.phytol.2017.05.017.

References

Aoki, K., Takahashi, M., Hashimoto, M., Okuno, T., Kurata, K., Suzuki, M., 2002. Total synthesis of both enantiomers of dictyochromenol and their (*Z*)-isomers. Biosci. Biotechnol. Biochem. 66, 1915–1924.

Bukuru, J.F., Van, T.N., Van Puyvelde, L., Mathenge, S.G., Mudida, F.P., De Kimpe, N., 2002. A benzochromene from the roots of *Pentas bussei*. J. Nat. Prod. 65, 783–785.

Changsen, C., Franzblau, S.G., Palittapongarnpim, P., 2003. Improved green fluorescent protein reporter gene-based microplate screening for antituberculosis compounds by utilizing an acetamidase promoter. Antimicrob. Agents Chemother. 47, 3682–3687.

Clericuzio, M., Mella, M., Toma, L., Finzi Paola, V., Vidari, G., 2002. Atlanticones, new protoilludane sesquiterpenes from the mushroom *Lactarius atlanticus* (Basidiomycetes). Eur. J. Org. Chem. 2002, 988–994.

Dave, M.-N., Kusumi, T., Ishitsuka, M., Iwashita, T., Kakisawa, H., 1984. A piscicidal chromanol and a chromenol from the brown alga *Dictyopteris undulata*. Heterocycles 22, 2301–2307.

Desjardins, R.E., Canfield, C.J., Haynes, J.D., Chulay, J.D., 1979. Quantitative assessment of antimalarial activity in vitro by a semiautomated microdilution technique. Antimicrob. Agents Chemother. 16, 710–718.

Fabian, K., Lorenzen, K., Anke, T., Johansson, M., Sterner, O., 1998. Five new bioactive sesquiterpenes from the fungus *Radulomyces confluens* (Fr.) Christ. Z. Naturforsch. C 53, 939–945.

Hiramatsu, F., Murayama, T., Koseki, T., Shiono, Y., 2007. Strobilols A–D: Four cadinane-type sesquiterpenes from the edible mushroom Strobilurus ohshimae. Phytochem. 68, 1267–1271.

Intaraudom, C., Boonyuen, N., Supothina, S., Tobwor, P., Prabpai, S., Kongsaeree, P., Pittayakhajonwut, P., 2013. Novel spiro-sesquiterpene from the mushroom *Anthracophyllum* sp. BCC18695. Phytochem. Lett. 6, 345–349.

Kokubun, T., Scott-Brown, A., Kite, G.C., Simmonds, M.S.J., 2016. Protoilludane, illudane, illudalane, and norilludane sesquiterpenoids from *Granulobasidium vellereum*. J. Nat. Prod. 79, 1698–1701.

Li, H.-J., Xie, Y.-L., Xie, Z.-L., Chen, Y., Lam, C.-K., Lan, W.-J., 2012. Chondrosterins A–E, triquinane-Type sesquiterpenoids from soft coral-Associated fungus *Chondrostereum* sp. Mar. Drugs 10, 627–638.

Malagòn, O., Porta, A., Clericuzio, M., Gilardoni, G., Gozzini, D., Vidari, G., 2014. Structures and biological significance of lactarane sesquiterpenes from the European mushroom *Russula nobilis*. Phytochem. 107, 126–134.

Murakami, T., Wada, H., Tanaka, N., Saiki, Y., Chen, C., 1980. Chemische und chemotaxonomische untersuchungen von filices: XXVII. chemische untersuchungen der inhaltsstoffe von *Dennstaedtia wilfordii* (MOORE) CHRIST. Chem. Pharm. Bull. 28, 1869–1872.

Nair, M.S., Takeshita, H., McMorris, T.C., Anchel, M., 1969. Metabolites of Clitocybe illudens. IV. Illudalic acid, a sesquiterpenoid, and illudinine, a sesquiterpenoid alkaloid. J. Org. Chem. 34, 240–243.

Nakano, Y., Lupton, D.W., 2016. Enantioselective N-heterocyclic carbene catalysis by the umpolung of α, β-unsaturated ketones. Angew. Chem. Int. Ed. 55, 3135–3139.

O'Brien, J., Wilson, I., Orton, T., Pognan, F., 2000. Investigation of the Alamar Blue (resazurin) fluorescent dye for the assessment of mammalian cell cytotoxicity. Eur. J. Biochem. 267, 5421–5426.

Suzuki, S., Murayama, T., Shiono, Y., 2005. Illudalane sesquiterpenoids, echinolactones A and B: from a mycelial culture of *Echinodontium japonicum*. Phytochem. 66, 2329–2333.

Tao, Q., Ma, K., Yang, Y., Wang, K., Chen, B., Huang, Y., Han, J., Bao, L., Liu, X.-B., Yang, Z., Yin, W.-B., Liu, H., 2016. Bioactive sesquiterpenes from the edible mushroom *Flammulina velutipes* and their biosynthetic pathway confirmed by genome analysis and chemical evidence. J. Org. Chem. 81, 9867–9877.

Weber, D., Erosa, G., Sterner, O., Anke, T., 2006. New bioactive sesquiterpenes from *Ripartites metrodii* and *R. tricholoma*. Z. Naturforsch. C 61, 663–669.

Yoo, N.H., Kim, J.P., Yun, B.S., Ryoo, I.J., Lee, I.K., Yoon, E.S., Koshino, H., Yoo, I.D., 2006. Hirsutenols D, E and F, new sesquiterpenes from the culture broth of *Stereum hirsutum*. J. Antibiot. 59, 110–113.

Phytochemistry Letters 25 (2018) 109–117

Contents lists available at ScienceDirect

Phytochemistry Letters

journal homepage: www.elsevier.com/locate/phytol

Anthrone derivatives from the terrestrial actinomycete, *Actinomadura* sp. BCC47066

Nantiya Bunbamrung[a], Khomsan Supong[b], Chakapong Intaraudom[a], Aibrohim Dramae[a], Patchanee Auncharoen[a], Pattama Pittayakhajonwut[a,*]

[a] The National Center for Genetic Engineering and Biotechnology (BIOTEC), 113 Thailand Science Park, Phaholyothin Road, Klong Luang, Pathumthani 12120, Thailand
[b] Department of Applied Science and Biotechnology, Faculty of Agro-Industrial Technology, Rajamangala University of Technology Tawan-ok, Chantaburi Campus, Chantaburi, 22210, Thailand

ARTICLE INFO

Keywords:
Actinomycetes
Actinomadura
Anthrones
Dimeric anthrone peroxide
Antimicrobial
Cytotoxicity

ABSTRACT

Eight new anthrone derivatives, which are (+)-oxanthromicins E (**1**), F (**4**), and G (**5**), (±)-*hemi*-oxanthromicin D (**2**), azanthromicin A (**7**), adxanthromicin A_2 (**10**), 3-methoxy oxanthromicin (**11**), and (±)-oxanthromicin G (**13**), along with eight previously described compounds (**6**, **8**, **9**, **12**, **14**–**17**) have been isolated from the terrestrial actinomycete, *Actinomodura* sp. BCC47066. The chemical structures have been determined on the basis of NMR spectroscopic information and chemical degradation. The configurations were assigned based upon CD spectral analyses, compared with the related compounds. Furthermore, the isolated compounds were assessed for biological activity. Compounds **10**, **12**, and **16** showed anti-*Bacillus cereus* with IC_{50} in a range of 1.56 − 12.50 μg/mL, while compounds **10** and **12** exhibited anti-phytopathogenic activity against *Colletotrichum capsici* and *C. gloeosporioides* with equal IC_{50} value of 6.25 μg/mL. All tested compounds possessed low cytotoxicity against both malignant and non-malignant cells.

1. Introduction

Actinomycetes are well known as an excellent producer for bioactive compounds and almost half of active molecules discovered from natural sources belongs to this group (Berdy, 2005). The genus most frequently found in this order is the genus *Streptomyces*, whose many secondary metabolites have been explored intensely. In order to find new bioactive molecules, the rare genera in this group have been identified and studied, including the genus *Actinomadura*. However, only few secondary metabolites from *Actinomycetes* spp. have been reported, which might be due to inappropriate growing conditions in the laboratory, diverse chemical structures with broad biological activity have been found. Examples of secondary metabolites isolated from the genus *Actinomadura* were antifungal pradimicins A–C from *Actinomadura hibisca* sp. nov. (ATCC 5357) (Tomita et al., 1990), anticancer chandrananimycins A–C from *Actinomadura* sp. M045 (Maskey et al., 2003), a γ-lactone actinomiaolone from *Actinomadura miaoliensis* BCRC 16873 (Cheng et al., 2013), and antibacterial actinomadurol from *Actinomadura* strain KC191 (Shin et al., 2016).

In our chemical screening program, *Actinomadura* sp. BCC47066 showed a prolific chemical profile, which deserved further chemical investigation. The investigation led to the isolation of eight new and eight known compounds. The isolated compounds were also evaluated for antimicrobial activity and for cytotoxicity against both cancerous (KB, MCF-7, NCI-H187) and non-cancerous (Vero) cells.

2. Results and discussion

The actinomycete *Actinomodura* sp. BCC47066 was cultivated in BIO19 for 7 days at 28 °C in shaking condition. The whole culture was extracted with EtOAc and after evaporation, its crude extract was then purified by column chromatography using Sephadex LH-20 column and followed by HPLC to furnish eight new compounds, namely, (+)-oxanthromicins E (**1**), F (**4**), and G (**5**), (±)-*hemi*-oxanthromicin D (**2**), azanthromicin A (**7**), adxanthromicin A_2 (**10**), 3-methoxy oxanthromicin (**11**), and (±)-oxanthromicin H (**13**) and eight known compounds, including (±)-*hemi*-oxanthromicin A (**6**), demethyl oxanthroquinone (**8**), oxanthroquinone (**9**), oxanthromicin (**12**), quercetin 3-glucoside (**14**), kaempferol 3-glucoside (**15**), (±)-*spiro*-oxanthromicin A (**16**), and indole-3-carboxylic acid (**17**).

Compound **1** was obtained as a brown solid and had the molecular formula $C_{24}H_{28}O_8$, which was established by HRESIMS (*m/z* 467.1679 $[M + Na]^+$). The ^{13}C NMR spectrum (Table 2) showed 24 signals, differentiated by DEPT-135 spectrum, consisting of four methyl, one

* Corresponding author.
E-mail address: pattamap@biotec.or.th (P. Pittayakhajonwut).

https://doi.org/10.1016/j.phytol.2018.04.002
Received 13 November 2017; Received in revised form 5 March 2018; Accepted 3 April 2018

methylene, five sp^3 methine, four aromatic methine, and ten quaternary carbons. The evidence from both ^{1}H NMR and ^{13}C NMR spectra indicated the presence of a sugar unit. The NMR spectral data (Tables 1 and 2) together with the positive optical rotation value ($[\alpha]_D^{28}$ + 132.9) suggested that the sugar unit was α-D-galactose (Takahashi et al., 2000). The remaining signals in the ^{1}H NMR spectrum contained signals of four singlet methyls (at δ_H 1.69, 1.70, 2.22, and 2.81), four doublet methines (at δ_H 7.05, 7.14, 7.44, and 7.47), and one chelated phenolic proton (δ_H 13.98). The doublet methines at δ_H 7.14 (H-5) and 7.44 (H-6) indicated an *ortho* position with a coupling constant of 8.0 Hz and correlated in HMBC spectrum to the carbons at C-7, C-8a, C-10 and C-8, C-10a, C-12, respectively, while the doublet methines at δ_H 7.05 (H-2) and 7.47 (H-4) indicated a *meta* position with a coupling constant of 1.9 Hz and correlated in HMBC spectrum to the carbons at C-3, C-4, C-9, C-9a and C-2, C-3, C-9a, C-10, respectively. Moreover, the HMBC spectrum showed correlations from 13-H_3 (δ_H 1.69) and 14-H_3 (δ_H 1.70) to C-4a, C-10, and C-10a; from 12-H_3 (δ_H 2.22) to C-6, C-7, and C-8; from 11-H_3 (δ_H 2.81) to C-1, C-2, and C-9a; and from 8-OH to C-7, C-8, and C-8a. The spectroscopic information suggested that the sugar unit was linked to the oxygen at C-3. Therefore, the chemical structure of compound **1** was depicted as shown in Fig. 1 and named (+)-oxanthromicin E.

Compound **2** was obtained as a brown solid with a molecular formula of $C_{23}H_{26}O_9$, 2 mass units higher than that of compound **1**, determined by HRESIMS (*m/z* 469.1468 $[M + Na]^+$). The ^{1}H NMR spectrum was similar to that of compound **1**, except an absence of a methyl group. Moreover, an absence of the quaternary carbon at δ_C 39.2 in the ^{13}C NMR spectrum and a presence of the quaternary carbon at δ_C 70.3 indicated a replacement of a methyl group at C-10 in compound **1** with a hydroxyl group in compound **2**. HMBC spectrum confirmed that a methyl at δ_H 1.57 (13-H_3) was situated at C-10 (δ_C 70.3) by correlating to the carbons at C-4a, C-10, and C-10a. The ^{13}C NMR spectrum also showed double signals indicating an isomeric mixture at C-10 of compound **2**. Thus compound **2** was assigned as shown in Fig. 1 and (±)-*hemi*-oxanthromicin D was given as its trivial name.

Compound **4** was obtained as a brown gum. The ^{1}H NMR spectrum was similar to that of (±)-*hemi*-oxanthromicin A (**6**), except an absence of a methyl signal and a presence of signals of three contiguous aromatic protons. The spectral information suggested the replacement of a methyl group at C-7 in compound **6** with an aromatic methine at δ_H 6.84 (1H, d, J = 8.1 Hz), showing correlations in HMBC spectrum to C-8 (δ_C 115.1), C-8 (δ_C 160.8), and C-8a (δ_C 115.0). HRESIMS confirmed the molecular formula of $C_{17}H_{13}O_6$ by giving the molecular ion peak at *m/z* 313.0706 $[M-H]^-$. In addition, compound **4** gave a positive optical rotation value ($[\alpha]_D^{25}$ + 40.7), which was opposite to the monomer of oxanthromicin (**12**) ($[\alpha]_D^{21}$ − 73.9) and the CD spectrum of compound **4** (Fig. 2) was opposite to the monomer of the known compound, oxanthormicin (**12**) (Wright et al., 1984). Therefore, the configuration at C-10 of compound **4** was opposite to the reported oxanthromicin (**12**). The chemical structure of compound **4** was thus illustrated as shown in Fig. 1 and compound **4** was then named (+)-oxanthromicin F.

Compound **5** was obtained as a brown gum with the molecular formula $C_{18}H_{16}O_7$, 30 mass units higher than that of compound **4**, established by HRESIMS (*m/z* 367.0790 $[M + Na]^+$). The ^{1}H NMR spectrum of compound **5** was similar to that of compound **6**, except an absence of one methyl signal and the additional oxymethylene signal resonating at δ_H 4.52 (1H, d, J = 15.6 Hz) and 4.54 (1H, d, J = 15.6 Hz). HMBC spectrum correlated these methylene protons to the carbons at C-6 (δ_C 132.9), C-7 (δ_C 128.7), and C-8 (δ_C 158.5), indicating the position of the oxymethylene at C-7. Moreover, compound **5** had the positive optical rotation value ($[\alpha]_D^{25}$ + 40.6), indicating that it has the same configuration at C-10 as compound **4**. Compound **5** was named (+)-oxanthromicin G.

Compound **7** was obtained as yellow gum and its molecular formula was deduced to be $C_{17}H_{17}NO_3$ from the molecular ion peak at *m/z* 284.1285 $[M+H]^+$ in HRESIMS spectrum. The ^{1}H NMR spectrum (Table 1) revealed four singlet methyls (at δ_H 1.58, 2.24, 2.57, and 2.93), three aromatic methines (at δ_H 7.33, 7.49, and 7.73), and a chelated hydroxyl proton (at δ_H 13.08). The ^{13}C NMR spectrum displayed only 15 signals, differentiated by DEPT-135 spectrum, consisting of four methyl, three methine, and eight quaternary carbons. HMBC spectrum showed correlations from H-5 to C-7, C8a, and C-10; from H-6 to C-8, C-10a, and C-13; from H_3-13 to C-6, C-7, and C-8; from 8-OH to C-7, C-8, and C-8a; from H_3-14 to C-4a, C-10, and C-10a; from H-4 to C-3, C-9a, C-10, and C-12; from H_3-11 to C-1 and C-9a; from H_3-12 to C-3 and C-4. HMBC information indicated a similar structure to that of compound **4**, except the two low field carbons at δ_C 160.3 (C-1) and 162.1 (C-3), indicating an attachment to a nitrogen. The remaining carbon at δ_C 190.3 was placed at C-9 due to chelation with a hydroxyl proton (δ_H 13.08) at C-8. Since compound **7** gave the same pattern of CD spectrum (Fig. 2) to those of (−)-*hemi*-oxanthromicin A, the configuration at C-10 was assigned to be the same as that of oxanthromicin **12**. Compound **7** (Fig. 1) was given as a trivial name azanthromicin A. Azanthromicin A is a reduced form of 2-aza-anthraquinone structure, which is rare in nature and had a broad range of antimicrobial and anticancer activities (Abdelfattah et al., 2012; Koyama et al., 2005). Examples of 3-methyl-2-aza-anthraquinone derivatives found in nature are bostrycoidin from *Fusarium bostrycoides* (Arsenault, 1965), tolypocaldin from *Tolypocladium inflatum* (Gräfe et al., 1990), scorpinone from unidentified fungus (Miljkovic et al., 2001), 5-deoxy-7-methylbostrycoidin from mycobionts of the lichen *Haematomma* sp. (Moriyasu et al., 2001), and utahmycin A from *Streptomyces* spp. (Abdelfattah et al., 2012; Bauer et al., 2010).

Compound **10** was obtained as a yellow solid and the molecular formula of $C_{42}H_{40}O_{17}$ was revealed by HRESIMS spectrum, giving the molecular ion peak at *m/z* 815.2190 $[M-H]^-$. The ^{1}H NMR spectrum was similar to that of compound **1**, except that they appeared as double signals with a complex sugar unit. The ^{13}C NMR spectrum gave doublet signals, indicating its presence of a mixture of sugar unit in compound **10**. The spectroscopic analyses including COSY, HMQC and HMBC spectra disclosed the similar chemical structure to adxanthromycin A, which was a dimeric anthrone peroxide structure with α-D-galactose (Takahashi et al., 2000). However, the optical rotation reported for adxanthromycin ($[\alpha]_D$ + 120.5) was opposite to that of compound **10** ($[\alpha]_D$ − 144.6). Hydrogenation of compound **10** with palladium on carbon gave compound **3** and (−)-form of monomer of oxanthromicin (**12**). Moreover, the same CD spectrum (Fig. 3) as that of compound **12** also confirmed the configurations at C-10 and C-10′ to be the same as those of oxanthromicin (**12**). The ^{1}H NMR and ^{13}C NMR spectral information of compound **3** (Tables 1 and 2) indicated a mixture of β- (δ_H 4.79, d, J = 8.0 Hz) and α-D-galactose (δ_H 5.55, d, J = 5.4 Hz) unit (Takahashi et al., 2000). The chemical structure of compound **3** was also reassured by 2D NMR spectral analysis. Compound **10** can therefore be illustrated as shown in Fig. 1 and was named adxanthromycin A_2.

Compound **11** was obtained as a brown gum and the ^{1}H NMR spectrum was similar to that of compound **12**, except the presence of unsymmetrical signal at aromatic region, an additional methoxy signal at δ_H 3.93, and an extra chelated hydroxyl proton. HRESIMS spectrum also confirmed the addition of methyl group, compared with that of compound **12**, by revealing the molecular ion peak at *m/z* 667.1823 $[M-H]^-$. The IR spectrum showing absorption of hydroxyl of acid (ν 2500–3600 cm^{-1}), carbonyl of carboxylic acid (ν_{max} 1706 cm^{-1}), and hydrogen bonded carbonyl ketone (ν_{max} 1624 cm^{-1}) suggested the methoxy group situated at C-3. In HMBC spectrum, the additional methoxy showed correlation to the carbon at δ_C 169.0 (C-3). The chemical structure of compound **11** was reassured by the 2D NMR analysis (COSY, HMQC, and HMBC), shown in Fig. 1. The optical rotation value of compounds **11** ($[\alpha]_D$ − 55.8) together with the similar CD pattern to that of compound **12** (Fig. 3) resulted in the assignment of configurations at C-10 and C-10′ to be the same as oxanthromicin (**12**) ($[\alpha]_D$ − 172.1) (Wright et al., 1984). Moreover, compound **12** could not

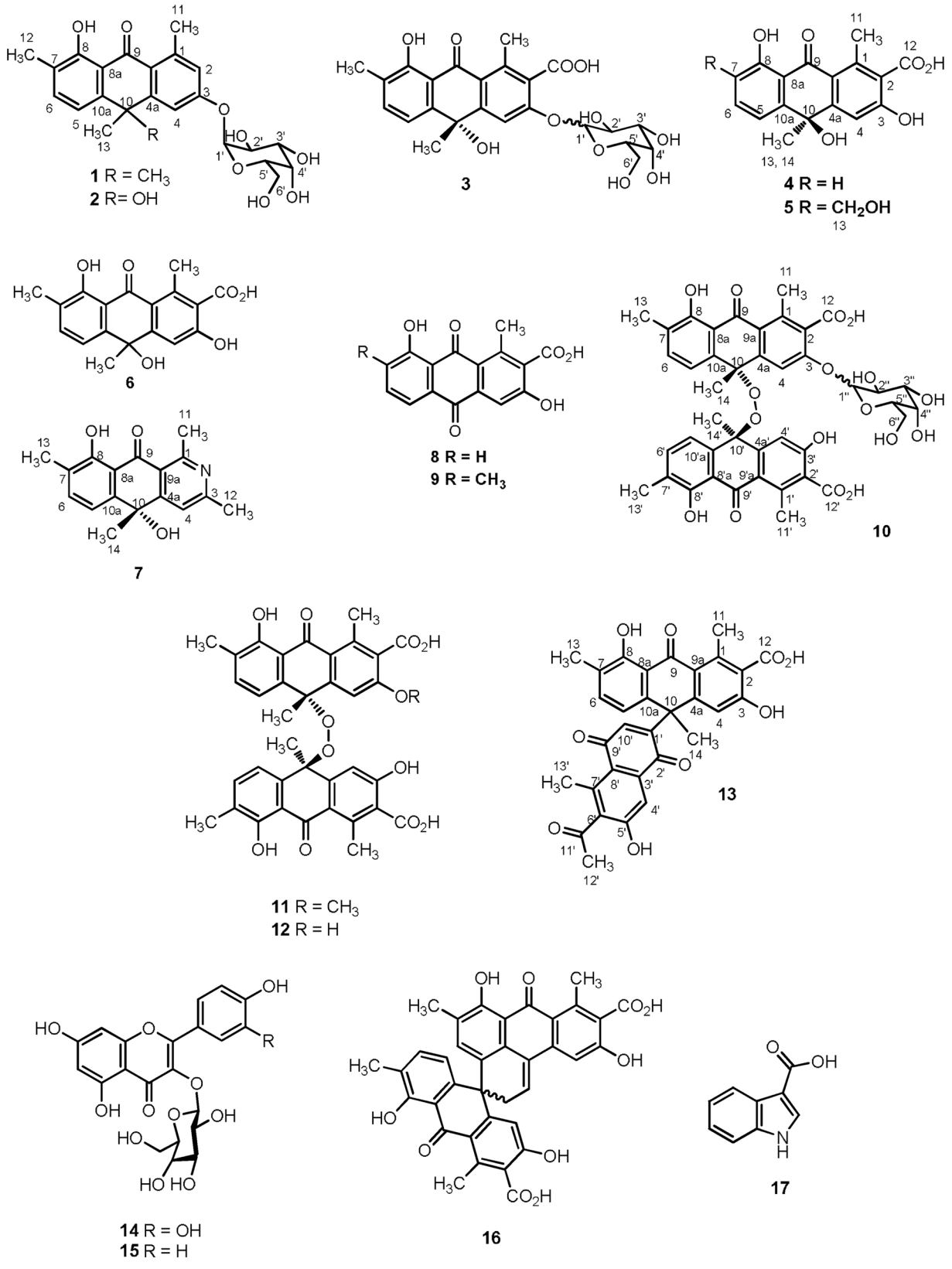

Fig. 1. Chemical structures of compounds **1–17** from *Actinomadura* sp. BCC47066.

be modified after treatment with 2% 1N HCl in MeOH for 3 days at room temperature, suggesting compound **11** is not an artifact formed from compound **12**. Thus, compound **11** is 3-methoxy oxanthromicin (Fig. 1).

Compound **13** was obtained as a brown gum and HRESIMS gave the molecular ion peak at *m/z* 539.1351 $[M-H]^-$, suggesting the molecular formula of $C_{31}H_{24}O_9$. Part of the ^{1}H NMR spectrum showed similar pattern to that of monomer of compound **12**, (−)-*hemi*-oxanthromicin A, and a lack of a quaternary carbon attached to oxygen at δ_C 69.6 in the ^{13}C NMR spectrum indicated a change of the substituent at

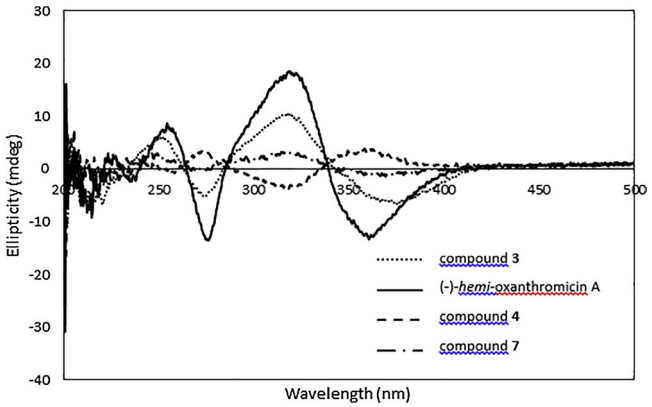

Fig. 2. CD spectra of compounds **3**, **4**, **7**, and (–)-*hemi*-oxanthromicin A (monomer of compound **12**).

C-10. In the ^{1}H NMR spectrum, there were two additional singlet methines at δ_H 7.43 and 7.56, and two singlet methyl signals at δ_H 2.10 and 2.43. These signals showed HMBC correlations as follows; from the methine at δ_H 7.43 (H-10′) to C-10, C-1′, and C-9′; from the methine at δ_H 7.56 (H-4′) to C-2′, C-6′, and C-8′; from the methyl at δ_H 2.10 (H_3-13′) to C-6′, C-7′, and C-8′; and from the methyl at δ_H 2.43 (H_3-12′) to C-6′ and C-11′. The spectroscopic evidence suggested the presence of 6′-acetyl-5′-hydroxy-7′-methylnaphthalene-2′,9′-dione (Husain et al., 2012) as a substituent at C-10. Compound **13** is present as an enantiomeric mixture since it gives 2 peaks (t_R 12.30 and 13.02 min) in a chiral HPLC analysis (using Chiral CD-Ph (5 µm), Shiseido® HPLC column, 250 mm x 4.6 mm) using linear gradient system (70–95% MeOH in water, for 30 min, at 254 nm, flow rate 1.0 mL/min) and also lacks a CD curve. Thus, chemical structure of compound **13** can be depicted as shown in Fig. 1 and (±)-oxanthromicin H was named for compound **13**.

The ^{1}H and ^{13}C NMR spectra of all known compounds (**6**, **8**, **9**, **12**, and **14–17**) were identical to those identified as (±)-*hemi*-oxanthromicin A (Salim et al., 2014), demethyl oxanthroquinone (Hawas et al., 2006), oxanthroquinone (Salim et al., 2014), oxanthromicin (Wright et al., 1984), quercetin 3-glucoside, kaempferal 3-glucoside (Kazuma et al., 2003), (±)-*spiro*-oxanthromicin A (Salim et al., 2014), and indole-3-carboxylic acid (Pouchert, 1993).

Compounds **1**, **2**, **6**, **8–10**, **12**, and **16** were evaluated for antimicrobial activity including antimalarial (*Plasmodium falciparum*, K-1 multidrug resistant strain), anti-TB (*Mycobacterium tuberculosis* H37Ra), anti-*Bacillus cereus*, anti-HSV-1, antiphytopathogenic (against *Colletotrichum capsici*, *C. gloeosporioides*, *Magnaporthe grisea* and *Alternaria brassicicola*) activities and for cytotoxicity against KB, MCF-7, NCI-H187, and Vero cells. Compounds **1**, **9**, and **10** exhibited anti-HSV-1 activity with IC_{50} in a range of 2.33–20.86 µg/mL (Table 5), while compound **1** was non-toxic against both cancerous and non-cancerous cells. Dimeric anthrone peroxides **10** and **12** were active against *B. cereus* (MIC 3.13 and 1·56 µg/mL), *C. capsici* (MIC 6.25 µg/mL), and *C. gloeosporioides* (MIC 6.25 µg/mL). Only compound **12** had anti-*M. grisea* activity with MIC value of 25 µg/mL, while compounds **12** and **16** exhibited anti-*A. brassicicola* activity at maximum tested concentration (50 µg/mL). All tested compounds, except compounds **9**, **10**, and **12**, showed non-cytotoxicity against both cancerous and non-cancerous cells (Table 5). In addition, all tested compounds were inactive for antimalarial and anti-TB activities at maximum tested concentration of 10 and 50 µg/mL, respectively.

Table 1
^{1}H NMR assignment of compounds **1–5** and compound **7** in acetone-d_6.

position	(1)[a] δ_H, (mult., *J* in Hz)	(2)[b] δ_H, (mult., *J* in Hz)	(3)[a] δ_H, (mult., *J* in Hz)	(4)[b,c] δ_H, (mult., *J* in Hz)	(5)[a,c] δ_H, (mult., *J* in Hz)	(7)[a] δ_H, (mult., *J* in Hz)
1	–	–	–	–	–	–
2	7.05 (d, 1.9)	7.04 (br s)	–	–	–	–
3	–	–	–	–	–	–
4	7.47 (d, 1.9)	7.66 (br s)	7.51 (s)	7.24 (s)	7.11 (s)	7.73 (s)
4a	–	–	–	–		–
5	7.14 (d, 8.0)	7.31 (d, 7.7)	7.29 (d, 7.7)	7.31 (d, 7.5)	7.28 (d, 7.8)	7.33 (d, 7.6)
6	7.44 (d, 8.0)	7.43 (d, 7.7)	7.43 (d, 7.7)	7.53 (t, 7.9)	7.59 (d, 7.8)	7.49 (d, 7.6)
7	–	–	–	6.84 (d, 8.1)	–	–
8	–	–	–	–	–	–
8a	–	–	–	–	–	–
9	–	–	–	–	–	–
9a	–	–	–	–	–	–
10	–	–	–	–	–	–
10a	–	–	–	–	–	–
11	2.81 (s)	2.72 (s)	2.80/2.82 (s)	2.78 (s)	2.97 (s)	2.93 (s)
12	2.22 (s)	2.22 (s)	–	–	–	2.57 (s)
13	1.69 (s)	1.57 (s)	2.22 (s)	1.44 (s)	4.52 (d, 15.6) and 4.54 (d, 15.6)	2.24 (s)
14	1.70 (s)	–	1.56 (s)	–	1.42 (s)	1.58 (s)
8-OH	13.98 (s)	13.34 (s)	13.16 (s)/13.19 (s)	13.02 (s)	13.48 (s)	13.08 (s)
10-OH	–	–	–	6.11 (s)	5.99 (s)	–
13-OH	–	–	–	–	5.08 (t, 5.5)	–
1′	5.74 (d, 2.08)	5.73/5.74 (br s)	5.55 (d, 5.4)/4.79 (d, 8.0)	–		
2′	4.07 (br s)	4.08 (br s)	5.30 (dd, 10.7, 3.6)/5.30 (dd, 10.1, 8.0)	–		
3′	3.97-4.04 (m)	4.00-4.04 (m)	4.16 (dd, 10.7, 3.1)/3.84 (dd, 10.1, 3.1)	–		
4′	3.97-4.04 (m)	4.00-4.04 (m)	4.09–4.14 (m)/4.04–4.08 (m)	–		
5′	3.89 (dd, 6.1, 5.7)	3.87 (dd, 5.9, 5.8)	4.09–4.14 (m)	–		
6′	3.70 (dd, 11.0, 6.1) 3.77 (dd, 11.0, 5.7)	3.70 (d, 10.9, 5.9) 3.76 (dd, 10.9, 5.8)	3.70–3.75 (m) 3.77–3.82 (m)	–		

[a] Recorded at 500 MHz.
[b] Recorded at 400 MHz.
[c] In DMSO-d_6.

Table 2
^{13}C NMR assignment of compounds **1–5** and compound **7** in acetone-d_6.

position	(1)[a] δ_C, type	(2)[b] δ_C, type	(3)[a] δ_C, type	(4)[b,c] δ_C, type	(5)[a,c] δ_C, type	(7)[a] δ_C, type
1	144.8 (C)	144.1/144.2 (C)	143.8/143.4 (C)	142.7 (C)[f]	148.8 (C)	160.3 (C)[g]
2	120.0 (CH)	119.5/119.6 (CH)	121.4 (C)	117.7 (C)	117.1 (C)[f]	–
3	161.2 (C)	161.1 (C)	160.5/160.6 (C)	160.8 (C)	167.3 (C)	162.1 (C)
4	113.0 (CH)	114.4 (CH)	112.2/112.3 (CH)	111.0 (CH)	112.3 (CH)	117.5 (CH)
4a	156.0 (C)	155.1 (C)	157.2/157.3 (C)	154.7 (C)	155.6 (C)	160.1 (C)[g]
5	116.3 (CH)	114.9(6)/115.0 (CH)	115.1 (CH)	115.1 (CH)[d]	115.0 (CH)	115.3 (CH)
6	136.8 (CH)	136.3 (CH)	134.1 (CH)	134.5(CH)	132.9 (CH)	137.0 (CH)
7	123.7 (C)	124.3/124.4 (C)	125.5 (C)	115.0 (CH)	128.7 (C)	124.8 (C)
8	161.5 (C)	160.2/160.5 (C)	161.18/161.20 (C)	160.8 (C)	158.5 (C)	160.1 (C)[g]
8a	115.2 (C)	114.3 (C)	115.45/115.47 (C)	115.0 (C)[d]	115.0 (C)	114.1 (C)
9	191.3 (C)	190.1(6)/190.2 (C)	190.9 (C)	188.8 (C)	189.9 (C)	190.3 (C)
9a	122.7 (C)	121.7 (C)	123.7/124.2 (C)	123.2 (C)[f]	119.9 (C)	120.4 (C)
10	39.2 (C)	70.3 (C)	71.1 (C)	69.4 (C)	70.1 (C)	70.0 (C)[f]
10a	149.3 (C)	148.1 (C)	148.38/148.42 (C)	150.0 (C)	148.8 (C)	147.5 (C)
11	24.9 (CH_3)	23.7 (CH_3)	20.8/20.9 (CH_3)	19.5 (CH_3)	20.9 (CH_3)	26.3 (CH_3)
12	14.8 (CH_3)	14.5 (CH_3)	168.2/168.3 (C)	–[e]	171.7 (C)[f]	24.2 (CH_3)
13	33.8 (CH_3)	38.7 (CH_3)	15.3 (CH_3)	40.2 (CH_3)	57.8 (CH_2)	14.4 (CH_3)
14	33.9 (CH_3)	–	39.5 (CH_3)	–	40.2 (CH_3)	37.9 (CH_3)
1′	98.6 (CH)	97.8/98.0 (CH)	91.1/96.12 (CH)	–		
2′	69.4 (CH)	68.8 (CH)	74.5/76.7 (CH)	–		
3′	70.7 (CH)	70.2 (CH)	68.4/73.0 (CH)	–		
4′	69.8 (CH)	69.2 (CH)	71.2/70.1 (CH)	–		
5′	72.7 (CH)	72.3 (CH)	70.9/76.3 (CH)	–		
6′	61.8 (CH_2)	61.2 (CH_2)	62.2/62.4 (CH_2)	–		

[a] Recorded at 125 MHz.
[b] Recorded at 100 MHz.
[c] In DMSO-d_6.
[d] Exchangeable.
[e] Do not observe in ^{13}C NMR.
[f] Observed in HMBC spectrum.
[g] Exchangeable.

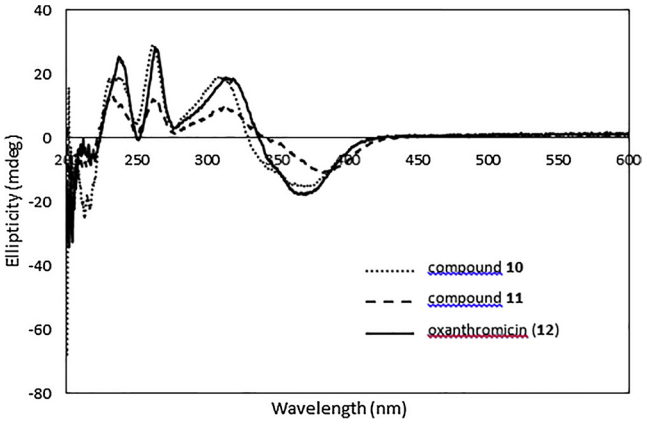

Fig. 3. CD spectra of compounds **10–12**.

(±)-*hemi*-Oxanthromicin A (**6**), oxanthroquinone (**9**), and (±)-*spiro*-oxanthromicin A were earlier isolated from the terrestrial *Streptomyces* sp. (MST-134270) and only compound **16** affected mislocalising oncogenic mutant K-Ras from the plasma membrane of intact Madin-Darby canine kidney (MDCK) cells (Salim et al., 2014). Compounds **8**, **14**, and **15** were previously isolated from the shrublets of *Emex spinosus* (L.) (Hawas et al., 2006) and the flowers of *Clitoria ternarea* (Kazuma et al., 2003), respectively, and have never been reported from microorganisms. Dimeric anthrone peroxide structure with one molecule of α-D-galactose (named adxanthromycin A), similar to compound **10**, was isolated *Streptomyces* sp. NA – 148 (Koiwa et al., 1999; Takahashi et al., 2000). Oxanthromicin (**12**) was formerly reported from *Actinomadura* sp. SCC 1646 with the relative configuration confirmed by X-ray crystallographic data (Wright et al., 1984) and possessed *in vitro* activity against dermatophytes (MIC 2–8 μg/mL) and *Candida* spp. (MIC 32– > 64 μg/mL) (Patel et al., 1984). Indole-3-carboxylic acid (**17**) was isolated from the plant-derived endophytic fungi, *Aspergillus* spp. and *Lasiodiplodia theobromae* (El-Hawary et al., 2017), and expected its role in survival of the collected plant (*Solanum nigrum* L.) in desert environment.

3. Experimental section

3.1. General procedures

Melting points were measured on a melting point MP90 apparatus from Mettler Toledo. UV spectra were performed in MeOH, using a Spekol 1200, Analytik Jena AG. IR spectra were recorded by using a Bruker ALPHA FT-IR spectrometer. Optical rotations were taken in either EtOH or MeOH on a JASCO P-1030 polarimeter. CD spectra were observed on a JASCO J-810 spectropolarimeter, using MeOH as a solvent. HRESIMS data were detected on a Bruker MicrOTOF mass spectrometer and Isotope Pattern from Hystar version 2.1 was used to calculate exact masses. NMR spectra, including ^{1}H, ^{13}C, DEPT-135, COSY, NOESY, HMQC (or HSQC) and HMBC experiments, were recorded on either Bruker Avance 500 NMR spectrometer (at 500 MHz for ^{1}H and 125 MHz for ^{13}C) or Bruker Avance III 400 NMR spectrometer (at 400 MHz for ^{1}H and 100 MHz for ^{13}C), using either acetone-d_6 (δ_H 2.08, δ_C 29.06) or DMSO-d_6 (δ_H 2.50, δ_C 39.50) as internal standards. HPLC were operated on a Dionex, Ultimate 3000 series model, equipped with a binary pump, an autosampler and a diode array detector. Preparative and semi-preparative HPLC were monitored at 210 nm and assembled with a Waters Sunfire C18 OBD column (diam. 19 mm × 250 mm, particle size 10 μm) at a flow rate of 15 mL/min and a Waters Sunfire C18 OBD column (diam. 19 mm × 150 mm, particle size 5 μm) at a flow rate of 9 mL/min, respectively. Mobile phase using for HPLC chromatography contained 0.005% TFA (trifluoroacetic acid).

3.2. Biological material

The actinomycete strain registered at BIOTEC Culture Collection (BCC) as BCC47066 was collected from soil at Phu Pha Man National Park, Khon Kaen province, Thailand. The sample was identified as *Actinomadura* sp. by Dr. Chanwit Suriyachadkun based on the 16S rRNA gene sequence. The 16S rRNA gene was amplified by PCR, and sequenced by Macrogen Inc., Korea using universal primers. BLASTZN analysis was used to compare 16S rRNA gene sequences with sequences from the EzBioCloud's nucleotide databases (Yoon et al., 2017). A phylogenetic tree was constructed by neighbor-joining method (Saitou and Nei, 1987) using MEGA 6 software. The results revealed that the strain BCC47066 belonged to the genus *Actinomadura*, which shared 99.01% similarity with *Actinomadura madurae*.

3.3. Fermentation, extraction, and isolation

The strain BCC47066 was grown on ISP2 agar (yeast extract-malt extract agar) at 25 °C for 30 days. The culture was cut into 1 cm^2 pieces and then inoculated into 10 × 250 mL Erlenmeyer flasks, containing 25 mL of BIO19 medium, which comprised (w/v): 2% glucose, 0.5% peptone, 0.3% yeast extract, 0.5% meat extract, 0.05% NaCl, and 0.3% $CaCO_3$. The culture broth was inoculated for 7 days at 28 °C on rotary shakers at 250 rpm and then consecutively transferred into 1 L Erlenmeyer flask, which contained 250 mL of the seed medium, BIO19. The seed culture (20 flasks) was cultivated on a rotary shaker (250 rpm) at 28 °C for 7 days and then transferred into 80 × 1 L Erlenmeyer flasks, which each contained 250 mL of BIO19 medium. The production medium (BIO19, 20 L) was cultivated for 7 days at 28 °C on rotary shakers (250 rpm). After 7 days of the cultivation, the whole culture (broth and cells) was extracted three times with an equal volume of EtOAc and the extract was then dried over Na_2SO_4. EtOAc was evaporated to dryness to yield a brown gummy solid (9.2 g), which was triturated in MeOH to obtain a brown solid (0.4 g) and the residue from the remaining methanolic solution was passed through a Sephadex LH-20 column (4.5 cm × 40 cm), eluted with 100% MeOH, to give three main fractions (F1–F3). The solid (0.4 g) was purified by preparative HPLC using a linear gradient system of 30–80% acetonitrile in water over 30 min to afford compounds **10** (23.1 mg), and **12** (6.9 mg), respectively.

The first fraction (F1, 4.0 g) was triturated in MeOH to give a brown solid (18.9 mg) of an impure compound **10** and the residue from the remaining methanolic solution was further purified by a Sephadex LH-20 column (4.5 × 40 cm^2) to afford 3 subfractions (F1F1–F1F3). Subfraction F1F1 (2.7 g) was further purified by another Sephadex LH-20 column (3.5 × 52 cm^2) eluted with MeOH to give 3 subfractions (F1F1-1–F1F1-3). Subfraction F1F1-1 (1.6 g) was further purified by a preparative HPLC using a linear gradient system of 30–80% acetonitrile in water over 30 min to give compounds **7** (2.5 mg), **2** (7.6 mg), **1** (3.9 mg), and **12** (1.93 mg), respectively. Subfraction F1F1-2 (52.3 mg) was further purified by a preparative HPLC using a linear gradient system of 30–80% acetonitrile in water over 50 min to obtain compounds **1** (1.2 mg), **10** (27.3 mg), and **12** (2.9 mg), respectively. Subfraction F1F1-3 (42.9 mg) was further purified by a preparative HPLC using a linear gradient system of 35–65% acetonitrile in water over 50 min to furnish compounds **10** (4.1 mg) and **12** (6.0 mg), respectively. Subfraction F1F2 (1.01 g) was passed through a Sephadex LH-20 column (4.5 × 40 cm^2), eluted with 100% MeOH to give 3 subfractions (F1F2-1–F1F2-3). Subfraction F1F2-1 (0.7 g) was further purified by a preparative HPLC using a linear gradient system of 20–70% acetonitrile in water over 50 min to furnish compounds **13** (3.2 mg), **10** (0.2 g), and **12** (20.0 mg). Subfraction F1F2-2 (72.0 mg) was further purified by a preparative HPLC using a linear gradient system of 30–80% acetonitrile in water over 30 min to obtain compounds **14** (2.0 mg), **15** (2.3 mg), *1H*-indole-3-carboxylic acid (**17**, 2.5 mg), compounds **13** (4.5 mg), **10** (12.7 mg), and **12** (8.3 mg), respectively. Subfraction F1F2-3 (0.2 g) was purified by a preparative HPLC using a linear gradient system of 30–80% acetonitrile in water over 30 min to yield compound **16** (58.8 mg).

The second fraction (F2, 0.6 g) was triturated in MeOH to afford a brown solid of compound **6** (56.9 mg) and the filtrate was passed through a Sephadex LH-20 column (4.5 × 40 cm^2) to give 2 subfractions (F2F1 and F2F2). Subfraction F2F1 (0.3 g) was passed through another Sephadex LH-20 column (2 × 90 cm^2) to furnish 2 subfractions (F2F1-1 and F2F1-2). Subfraction F2F1-1 (0.2 g) was further purified by a preparative HPLC using a linear gradient system of 35–65% acetonitrile in water over 50 min to obtain compounds **5** (2.7 mg), **4** (2.2 mg), **6** (31.0 mg), and **10** (56.3 mg), respectively. Subfraction F2F1-2 (51.6 mg) was further purified by a preparative HPLC using a linear gradient system of 50–65% acetonitrile in water over 40 min to yield compound **16** (11.4 mg). Subfraction F2F2 (0.1 g) was further purified by a preparative HPLC using a linear gradient system of 40–60% acetonitrile in water over 55 min to afford compounds **6** (34.9 mg), **10** (19.5 mg), and **12** (8.9 mg), respectively.

The third fraction (F3, 1.4 g) was triturated in MeOH to yield a brown solid (0.2 g), which was further purified by a preparative HPLC using a linear gradient system of 30–80% acetonitrile in water over 30 min to yield compounds **6** (66.3 mg) and **9** (2.3 mg), respectively. The filtrate was passed through a Sephadex LH-20 column (4.5 × 40 cm^2), eluted with 100% MeOH to give 4 subfractions (F3F1–F3F4). Compound **6** (71.7 mg) was given in the subfraction F3F1. Subfraction F3F2 (0.4 g) was triturated in MeOH to give a brown solid of compound **6** (0.2 g) and the filtrate was passed through a Sephadex LH-20 column (2 × 90 cm^2), eluted with 100% MeOH to give 2 subfractions (F3F2-1 and F3F2-2). Compound **16** (21.2 mg) was obtained in the subfraction F3F2-2. Subfraction F3F2-1 (85.7 mg) was further purified by a preparative HPLC using a linear gradient system of 35–65% acetonitrile in water over 50 min to furnish compounds **6** (1.6 mg), **10** (12.2 mg), **12** (1.3 mg), and **11** (1.4 mg), respectively. Subfraction F3F3 (0.2 g) was further purified by a preparative HPLC using 40–100% acetonitrile in water over 30 min to obtain compounds **4** (2.8 mg), **16** (15.2 mg), **9** (3.7 mg), **10** (7.7 mg), and **12** (12.6 mg), respectively. Subfraction F3F4 (0.2 g) was triturated in MeOH to give a brown solid (14.0 mg), which was further purified by a semi-preparative HPLC using a linear gradient system of 35–75% acetonitrile in water over 30 min to afford compounds **8** (4.0 mg) and **9** (3.5 mg), respectively. The filtrate was further purified by a semi-preparative HPLC using a linear gradient system of 40–100% acetonitrile in water over 40 min to give compounds **10** (7.5 mg), **12** (14.9 mg), and **11** (2.9 mg), respectively.

3.3.1. (+)-Oxanthromicin E (1)

Brown solid, $[\alpha]_D^{28}$ +132.89 (*c* 0.06, EtOH); UV (MeOH) λ_{max} (log ε) 221 (4.06), 269 (3.89), 304 (4.12), 358 (3.77), 426 (2.80) nm; FTIR (ATR) ν_{max} 3371, 2855, 1712 (w), 1618, 1599, 1571, 1456, 1423, 1350, 1292, 1260, 1186, 1150, 1114, 1081, 1028, 1007, 773 cm^{-1}; ^1H NMR (500 MHz, acetone-d_6) and ^{13}C NMR (125 MHz, acetone-d_6) data, see Tables 1 and 2; HRESIMS *m/z* 467.1679 $[M + Na]^+$ (calcd for $C_{24}H_{28}O_8Na$, 467.1676).

3.3.2. (±)-hemi-Oxanthromicin D (2)

Brown solid, $[\alpha]_D^{29}$ +174.95 (*c* 0.06, EtOH); UV (MeOH) λ_{max} (log ε) 222 (4.04), 270 (3.91), 309 (4.09), 357 (3.82), 421 (2.83) nm; FTIR (ATR) ν_{max} 3362, 2856, 1705 (w), 1622, 1600, 1568, 1449, 1421, 1347, 1290, 1258, 1176, 1163, 1083, 1027, 1002, 829, 785 cm^{-1}; ^1H NMR (400 MHz, acetone-d_6) and ^{13}C NMR (100 MHz, acetone-d_6) data, see Tables 1 and 2; HRESIMS *m/z* 469.1468 $[M + Na]^+$ (calcd for $C_{23}H_{26}O_9Na$, 469.1469).

3.3.3. Compound 3

Yellow gum; $[\alpha]_D^{26}$ −18.57 (*c* 0.16, EtOH); ^1H NMR (500 MHz, acetone-d_6) and ^{13}C NMR (125 MHz, acetone-d_6) data, see Tables 1 and

2; HRESIMS *m/z* 489.1407 $[M-H]^-$ (calcd for $C_{24}H_{25}O_{11}$, 489.1402).

3.3.4. (+)-Oxanthromicin F (4)

Brown gum; $[\alpha]_D^{25}$ +40.68 (*c* 0.11, EtOH); UV (MeOH) λ_{max} (log ε) 224 (3.89), 258 (3.82), 323 (3.76), 348 (3.79), 419 (3.08) nm; FTIR (ATR) ν_{max} 2500–3600, 3399, 2926, 1703 (w), 1628, 1586, 1476, 1452, 1267, 1229, 1178, 1076, 1042, 883, 825, 789 cm^{-1}; ^1H NMR (400 MHz, DMSO-d_6) and ^{13}C NMR (100 MHz, DMSO-d_6) data, see Tables 1 and 2; HRESIMS *m/z* 313.0706 $[M-H]^-$ (calcd for $C_{17}H_{13}O_6$, 313.0718).

3.3.5. (+)-Oxanthromicin G (5)

Brown gum; $[\alpha]_D^{24}$ +40.60 (*c* 0.07, EtOH); UV (MeOH) λ_{max} (log ε) 222 (4.05), 260 (3.93), 324 (3.88), 349 (3.90), 424 (3.41) nm; FTIR (ATR) ν_{max} 2500–3600, 3370, 2925, 1710 (w), 1621, 1593, 1569, 1428, 1329, 1263, 1194, 1173, 1080, 1043, 829 cm^{-1}; ^1H NMR (500 MHz, DMSO-d_6) and ^{13}C NMR (125 MHz, DMSO-d_6) data, see Tables 1 and 2; HRESIMS *m/z* 367.0790 $[M+Na]^+$ (calcd for $C_{18}H_{16}O_7Na$, 367.0788).

3.3.6. Azanthromicin A (7)

Yellow gum; $[\alpha]_D^{23}$ +13.81 (*c* 0.13, EtOH); UV (MeOH) λ_{max} (log ε) 234 (3.89), 246 (3.81), 302 (3.84), 365 (3.55), 422 (3.18) nm; FTIR (ATR) ν_{max} 3360, 2926, 1718 (w), 1630, 1593, 1579, 1418, 1380, 1327, 1312, 1257, 1186, 1164, 1145, 1108, 1035, 889, 829, 796 cm^{-1}; ^1H NMR (500 MHz, acetone-d_6) and ^{13}C NMR (125 MHz, acetone-d_6) data, see Tables 1 and 2; HRESIMS *m/z* 284.1285 $[M+H]^+$ (calcd for $C_{17}H_{18}NO_3$, 284.1281).

3.3.7. Adxanthromicin A_2 (10)

Yellow solid; mp 179.5–181.8 °C; $[\alpha]_D^{28}$ −144.64 (*c* 0.07, MeOH); UV (MeOH) λ_{max} (log ε) 221 (4.34), 259 (4.24), 316 (4.21), 357 (4.11) nm; FTIR (ATR) ν_{max} 3407, 2925, 1715, 1625, 1595, 1574, 1488, 1420, 1336, 1316, 1256, 1190, 1158, 1142, 1115, 1074, 1046, 1027, 885, 805 cm^{-1}; ^1H NMR (400 MHz, acetone-d_6) and ^{13}C NMR (100 MHz, acetone-d_6) data, see Table 3; HRESIMS *m/z* 815.2190 $[M-H]^-$ (calcd for $C_{42}H_{39}O_{17}$, 815.2193).

Table 3
^1H and ^{13}C NMR assignments of compound **10** in acetone-d_6.

position	(**10**)[a]	
	δ_H, (mult., *J* in Hz)	δ_C, type
1/1′	–	142.0/142.1 (C)
2/2′	–	121.1/121.4 (C)
3/3′	–	160.7/160.8 (C)
4/4′	7.02 (1H, s)/7.08 (1H, s)	113.8 (CH)
4a/4′a	–	150.5 (C)
5/5′	6.72 (2H, d, 7.1)	117.4/117.5 (CH)
6/6′	7.39 (2H, d, 7.1)	135.9/136.2 (CH)
7/7′	–	125.4/125.5 (C)
8/8′	–	160.4/160.5 (C)
8a/8′a	–	115.4/115.6 (C)
9/9′	–	190.09/190.13 (C)
9a/9′a	–	125.3 (C)
10/10′	–	80.2 (C)
10a/10′a	–	142.0/142.1 (C)
11/11′	2.85 (3H, s)/2.87 (3H, s)	20.7/20.9 (CH_3)
12/12′	–	167.6 (C)
13/13′	2.29 (6H, s)	14.87/14.91 (CH_3)
14/14′	1.34 (6H, s)	33.4/33.7 (CH_3)
8-OH/8′ −OH	13.65 (1H, s)/13.72 (1H, s)	–
1”	5.30 (1H, br s)/5.60 (1H, s)	90.5/95.5 (CH)
2”	4.10-4.30 (1H, m)	67.7 (CH)
3”	3.75-3.90 (1H, m)	70.4 (CH)
4”	3.75-3.90 (1H, m)	73.9 (CH)
5”	3.75-3.90 (1H, m)	73.9 (CH)
6”	4.10 − 4.30 (1H, m)/3.75 − 3.90 (1H, m)	61.8 (CH_2)

[a] Recorded at 400 MHz for ^1H NMR and 100 MHz for ^{13}C NMR.

Table 4
^1H and ^{13}C NMR assignments of compounds **11** and **13** in acetone-d_6.

position	**11**[a]		**13**[a]	
	δ_H, (mult., *J* in Hz)	δ_C, type	δ_H, (mult., *J* in Hz)	δ_C, type
1	–	151.8 (C)[b]	–	144.4 (C)
2	–	120.2 (C)[b]	–	120.5 (C)
3	–	169.0 (C)	–	160.5 (C)
4	6.90 (s)	118.7 (CH)	6.84 (s)	111.2 (CH)
4a	–	150.3 (C)	–	154.4 (C)[d]
5	6.76 (d, 7.8)	118.2 (CH)	6.71 (d, 7.8)/6.72 (d, 7.8)	111.1 (CH)
6	7.48 (d, 7.8)	135.5 (CH)	7.26 (d, 7.8)	136.7 (CH)
7	–	126.1 (C)	–	123.9 (C)
8	–	161.2 (C)	–	131.2 (C)
8a	–	116.0 (C)	–	114.7 (C)
9	–	190.3 (C)	–	190.5 (C)
9a	–	121.2 (C)	–	122.2 (C)
10	–	81.3 (C)	–	46.1 (C)
10a	–	142.8 (C)	–	145.8 (C)
11	3.19 (s)	21.5 (CH_3)	2.97 (s)	20.9 (CH_3)
12	–	–[c]	–	170.0 (C)[b]
13	2.29 (s)	15.5 (CH_3)	2.19 (s)	14.5 (CH_3)
14	1.33 (s)	33.6 (CH_3)	1.76 (s)	34.4 (CH_3)
1′	–	141.3 (C)	–	155.8 (C)[d]
2′	–	121.2 (C)	–	184.6 (C)
3′	–	–[c]	–	135.1 (C)
4′	7.17 (s)	115.8 (C)	7.56 (s)	110.8 (CH)
4′a	–	150.7 (C)	–	–
5′	6.78 (d, 7.8)	118.4 (CH)	–	157.1 (C)
6′	7.50 (d, 7.8)	136.5 (CH)	–	136.8 (C)
7′	–	126.0 (C)	–	139.4 (C)
8′	–	160.9 (C)	–	123.7 (C)
8′a	–	116.9 (C)	–	–
9′	–	190.6 (C)	–	183.7 (C)
9′a	–	128.1 (C)	–	–
10′	–	81.4 (C)	7.43 (s)	133.9 (CH)
10′a	–	143.4 (C)	–	–
11′	2.73 (s)	20.9 (CH_3)	–	203.2 (C)
12′	–	–[c]	2.43 (s)	31.2 (CH_3)
13′	2.29 (s)	15.7 (CH_3)	2.10 (s)	17.5 (CH_3)
14′	1.27 (s)	34.7 (CH_3)	–	–
8-OH	13.65 (s)	–	13.96 (s)	–
8′-OH	13.72 (s)	–	–	–
3-OCH_3	3.93 (s)	52.3 (CH_3)	–	–

[a] Recorded at 500 MHz for ^1H NMR and 125 MHz for ^{13}C NMR.
[b] Observed in HMBC spectrum.
[c] Do not observe in ^{13}C NMR spectrum.
[d] Exchangeable.

3.3.8. 3-Methoxy oxanthromicin (11)

Brown gum; $[\alpha]_D^{25}$ − 55.81 (*c* 0.15, EtOH); UV (MeOH) λ_{max} (log ε) 228 (4.34), 259 (4.26), 317 (4.20), 357 (4.16), 423 (3.58) nm; FTIR (ATR) ν_{max} 2500–3600, 2925, 1706, 1624, 1594, 1572, 1421, 1336, 1256, 1195, 1156, 1141, 1077, 884, 826, 804 cm^{-1}; ^1H NMR (500 MHz, acetone-d_6) and ^{13}C NMR (125 MHz, acetone-d_6) data, see Table 4; HRESIMS *m/z* 667.1823 $[M-H]^-$ (calcd for $C_{37}H_{31}O_{12}$, 667.1821).

3.3.9. (±)-Oxanthromicin H (13)

Brown gum; $[\alpha]_D^{25}$ + 38.38 (*c* 0.09, EtOH); UV (MeOH) λ_{max} (log ε) 231 (4.23), 266 (4.26), 316 (4.05), 353 (3.98), 421 (3.33) nm; FTIR (ATR) ν_{max} 2500–3600, 2926, 1703, 1664, 1619, 1572, 1423, 1379, 1327, 1256, 1212, 1193, 1147, 1078, 1047, 1032, 827, 654 cm^{-1}; ^1H NMR (500 MHz, acetone-d_6) and ^{13}C NMR (125 MHz, acetone-d_6) data, see Table 4; HRESIMS *m/z* 539.1351 $[M-H]^-$ (calcd for $C_{31}H_{23}O_9$, 539.1348).

3.3.10. Hydrogenation of compound 10

Compound **10** (30.0 mg) was stirred in dried MeOH (1.2 mL) with a presence of Pd-C/H_2 at room temperature for 8 h. The mixture was then

Table 5
Antimicrobial activity and cytotoxicity of the isolated compounds.

Compound	Anti *B. cereus*[a]	Anti-HSV−1[b]	Anti-*C. capsici*[a]	Anti-*C. gloeosporioides*[a]	Anti-*A. brassicicola*[b]	Anti-*M. grisea*[b]	Cytotoxicity[b] (IC_{50}, μg/mL)			
	(MIC, μg/mL)	(IC_{50}, μg/mL)	(MIC, μg/mL)	(MIC, μg/mL)	(MIC, μg/mL)	(MIC, μg/mL)	MCF-7	KB	NCI-H187	Vero
1	> 25	2.33	> 25	> 25	> 50	> 50	> 50	> 50	> 50	> 50
2	> 25	> 50	> 25	> 25	> 50	> 50	> 50	> 50	> 50	> 50
6	> 25	> 50	> 25	> 25	> 50	> 50	> 50	> 50	> 50	> 50
8	> 25	> 50	> 25	> 25	> 50	> 50	> 50	> 50	> 50	> 50
9	> 25	20.86	> 25	> 25	> 50	> 50	> 50	31.72	33.19	> 50
10	3.13	10.32	6.25	6.25	> 50	> 50	> 50	30.13	> 50	> 50
12	1.56	> 50	6.25	6.25	50.0	25.0	> 50	> 50	> 50	27.64
16	12.50	> 50	> 25	> 25	50.0	> 50	> 50	> 50	> 50	> 50
vancomycin	2.0	–	–	–	–	–	–	–	–	–
acyclovir	–	4.99	–	–	–	–	–	–	–	–
amphotericin B	–	–	1.56 – 3.13	1.56 – 3.13	1.56	3.13	–	–	–	–
ellipticine	–	–	–	–	–	–	–	2.60	1.94	1.53
doxorubicin	–	–	–	–	–	–	8.59	0.353	0.079	–
tamoxifen	–	–	–	–	–	–	8.17	–	–	–

[a] = maximum tested concentration was done at 25 μg/mL.
[b] = maximum tested concentration was done at 50 μg/mL.

filtrated through a pad of Celite®545 and evaporated to dryness. The crude was purified by semi-preparative HPLC, eluted with a linear gradient system of 30 − 70% acetonitrile in water over 40 min at the flow rate 8 mL/min, to afford compound **3** (10.9 mg, 60.6%) and *(−)-hemi*-oxanthromicin A (7.2 mg, 60.0%).

3.4. Biological assays

All compounds with sufficient amount were evaluated for antimicrobial activity including malaria against *P. falciparum* (K1-multidrug resistant strain), bacteria against *Mycobacterium tuberculosis* H37Ra and *Bacillus cereus*, phytopathogenic fungi against *Colletotrichum capsici*, *C. gloeosporioides*, *Magnaporthe grisea* and *Alternaria brassicicola*, for anti-*Herpes simplex* virus type 1 (HSV-1) activity, and for cytotoxicity against both cancerous (KB, MCF-7, NCI-H187) and non-cancerous (Vero) cells. The microculture radio isotope technique was employed for antimalarial activity against the multidrug–resistant *Plasmodium falciparum*, K1 strain (Desjardins et al., 1979). The green fluorescent protein microplate assay (GFPMA) was performed to evaluate for anti-HSV- 1 (ATCC VR260) (Hunt et al., 1999), anti-*M. tuberculosis* H37Ra (ATCC 25177), cytotoxicity against Vero cells (African green monkey kidney fibroblasts, ATCC CCL-81) (Changsen et al., 2003), and anti-phytopathogenic fungi including *C. capsici* (BMGC 106) and *C. gloeosporioides* (BMGC 107) (Chutrakul et al., 2013). The resazurin microplate assay (REMA) was used for anti-*B. cereus* (ATCC 11778) and cytotoxicity against KB (human epidermoid carcinoma, ATCC CCL-17), MCF-7 (human breast cancer, ATCC HTC-22) and NCI-H187 (human small lung cancer, ATCC CRL-5804) cells (O'Brien et al., 2000; Sarker et al., 2007). 5 (and 6)-Carboxyfluorescein diacetate (CFDA) for fluorometric detection was used for anti- *A. brassicicola* (BCC 42724) (Aremu et al., 2003) and anti-*M. grisea* (BCC 10261) (Guarro et al., 1998).

Dihydroartemisinine and mefloquine were used as positive controls for antimalarial activity and showed IC_{50} values of 7.17×10^{-4} and 0.0107 μg/mL, respectively. Rifampicin, ofloxacin, streptomycin, isoniazid and ethambutol were used as positive controls for anti-TB activity and displayed MIC values of 0.013, 0.391, 0.313, 0.047, 0.938 μg/mL, respectively. Vancomycin was used as a positive control for anti-*B. cereus* activity and exhibited MIC value of 2.00 μg/mL. Acyclovir was used as a positive control for anti-HSV-1 activity and displayed IC_{50} value of 4.99 μg/mL. Amphotericin B was used as a positive control for anti-phytopathogenic fungi and showed MIC values of 1.56–3.13 μg/mL. Tamoxifen and doxorubicin were used as positive controls for anti-MCF-7 activity and showed IC_{50} values of 8.17 and 8.59 μg/mL. Ellipticine and doxorubicin were used as positive controls for anti-KB and anti-NCI-H187 activities and showed IC_{50} values of 2.60, 0.353 and 1.94, 0.079 μg/mL, respectively. Ellipticine was used as a positive control for cytotoxicity against Vero cell and exhibited IC_{50} value of 1.53 μg/mL. Maximum tested concentration was done at 50 μg/mL, except for anti-*B. cereus*, anti-*C. capsici*, anti-*C. gloeosporioides* were done at 25 μg/mL and antimalarial activity was done at 10 μg/mL.

Acknowledgements

Financial support from the Thailand Research Fund (TRF grant number: RSA5980001) and the National Center for Genetic Engineering and Biotechnology (BIOTEC grant number: P16-51093) are gratefully acknowledged.

Appendix A. Supplementary data

Supplementary data associated with this article can be found, in the online version, at https://doi.org/10.1016/j.phytol.2018.04.002.

References

Abdelfattah, M.S., Toume, K., Arai, M.A., Masu, H., Ishibashi, M., 2012. Katorazone, a new yellow pigment with a 2-azaquinone-phenylhydrazone structure produced by *Streptomyces* sp. IFM 11299. Tetrahedron Lett. 53, 3346–3348.
Aremu, E.A., Furumai, T., Igarashi, Y., Sato, Y., Akamatsu, H., Kodama, M., Otani, H., 2003. Specific inhibition of spore germination of *Alternaria brassicicola* by fistupyrone from *Streptomyces* sp. TP-A0569. J. Gen. Plant Pathol. 69, 211–217.
Arsenault, G.P., 1965. The structure of bostrycoidin, a β-aza-anthraquinone from *Fusarium solani* D2 purple. Tetrahedron Lett. 6, 4033–4037.
Bauer, J.D., King, R.W., Brady, S.F., 2010. Utahmycins A and B, azaquinones produced by an environmental DNA clone. J. Nat. Prod. 73, 976–979.
Berdy, J., 2005. Bioactive microbial metabolites. J. Antibiot. 58, 1–26.
Changsen, C., Franzblau, S.G., Palittapongarnpim, P., 2003. Improved green fluorescent protein reporter gene-based microplate screening for antituberculosis compounds by utilizing an acetamidase promoter. Antimicrob. Agents Chemother. 47, 3682–3687.
Cheng, M.-J., Tseng, M., Yuan, G.-F., Chen, I.-S., 2013. Phytochemical investigation of the culture broth of actinomycete *Actinomadura miaoliensis* BCRC 16873. Chem. Nat. Comp. 49, 226–228.
Chutrakul, C., Khaokhajorn, P., Auncharoen, P., Boonruengprapa, T., Mongkolporn, O., 2013. The potential of a fluorescent-based approach for bioassay of antifungal agents against chili anthracnose disease in Thailand. Biosci. Biotechnol. Biochem. 77, 259–265.
Desjardins, R.E., Canfield, C.J., Haynes, J.D., Chulay, J.D., 1979. Quantitative assessment of antimalarial activity in vitro by a semiautomated microdilution technique. Antimicrob. Agents Chemother. 16, 710–718.
El-Hawary, S.S., Sayed, A.M., Rateb, M.E., Bakeer, W., AbouZid, S.F., Mohammed, R., 2017. Secondary metabolites from fungal endophytes of *Solanum nigrum*. Nat. Prod. Res. 1–4.
Gräfe, U., Ihn, W., Tresselt, D., Miosga, N., Kaden, U., Schlegel, B., Bormann, E.-J., Sedmera, P., Novák, J., 1990. Tolypocladin — a new metal-chelating 2-aza-anthraquinone from *Tolypocladium inflatum*. Biol. Met. 3, 39–44.
Guarro, J., Pujol, I., Aguilar, C., Llop, C., Fernández-Ballart, J., 1998. Inoculum

preparation for in-vitro susceptibility testing of filamentous fungi. J. Antimicrob. Chemother. 42, 385–387.
Hawas, U.W., El-Ansari, M.A., Laatsch, H., 2006. A new alpha-methylanthraquinone glucoside from *Emex spinosus*. Nat. Prod. Res. 20, 742–747.
Hunt, L., Jordan, M., De Jesus, M., Wurm, F.M., 1999. GFP-expressing mammalian cells for fast, sensitive, noninvasive cell growth assessment in a kinetic mode. Biotechnol. Bioeng. 65, 201–205.
Husain, S.M., Schätzle, M.A., Röhr, C., Lüdeke, S., Müller, M., 2012. Biomimetic asymmetric synthesis of (*R*)-GTRI-02 and (3*S*,4*R*)-3,4-dihydroxy-3,4-dihydronaphthalen-1(2*H*)-ones. Org. Lett. 14, 3600–3603.
Kazuma, K., Noda, N., Suzuki, M., 2003. Malonylated flavonol glycosides from the petals of *Clitoria ternatea*. Phytochemistry 62, 229–237.
Koiwa, T., Nakano, T., Takahashi, S., Koshino, H., Yamazaki, M., Takashi, T., Nakagawa, A., 1999. Adxanthromycin: a new inhibitor of ICAM-1/LFA-1 mediated cell adhesion from *Streptomyces* sp. NA-148. J. Antibiot. 52, 198–200.
Koyama, J., Morita, I., Kobayashi, N., Osakai, T., Usuki, Y., Taniguchi, M., 2005. Structure-activity relations of azafluorenone and azaanthraquinone as antimicrobial compounds. Bioorg. Med. Chem. Lett. 15, 1079–1082.
Maskey, R.P., Li, F., Qin, S., Fiebig, H.H., Laatsch, H., 2003. Chandrananimycins A approximately C: production of novel anticancer antibiotics from a marine *Actinomadura* sp. isolate M048 by variation of medium composition and growth conditions. J. Antibiot. 56, 622–629.
Miljkovic, A., Mantle, P.G., Williams, D.J., Rassing, B., 2001. Scorpinone: a new natural azaanthraquinone produced by a Bispora-like tropical fungus. J. Nat. Prod. 64, 1251–1253.
Moriyasu, Y., Miyagawa, H., Hamada, N., Miyawaki, H., Ueno, T., 2001. 5-Deoxy-7-methylbostrycoidin from cultured mycobionts from *Haematomma* sp. Phytochemistry 58, 239–241.
O'Brien, J., Wilson, I., Orton, T., Pognan, F., 2000. Investigation of the Alamar Blue (resazurin) fluorescent dye for the assessment of mammalian cell cytotoxicity. Eur. J. Biochem. 267, 5421–5426.
Patel, M., Horan, A.C., Gullo, V.P., Loebenberg, D., Marquez, J.A., Miller, G.H., Waitz, J.A., 1984. Oxanthromicin, a novel antibiotic from *Actinomadura*. J. Antibiot. 37, 413–415.
Pouchert, C., 1993. Aldrich Library of ^{13}C and ^{1}H FT-NMR Spectra. Wiley, pp. 138.
Saitou, N., Nei, M., 1987. The neighbor-joining method: a new method for reconstructing phylogenetic trees. Mol. Biol. Evol. 4, 406–425.
Salim, A.A., Xiao, X., Cho, K.J., Piggott, A.M., Lacey, E., Hancock, J.F., Capon, R.J., 2014. Rare *Streptomyces* sp. polyketides as modulators of K-Ras localisation. Org. Biomol. Chem. 12, 4872–4878.
Sarker, S.D., Nahar, L., Kumarasamy, Y., 2007. Microtitre plate-based antibacterial assay incorporating resazurin as an indicator of cell growth, and its application in the in vitro antibacterial screening of phytochemicals. Methods 42, 321–324.
Shin, B., Kim, B.-Y., Cho, E., Oh, K.-B., Shin, J., Goodfellow, M., Oh, D.-C., 2016. Actinomadurol, an antibacterial norditerpenoid from a rare actinomycete, *Actinomadura* sp. KC 191. J. Nat. Prod. 79, 1886–1890.
Takahashi, S., Nakano, T., Koiwa, T., Noshita, T., Funayama, S., Koshino, H., Nakagawa, A., 2000. Adxanthromycins A and B: new inhibitors of ICAM-1/LFA-1 mediated cell adhesion molecule from *Streptomyces* sp. NA-148. II. Physico-chemical properties and structure elucidation. J. Antibiot. 53, 163–170.
Tomita, K., Nishio, M., Saitoh, K., Yamamoto, H., Hoshino, Y., Ohkuma, H., Konishi, M., Miyaki, T., Oki, T., 1990. Pradimicins A, B and C: new antifungal antibiotics I. Taxonomy, production, isolation and physico-chemical properties. J. Antibiot. 43, 755–762.
Wright, J.J.K., Merill, Y., Puar, M.S., McPhail, A.T., 1984. Structure of oxanthromicin (antibiotic 16–550), a novel dimeric anthrone peroxide. J. Chem. Soc., Chem. Commun. 473–474.
Yoon, S.H., Ha, S.M., Kwon, S., Lim, J., Kim, Y., Seo, H., Chun, J., 2017. Introducing EzBioCloud: a taxonomically united database of 16S rRNA gene sequences and whole-genome assemblies. Int. J. Syst. Evol. Microbiol. 67, 1613–1617.

Phytochemistry Letters 26 (2018) 33–37

Contents lists available at ScienceDirect

Phytochemistry Letters

journal homepage: www.elsevier.com/locate/phytol

Antagonistic metabolites produced by the fungus *Curvularia* sp. BCC52426 against *Aspergillus* sp. BCC51998

Nantiya Bunbamrung, Chakapong Intaraudom, Aibrohim Dramae, Nattawut Boonyuen, Rungtiwa Chanthaket, Pranee Rachtawee, Pattama Pittayakhajonwut*

The National Center for Genetic Engineering and Biotechnology (BIOTEC), 113 Thailand Science Park, Phaholyothin Road, Klong Luang, Pathum Thani, 12120, Thailand

ARTICLE INFO

Keywords:
Curvularia
Chloro-containing xanthone
Chromone derivatives
Antimicrobial

ABSTRACT

Four previously undescribed compounds, including (*Z*)-chloromonilinic acid B (**1**), (*E*)-chloromonilinic acid C (**2**), 4-chlorocurvularin (**5**), and 4-chlorocurvularinic acid (**6**), together with four known compounds, (*E*)-chloromonilinic acids A and B, pinselin, and anhydromevalonolactone, were isolated from the fungus *Curvularia* sp. BCC52426. The chemical structures were determined by comparing their NMR spectra to documented spectra of the related compounds and the isolated compounds were also appraised for antimicrobial activity and cytotoxicity.

1. Introduction

The genus *Curvularia* has been isolated from various environments such as plants, soil, and marine. Diverse chemical structures with a broad range of biological activity have been identified and isolated from this genus. For example, murranofuran A, murranolide A, murranopyrone, and murranoic acid A were isolated from the endophytic fungus *Curvularia* sp. M12. Murranolide A and murranopyrone show more than 50% motility inhibitory activity against the late blight phytopathogen (*Phytophthora capcisi*) at a concentration of 50–100 μg/mL (Mondol et al., 2017). A pyrrole alkaloid named curindolizine was isolated from a white croaker-associated fungus, *Curvularia* sp. IFB-Z10, which has anti-inflammatory properties (Han et al., 2016). Pentanorlanostane derivatives, named curvalarols A and B, were isolated from the soil fungus *Curvularia borreriae* HS-FG-237 and display cytotoxicity against A549, K562, and MDA-MB-231 cells (Xue et al., 2013). Curvularone A and 4-hydroxyradianthin were isolated from the soil fungus *Curvularia inaequalis* strain HS-FG-257 and show cytotoxicity against ACHN and HepG2 (Pang et al., 2013). Curvulapyrone, curvulalide, and curvularic acid were isolated from the sea fan-fungus, *Curvularia* sp. PSU-F22 and two other compounds are inactive as antibacterial agents against *Staphylococcus aureus* ATCC 25923 and methicillin-resistant *S. aureus* SK1 and as antifungal agents against *Microsporum gypseum* SH-MU-4 activities (Trisuwan et al., 2011). A 14-membered macrolide, apralactone, was isolated from the marine-derived fungus, *Curvularia* sp. (strain no. 768) and possess cytotoxic activity against human tumour cells (Greve et al., 2008).

Two strains of fungi, registered as BCC51998 and BCC52426, were collected from 1 to 3-year-old bagasse at a depth of 30 cm from the surface and identified by morphology and partial gene sequences to be *Aspergillus* sp. and *Curvularia* sp., respectively. These two strains were co-cultured on a PDA (potato dextrose agar) plate and unexpectedly, after 7 days, the fungus *Curvularia* sp. BCC52426 showed antagonistic behavior, producing an inhibition area that did not allow the fungus *Aspergillus* sp. BCC51998 to invade. We investigated potentially antagonistic metabolites produced by *Curvularia* sp. BCC52426. In addition, as part of our continuing search for new antimicrobial agents, crude extracts of *Curvularia* sp. BCC52426 were also appraised for antimalarial, antitubercular, antibacterial, anti-phytopathogenic fungus and cytotoxic activities, and the results showed that these extracts were inactive in all tests at the maximum tested concentrations. Chemical analysis of the culture broth led to the isolation of four new compounds, (*Z*)-chloromonilinic acid B (**1**), (*E*)-chloromonilinic acid C (**2**), 4-chlorocurvularin (**5**), and 4-chlorocurvularinic acid (**6**), together with three known compounds, (*E*)-chloromonilinic acids A (**3**) and B (**4**) and anhydromevalonolactone. The crude extract from cells yielded only compound **5** and pinselin.

2. Results and discussion

Compound **1** was obtained as a brown gum. The ^{1}H NMR spectrum (Table 1) was almost identical to that of compound **4**, whose spectroscopic data were identical to those of (*E*)-chloromonilinic acid B (Sassa et al., 1989), except for a downfield shift of a methine proton. The

* Corresponding author.
E-mail address: pattamap@biotec.or.th (P. Pittayakhajonwut).

https://doi.org/10.1016/j.phytol.2018.05.009
Received 19 December 2017; Received in revised form 20 April 2018; Accepted 1 May 2018

Table 1
^{1}H and ^{13}C NMR assignments of compounds **1**, **2**, **5**, and **6**.

position	**1**[a] in DMSO-d_6		**2**[b] in DMSO-d_6		**5**[a] in acetone-d_6		**6**[b] in DMSO-d_6	
	δ_H, (mult.)	δ_C, type	δ_H, (mult.)	δ_C, type	δ_H, (mult.)	δ_C, type	δ_H, (mult.)	δ_C, type
1	–	170.8, C	–	169.1, C	–	133.4, C	–	117.5, C
2	3.58 (s)	30.6, CH_2	3.49 (s)	29.8, CH_2	7.08 (s)	112.4, CH	–	151.3, C
3	–	115.8, C	–	115.5, C	–	161.4, C	7.67 (s)	125.5, CH
4	–	181.9, C	–	181.3, C	–	108.8, C	–	123.4, C
4a	–	–	–	–	–	160.3, C	–	145.3, C
5	–	107.8, C	–	111.4, C	6.67 (s)	110.8(5), CH	7.49 (s)	108.1, CH
6	–	159.8, C	–	155.4, C	–	149.5, C	–	125.5, C
7	6.73 (s)	112.7, CH	7.54 (s)	108.1, CH	6.93 (s)	107.7, CH	7.25 (s)	111.0, CH
8	–	149.2, C	–	138.6, C	–	155.8, C	–	160.9, C
8a	–	–	–	–	–	106.4, C	–	110.1, C
9	6.98 (s)	108.1, CH	7.30 (s)	111.4, CH	–	179.6, C	–	180.6, C
9a	–	–	–	–	–	110.8(6), C	–	119.3, C
10	–	155.9, C	–	159.3, C	–	–	–	–
10a	–	–	–	–	–	153.9, C	–	155.5, C
11	–	158.6, C	–	159.5, C	–	168.2, C	–	167.0[c], C
12	–	129.5[c], C	–	132.0, C	2.46 (s)	21.7, CH_3	–	166.5, C
13	6.82 (s)	129.4, CH	6.82 (s)	131.2, CH	–	–	–	–
14	–	164.0, C	–	163.3, C	–	–	–	–
1-OCH_3	3.63 (s)	52.4, CH_3	3.60 (s)	51.9, CH_3	–	–	–	–
8-CH_3	2.40 (s)	22.3, CH_3	–	–	–	–	–	–
8-COOH	–	–	–	165.5, C	–	–	–	–
8-OH	–	–	–	–	12.27 (s)	–	11.97 (s)	–
11-OCH_3	–	–	–	–	3.91 (s)	52.4, CH_3	–	–
12-OCH_3	–	–	–	–	–	–	3.86, s	52.8, CH_3

[a] Recorded at 400 MHz for ^{1}H NMR and at 100 MHz for ^{13}C NMR.
[b] Recorded at 500 MHz for ^{1}H NMR and at 125 MHz for ^{13}C NMR.
[c] Observed in HMBC spectrum.

downfield methine at δ_H 6.82 (H-13) correlated in HMBC to C-11 (δ_C 158.6) and C-12 (δ_C 129.5). The remaining HMBC correlations indicated that compound **1** had the same chemical structure as chloromonilinic acid B, also confirmed by HRESIMS, which gave a sodium-adducted mass ion peak at *m/z* 375.0241 $[M+Na]^+$. However, the observation of correlation from H-13 and H_2-2 in the NOESY spectrum suggested that the configuration of double bond at C-12/C-13 was *Z*. Thus, compound **1** was the first isolation of a *Z* form of chloromonilinic acid B.

Likewise, the ^{1}H NMR spectrum (Table 1) of compound **2** showed downfield shifts of two aromatic methine protons and a lack of methyl signal at C-8, compared with that of compound **4** (Sassa et al., 1989). In the HMBC spectrum, two downfield methine protons (δ_H 7.30, H-9 and 7.54, H-7) correlated to an extra quaternary carbon at δ_C 165.5, suggesting a replacement of a methyl group with a carboxylic group. The rest of the structure was determined by NMR spectroscopic data, and the HRESIMS spectrum confirmed the molecular formula $C_{16}H_{11}ClO_9$ by showing a mass ion peak at *m/z* 381.0016 $[M-H]^-$. The lack of a correlation from H-13 (δ_H 6.82) to H_2-2 (δ_H 3.49) in the NOESY spectrum suggested that the configuration of the double bond at C-12/C-13 was *E*. The chemical structure of compound **2** is shown in Fig. 1 and (*E*)-chloromonilinic acid C was given as its trivial name.

Compound **5** was obtained as an orange solid. HRESIMS spectrum revealed a sodium-adduct mass ion peak at *m/z* 357.0139 $[M+Na]^+$, establishing a molecular formula $C_{16}H_{11}ClO_6$. The ^{1}H NMR spectrum (Table 1) was similar to that of 4-chloropinselin (Kachi et al., 1986), apart from an upfield shift of a methine proton at δ_H 7.08 (H-2). In the HMBC spectrum, H-2 correlated to C-4 (δ_C 108.8), C-9a (δ_C 110.9), and C-11 (δ_C 168.2), indicating its position at C-2. In addition, the methoxy protons at δ_H 3.91 correlated to C-11 in the HMBC spectrum, suggesting a methyl ester at C-1. The remaining signals showed HMBC correlations that were the same as those described for 4-chloropinselin. The ^{13}C NMR signals at C-2 (δ_C 112.4) and C-4 suggested a hydroxyl substituent at C-3. Thus, compound **5** possessed the chemical structure shown in Fig. 1 and was named 4-chlorocurvularin.

Compound **6** was obtained as a yellow solid and the ^{1}H NMR spectrum (Table 1) was similar to that of compound **5**, except for the absence of the methyl signal. HRESIMS spectrum revealed the presence of a Cl atom in the molecule with a mass ion peak at *m/z* 362.9920 $[M-H]^-$, establishing the molecular formula of $C_{16}H_9ClO_8$. The ^{13}C NMR spectrum showed only fourteen signals consisting of one methyl, three methine, and ten quaternary carbons. Two aromatic methine protons at δ_H 7.25 (H-7), 7.49 (H-5), and a methoxy group at δ_H 3.86 correlated in the HMBC spectrum to a carbonyl carbon at δ_C 166.5 (C-12), indicating a carbomethoxy group attached at C-6. Moreover, the HMBC spectrum showed correlations from H-3 to C-1, C-2, C-4, and C-4a; from H-5 to C-7, C-8a, and C-10a; and from H-7 to C-5, C-8, and C-8a. The remaining signal at δ_C 180.6 indicated a carbonyl of xanthone, whose UV spectrum showed a similar pattern to that of fischexanthone (Bunbamrung et al., 2015). The IR spectrum displayed absorption of a carboxylic acid hydroxyl group (ν 3500–2800 cm^{-1}) and an ester carbonyl (ν_{max} 1737 cm^{-1}). Therefore, compound 6 was assigned as 4-chloro-2,8-dihydroxy-6-(methoxycarbonyl)-9-oxo-9*H*-xanthene-1-carboxylic acid, shown in Fig. 1, and was named 4-chlorocurvularinic acid.

The ^{1}H and ^{13}C NMR spectra of compounds **3**, **4**, and **7** were identical to those of (*E*)-chloromonilinic acids A and B (Sassa et al., 1989) and pinselin (Yamazaki and Okuyama, 1980), respectively. All tested compounds, except compounds **1** and **5**, showed no cytotoxicity (IC_{50} > 10 μM) against either cancerous (MCF-7, KB, NCI-H187) or non-cancerous (Vero) cells and were inactive in all tests. Compound **1** exhibited anti-TB activity at the maximum tested concentration (MIC 50 μg/mL), whereas compound **5** showed antibacterial activity against *B. cereus* and *E. faecium*, with MIC values of 25 and 50 μg/mL, respectively. The results indicated that (*Z*)-chloromonilinic acid B (**1**) had higher anti-TB activity than that of (*E*)-chloromonilinic acid B (**4**) and that 4-chlorocurvularin (**5**) had higher antibacterial activity than that of the related compound, pinselin (**7**). Moreover, the isolated compounds should have biological activity against the fungus *Aspergillus*, but this test has not been performed.

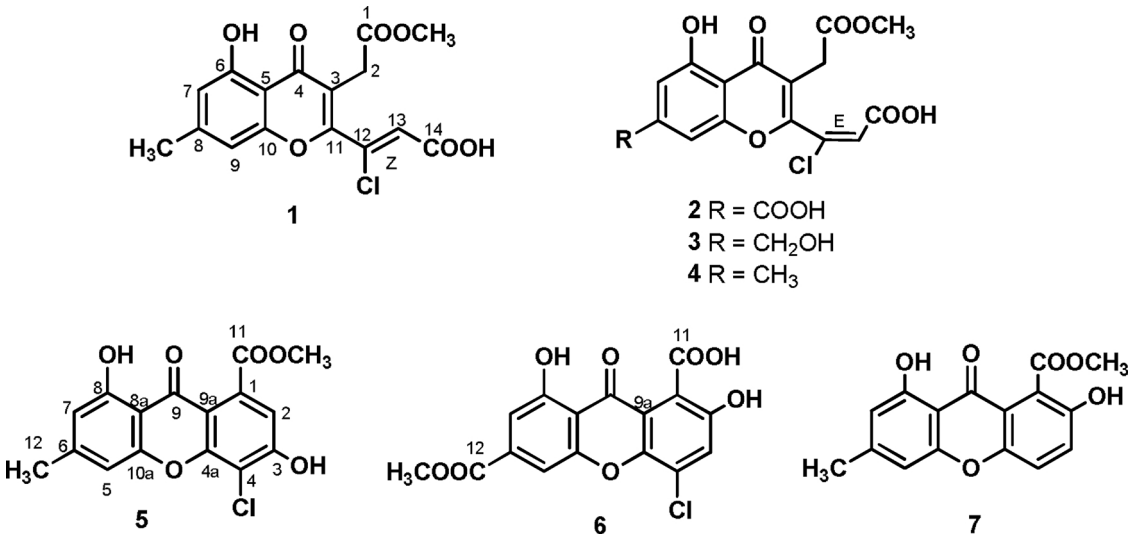

Fig. 1. Chemical structures of compounds isolated from the fungus *Curvularia* sp. BCC52426.

3. Experimental section

3.1. General procedures

NMR spectra, including ^{1}H, ^{13}C, DEPT-135, COSY, NOESY, HMQC and HMBC experiments, were recorded on either a Bruker Avance 500 NMR spectrometer (at 500 MHz for ^{1}H and 125 MHz for ^{13}C) or a Bruker Avance III 400 NMR spectrometer (at 400 MHz for ^{1}H and 100 MHz for ^{13}C), using either acetone-d_6 or DMSO-d_6 as internal standards. UV spectroscopy was performed in MeOH, using a Spekol 1200, Analytik Jena AG. IR spectra were obtained from a Bruker ALPHA FT-IR spectrometer. HRESIMS data were acquired on a Bruker MicrOTOF mass spectrometer. Preparative HPLC was performed using the Dionex, Ultimate 3000 series model, which was equipped with a binary pump, an autosampler and a diode array detector. Preparative and semi-preparative HPLC were performed with a Sunfire C18 OBD column from Waters (diam. 19 mm × 250 mm, particle size 10 µm for preparative HPLC and diam. 19 mm × 150 mm, particle size 5 µm for semi-preparative HPLC) at flow rates of 15 and 9 mL/min, respectively.

3.2. Fungal material

The fungus was isolated from 1 to 3-year-old bagasse collected at a depth of 30 cm from the surface at Eastern Sugar and Cane Public Company Limited, Sa Kaeo province, Thailand. The fungus was identified based on the partial nuclear large subunits ribosomal DNA (nc28S rDNA, 1159 bps), the internal transcribed spacer (ITS region, 577 bps) and the partial RPB2 gene for RNA polymerase II subunit 2 (RPB2, 947 bps). The combined nc28S rDNA and RPB2 sequences (2106 bps) indicated affinity with fungal taxa within Pleosporales, Dothideomycetes, and Ascomycota, and the ITS sequence of the fungus showed 99–100% similarity with *Curvularia* sp. using BLAST (the Basic Local Alignment Search Tool; https://blast.ncbi.nlm.nih.gov/Blast.cgi) from the National Center for Biotechnology Information (NCBI) and Pairwise Sequence Alignment (PSA; http://www.mycobank.org/) from Mycobank. Therefore, the fungus was identified as *Curvularia* sp. in family Pleosporaceae, order Pleosporales, class Dothideomycetes, phylum Ascomycota, registered as BCC52426 at BIOTEC Culture Collection (BCC). The ITS, nc28S rDNA and RPB2 sequences were submitted to GenBank with accession numbers MG661738, MG661740, and MG674189, respectively.

3.3. Fermentation, extraction, and isolation

The fungus BCC52426, previously induced by co-cultured with *Aspergillus* sp. BCC51998, was grown on PDA (potato dextrose agar) at 25 °C for 19 days, and the agar was then cut into small pieces (1 × 1 cm^2) prior to transferring into four 250 mL Erlenmeyer flasks, each containing 25 mL PDB (potato dextrose broth). The culture was grown for 6 days at 25 °C in a shaker and was later transferred into sixteen 1 L Erlenmeyer flasks, each containing 250 mL PDB. The seed culture was then incubated for 6 days at 25 °C in a shaker and transferred into eighty 1 L Erlenmeyer flasks, each containing 250 mL MEB (malt extract broth). This production culture (20 L) was grown for 40 days at 25 °C in shakers (250 rpm). After 40 days, the broth and cell were separated by simple filtration. The broth was extracted with an equal volume of EtOAc three times. The EtOAc was dried over Na_2SO_4 and then evaporated to dryness to give a brown gum (0.81 g). The cells were submerged in MeOH for 3 days and consecutively in CH_2Cl_2 for 3 days. The organic solvents were then combined and concentrated. Water (50 mL) was added and the mixture was then extracted thrice with equal volumes of EtOAc. EtOAc was then dried over Na_2SO_4 and evaporated to dryness to obtain a brown gum (4.68 g).

Broth (0.81 g) was passed through a Sephadex LH-20 column (4.5 cm × 40 cm) and eluted with 100% MeOH to give two main fractions. The first fraction (0.57 g) was passed through another Sephadex LH-20 column (2.5 cm × 75 cm) and eluted with 100% MeOH to obtain three subfractions (f1-f3). Subfraction f1 (0.18 g) was further purified by preparative HPLC using a linear gradient system of 5–85% CH_3CN in water over 30 min, to yield compound anhydromevalonolactone (9.2 mg). Subfraction f2 (0.25 g) was purified by preparative HPLC, using a linear gradient system of 10–65% CH_3CN in water over 30 min, to yield 3 subfractions (f2f1–f2f3). Anhydromevalonolactone (3.9 mg) and compound **4** (26.8 mg) were obtained from subfractions f2f1 and f2f3, respectively. Subfraction f2f2 (46.0 mg) was further purified using a Sephadex LH-20 column (using 100% MeOH as the mobile phase) followed by purification on TLC plates (using 1:1, *n*-hexane:acetone in a presence of 1% acetic acid as a mobile phase) to yield compounds **4** (22.1 mg) and **1** (7.6 mg). Subfraction f3 (58.5 mg) was further purified by semi-preparative HPLC using a linear gradient system of 30–70% CH_3CN in water in the presence of 0.05% HCOOH over 30 min, to yield compounds **3** (2.3 mg) and **2** (7.0 mg). The second fraction (25.7 mg) was purified by semi-preparative HPLC using a linear gradient system of 10–65% CH_3CN in water over 30 min to yield compounds **6** (2.9 mg) and **5** (1.8 mg).

The brown gum (4.7 g) from cell extraction was passed through a Sephadex LH-20 column to yield two main fractions. The first fraction (69.5 mg) was further purified by preparative HPLC using a linear gradient system of 10–70% CH_3CN in water over 30 min to yield pinselin (**7**, 2.7 mg). The second fraction (20.7 mg) was purified by semi-preparative HPLC, using 20–80% CH_3CN in water over 30 min to yield compound **5** (3.1 mg).

3.3.1. (Z)-Chloromonilinic acid B (1)

Brown gum; UV (MeOH) λ_{max} (log ε) 243 (4.15), 263 (4.21), 337 (3.74) nm; FTIR (ATR) ν_{max} 3500-2500 (br), 1738, 1656, 1610, 1437, 1364, 1351, 1294, 1207, 1165, 1083, 958, 826 cm^{-1}; HRESIMS *m/z* 375.0241 $[M+Na]^+$ (calcd for $C_{16}H_{13}ClO_7Na$, 375.0242).

3.3.2. (E)-Chloromonilinic acid C (2)

Brown gum; UV (MeOH) λ_{max} (log ε) 243 (4.08), 261 (4.07), 351 (3.73) nm; FTIR (ATR) ν_{max} 3500-2500 (br), 1736, 1727, 1657, 1611, 1439, 1413, 1365, 1349, 1288, 1228, 1217, 1197, 1165, 1079 cm^{-1}; HRESIMS *m/z* 381.0016 $[M-H]^-$ (calcd for $C_{16}H_{10}ClO_9$, 381.0019).

3.3.3. 4-Chlorocurvularin (5)

Orange solid; UV (MeOH) λ_{max} (log ε) 240 (4.27), 262 (4.10), 294 (3.80), 359 (4.08) nm; FTIR (ATR) ν_{max} 3500-3000 (br), 2954, 2924, 2854, 1737, 1722, 1650, 1596, 1529, 1502, 1439, 1379, 1275, 1210, 1164, 1107, 1051, 1028, 830, 773 cm^{-1}; HRESIMS *m/z* 357.0139 $[M+Na]^+$ (calcd for $C_{16}H_{11}ClO_6Na$, 357.0136).

3.3.4. 4-Chlorocurvularinic acid (6)

Yellow solid; UV (MeOH) λ_{max} (log ε) 241 (4.36), 268 (4.36), 297 (4.04), 332 (3.84), 404 (3.96) nm; FTIR (ATR) ν_{max} 3500-2800 (br), 2925, 2853, 1737 (overlapping), 1716, 1650, 1620, 1587, 1570, 1499, 1436, 1412, 1359, 1283, 1232, 1192, 1083, 1017, 879, 757 cm^{-1}; HRESIMS *m/z* 362.9920 $[M-H]^-$ (calcd for $C_{16}H_8ClO_8$, 362.9913).

3.4. Biological assays

Isolated compounds that were obtained at adequate amounts (excluding compounds **3** and **6**) were evaluated for antimicrobial activity against the malaria parasite *P. falciparum* (K1-multidrug resistant strain), the bacteria *Mycobacterium tuberculosis* H37Ra, *Bacillus cereus*, *Enterococcus faecium*, *Escherichia coli*, *Acinetobacter baumannii*, *Klebsiella pneumoniae*, and *Pseudomonas aeruginosa*, and the phytopathogenic fungi *Colletotrichum capsici*, *C. gloeosporioides*, *Magnaporthe grisea* and *Alternaria brassicicola*. The compounds were also tested for cytotoxicity against both cancerous (KB, MCF-7, and NCI-H187) and non-cancerous (Vero) cells. The microculture radio isotope technique was employed to evaluate antimalarial activity against the multidrug–resistant *Plasmodium falciparum* K1 strain (Desjardins et al., 1979). The green fluorescent protein microplate assay (GFPMA) was performed to evaluate anti-*M. tuberculosis* H37Ra (ATCC 25177), cytotoxicity against Vero cells (African green monkey kidney fibroblasts, ATCC CCL-81) (Changsen et al., 2003), and anti-phytopathogenic fungi including *C. capsici* (BMGC 106) and *C. gloeosporioides* (BMGC 107) (Chutrakul et al., 2013). The resazurin microplate assay (REMA) was used to evaluate anti-*B. cereus* (ATCC 11778) and cytotoxicity against KB (human epidermoid carcinoma, ATCC CCL-17), MCF-7 (human breast cancer, ATCC HTC-22) and NCI-H187 (human small lung cancer, ATCC CRL-5804) cells (O'Brien et al., 2000; Sarker et al., 2007). Antibacterial activity against *E. faecium* (ATCC 51559), *E. coli* (ATCC 25922), *A. baumannii* (ATCC 19606), *K. pneumoniae* (ATCC 700603), and *P. aeruginosa* (ATCC 15692) was evaluated by using the standard protocols published by Clinical and Laboratory Standard Institute (Wayne, 2006a,b). 5- (and 6)-Carboxyfluorescein diacetate (CFDA) for fluorometric detection was used for anti-*A. brassicicola* (BCC 42724) (Aremu et al., 2003) and anti-*M. grisea* (BCC 10261) (Guarro et al., 1998).

Dihydroartemisinine and mefloquine were used as positive controls for antimalarial activity and had IC_{50} values of 8.05×10^{-4} and 0.024 μg/mL, respectively. Rifampicin, ofloxacin, streptomycin, isoniazid and ethambutol were used as positive controls for anti-TB activity and displayed MIC values of 0.025, 0.391, 0.313, 0.047, 0.47 μg/mL, respectively. Vancomycin was used as a positive control for anti-*B. cereus* activity and exhibited an MIC value of 2.00 μg/mL. Rifampicin and tetracycline HCl were used as standard references for activity against *E. faecium* and *E. coli* and showed the same MIC value of 3.13 μg/mL, whereas rifampicin and erythromycin were used as standard references for anti-*A. baumannii* and anti-*K. pneumoniae* and exhibited MIC values of 3.13, 12.50 and 25.0, 100.0 μg/mL, respectively. Erythromycin and chloramphenicol were used as standard references for anti-*P. aeruginosa* and had MIC values of > 32 and > 8 μg/mL. Amphotericin B was used as a positive control for anti-phytopathogenic fungi with MIC values in the range of 1.56–3.13 μg/mL. The maximum tested concentration was 50 μg/mL, except for anti-*B. cereus*, anti-*C. capsici*, and anti-*C. gloeosporioides*, which were tested at 25 μg/mL, and antimalarial activity, which was tested at 10 μg/mL.

Acknowledgements

Financial support from the Thailand Research Fund (TRF grant number: RSA5980001) and the National Center for Genetic Engineering and Biotechnology (BIOTEC grant number: P16-51093) are gratefully acknowledged.

Appendix A. Supplementary data

Supplementary data associated with this article can be found, in the online version, at https://doi.org/10.1016/j.phytol.2018.05.009.

References

Aremu, E.A., Furumai, T., Igarashi, Y., Sato, Y., Akamatsu, H., Kodama, M., Otani, H., 2003. Specific inhibition of spore germination of Alternaria brassicicola by fistupyrone from *Streptomyces* sp. TP-A0569. J. Gen. Plant Pathol. 69, 211–217.

Bunbamrung, N., Intaraudom, C., Supothina, S., Komwijit, S., Pittayakhajonwut, P., 2015. Antibacterial and anti-phytopathogenic substances from the insect pathogenic fungus *Gibellula* sp. BCC36964. Phytochem. Lett. 12, 142–147.

Changsen, C., Franzblau, S.G., Palittapongarnpim, P., 2003. Improved green fluorescent protein reporter gene-based microplate screening for antituberculosis compounds by utilizing an acetamidase promoter. Antimicrob. Agents Chemother. 47, 3682–3687.

Chutrakul, C., Khaokhajorn, P., Auncharoen, P., Boonruengprapa, T., Mongkolporn, O., 2013. The potential of a fluorescent-based approach for bioassay of antifungal agents against chili anthracnose disease in Thailand. Biosci. Biotechnol. Biochem. 77, 259–265.

Desjardins, R.E., Canfield, C.J., Haynes, J.D., Chulay, J.D., 1979. Quantitative assessment of antimalarial activity in vitro by a semiautomated microdilution technique. Antimicrob. Agents Chemother. 16, 710–718.

Greve, H., Schupp, P.J., Eguereva, E., Kehraus, S., Kelter, G., Maier, A., Fiebig, H.H., Konig, G.M., 2008. Apralactone A and a new stereochemical class of curvularins from the marine-derived fungus *Curvularia* sp. Eur. J. Org. Chem. 2008, 5085–5092.

Guarro, J., Pujol, I., Aguilar, C., Llop, C., Fernández-Ballart, J., 1998. Inoculum preparation for in-vitro susceptibility testing of filamentous fungi. J. Antimicrob. Chemother. 42, 385–387.

Han, W.B., Zhang, A.H., Deng, X.Z., Lei, X., Tan, R.X., 2016. Curindolizine, an anti-inflammatory agent assembled via michael addition of pyrrole alkaloids inside fungal cells. Org. Lett. 18, 1816–1819.

Kachi, H., Hattori, H., Sassa, T., 1986. A new antifungal substance, bromomonilicin, and its precursor produced by *Monilinia fructicola*. J. Antibiot. 39, 164–166.

Mondol, M.A.M., Farthouse, J., Islam, M.T., Schüffler, A., Laatsch, H., 2017. Metabolites from the endophytic fungus *Curvularia* sp: m12 act as motility inhibitors against *Phytophthora capsici* zoospores. J. Nat. Prod. 80, 347–355.

O'Brien, J., Wilson, I., Orton, T., Pognan, F., 2000. Investigation of the Alamar Blue (resazurin) fluorescent dye for the assessment of mammalian cell cytotoxicity. Eur. J. Biochem. 267, 5421–5426.

Pang, Y.-W., Zhang, L.-J., Fang, J.-S., Liu, Q.-F., Zhang, H., Xiang, W.-S., Wang, J.-D., Wang, X.-J., 2013. Two new antitumor constituents from a soil fungus *Curvularia inaequalis* (strain HS-FG-257). J. Antibiot. 66, 287–289.

Sarker, S.D., Nahar, L., Kumarasamy, Y., 2007. Microtitre plate-based antibacterial assay incorporating resazurin as an indicator of cell growth, and its application in the in vitro antibacterial screening of phytochemicals. Methods 42, 321–324.

Sassa, T., Horiguchi, K., Suzuki, Y., 1989. Chloromonilinic acids A and B: novel catabolites of the growth self-inhibitor chloromonilicin isolated from *Monilinia fructicola*. Agric. Biol. Chem. 53, 1337–1341.

Trisuwan, K., Rukachaisirikul, V., Phongpaichit, S., Preedanon, S., Sakayaroj, J., 2011. Modiolide and pyrone derivatives from the sea fan-derived fungus *Curvularia* sp. PSU-F22. Arch. Pharm. Res. 34, 709–714.

Wayne, P.A., 2006a. M7-A7. Methods for Dilution Antimicrobial Susceptibility Tests for Bacteria That Grow Aerobically; Approved Standard, 7th ed. Clinical and Laboratory Standards Institute.

Wayne, P.A., 2006b. M100-S16, Performance Standards for Antimicrobial Susceptibility Testing; 16th Informational Supplement. Clinical and Laboratory Standards Institute.

Xue, C.-Y., Li, J.-S., Qi, H., Xi, F.-Y., Xiang, W.-S., Wang, J.-D., Wang, X.-J., 2013. Two new pentanorlanostane metabolites from a soil fungus *Curvularia borreriae* strain HS-FG-237. J. Antibiot. 66, 735–737.

Yamazaki, M., Okuyama, E.M.I., 1980. Isolation and structures of oxaphenalenone dimers from *Talaromyces bacillosporus*. Chem. Pharm. Bull. 28, 3649–3655.

Tetrahedron 74 (2018) 6907–6916

Contents lists available at ScienceDirect

Tetrahedron

journal homepage: www.elsevier.com/locate/tet

Antimicrobial activity of cyathane derivatives from *Cyathus subglobisporus* BCC44381

Sutichai Nitthithanasilp, Chakapong Intaraudom, Nattawut Boonyuen, Rapheephat Suvannakad, Pattama Pittayakhajonwut*

National Center for Genetic Engineering and Biotechnology (BIOTEC), National Science and Technology Development Agency (NSTDA), Thailand Science Park, Phaholyothin Road, Klong Luang, Pathum Thani 12120, Thailand

ARTICLE INFO

Article history:
Received 27 June 2018
Received in revised form
4 October 2018
Accepted 8 October 2018
Available online 10 October 2018

Keywords:
Cyathus
Cyathane derivatives
Antimicrobial
Anticancer
Cytotoxicity

ABSTRACT

Six unknown cyathane diterpenes, named cyathinins A – E, and 10-hydroxyerinacine S, were isolated from *Cyathus subglobisporus* BCC44381 along with six known compounds, striatoid C, striatin C, striatals A, C, D, and glochidone. The chemical structures were determined by means of high resolution mass spectrometry (HRESI-MS) and nuclear magnetic resonance (NMR) spectroscopy. The absolute configurations were confirmed by X-ray diffraction analysis. The isolated active compounds exhibited antimalarial against *Plasmodium falciparum* (IC_{50} 0.88–7.51 μM), antibacterial activities against *Mycobacterium tuberculosis* (MIC 25–50 μg/mL), Gram-positive bacteria of *Bacillus cereus* and *Enterococcus faecium* (MIC 0.78–50 μg/mL) and Gram-negative bacteria of *Escherichia coli*, *Acinetobacter baumannii* and *Klebsiella pneumoniae* in a presence of phenylalanine-arginine β-naphthylamide (MIC 3.13–50 μg/mL), antifungal activity against *Candida albicans* (IC_{50} 8.6–80.3 μM) activities, and cytotoxic activity against both cancerous (MCF-7, KB, NCI-H187, IC_{50} 0.36–28.32 μM) and non-cancerous (Vero, IC_{50} 0.13–91.50 μM) cells.

1. Introduction

Cyathanes are tricyclic diterpenes with annelated 5–6–7-memebered ring skeleton and have been widely isolated from mushrooms of the genus *Cyathus* and edible mushrooms of the genera *Hericium* [1] and *Sarcodon*. The genus *Sarcodon* can be considered as inedible due to the bitter taste, but this is less apparent in younger samples [2]. Many cyathane diterpenes have been described, for examples cyafrins and cyathins D–H, Q, R from *Cyathus africanus* Brodie, [3–6] cyathatriols from *C. earlei* [7], striatins, striatoids A–F, and pyristriatins A, B from *C. striatus* [8–11], cyathins J–P from *C. gansuensis* [12], erinacines and hericenones from *Hericium erinaceus* [13–18], *H. ramosum* (currently valid name *H. coralloides*) CL24240 [19] and *H. flagellum* [20], scabronines, sarcodonins, and neosarcodonins from *Sarcodon scabrosus* [21–25], glaucopines from *S. glaucopus* [26,27], cyrneines from *S. cyrneus* [28,29], and laxitextines A and B from *Laxitextum incrustatm* [30]. These compounds exhibited various biological activities such as antibacterial activity, anti-inflammatory, inductive activity of nerve growth factor (NGF)-synthesis, neurotrophin inducing effects, and antitumor activity [20,31]. Moreover, the profound study of the cyathane diterpene named cyathin R, which had apoptosis induction property in Bax/Bak-deficient mouse embryonic fibroblasts, showed that the compound could activate apoptosis via a novel mechanisms by promoting of the VDAC1 oligomerization [5]. Recently, the enzyme involved in cyclization of the cyathane skeleton in *H. erinaceum* was characterized [32].

As part of our ongoing search for new antimicrobial compounds from Thai microorganisms, the crude extracts from *Cyathus subglobisporus* BCC43381 exhibited significant antimicrobial activity (against *Plasmodium falciparum*, *Mycobacterium tuberculosis*, *Candida albicans*, Gram-Positive and Gram-negative bacteria) and the strain was then subjected to the identification of its active principles.

2. Results and discussion

2.1. Compound isolation and structure elucidation

The strain *Cyathus subglobisporus* BCC44381 was grown on malt

* Corresponding author.
E-mail address: pattamap@biotec.or.th (P. Pittayakhajonwut).

https://doi.org/10.1016/j.tet.2018.10.012
0040-4020/

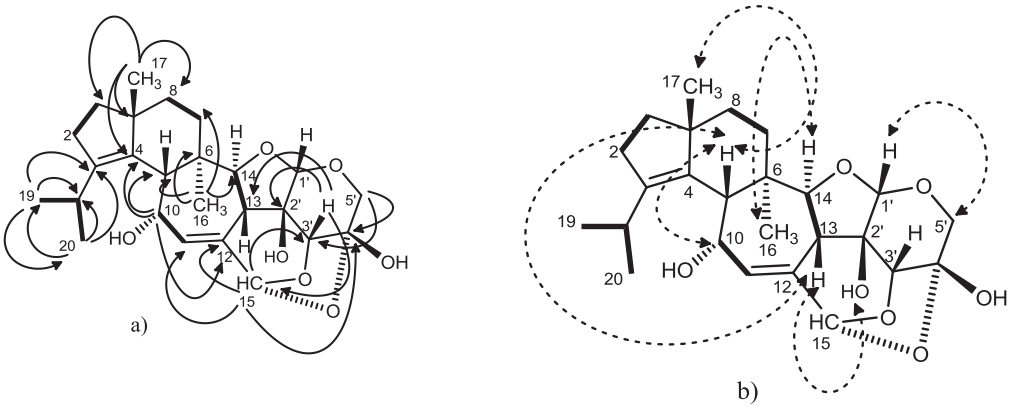

Fig. 1. a) COSY (bold bonds), selected HMBC (arrows) correlations of compound **1** and b) key NOESY correlations (dash arrows) of compound **1**.

extract medium under shaking. The culture was extracted with EtOAc, while cells were macerated with MeOH for 3 days, followed by CH_2Cl_2 for 3 days. For cells, the organic solvents were later combined, concentrated, and extracted with *n*-hexane and EtOAc, respectively. After TLC and HPLC analyses of all crude extracts, the EtOAc crude extract from cells was discarded due to lack of significant amount of material. The crude extract from broth, which was purified by chromatographic techniques (using Sephadex LH-20 columns and HPLC), contained eight compounds, including four new compounds (compounds **1**, **2**, **3**, and **5**) and four known compounds (compounds **4**, **6**, **8**, and **9**). The *n*-hexane crude extract from cells, after purification by silica gel column chromatography and HPLC, contained two known compounds (compounds **7** and **13**). In addition, during the purification process, a part of the fraction F1 of the broth crude extract was purified by using a silica gel column chromatography and yielded four compounds, which were two new (compounds **10** and **12**) and two known (compounds **8** and **9**). The ^{1}H and ^{13}C NMR spectroscopic data together with the physical properties of the known compounds were compared with the data given in the literature for striatoid C (**4**) [10], stratin C (**6**) [33,34], striatals A (**7**), C (**8**), D (**9**) [35], and glochidone (**13**) [36].

Compound **1** was obtained as colorless crystals with the molecular formula of $C_{25}H_{34}O_7$, revealed by the mass ion peak at *m/z* 445.2236 $[M-H]^-$ in the HRESIMS spectrum. The molecular formula indicated nine degrees of unsaturation. The ^{1}H and ^{13}C NMR spectra of compound **1** were similar to those of striatoid B (**4a**) [10], except the absence of a quaternary carbon attached to two oxygens and the presence of an extra oxymethine signal. Obviously, two oxymethine protons at δ_H 4.38 and 4.74, attributed to the carbons at δ_C 86.1 and 70.6, respectively in HSQC spectrum, resonated at lower field than the oxymethine proton at C-1 of striatoid B (δ_H 3.74). The HMBC spectrum (Fig. 1a) confirmed the position of the oxymethine at δ_H 4.38 at C-3′ by showing correlations from H-3′ to C-2′ (δ_C 76.4), C-13 (δ_C 44.9), and C-15 (δ_C 103.3); H_2-5′ to C-3′ and C-4′ (δ_C 97.7); from H-15 to C-3′, C-4′, C-12 (δ_C 137.5), and C-11 (δ_C 128.6). Moreover, the oxymethine at δ_H 4.74 showed correlations in HMBC spectrum to C-4 (δ_C 137.9), C-5 (δ_C 47.8), C-6 (δ_C 41.1), and C-12, suggesting its position at C-10. Thus, the upfield methylene at δ_H 1.51–1.55, attributed to the carbon at δ_C 37.8 in HSQC spectrum, must be placed at C-1, which confirmed by HMBC correlations from H_3-17 (δ_H 1.02) to C-1 (δ_C 37.8), C-4 (δ_C 137.9), C-8 (δ_C 40.2), and C-9 (δ_C 50.2). The spectroscopic evidence indicated that compound **1** was different from striatoid B (**4a**) at positions 1, 10, and 3′. In addition, the NOESY spectrum showed correlations (Fig. 1b) from H-5 to H_3-17, H-10, and H-13; from H-14 to H_3-16; from H-1′ and H_β-5′; and from H-13 to OH-2′. The stereochemistry, which was

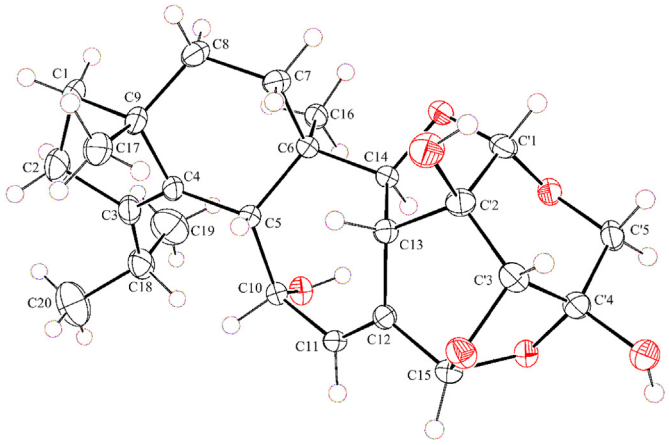

Fig. 2. X-ray crystallographic data of compound **1**.

corroborated by X-ray crystallographic data (Fig. 2) using a graphite-monochromated Cu K_α radiation giving the value of the absolute structure parameter 0.1(2), was consistent with the absolute configurations at C-5, C-6, and C-9 of those previously identified cyathane diterpenoids assigned as 5R, 6R, and 9R, respectively [4,37]. Therefore, the evidence from NOESY information and X-ray data suggested that the chemical structure with absolute configurations of compound **1** could be assigned as shown in Fig. 3. Compound **1** is categorized in cyathane-xyloside diterpene and given the trivial name cyathinin A.

Compound **2** was obtained as a pale yellow solid and had the same molecular formula as compound **1**, revealed by HRESIMS (*m/z* 445.2216 $[M-H]^-$), suggesting that compound **2** was an isomer of compound **1**. The ^{1}H NMR spectrum (Table 1) was similar to that of compound **1**, except the upfield shifts of three methine protons at H-15 ($\Delta\delta_H$[1] −0.13), H-1′ ($\Delta\delta_H$[1] −0.15), and H-3′ ($\Delta\delta_H$[1] −0.85), suggesting the difference at the xyloside moiety. Obviously, the oxymethine proton at H-3′ (δ_H 4.38) in **1** was shifted to δ_H 3.53 in compound **2** and the evidence from COSY spectrum suggested its situation at C-4′ in compound **2** by showing cross-peak correlation between δ_H 3.53 and H_2-5′. A small coupling ($J = 1.0$ Hz) between H_α-5′ and H-4′ implied the dihedral angle of approx. 67°. Moreover, the HMBC spectrum showed partial correlations from H-15 to C-11

[1] $\Delta\delta_H$ as the difference in chemical shift of the protons in compound 1 versus those of compound 2.

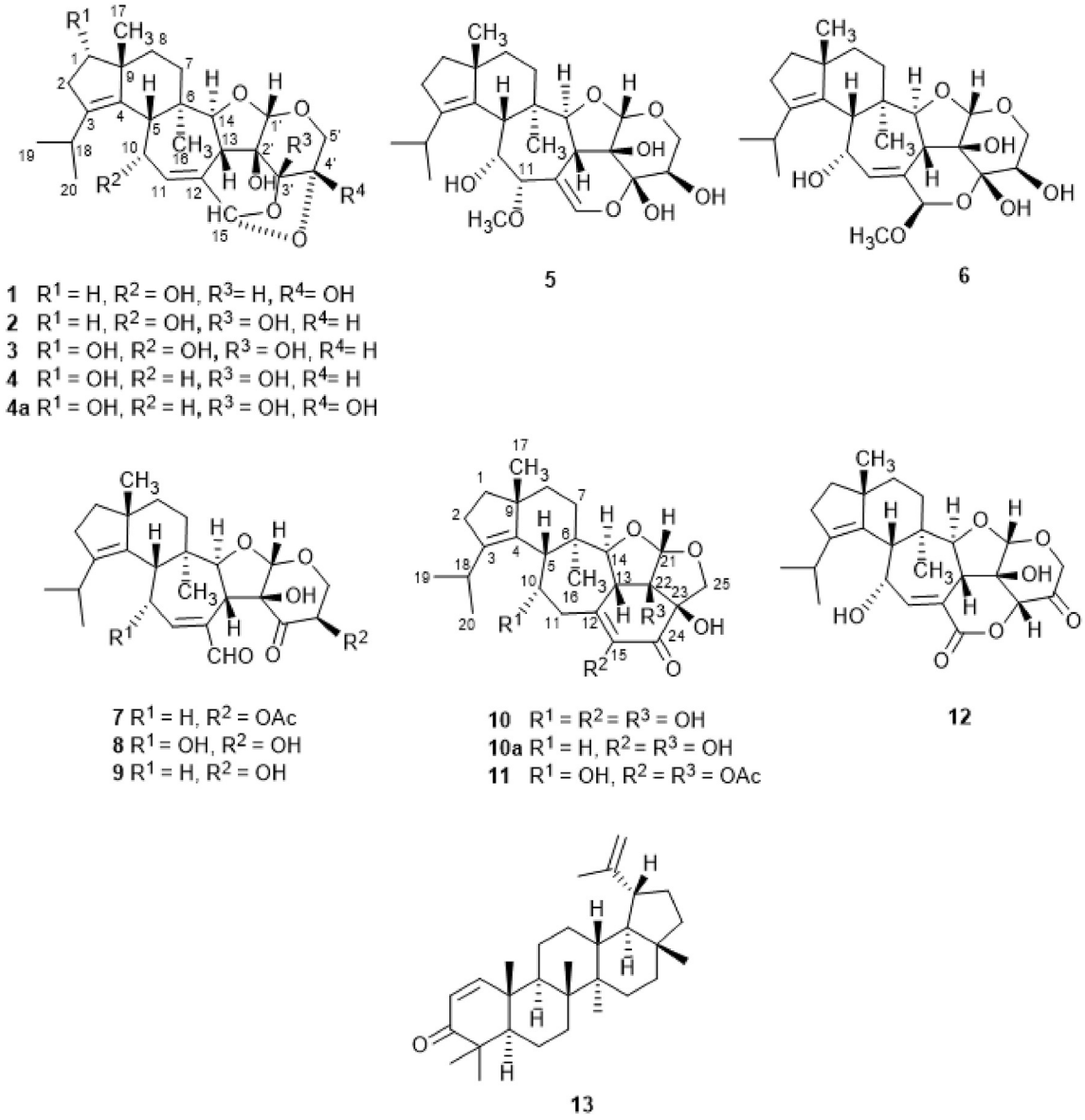

Fig. 3. Chemical structures of compounds **1**–**13** isolated from *Cyathus subglobisporus* BCC44381.

(δ_C 128.6), C-12 (δ_C 139.6), C-3′ (δ_C 100.8), and C-4′ (δ_C 73.8); from H_2-5′ to C-1′ (δ_C 105.3), C-3′, and C-4′; and from H-4′ to C-2′ (δ_C 78.4), C-3′, and C-5′ (δ_C 61.6), confirming a hydroxyl group at C-3′ and a methine proton at C-4′ in compound **2**. In addition, the NOESY spectrum (Fig. 4a) showed the same cross-peak correlations as those of compound **1** and had an extra correlation between H_α-5′ and H-4′, implying the *cis* relationship of the two protons. The spectral analyses from HMBC and NOESY data revealed that compound **2** had the same stereoconfigurations as those in compound **1**. Therefore, the chemical structure of compound **2** with absolute configuration, based on biosynthetic consideration, could be illustrated as shown in Fig. 3 and compound **2** is named cyathinin B.

Compound **3** was obtained as a yellow solid. HRESIMS displayed the mass ion at *m/z* 461.2186 $[M-H]^-$, indicating the molecular formula of $C_{25}H_{33}O_8$ with one more oxygen than that of compound **2**. The ^1H and ^{13}C NMR spectral data (Tables 1 and 2) were also similar to those of compound **2**, apart from an additional oxymethine at δ_H 3.77–3.82, an extra hydroxyl signal at δ_H 3.42, and a lack of a methylene carbon. In the ^1H NMR spectrum (Table 1), the signals for a xyloside moiety were identical to those of compound **2**, indicating the same xyloside unit as in compound **2**. The COSY spectrum showed cross-peak correlation between an extra oxymethine at δ_H 3.77–2.82 (attributed to δ_C 77.8 in HSQC spectrum) and two non-equivalent methylene protons at δ_H 2.25 (1H, dd, J = 16.1, 1.9 Hz) and 2.67 (1H, ddd, J = 16.1, 6.4, 2.6 Hz). In addition, the HMBC spectrum showed correlations (Fig. 4b) from H_3-17 to carbons at δ_C 77.8 (C-1), C-4 (δ_C 136.0), C-8 (δ_C 26.6), and C-9 (δ_C 53.6); and from H-2 to C-1, C-3 (δ_C 137.2), and C-4 (δ_C 136.0), indicating that the extra oxymethine was situated at C-1. In addition, the NOESY spectrum (Fig. 4b) showed an extra cross-peak correlation between H-1 and H-17, confirming a *syn* relationship, while the rest of the NOESY correlations were identical to compound **2**. The evidence from NOESY data in conjunction with the definite absolute configurations at C-5, C-6, and C-9 led to the chemical structure of compound **3** as shown in Fig. 3. Cyathinin C is named for compound **3** and should derive from the same biosynthesis pathway as compounds **1** and **2**.

Compound **5** was obtained as a pale yellow solid and HRESIMS

Table 1
The ^{1}H NMR assignments of compounds **1**–**3**, **5** and **12** in acetone-d_6.

position	**1**[a]	**2**[b]	**3**[a]	**5**[b]	**12**[b,c]
	δ_H, mult. (J in Hz)	δ_H, mult. (J in Hz)	δ_H, mult. (J in Hz)	δ_H, mult. (J in Hz)	δ_H, mult. (J in Hz)
1	1.51–1.55 (m)	1.47–1.54 (m), 1.52–1.58 (m)	3.77–3.82 (m)	1.53–1.57 (m); 1.62–1.70 (m)	1.38–1.50 (m)
2	1.70–1.78 (m), 2.32–2.36 (m)	1.39–1.42 (m), 2.30–2.38 (m)	2.25 (H_b, dd, 16.1, 1.9[d]), 2.67 (H_a, ddd, 16.1, 6.4, 2.6)	2.27–2.37 (m)	158–1.68 (m)
5	2.31 (s)	2.28 (s)	2.30 (br s)	2.84 (s)	2.06 (br s)
7	1.37 (dt, 13.6, 3.3) 1.70 –1.78 (m)	1.35–1.39 (m), 2.30–2.38 (m)	1.46 (ddd, 13.6, 5.0, 2.2)[d], 1.80 (td, 13.6, 4.3)	1.41–1.47 (m), 1.57–1.62 (m)	1.38–1.50 (m)
8	1.46–1.52 (m), 1.66–1.71 (m)	1.62–1.72 (m), 1.73–1.82 (m)	1.12 (dm, 13.9, <1), 2.19 (td, 13.9, 5.0)	1.49–1.53 (m), 1.53–1.57 (m)	2.22–2.28 (m)
10	4.74 (t, 4.9)	4.75 (dd, 6.0, 4.8)	4.72 (dd, 5.9[e], 4.8)	4.32 (dd, 4.6[e], 3.4)	4.56 (dd, 6.6, 3.7)
11	5.63 (dd, 6.0, 2.7)	5.62 (dd, 6.0, 2.9)	5.62 (dd, 5.9, 2.7)	3.52 (d, 4.6)	6.73 (dd, 6.6, 2.7)
13	2.72 (dd, 8.5, 1.5)	2.98 (dd, 8.4, 2.9)	3.00 (d, 8.4, 2.7)	2.57 (d, 9.8)	3.23–3.29 (m)
14	4.51 (d, 8.5)	4.59 (d, 8.4)	4.58 (d, 8.4)	4.33 (d, 9.8)	4.13 (d, 7.7)
15	5.73 (s)	5.60 (s)	5.60 (s)	6.24 (s)	–
16	1.22 (s)	1.25 (s)	1.24 (s)	1.13 (s)	1.09 (s)
17	1.02 (s)	1.02 (s)	0.99 (s)	1.06 (s)	0.95 (s)
18	3.52 (sept, 6.8)	3.53 (sept, 6.8)	3.50–3.57 (m)	3.34 (sept, 6.8)	3.23–3.29 (m)
19	0.94 (d, 6.9)	0.94 (d, 6.9)	0.93 (d, 6.9)	0.94 (d, 6.9)	0.91 (d, 6.9)
20	1.00 (d, 6.7)	1.01 (d, 6.7)	1.00 (d, 6.7)	0.99 (d, 6.7)	0.94 (d, 6.7)
1′	4.99 (s)	4.84 (s)	4.85 (s)	5.15 (s)	5.52 (s)
3′	4.38 (s)	–	–	–	5.47 (d, 1.7)
4′	–	3.53 (s)	3.53 (s)	3.96 (br s)	–
5′	3.64 (H_β, d, 12.8), 3.77 (H_α, d, 12.8)	3.61 (H_β, d, 13.6), 3.96 (H_α, dd, 13.6, 1.0)	3.61 (H_β, d, 13.6), 3.96 (H_α, d. 13.6, 1.5[d])	3.74 (H_β, d, 11.5), 4.10 (H_α, d, 11.5, 5.7)	4.11 (d, 18.8), 4.43 (d, 18.8)
2′-OH	4.55 (s)	5.11 (s)	5.12 (s)	4.09 (s)	6.79 (s)
3′-OH	–	6.14 (s)	6.15 (s)	5.61 (s)	–
4′-OH	5.52 (s)	–	–	4.75 (s)	–
10-OH	3.94 (d, 3.7)	3.94 (d, 4.8)	3.95 (d, 4.8)	3.89 (d, 3.4)	5.28 (d, 3.7)
1-OH	–	–	3.42 (d, 4.9)	–	–
11-OCH_3	–	–	–	3.19 (s)	–

[a] Recorded on a 500 MHz NMR spectrometer.
[b] Recorded on a 400 MHz NMR spectrometer.
[c] Recorded in DMSO-d_6 due to the solubility.
[d] Coupling patterns appeared after ^{1}H decoupling experiment.
[e] Coupling patterns revealed after addition of D_2O.

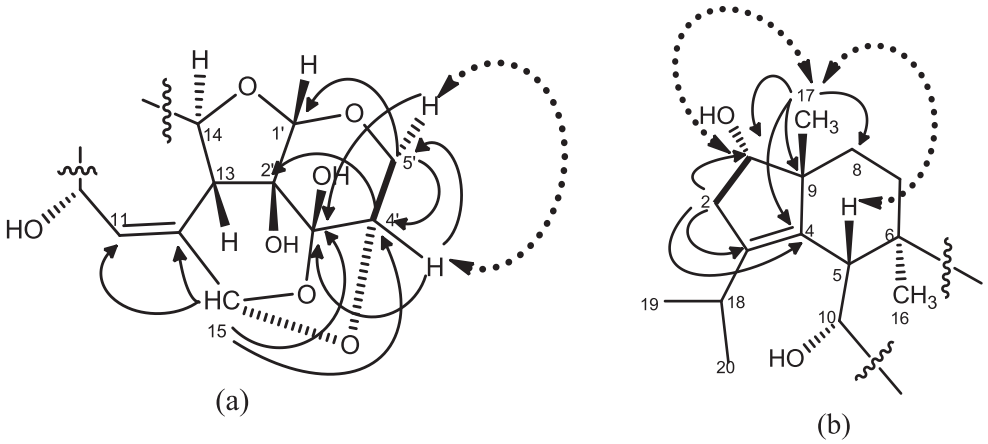

Fig. 4. Key COSY (bold bond), HMBC (arrows) and NOESY (dash arrows) correlations of compound **2** (a) and **3** (b).

data gave the same mass ion peak at *m/z* 477.2490 $[M-H]^-$ as that of striatin C (**6**). The ^{13}C NMR spectrum was also similar to that of compound **6**, except two upfield signals of an oxymethine carbon at δ_C 84.8 (C-11) and a quaternary carbon at δ_C 114.0 (C-12), and a downfield shift of a methine signal at δ_C 139.9 (C-15). Furthermore, the HMBC spectrum showed correlations (Fig. 5) from H-10 (δ_H 4.32) to C-5 (42.1), C-11 (δ_C 84.8) and C-12 (δ_C 114.0); from H-15 (δ_H 6.24) to C-11, C-12, C-13 (δ_C 42.3), and C-3′ (δ_C 96.8); and from 11-OCH_3 (δ_H 3.19) to C-11, indicating that compound **5** was a regioisomer of compound **6**. Moreover, the methine at δ_H 3.52 (H-11) coupled to a methine at δ_H 4.32 (H-10) with a coupling constant value of 4.6 Hz (Table 1), indicating a *cis*-relationship. The NOESY spectrum (Fig. 5a) showed cross-peak correlations from H_3-17 to H-5 and H-13; from H_3-16 and H-14; from H-11 to H-10 and H-15; and from H-1′ to H-5 and H_β-5′; and from H-4′ to H_α-5′. Together with biogenetic consideration, the absolute configurations of compound **5** were assigned as shown in Fig. 2 and cyathinin D is given as its trivial name.

Compound **10** was obtained as a colorless solid and the molecular formula was determined to be $C_{25}H_{34}O_7$ by HRESIMS data,

Table 2
The ^{13}C NMR assignments of compounds **1**–**3**, **5** and **12** in acetone-d_6.

position	δ_C, type				
	1[a]	**2**[b]	**3**[a]	**5**[b]	**12**[b,c]
1	37.8 (CH_2)	38.0 (CH_2)	77.8 (CH)	39.9 (CH_2)	38.9 (CH_2)
2	29.1 (CH_2)	29.2 (CH_2)	39.2 (CH_2)	29.0 (CH_2)	29.1 (CH_2)
3	140.1 (C)	140.4 (C)	137.2 (C)	138.8 (C)	139.2 (C)
4	137.9 (C)	137.8 (C)	136.0 (C)	140.2 (C)	135.6 (C)
5	47.8 (CH)	48.1 (CH)	47.9 (CH)	42.1 (CH)	44.3 (CH)
6	41.1 (C)	41.5 (C)	41.3 (C)	42.0 (C)	41.5 (C)
7	29.4 (CH_2)	29.8 (CH_2)	28.6 (CH_2)	30.2 (CH_2)	27.9 (C)
8	40.2 (CH_2)	40.4 (CH_2)	26.6 (CH_2)	38.8 (CH_2)	28.3 (CH_2)
9	50.2 (C)	50.5 (C)	53.6 (C)	50.8 (C)	48.9 (C)
10	70.6 (CH)	70.9 (CH)	70.4 (CH)	74.4 (CH)	67.7 (CH)
11	128.6 (CH)	128.6 (CH)	128.5 (CH)	84.8 (CH)	146.8 (CH)
12	137.5 (C)	139.6 (C)	139.2 (C)	114.0 (C)	124.6 (C)
13	44.9 (CH)	46.1 (CH)	45.7 (CH)	42.3 (CH)	46.9 (CH)
14	92.0 (CH)	92.3 (CH)	91.9 (CH)	93.8 (CH)	93.0 (CH)
15	103.3 (CH)	102.8 (CH)	102.4 (CH)	139.9 (CH)	165.6 (C)
16	21.7 (CH_3)	21.9 (CH_3)	21.7 (CH_3)	21.7 (CH_3)	21.0 (CH_3)
17	24.3 (CH_3)	24.6 (CH_3)	24.3 (CH_3)	25.1 (CH_3)	23.9 (CH_3)
18	26.2 (CH)	26.5 (CH)	26.1 (CH)	26.5 (CH)	25.1 (CH)
19	21.9 (CH_3)	22.0 (CH_3)	22.0 (CH_3)	22.0 (CH_3)	21.6 (CH_3)
20	22.3 (CH_3)	22.4 (CH_3)	22.1 (CH_3)	22.2 (CH_3)	21.9 (CH_3)
1′	106.3 (CH)	105.3 (CH)	105.0 (CH)	108.6 (CH)	108.6 (CH)
2′	76.4 (C)	78.4 (C)	78.1 (C)	81.3 (C)	79.5 (C)
3′	86.1 (CH)	100.8 (C)	100.7 (C)	96.8 (C)	83.5 (CH)
4′	97.7 (C)	73.8 (CH)	73.5 (CH)	70.6 (CH)	204.6 (C)
5′	64.2 (CH_2)	61.6 (CH_2)	61.3 (CH_2)	68.6 (CH_2)	67.5 (CH_2)
11-OCH_3	–	–	–	55.7 (CH_3)	–

[a] Recorded at 125 MHz.
[b] Recorded at 100 MHz.
[c] Recorded in DMSO-d_6.

showing a mass ion peak at *m/z* 445.2225 $[M-H]^-$. The ^1H and ^{13}C NMR spectra were similar to those of erinacine S (**10a**) [33], except a lack of a methylene carbon and an additional oxymethine at δ_H 4.31 (δ_C 69.0). The extra oxymethine signal coupled to H_2-11 (δ_H 2.01 and 2.32) in the COSY spectrum and showed correlations in the HMBC spectrum to C-4 (δ_C 138.0), C-6 (δ_C 41.6), and C-12 (δ_C 127.1), confirming its position at C-10. The NOESY spectrum showed cross-peak correlations (Fig. 5b) from H_3-17 to H-5; from H-5 to H-10; from H_3-16 to H-14 and 10-OH; from H-13 to H-21; and from H-14 to H_α-25. Moreover, the reaction of compound **10** with acetic anhydride in pyridine yielded compound **11**, which was crystallized in MeOH–H_2O to obtain a single needle for X-ray crystallographic analysis. The X-ray data of compound **11** (Fig. 6), obtained from a graphite-monochromated Cu K_α radiation with the value of the absolute structure parameter −0.009(17), together with the NOESY information of compound **10** confirmed the absolute configurations

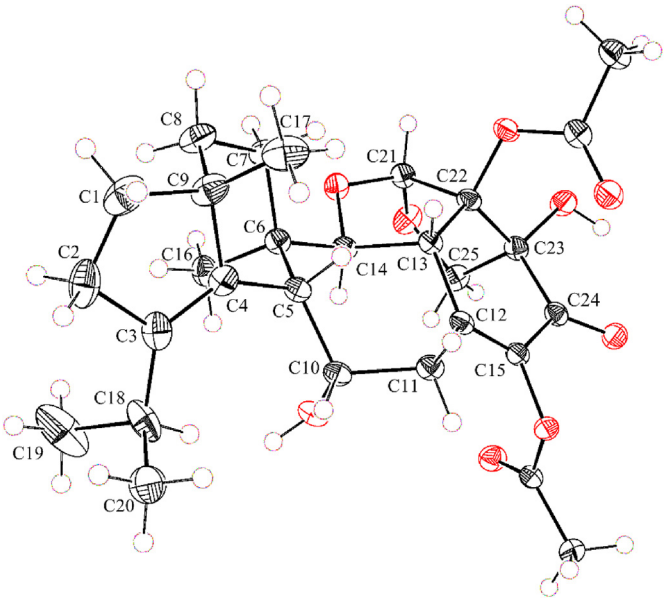

Fig. 6. X-ray crystallographic data of compound **11**.

of compound **10**, whose chemical structure is illustrated in Fig. 2. The structure of compound **10** is closely related to erinacine S (**10a**), thus the name 10-hydroxyerinacine S is given as an informal name for compound **10**.

Compound **12** was obtained as a colorless solid. HRESIMS spectrum revealed the molecular formula $C_{25}H_{32}O_7$ by giving the sodium-adduct mass ion peak at *m/z* 467.2033 $[M+Na]^+$. The ^1H and ^{13}C NMR spectral data (Tables 1 and 2) of compound **12** indicated the presence of a cyathane skeleton with a different xyloside moiety, whose cythane backbone was confirmed by the extensive 2D NMR analysis (including COSY, HSQC, HMBC). The NOESY spectrum together with biogeneric consideration suggested the absolute configurations at C-5, C-6, C-9, C-10, C-13, and C-14 of cyathane unit to be the same as those of aforementioned compounds. In addition, the ^{13}C NMR spectrum also displayed two additional quaternary carbons at δ_C 165.6 and 204.6, indicating the existence of lactone and ketone carbonyls, whose IR spectrum showing the absorptions at ν_{max} 1750 and 1724 cm^{-1}, respectively. Moreover, the HMBC correlations showed partial correlations from H-11 (δ_H 6.73) to C-15 (δ_C 165.6); from H-14 (δ_H 4.13) to C-12 (δ_C 124.6) and C-16 (δ_C 21.0); from H-13 (δ_H 3.23–3.29) to C-12, C-14 (δ_C 93.0), and C-2′ (δ_C 79.5); from H-1′ (δ_H 5.52) to C-14 and C-5′ (δ_C

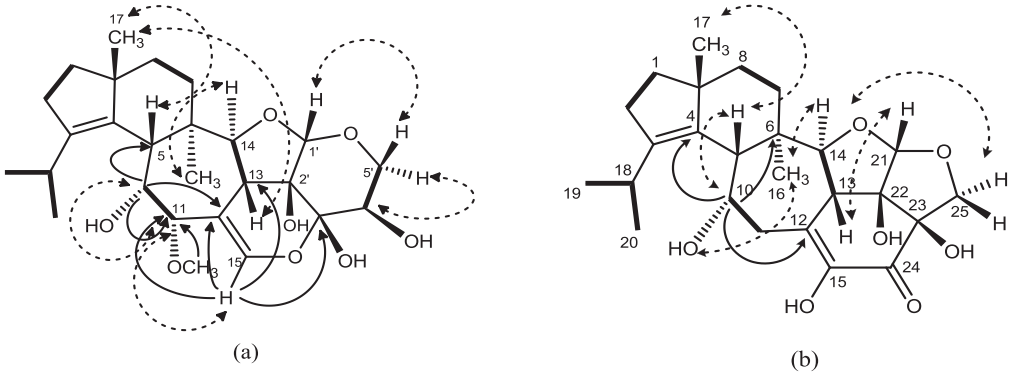

Fig. 5. Key COSY (bold bond), HMBC (arrows) and NOESY (dash arrows) correlations of compound**s 5** (a) and **10** (b).

67.5); from H-3′ (δ_H 5.47) to C-13 (δ_C 46.9), C-15 (δ_C 165.6), C-2′ (δ_C 79.5) and C-4′ (δ_C 204.6); and from H-5′ (δ_H 4.43) to C-1′ (δ_C 108.6) and C-4′, which led to the xyloside structure as delineated in Fig. 3. Together with the evidence from the additional NOESY spectrum, the cross-peak correlation from H-1′ to H-3′ and OH-2′ was observed. Thus, chemical structure of compound **12** with the absolute configurations could be assigned as shown in Fig. 3. Cyathinin E is given as its trivial name.

The known compounds **4**, **6**–**9** were identified as striatoid C, striatin C, striatals A, C, and D and formerly isolated from *Cyathus striatus*. Striatins were reported to be artefacts of striatals formed by extraction of mycelia of *Cyathus striatus* and *Gerronema fibula* with methanol [35]. Likewise, compounds **10** and **12** could be considered as artefacts of striatin C (**6**) and striatal C (**8**), given after passing through a silica gel column chromatography. Herein, the complete ^{1}H and ^{13}C NMR spectral data of striatal D (**9**) are also given. Glochidone (**13**) was originally isolated from *Cyathus helenae* [38] and later found in *Cyathus striatus* [39].

2.2. Biological activity

All compounds except compound **2** were tested for antimicrobial activity (Table 3) including antimalarial activity against *P. falciparum* (K1, multidrug-resistant strain), antibacterial activity against Gram-positive (*Bacillus cereus*, *Enterococcus faecium*) and Gram-negative (*Escherichia coli*, *Pseudomonas aeruginosa, Acinetobacter baumannii, Klebsiella pneumoniae*) bacteria, and antifungal activity against *C. albicans* (Table 4) and for cytotoxicity (Table 5) against cancerous (MCF-7, KB, NCI-H187) and non-cancerous (Vero) cells.

Compounds **1** and **4**–**9** exhibited antimalarial activity with IC_{50} in a range of 0.88–7.51 μM, while compounds **5**–**8** showed antifungal activity against *C. albicans* with IC_{50} in a range of 8.6–80.3 μM. In addition, compounds **1** and **5**–**8** displayed anti-*M. tuberculosis* activity with MIC values in a range of 25.0–50.0 μg/mL. Furthermore, compounds **1** and **5**–**9** showed antibacterial activity against Gram-positive bacteria with MIC values in a range of 0.78–50.0 μg/mL (Table 4) and compounds **6**–**8** showed antibacterial activity against three Gram-negative bacteria (*E. coli*, *A. baumannii*, and *K. pneumoniae*) in a presence of PAβN (phenylalanine-arginine β-naphthylamide) with MIC values in a range of 3.13–50 μg/mL. Moreover, compound **1**, **4**, and **5** also possessed antibacterial activity against *E. coli* and *A. baumannii* in a presence of PAβN with MIC values in a range of 6.25–50.0 μg/mL. All tested compounds were inactive for antibacterial activity against Gram-negative bacteria without PAβN at maximum tested concentration (50 μg/mL). The results evidenced a beneficial effect of a hydroxyl group at C-10 on antimicrobial activity. For example, compound **4** exhibited a better antimalarial, anti-*E. coli*, and anti-*A. baumannii* activities than compound **3** and compounds **7** and **9** showed stronger antimicrobial activity than compound **8**. Although, compounds **10**–**12** also possessed the hydroxyl group at C-10, the results implied that xyloside unit plays a role in antimicrobial activity. For cytotoxicity (Table 5), compounds **5**–**8** were toxic against both cancerous and non-cancerous cells with IC_{50} in a range of 0.13–6.91 μM. Moreover, compound **1** showed cytotoxicity against NCI-H187 (IC_{50} 8.48 μM) and Vero (IC_{50} 6.93 μM) cells, while compounds **4** and **9** possessed cytotoxicity against Vero cells with IC_{50} values of 1.69 and 3.62 μM. Compound **4** also displayed cytotoxicity against KB cell with IC_{50} value of 2.94 μM.

Table 3
The ^{1}H and ^{13}C NMR assignments of compounds **10** and **11** in acetone-d_6 (500 MHz).

position	**10**		**11**	
	δ_H, mult. (*J* in Hz)	δ_C, type	δ_H, mult. (*J* in Hz)	δ_C, type
1	1.46–1.56 (m)/1.59–1.67 (m)	38.6 (CH_2)	1.52–1.62 (m)/1.62–1.72 (m)	40.0 (CH_2)
2	2.23–2.32 (m)	28.0 (CH_2)	2.30–2.38 (m)	29.0 (CH_2)
3	–	137.6 (C)	–	139.4 (C)
4	–	138.0 (C)	–	138.7 (C)
5	2.40 (s)	47.0 (CH)	2.54 (s)	48.5 (CH)
6	–	41.6 (C)	–	42.5 (C)
7	1.48–1.56 (m)	29.1 (C)	1.62–1.72 (m)	30.1 (C)
8	1.40–1.48 (m)	37.0 (CH_2)	1.52–1.62 (m)	38.1 (CH_2)
9	–	48.8 (C)	–	39.8(C)
10	4.31 (br m)	69.0 (CH)	4.54 (br s)	70.4 (CH)
11	2.01 (d, 16.0)/2.32 (dd, 16.0, 4.1)	39.5 (CH_2)	2.22 (d, 15.9)/2.38 (dd, 15.9, 4.6)	41.1 (CH_2)
12	–	127.1 (C)	–	141.4 (C)
13	3.18 (d, 10.8)	48.1 (CH)	3.48 (d, 10.2)	48.8 (CH)
14	4.41 (d, 10.8)	88.9 (CH)	4.76 (d, 10.2)	90.2 (CH)
15	–	142.3 (C)	–	141.2 (C)
16	1.06 (s)	20.6 (CH_3)	1.20 (s)	21.3 (CH_3)
17	1.03 (s)	24.4 (CH_3)	1.04 (s)	24.7(CH_3)
18	3.22 (sept, 6.7)	24.9 (CH)	3.28 (sept, 6.6)	26.3 (CH)
19	0.92 (d, 6.4)	21.5(9) (CH_3)	0.94 (d, 6.9)	21.8(7) (CH_3)
20	0.93 (d, 6.3)	21.6(1) (CH_3)	0.98 (d, 6.6)	21.9(2) (CH_3)
21	5.31 (s)	111.3 (C)	5.77 (s)	113.1 (C)
22	–	91.6 (C)	–	97.1(C)
23	–	81.6 (C)	–	82.0 (C)
24	–	191.8 (C)	–	-[a] (C)
25	3.88 (d, 9.8)/4.01 (d, 9.8)	79.2 (CH_2)	3.95 (d, 10.1)/4.58 (d, 10.1)	81.3 (CH_2)
10-OH	4.79 (d, 3.1)	–	4.16 (s)	–
15-OH	8.29 (s)	–	–	–
15-$OCOCH_3$	–	–	2.17 (s)	169.0 (C)/20.2 (CH_3)
22-OH	5.53 (s)	–	–	–
22-$OCOCH_3$	–	–	2.01 (s)	170.8 (C)/20.7 (CH_3)
23-OH	5.99 (s)	–	4.93 (s)	–

[a] Did not observe in the ^{13}C NMR spectrum.

Table 4
Antimicrobial activity of the isolated compounds **1** and **3**–**12**.

Compound	Anti-*P. falciparum*[a] (IC_{50}, μM)	Anti-*C. albicans*[c]	Antibacterial activity (MIC, μg/mL)						
		(IC_{50}, μM)	*M. tuberculosis*[c]	*B. cereus*[b]	*E. faecium*[c]	*E. coli*[c] +PAβN[d]	*P. aeruginosa*[c] + PAβN[d]	*A. baumannii*[c] +PAβN[d]	*K. pneumoniae*[c] +PAβN[d]
1	7.51	inactive	50.0	25.0	50.0	25.0	inactive	nt	inactive
3	inactive	inactive	inactive	inactive	inactive	inactive	inactive	inactive	inactive
4	7.33	inactive	inactive	12.5	inactive	50.0	inactive	12.5	inactive
5	2.13	80.3	50.0	3.13	50.0	12.5	inactive	6.25	inactive
6	1.40	75.8	50.0	1.56	25.0	6.25	inactive	3.13	50.0
7	1.03	72.3	50.0	1.56	25.0	6.25	inactive	12.5	50.0
8	0.88	8.6	25.0	0.78	6.25	3.13	inactive	6.25	25.0
9	2.12	inactive	inactive	6.25	50.0	50.0	inactive	nt	inactive
10	inactive	inactive	inactive	inactive	inactive	inactive	inactive	inactive	inactive
11	inactive	inactive	inactive	inactive	inactive	inactive	inactive	inactive	inactive
12	inactive	inactive	inactive	25.0	inactive	inactive	inactive	inactive	inactive
Dihydroartemisinin	0.0029	–	–	–	–	–	–	–	–
Mefloquine	0.043	–	–	–	–	–	–	–	–
Amphotericin B	–	0.08	–	–	–	–	–	–	–
Vancomycin	–	–	–	2.0	–	–	–	–	–
Rifampicin	–	–	0.013	–	1.56	0.05	–	0.10	0.20
Streptomycin	–	–	0.63	–	–	–	–	–	–
Isoniazid	–	–	0.047	–	–	–	–	–	–
Ofloxacin	–	–	0.78	–	–	–	–	–	–
Ethambutol	–	–	0.94	–	–	–	–	–	–
Tetracycline HCl	–	–	–	–	0.10–0.20	–	–	–	–
Erythromycin	–	–	–	–	–	0.78	>32	0.78	6.25

nt = not being tested.
[a] Maximum tested concentration was done at 10 μg/mL.
[b] Maximum tested concentration was done at 25 μg/mL.
[c] Maximum tested concentration was done at 50 μg/mL.
[d] PAβN = Phenylalanine-arginine β-naphthylamide.

Table 5
Cytotoxicity against KB, MCF-7, NCI-H187 and Vero cells of the isolated compounds.

Compound	Cytotoxicity[a] (IC_{50}, μM)			
	MCF-7	KB	NCI-H187	Vero
1	28.32	12.85	8.48	6.93
3	inactive	inactive	inactive	inactive
4	18.14	2.94	20.85	1.69
5	3.87	0.48	0.44	0.13
6	3.58	0.36	4.02	0.15
7	1.41	0.6	3.97	0.20
8	6.91	0.84	6.21	0.51
9	inactive	inactive	17.73	3.62
10	inactive	inactive	inactive	91.50
11	inactive	inactive	inactive	inactive
12	inactive	39.17	109.37	13.11
Tamoxifen	19.22	–	–	–
Doxorubicin	12.14	1.06	0.36	–
Ellipticine	–	5.81	5.40	4.38

[a] Maximum tested concentration was done at 50 μg/mL.

3. Conclusion

Twelve compounds, including six unknown compounds (cyathinins A – E and 10-hydroxyerinacine S) and six previously described compounds (striatoid C, striatin C, striatals A, C, D, and glochidone), were isolated from *Cyathus subglobisporus* BCC43381. The absolute configurations of cyathinin A (**1**) and 10-hydroxyerinacine S (**10**) were confirmed by based on NOESY spectral data together with X-ray crystallographic analyses of cyathinin A and its derivative, respectively, in comparison with the related cyathane diterpenes with the reported absolute configurations. Compounds **1** and **4**–**9** exhibited antimalarial activity (IC_{50} 0.88–7.51 μM), while compounds **5**–**8** showed weak anti-*M. tuberculosis* (MIC 25.0–50.0 μg/mL) and anti-*C. albicans* (IC_{50} 8.60–80.33 μM) activities. In addition, compounds **1** and **5**–**9** possessed broad spectrum of antibacterial activity against Gram-positive bacteria (*B. cereus* and *E. faecium*, MIC 0.78–50.0 μg/mL), whereas compounds **6**–**8** displayed antibacterial activity against all tested Gram-negative bacteria, except *P. aeruginosa*, in a presence of PAβN (MIC 3.13–50.0 μg/mL). Compounds **5**–**8** had strong cytotoxicity (IC_{50} < 10 μM) against malignant (IC_{50} 0.26–6.91 μM) and non-malignant (IC_{50} 0.13–0.51 μM) cells, while compounds **3**, **10**, and **11** were inactive to all tests. The biological results demonstrated that the hydroxyl group at C-10 and the xyloside unit had an effect on antimicrobial activity.

4. Experimental

4.1. General experimental procedures

Melting points were measured by using a melting point M565 apparatus from Buchi. Specific rotations were recorded by using JASCO P-1030 digital polarimeter. UV spectra were taken in MeOH on a Spekol 1200 UV–Vis spectrophotometer from Analytik Jena. FTIR spectra were done on a Bruker ALPHA spectrometer. NMR spectra were performed on either Bruker Avance-III 400 (400 MHz for ^{1}H and 100 MHz for ^{13}C) or Bruker Avance 500 (500 MHz for ^{1}H and 125 MHz for ^{13}C) NMR spectrometers. HRESIMS data were obtained from a Bruker MicrOTOF mass spectrometer. X-ray diffraction data were collected on Bruker V8 Venture diffractometer equipped with graphite monochromated Cu Kα radiation (λ = 1.54178 Å) at 100(2) K. Preparative and semi-preparative HPLC were performed on a Dionex–Ultimate 3000 series equipped with a binary pump, an autosampler, and a diode array detector. Capcell Pak C18 column, MG-II from Shiseido (particle size 10 μm, diam. 20 mm × 250 mm) was used for preparative HPLC at flow rate of 12 mL/min. SunFire C18 OBD column from Waters (particle size 5 μm, diam. 19 mm × 150 mm) was used for semi-preparative HPLC at flow rate of 8 mL/min. Silica gel column chromatography was performed by using silica gel 60 (70–230 Mesh ASTM) from Merck.

4.2. Fungal material

The unidentified fungus was collected on unidentified wood at Khao Yai National Park, Nakhon Nayok province, Thailand by Dr. Rattaket Choeyklin and the axenic culture was deposited at BIOTEC Culture Collection (BCC), the National Center for Genetic Engineering and Biotechnology (BIOTEC), Thailand with the registration code BCC44381. Its fruiting bodies (peridia) are pale yellow to pale brown and outside covered with shaggy hairs, while inner peridium surface are smooth with grey to brownish grey. Small capsules of their spores (peridioles) are eggs-like with greyish brown to pale brown and attached to the inner surface of the fruit body. Basidiospores are mostly spherical, no color, smooth, and thick-walled. The fungus was also identified by using the partial nuclear large subunits ribosomal DNA (nc28S rDNA; 1186 bps), and the internal transcribed spacer region (ITS region; 747 bps). The nc28S sequence had affinity with fungal taxa within Basidiomycota, Agaricales, Agaricomycetidae, Agaricomycetes, analyzed by the Basic Local Alignment Search Tool (BLAST; http://www.ncbi.nlm.nih.gov) from the National Center for Biotechnology Information (NCBI). Whilst the ITS data showed 100% similarity with *Cyathus subglobisporus*, compared with the strain accession numbers NR_137683, deposited by Zhao et al. [40] as a new basidiomycetous species from Thailand. Compared with the sequence availability in NCBI (nc28S and ITS sequence data) of 40 species in the genus *Cyathus*, the fungus BCC44381 was thus identified as *Cyathus subglobisporus*, which was a member in the Agaricaceae, Agaricales, Agaricomycetidae, Agaricomycetes, Agaricomycotina, Basidiomycota. The ITS and nc28S rDNA sequences of this fungus have been submitted to GenBank with the accession numbers MH156046, and MH156047, respectively.

4.3. Fermentation, extraction, and isolation

The strain was inoculated on potato dextrose agar (PDA) plate at 25 °C for 11 days and then cut into small pieces (1×1 cm^2). The pieces were added into ten 250 mL Erlenmeyer flasks, each contained 25 mL of potato dextrose broth (PDB), comprising potato starch 4.0 g/L, dextrose 20.0 g/L in distilled water. The culture was incubated at 25 °C for 5 days in a shaker (250 rpm) and equally transferred into ten 1 L Erlenmeyer flasks, containing 250 mL of PDB medium. The seed culture was cultivated at 25 °C for 5 days in a rotary shakers at 250 rpm and was transferred into eighty 1 L Erlenmeyer flask, which each contained 250 mL of MEB (malt extract broth). The culture was incubated at 25 °C on a rotary shaker at 250 rpm. After 10 days, the cell was separated by filtration and the broth was extracted three times with equal volume of EtOAc. EtOAc was dried over Na_2SO_4 and evaporated to dryness to yield a brown gum (9.4 g).

The cells were macerated in MeOH (1 L) for 3 days and then in CH_2Cl_2 (1 L) for 3 days. Organic solvents were combined and concentrated in *vacuo*. Later, water (100 mL) was added and the mixture was extracted three times with equal volume of *n*-hexane, followed by three times with equal volume of EtOAc. *n*-Hexane and EtOAc extracts were separately dried over Na_2SO_4 and then evaporated to dryness to obtain crude extracts as brown gum from *n*-hexane (0.5 g) and from EtOAc (3.9 g), respectively. The EtOAc crude extract from cells was discarded due to lack of material as shown by TLC and HPLC analyses.

The crude extract from broth (9.4 g) was passed through a Sephadex LH-20 column (4.5 cm × 30 cm), eluted with 100% MeOH to give two main fractions (F1, 7.3 g and F2, 0.24 g). A part of fraction F1 (0.24 g) was further purified by a preparative HPLC, using linear gradient system of 15–85% CH_3CN in water over 22 min, then at 85% CH_3CN in water over 3 min, and followed by a linear gradient system of 85–100% CH_3CN in water over 5 min, to afford compounds **8** (0.10 g), **6** (22.2 mg), and **9** (11.3 mg), respectively. Fraction F2 (0.24 g) was further purified by a preparative HPLC, using a linear gradient system of 10–75% CH_3CN in water over 22 min, then left at 75% CH_3CN in water for 3 min, and followed by a linear gradient system of 75–100% CH_3CN in water over 5 min, to yield compounds **3** (4.7 mg), **4** (8.9 mg), **1** (3.3 mg), **5** (5.9 mg), **8** (43.0 mg), and **9** (1.5 mg) from subfractions F2F1, F2F2, F2F3, F2F4, F2F6, F2F7, respectively. Subfraction F2F5 (36.9 mg) was further purified by a preparative HPLC, using a linear gradient system of 35–75% CH_3CN in water over 30 min, to obtain compounds **6** (12.2 mg), **2** (2.5 mg), and **8** (3.5 mg), respectively.

In addition, a part of fraction F1 (2.39 g) was also purified by Sephadex LH-20 (4.5 cm × 40 cm) to give three subfractions (F1S1 – F1S3). Compound **9** (65.1 mg) was obtained from the subfraction F1S1. Subfraction F1S2 (1.5 g) was further purified by a silica gel column chromatography (4 cm × 20 cm), eluted with 20% acetone in CH_2Cl_2 to afford compound **10** (0.5 g). Subfraction F1S3 (0.3 g) was further purified by a silica gel column chromatography (4 cm × 40 cm), eluted with 20% acetone in CH_2Cl_2 to furnish compounds **12** (15.9 mg), **10** (0.13 g), and **8** (13.9 mg), respectively.

The *n*-hexane crude extract from cells (0.5 g) was purified by a silica gel column chromatography eluted with 60% CH_2Cl_2 in hexane to obtained three fractions, each of which was further purified by semi-preparative HPLC, eluted with a linear gradient system of 5–75% CH_3CN in water over 20 min, to yield compounds **7** (3.71 mg) and **13** (14.1 mg), respectively.

4.3.1. Cyathinin A (*1*)

Colorless crystals (from MeOH–H_2O); $[\alpha]_D^{22}$ –4.68 (c 0.17, MeOH); UV (MeOH) λ_{max} (log ε) nm: 220 (3.90), 271 (3.58); FTIR (ATR) ν_{max} cm^{-1}: 3432, 2948, 2931, 2864, 1724, 1453, 1377, 1191, 1099, 1073, 1037, 1006, 989, 935, 912, 874, 796, 696; HRESIMS at *m/z* 445.2236 $[M-H]^-$ (calcd for $C_{25}H_{33}O_7$, 445.2232); ^{1}H and ^{13}C NMR data, see Tables 1 and 2

X-ray crystallographic analysis of ***1***. $C_{25}H_{34}O_7$, $M = 446.52$, orthorhombic, space group $P2_12_12_1$, $a = 6.6228(3)$ Å, $b = 9.7847(5)$ Å, $c = 37.3196(17)$ Å, $\alpha = 90.0°$, $\beta = 90.0°$, $\gamma = 90.0°$, $V = 2418.4(2)$ Å^3, $F(000) = 960$, $Z = 4$, $T = 100(2)$ K, μ (Cu Kα) $= 0.73$ mm^{-1}, $D_x = 1.226$ Mg/m^3, reflections measured/unique: 19657/4767, number of observations $[I > 2\sigma(I)]$ 4706. The final *R* indices $[I > 2\sigma(I)]$: $R_1 = 0.043$, wR_2 was 0.11680 (all data), Flack x determined using 1928 quotients $[(I^+)-(I^-)]/[(I^+)+(I^-)]$ [41], and absolute structure parameter = 0.1(2). The structure was solved in the space group *P*1 with the ShelXT structure solution program using combined Patterson and dual-space recycling methods [42]. and refined by least squares using version 2014/7 of ShelXL [43]. All non-hydrogen atoms were refined anisotropically. Hydrogen atom positions were calculated geometrically and refined using riding model. In compound **1**, the disordered solvent molecules could not be located in the successive difference Fourier maps, and hence the solvent masking procedure as implemented in OLEX2 [44] was used to remove the electronic contribution of disordered and partially occupied solvent molecules from the refinement. Crystallographic data have been deposited at the Cambridge Crystallographic Data Centre under the reference number CCDC 1832375. Copies of the data can be obtained, free of charge, on application to the Director, CCDC, 12 Union Road, Cambridge CB2 1EZ, UK (e-mail: deposit@ccdc.cam.ac.uk).

4.3.2. Cyathinin B (*2*)

Yellow needles; $[\alpha]_D^{24}$ –19.60 (c 0.12, MeOH); UV (MeOH) λ_{max} (log ε) nm: 219 (3.90), 234 (3.83), 279 (3.59); FTIR (ATR) ν_{max} cm^{-1}: 3431, 2933, 2864, 1694, 1630, 1454, 1377, 1357, 1330, 1287, 1226, 1190, 1128, 1097, 1066, 1038, 1006, 920, 854; HRESIMS at *m/z*

445.2216 [M−H]$^-$ (calcd for $C_{25}H_{33}O_7$, 445.2232); ^{1}H and ^{13}C NMR data, see Tables 1 and 2

*4.3.3. Cyathinin C (**3**)*

A yellow solid; $[\alpha]_D^{26}$ −23.00 (c 0.24, MeOH); UV (MeOH) λ_{max} (log ε) nm: 216 (3.62), 237 (3.44); FTIR (ATR) ν_{max} cm^{-1}: 3411, 2951, 2927, 2869, 1641, 1454, 1377, 1358, 1328, 1288, 1267, 1222, 1191, 1128, 1093, 1070, 1044, 1005, 912, 858, 771; HRESIMS at *m/z* 461.2186 [M−H]$^-$ (calcd for $C_{25}H_{33}O_8$, 461.2181); ^{1}H and ^{13}C NMR data, see Tables 1 and 2

*4.3.4. Striatoid C (**4**)*

Colorless solid; $[\alpha]_D^{24}$ −56.52 (c 0.13, MeOH); HRESIMS at *m/z* 445.2239 [M−H]$^-$ (calcd for $C_{25}H_{33}O_7$, 445.2232); ^{1}H and ^{13}C NMR data, see Figs. S26 and S27 in Supplementary information.

*4.3.5. Cyathinin D (**5**)*

A pale yellow solid; $[\alpha]_D^{24}$ −7.61 (c 0.30, MeOH); UV (MeOH) λ_{max} (log ε) nm: 213 (3.40), 217 (3.36), 278 (2.96); FTIR (ATR) ν_{max} cm^{-1}: 3458, 2929, 2866, 1679, 1454, 1374, 1219, 1123, 1082, 1048, 994, 773; HRESIMS at *m/z* 477.2490 [M−H]$^-$ (calcd for $C_{26}H_{37}O_8$, 477.2494); ^{1}H and ^{13}C NMR data, see Tables 1 and 2

*4.3.6. Striatin C (**6**)*

Pale yellow solid; $[\alpha]_D^{22}$ −12.37 (c 0.13, MeOH); HRESIMS at *m/z* 477.2490 [M−H]$^-$ (calcd for $C_{26}H_{37}O_8$, 477.2494); ^{1}H and ^{13}C NMR data, see Figs. S37 and S38 in Supplementary information.

*4.3.7. Striatal A (**7**)*

Pale yellow solid; $[\alpha]_D^{24}$ −77.44 (c 0.37, MeOH); HRESIMS at *m/z* 495.2357 [M+Na]$^+$ (calcd for $C_{27}H_{36}O_7Na$, 495.2353); ^{1}H and ^{13}C NMR data, see Figs. S40 and S41 in Supplementary information.

*4.3.8. Striatal B (**8**)*

Pale yellow solid; $[\alpha]_D^{24}$ −56.52 (c 0.13, MeOH); HRESIMS at *m/z* 445.2259 [M−H]$^-$ (calcd for $C_{25}H_{33}O_7$, 445.2232); ^{1}H and ^{13}C NMR data, see Figs. S43 and S44 in Supplementary information.

*4.3.9. Striatal D (**9**)*

Pale yellow solid; $[\alpha]_D^{24}$ −42.74 (c 0.05, $CHCl_3$); ^{1}H NMR data ($CDCl_3$, 400 MHz), δ_H (ppm): 0.99 (d, J = 6.2 Hz, 3H, 19-H), 1.00 (d, J = 6.2 Hz, 3H, 20-H), 1.02 (s, 3H, 16-H), 1.03 (s, 3H, 17-H), 1.52–1.60 (m, 4H, 1-H$_a$, 8-H$_2$, and 7-H$_a$), 1.60–1.70 (m, 2H, 1-H$_b$ and 7-H$_b$), 2.28–2.34 (m, 2H, 2-H$_2$), 2.42 (d, J = 11.1 Hz, 1H, 5-H), 2.73 (sept, J = 6.2 Hz, 1H, 18-H), 2.77 (t, J = 7.1 Hz, 1H, 10-H$_a$), 2.82–2.87 (m, 10-H$_b$), 3.36 (d, J = 10.5 Hz, 1H, 13-H), 3.69 (dd, J = 11.7, 5.4 Hz, 1H, 5′-H$_a$), 3.92 (d, J = 8.8 Hz, 1H, 4′-OH), 4.00 (ddd, J = 8.8, 5.4, 3.9 Hz, 1H, 4′-H$_\alpha$), 4.11 (d, J = 1 Hz, 3H, 14-H), 4.24 (dd, J = 11.7, 3.9 Hz, 1H, 5′-H$_\beta$), 5.23 (s, 1H, 1′-H); 6.11 (s, 1H, 2′-OH), 6.99 (dt, J = 8.2, 2.5 Hz, 1H, 11-H), 9.28 (s, 1H, 15-H); ^{13}C NMR data ($CDCl_3$, 100 MHz) δ_C (ppm): 17.3 (C-16), 21.5 (C-20), 21.9 (C-19), 24.6 (C-17), 26.9 (C-7), 27.1 (C-18), 28.4 (C-2), 29.5 (C-10), 36.3 (C-8), 38.3 (C-1), 41.7 (C-6), 42.7 (C-5), 45.8 (C-13), 49.6 (C-9), 68.6 (C-5′), 74.9 (C-4′), 83.7 (C-2′), 87.3 (C-14), 108.3 (C-1′), 135.9 (C-4), 140.0 (C-3), 142.2 (C-12), 159.3 (C-11), 196.2 (C-15), 204.2 (C-3′); HRESIMS at *m/z* 453.2255 [M+Na]$^+$ (calcd for $C_{25}H_{34}O_6Na$, 453.2248).

*4.3.10. 10-Hydroxyerinacine S (**10**)*

Colorless needles; mp 282 °C (dec); $[\alpha]_D^{23}$ −38.48 (c 0.14, MeOH); UV (MeOH) λ_{max} (log ε) nm: 239 (4.69), 264 (4.53), 349 (4.46); FTIR (ATR) ν_{max} cm^{-1}: 3331, 2956, 2923, 2853, 1733, 1674, 1649, 1541, 1459, 1384, 1245, 1223, 1145, 1098, 1070, 1045, 1022, 1001, 947, 917, 820, 792, 686, 669; HRESIMS at *m/z* 445.2225 [M−H]$^-$ (calcd for $C_{25}H_{33}O_7$, 445.2232); ^{1}H and ^{13}C NMR data, see Table 3.

*4.3.11. 15, 22-Diacetyloxy-10-hydroxyerinacine S (**11**)*

Compound **10** (7.0 mg, 0.0156 mmol) was treated with excess acetic anhydride (400 μL) and pyridine (400 μL) at room temperature and the mixture was stirred at room temperature for 12 h. The crude was then purified directly by semi-preparative HPLC (SunFire C_{18} OBD, diam. 10 μm, diam. 19 mm × 250 mm), eluted with a linear gradient system of 40–85% aqueous CH_3CN over 24 min at the flow rate 15 mL/min, to provide compound **11** (4.8 mg, 0.0091 mmol), which was crystallized in MeOH − H_2O to give colorless needles; $[\alpha]_D^{22}$ −55.09 (c 0.09, MeOH); UV (MeOH) λ_{max} (log ε) nm: 218 (3.65), 243 (3.85), 292 (3.29); FTIR (ATR) ν_{max} cm^{-1}: 3447, 2927, 2859, 1749, 1698, 1647, 1455, 1372, 1233, 1185, 1144, 1095, 1051, 1029, 952, 891; HRESIMS at *m/z* 529.2444 [M−H]$^-$ (calcd for $C_{29}H_{37}O_9$, 529.2443); ^{1}H and ^{13}C NMR data, see Table 3.

*X-ray crystallographic analysis of **11**.* $C_{29}H_{38}O_9$, M = 530.59, tetragonal, space group $P4_12_12$, a = 14.8991(5) Å, c = 24.1106(9) Å, α = 90.0°, β = 90.0°, γ = 90.0°, V = 5352.1(2) Å^3, F(000) = 2272, Z = 8, T = 100(2) K, μ (Cu Kα) = 0.80 mm^{-1}, D_x = 1.317 Mg/m^3, reflections measured/unique: 80902/5285, number of observations [$I > 2\sigma(I)$] 5204. The final R indices [$I > 2\sigma(I)$]: R_1 = 0.033, wR_2 was 0.0652 (all data), Flack x determined using 2188 quotients $[(I^+)-(I^-)]/[(I^+)+(I^-)]$ [41], S = 1.04, and absolute structure parameter = −0.009(17). The structure was solved in the space group $P1$ with the ShelXT structure solution program using combined Patterson and dual-space recycling methods [42]. The crystal structure was refined by least squares using version 2014/7 of ShelXL [43]. All non-hydrogen atoms were refined anisotropically. Hydrogen atom positions were calculated geometrically and refined using the riding model. Crystallographic data have been deposited at the Cambridge Crystallographic Data Centre under the reference number CCDC 1832377. Copies of the data can be obtained, free of charge, on application to the Director, CCDC, 12 Union Road, Cambridge CB2 1EZ, UK (e-mail: deposit@ccdc.cam.ac.uk).

*4.3.12. Cyathinin E (**12**)*

A colorless solid; $[\alpha]_D^{23}$ −19.88 (c 0.08, MeOH); UV (MeOH) λ_{max} (log ε) nm: 213 (2.09), 278 (2.31); FTIR (ATR) ν_{max} cm^{-1}: 3432, 2949, 2928, 2857, 1750, 1724, 1639, 1455, 1373, 1253, 1234, 1210, 1136, 1108, 1088, 1039, 1001, 752, 668; HRESIMS at *m/z* 467.2033 [M+Na]$^+$ (calcd for $C_{25}H_{32}O_7Na$, 467.2040); ^{1}H and ^{13}C NMR data, see Tables 1 and 2

*4.3.13. Glochidone C (**13**)*

A colorless solid; $[\alpha]_D^{26}$ 47.04 (c 0.41, $CHCl_3$); HRESIMS at *m/z* 445.3443 [M+Na]$^+$ (calcd for $C_{30}H_{46}ONa$, 445.3441); ^{1}H and ^{13}C NMR data, see Figs. S69–S71 in Supplementary information.

4.4. Biological tests

The microculture radioisotope technique was employed for evaluation of antimalarial activity against *P. falciparum* (K1, multidrug-resistant strain) [45]. Dihydroartemisinin and mefloquine were used as positive controls. The resazurin microplate assay (REMA) was applied for the evaluation of cytotoxicity against cancerous cells including MCF-7 (human breast cancer, ATCC HTC-22), KB (human oral epidermoid carcinoma, ATCC CCL-17), and NCI-H187 (human small-cell lung cancer, ATCC CRL-5804) cells, of anti-*C. albicans*, and of antibacterial activity against *B. cereus* (ATCC11778) [46,47]. Doxorubicin and tamoxifen were used as positive controls for cytotoxicity against MCF-7 cells, while doxorubicin and ellipticine were used as standard references for cytotoxicity against KB and NCI-H187 cells. Amphotericin B was used as a positive control for anti-*C. albicans* and vancomycin was used as a standard reference for anti-*B. cereus*. Antibacterial activity against *E. faecium* (ATCC51559), *E. coli* (ATCC25922), *A. baumannii*

(ATCC19606), *K. pneumoniae* (ATCC700603), and *P. aeruginosa* (ATCC15692) was performed by using the standard protocols published by Clinical and Laboratory Standard Institute [48,49]. Phenylalanine-arginine β-naphthylamide (PAβN) was also added for anti-Gram-negative bacteria tests to compare with the results of the tests without addition of PAβN. Rifampicin and tetracycline HCl were used as positive control for anti-*E. faecium*, while rifampicin and erythromycin were used as positive controls for anti-*E. coli*, anti-*A. baumannii* and anti-*K. pneumoniae*. Erythromycin was used as a positive control for anti-*P. aeruginosa*. The green fluorescent protein microplate assay (GFPMA) was used to evaluate anti-*M. tuberculosis* H37Ra (ATCC25177) and cytotoxicity against non-cancerous cells (Vero, African green monkey kidney fibroblasts, ATCC CCL-81) [50]. Rifampicin, ofloxacin, streptomycin, isoniazid and ethambutol were used as positive controls for anti-*M. tuberculosis* activity, while ellipticine was used as a positive control for cytotoxicity against Vero cell. Maximum tested concentration was done at 50 μg/mL, except for antimalarial and anti-*B. cereus* activities were done at 10 and 25 μg/mL, respectively.

Acknowledgements

The financial support from Thailand Research Fund (TRF grant number: RSA5980001) and the National Center for Genetic Engineering and Biotechnology (BIOTEC grant number: P16-51093) are gratefully acknowledged.

Appendix A. Supplementary data

Supplementary data to this article can be found online at https://doi.org/10.1016/j.tet.2018.10.012.

References

[1] B. Thongbai, S. Rapior, K.D. Hyde, K. Wittstein, M. Stadler, Mycol. Prog. 14 (2015) 91–113.
[2] M.C. Marcotullio, in: I. Rasooli (Ed.), Phytochemicals-bioactivities and Impact on Health, Intech, 2011, pp. 77–94.
[3] W.A. Ayer, T. Yoshida, D.M. van Schie, J. Can, J. Chem. 56 (1978) 2113–2120.
[4] J. Han, Y. Chen, L. Bao, X. Yang, D. Liu, S. Li, F. Zhao, H. Liu, Fitoterapia 84 (2013) 22–31.
[5] L. Huang, J. Han, D. Ben-Hail, L. He, B. Li, Z. Chen, Y. Wang, Y. Yang, L. Liu, Y. Zhu, V. Shoshan-Barmatz, H. Liu, Q. Chen, J. Biol. Chem. 290 (2015) 23563–23578.
[6] L. He, J. Han, B. Li, L. Huang, K. Ma, Q. Chen, X. Liu, L. Bao, H. Liu, Eur. J. Med. Chem. 111 (2016) 183–192.
[7] W.A. Ayer, S.P. Lee, Can. J. Chem. 57 (1979) 3332–3337.
[8] T. Anke, F. Oberwinkler, J. Antibiot. 30 (1977) 221–225.
[9] H.-J. Hecht, G. Hofle, W. Steglich, T. Anke, F. Oberwinkler, J. Chem. Soc., Chem. Commun. (1978) 665–666.
[10] R. Bai, C.C. Zhang, X. Yin, J. Wei, J.M. Gao, J. Nat. Prod. 78 (2015) 783–788.
[11] C. Richter, S.E. Helaly, B. Thongbai, K.D. Hyde, M. Stadler, J. Nat. Prod. 79 (2016) 1684–1688.
[12] B. Wang, J. Han, W. Xu, Y. Chen, H. Liu, Food Chem. 152 (2014) 169–176.
[13] H. Kawagishi, M. Ando, H. Sakamoto, S. Yoshida, F. Ojima, Y. Ishiguro, N. Ukai, S. Furukawa, Tetrahedron Lett. 32 (1991) 4561–4564.
[14] H. Kawagishi, M. Ando, K. Shinba, H. Sakamoto, S. Yoshida, F. Ojima, Y. Ishiguro, N. Ukai, S. Furukawa, Phytochemistry 32 (1992) 175–178.
[15] H. Kawagishi, A. Shimada, R. Shirai, K. Okamoto, F. Ojima, H. Sakamoto, Y. Ishiguro, S. Furukawa, Tetrahedron Lett. 35 (1994) 1569–1572.
[16] H. Kawagishi, A. Shimada, S. Hosokawa, H. Mori, H. Sakamoto, Y. Ishiguro, S. Sakemi, J. Bordner, N. Kojima, S. Furukawa, Tetrahedron Lett. 37 (1996) 7399–7402.
[17] H. Kawagishi, A. Simada, K. Shizuki, F. Ojima, H. Mori, K. Okamoto, H. Sakamoto, S. Furukawa, Heterocycl. Commun. 2 (1996) 51–54.
[18] E.W. Lee, K. Shizuki, S. Hosokawa, M. Suzuki, H. Suganuma, T. Inakuma, J. Li, M. Ohnishi-Kameyama, T. Nagata, S. Furukawa, H. Kawagishi, Biosci. Biotechnol. Biochem. 64 (2000) 2402–2405.
[19] T. Saito, F. Aoki, H. Hirai, T. Inagaki, Y. Matsunaga, T. Sakakibara, S. Sakemi, Y. Suzuki, S. Watanabe, O. Suga, T. Sujaku, A.A. Smogowicz, S.J. Truesdell, J.W. Wong, A. Nagahisa, Y. Kojima, N. Kojima, J. Antibiot. 51 (1998) 983–990.
[20] Z. Rupcic, M. Rascher, S. Kanaki, R.W. Köster, M. Stadler, K. Wittstein, Int. J. Mol. Sci. 19 (2018) 740–751.
[21] H. Shibata, T. Tokunaga, D. e. Karasawa, A. Hirota, M. Nakayama, H. Nozaki, T. Tada, Agric. Biol. Chem. 53 (1989) 3373–3375.
[22] T. Kita, Y. Takaya, Y. Oshima, T. Ohta, K. Aizawa, T. Hirano, T. Inakuma, Tetrahedron 54 (1998) 11877–11886.
[23] T. Ohta, T. Kita, N. Kobayashi, Y. Obara, N. Nakahata, Y. Ohizumi, Y. Takaya, Y. Oshima, Tetrahedron Lett. 39 (1998) 6229–6232.
[24] M. Hirota, K. Morimura, H. Shibata, Biosci. Biotechnol. Biochem. 66 (2002) 179–184.
[25] X.W. Shi, L. Liu, J.M. Gao, A.L. Zhang, Eur. J. Med. Chem. 46 (2011) 3112–3117.
[26] M. Curini, F. Maltese, M.C. Marcotullio, L. Menghini, R. Pagiotti, O. Rosati, G. Altinier, A. Tubaro, Planta Med. 71 (2005) 194–196.
[27] M.C. Marcotullio, R. Pagiotti, V. Campagna, F. Maltese, G. Fardella, G. Altinier, A. Tubaro, Nat. Prod. Res. 20 (2006) 917–921.
[28] M.C. Marcotullio, R. Pagiott, F. Maltese, Y. Obara, T. Hoshino, N. Nakahata, M. Curini, Planta Med. 72 (2006) 819–823.
[29] Y. Obara, T. Hoshino, M.C. Marcotullio, R. Pagiotti, N. Nakahata, Life Sci. 80 (2007) 1669–1677.
[30] C.M. Mudalungu, C. Richter, K. Wittstein, M.A. Abdalla, J.C. Matasyoh, M. Stadler, R.D. Sussmuth, J. Nat. Prod. 79 (2016) 894–898.
[31] I.S. Marcos, R.F. Moro, A. Gil-Mesón, D. Díez, in: R. Atta ur (Ed.), Studies in Natural Products Chemistry, Elsevier, 2016, pp. 137–207.
[32] Y.L. Yang, S. Zhang, K. Ma, Y. Xu, Q. Tao, Y. Chen, J. Chen, S. Guo, J. Ren, W. Wang, Y. Tao, W.B. Yin, H. Liu, Angew. Chem., Int. Ed. Engl. 56 (2017) 4749–4752.
[33] C.C. Chen, T.T. Tzeng, C.C. Chen, C.L. Ni, L.Y. Lee, W.P. Chen, Y.J. Shiao, C.C. Shen, J. Nat. Prod. 79 (2016) 438–441.
[34] D. Arad, A.P. Bollon, D.C. Young, B.W. Poland, A.S. Peek, Google Patents, 2001.
[35] T. Anke, U. Rabe, P. Schu, T. Eizenhofer, M. Schrage, W.Z. Steglich, Naturforscher C 57 (2002) 263–271.
[36] P. Puapairoj, W. Naengchomnong, A. Kijjoa, M.M. Pinto, M. Pedro, M.S. Nascimento, A.M. Silva, W. Herz, Planta Med. 71 (2005) 208–213.
[37] H.Y. Tang, X. Yin, C.C. Zhang, Q. Jia, J.M. Gao, Curr. Med. Chem. 22 (2015) 2375–2391.
[38] W.A. Ayer, L.M. Browne, J.R. Mercer, D.R. Taylor, D.E. Ward, Can. J. Chem. 56 (1978) 717–721.
[39] W.A. Ayer, R.J. Flanagan, T. Reffstrup, Tetrahedron 40 (1984) 2069–2082.
[40] R.L. Zhao, D.E. Desjardin, K. Soytong, K.D. Hyde, Persoonia 21 (2008) 71–76.
[41] S. Parsons, H.D. Flack, T. Wagner, Acta Crystallogr. B Struct. Sci. Cryst. Eng. Mater. 69 (2013) 249–259.
[42] G. Sheldrick, Acta Crystallogr. A 71 (2015) 3–8.
[43] G.M. Sheldrick, Acta Crystallogr. C Struct. Chem. 71 (2015) 3–8.
[44] O.V. Dolomanov, L.J. Bourhis, R.J. Gildea, J.A.K. Howard, H.J. Puschmann, Appl. Cryst. 42 (2009) 339–341.
[45] R.E. Desjardins, C.J. Canfield, J.D. Haynes, J.D. Chulay, Antimicrob. Agents Chemother. 16 (1979) 710–718.
[46] J. O'Brien, I. Wilson, T. Orton, F. Pognan, Eur. J. Biochem. 267 (2000) 5421–5426.
[47] S.D. Sarker, L. Nahar, Y. Kumarasamy, Methods 42 (2007) 321–324.
[48] P.A. Wayne, M7-A7. Methods for Dilution Antimicrobial Susceptibility Tests for Bacteria that Grow Aerobically; Approved Standard, seventh ed., Clinical and Laboratory Standards Institute, Pennsylvania, USA, 2006.
[49] P.A. Wayne, M100-S16, Performance Standards for Antimicrobial Susceptibility Testing; Sixteenth Informational Supplement, Clinical and Laboratory Standards Institute, Pennsylvania, USA, 2006.
[50] C. Changsen, S.G. Franzblau, P. Palittapongarnpim, Antimicrob. Agents Chemother. 47 (2003) 3682–3687.

รายละเอียดการประดิษฐ์

ชื่อที่แสดงถึงการประดิษฐ์

สารประกอบเฟนเลอรัล และองค์ประกอบทางเภสัชกรรมของสารดังกล่าว

สาขาวิทยาการที่เกี่ยวข้องกับการประดิษฐ์

จุลชีววิทยา เคมี และการแพทย์ ที่เกี่ยวข้องกับสารประกอบเฟนเลอรัล และองค์ประกอบทางเภสัชกรรมของสารดังกล่าว

ภูมิหลังของศิลปะหรือวิทยาการที่เกี่ยวข้อง

จากการรายงานผลของกระทรวงสาธารณสุขไทย พบว่ามะเร็งเป็นปัญหาการเสียชีวิตอันดับต้นๆ ของไทยติดต่อกันมาหลายปี และมีแนวโน้มเพิ่มขึ้น รวมทั้งทั่วโลกก็ประสบกับปัญหาเช่นเดียวกัน เนื่องจากโครงสร้างประชากรกำลังเข้าสู่สังคมผู้สูงอายุ และการพบความสัมพันธ์ของมะเร็งกับการสูบบุหรี่ อาหาร และมลพิษ ดังนั้น ที่ผ่านมาจึงมีรายงานจำนวนมากที่พยายามจะพัฒนาสารใหม่ที่ออกฤทธิ์ในการยับยั้งเซลล์มะเร็งต่างๆ ยาที่ออกฤทธิ์ยับยั้งเซลล์มะเร็งที่ใช้ในปัจจุบันมีหลากหลาย โดยแบ่งตามการออกฤทธิ์ต่อเป้าหมายต่างกัน ตัวอย่าง เช่น กลุ่มที่มีผลต่อดีเอ็นเอ โดยทำให้สายดีเอ็นเอไม่พร้อมสำหรับการจำลองตัวเอง ยาในกลุ่มนี้ ได้แก่ ด๊อกโซรูบิซิน (doxorubicin) อีพิรูบิซิน (epirubicin), กลุ่มที่มีผลต่อการแบ่งเซล์ ได้แก่ แพคลิแทกเซล (paclitaxel) โดซีแทกเซิล (docetaxel) นอกจากนั้น ยังมีกลุ่มที่ออกฤทธิ์เกี่ยวข้องกับฮอร์โมน เช่น ยายับยั้งมะเร็งเต้านมที่ไวต่อเอสโตรเจน เป็นยาที่ใช้เพื่อไม่ให้ฮอร์โมนดังกล่าวกระตุ้นการเจริญเติบโตของมะเร็งหรือลดการสร้างฮอร์โมนนั้นๆ ในร่างกาย โดยยาในกลุ่มนี้ ได้แก่ ยาราโลซิฟีน (raloxifene) ทาม็อกซิเฟน (tamoxifen) เป็นต้น

ถึงแม้ว่าปัจจุบันจะมีการพัฒนาสารประกอบที่ออกฤทธิ์ในการยับยั้งเซลล์มะเร็งชนิดต่างๆ ในระดับหนึ่งแล้วดังที่กล่าวข้างต้น แต่พบว่าสารที่มีฤทธิ์สูงในการยับยั้งเซลล์มะเร็งจะมีความเป็นพิษต่อเซลล์ปกติสูงเช่นกัน ดังนั้นในปัจจุบันจึงยังคงมีความพยายามในการพัฒนาสารชนิดใหม่ที่ออกฤทธิ์สูงในการยับยั้งเซลล์มะเร็ง โดยที่มีความเป็นพิษต่อเซลล์ปกติต่ำ และการประดิษฐ์นี้ก็มีจุดมุ่งหมายในการพัฒนาสารออกฤทธิ์ชนิดใหม่ที่มีลักษณะดังกล่าว

ลักษณะและความมุ่งหมายของการประดิษฐ์

การประดิษฐ์นี้เกี่ยวกับการพัฒนาสารประกอบเฟนเลอรัลซึ่งเป็นสารประกอบชนิดใหม่ที่มีฤทธิ์ยับยั้งเซลล์มะเร็งได้ดี โดยที่มีความเป็นพิษต่อเซลล์ปกติต่ำ ซึ่งผลิตได้จากกรรมวิธีการเลี้ยงเชื้อราไฮปอกซิลอน เฟน-เลอรี (*Hypoxylon fendleri*) สายพันธุ์ BCC32408 ที่พัฒนาขึ้น ประกอบกับวิธีการแยกสารประกอบออกจากสารสกัดหยาบและการทำให้สารบริสุทธิ์ นอกจากนี้ ยังพบว่าสารประกอบเฟนเลอรัลยังมีฤทธิ์ในการยับยั้งเชื้อมาลาเรียอีกด้วย ดังนั้น จึงสามารถใช้สารประกอบตามการประดิษฐ์นี้เป็นสารออกฤทธิ์ในองค์ประกอบทางเภสัชกรรมที่ออกฤทธิ์ ยับยั้งเซลล์มะเร็ง หรือ ยับยั้งเชื้อมาลาเรียได้

สารประกอบเฟนเลอรัลตามการประดิษฐ์นี้ มีสูตรโครงสร้าง (I) ดังนี้

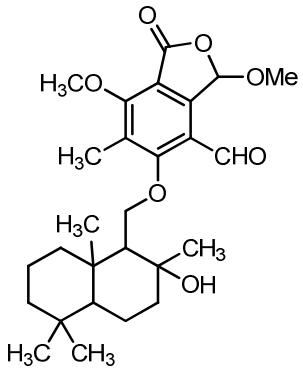

(I)

คำอธิบายรูปเขียนโดยย่อ

รูปที่ 1 แสดงสเปกตรัมของการดูดกลืนแสง UV ของสารประกอบ (I) ในเมทธานอล

รูปที่ 2 แสดงสเปกตรัมของการดูดกลืนแสง IR ของสารประกอบ (I) (ATR)

รูปที่ 3 แสดง ^{1}H-NMR สเปกตราของสารประกอบ (I) (500 MHz, $CDCl_3$)

รูปที่ 4 แสดง ^{13}C-NMR สเปกตราของสารประกอบ (I) (125 MHz, $CDCl_3$)

การเปิดเผยการประดิษฐ์โดยสมบูรณ์

การประดิษฐ์สารประกอบเฟนเลอรัล (I) ตามการประดิษฐ์นี้ ได้จากกรรมวิธีการผลิต ที่ประกอบด้วยขั้นตอนการเลี้ยงเชื้อรา *Hypoxylon fendleri* สายพันธุ์ BCC32408 ที่เริ่มจากการปลูกถ่ายเส้นใยเชื้อราหรือสปอร์ของเชื้อรา การบ่มเพาะเชื้อรา การสกัดสารประกอบออกจากส่วนของอาหารเลี้ยงเชื้อและตัวเซลล์ การแยกสารประกอบออกจากสารสกัด และการทำให้บริสุทธิ์จนกระทั่งได้สารประกอบเฟนเลอรัล ที่แสดงด้วยสูตรโครงสร้าง (I) ดังต่อไปนี้

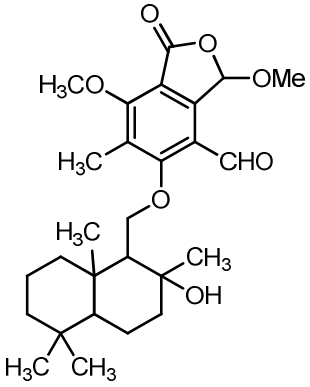

(I)

เมื่อทำการเปรียบเทียบโครงสร้างสารประกอบเฟนเลอรัล (I) กับฐานข้อมูลทางเคมี พบว่าสารประกอบนี้เป็นสารประกอบชนิดใหม่ที่ไม่เหมือนกับสารใดที่รายงานมาก่อนหน้านี้ โดยสารประกอบชนิดนี้มีฤทธิ์ยับยั้งเซลล์มะเร็งได้ดี และมีความเป็นพิษต่อเซลล์ปกติต่ำ อีกทั้งยังพบว่าสารประกอบชนิดนี้มีฤทธิ์ในการยับยั้งเชื้อ

มาลาเรียอีกด้วย นอกจากนี้ พบว่าเชื้อรา *Hypoxylon fendleri* สายพันธุ์ BCC32408 ที่นำมาเลี้ยงด้วยกรรมวิธีตามการประดิษฐ์นี้เพื่อผลิตสารประกอบสูตร (I) โดยในธรรมชาติเชื้อราชนิดนี้ไม่มีรายงานว่าสามารถผลิตสารประกอบดังกล่าวนี้ได้

การประดิษฐ์นี้ ยังครอบคลุมถึงเกลือของสารประกอบเฟนเลอรัลที่มีสูตรโครงสร้าง (I) รวมทั้งองค์ประกอบทางเภสัชกรรม ที่ออกฤทธิ์ยับยั้งเซลล์มะเร็ง หรือ ยับยั้งเชื้อมาลาเรีย ที่ประกอบด้วย

ก. สารออกฤทธิ์ ที่เลือกได้จากกลุ่มที่ประกอบด้วย สารประกอบเฟนเลอรัลที่มีสูตรโครงสร้าง (I), เกลือของสารประกอบเฟนเลอรัลที่มีสูตรโครงสร้าง (I) หรือ สารผสมของสารดังกล่าว

ข. สารตัวพาที่ยอมรับได้ทางเภสัชกรรม

ลำดับต่อไปจะขอกล่าวถึงรายละเอียดตัวอย่างในการผลิตสารประกอบใหม่ตามการประดิษฐ์นี้ และตัวอย่างการทดสอบประสิทธิภาพการออกฤทธิ์ของสาร

1. การเลี้ยงเชื้อรา *Hypoxylon fendleri* สายพันธุ์ BCC32408

การเลี้ยงเชื้อรา *Hypoxylon fendleri* สายพันธุ์ BCC32408 เพื่อผลิตสารประกอบเฟนเลอรัล (I) ในการประดิษฐ์นี้สามารถทำได้ในอาหารเหลวหลายชนิด โดยทั่วไปอาหารเลี้ยงเชื้อที่จะทำให้เชื้อเจริญเติบโตและส่งผลดีต่อการผลิตสาร ประกอบด้วยแหล่งคาร์บอน เช่น แป้ง น้ำตาล แหล่งไนโตรเจน ทริปโตน (tryptone) กรดอะมิโน โพลีเปปไทด์ เป็นต้น แหล่งสารองค์ประกอบเชิงซ้อน สารสกัดยีสต์ (yeast extract) เกลืออนินทรีย์ อีกทั้งมีการเติมแร่ธาตุต่างๆ ในปริมาณเล็กน้อย

การเลี้ยงเชื้อรา *Hypoxylon fendleri* สายพันธุ์ BCC32408 ที่เหมาะสมในการผลิตสารประกอบเฟนเลอรัล (I) ประกอบด้วยการปลูกถ่ายเส้นใยของเชื้อราในอาหารเลี้ยงเชื้อเหลวที่เหมาะสม และการบ่มเพาะในสภาวะที่มีอากาศดังนี้

1.1 กระบวนการหมัก เริ่มต้นจากการปลูกถ่ายเส้นใยเชื้อหรือสปอร์ของเชื้อที่เก็บรักษาเอาไว้ไปยังอาหารเลี้ยงหัวเชื้อ ในที่นี้ใช้อาหารเหลวโปเตโต้ เด็คโตรส (Potato Dextrose Broth, PDB) ปล่อยให้การเจริญเติบโตของเชื้อเหมาะสมสำหรับใช้เป็นจุดตั้งต้นในการผลิตสารทุติยภูมิ

1.2 บ่มหัวเชื้อที่อยู่ในอาหารเหลวโปเตโต้ เด็คโตรส (Potato Dextrose Broth) ในสภาวะที่มีอากาศโดยการเขย่า ด้วยความเร็ว 200 รอบต่อนาที (rpm) ที่อุณหภูมิ 25 องศาเซลเซียส เป็นเวลา 5 วัน แล้วถ่ายหัวเชื้อไปในขวดที่ใหญ่ขึ้น โดยใช้อาหารสูตรเดิมที่มีปริมาตร 250 มิลลิลิตร โดยใช้ขวดปริมาตร 1,000 มิลลิลิตร

1.3 การหมักบ่มเชื้อ โดยการถ่ายหัวเชื้อไปยังอาหารเลี้ยงเชื้อที่เหมาะในการสร้างสารทุติยภูมิ ในที่นี้ใช้สูตรอาหารที่สกัดจากข้าวบาร์เล่ย์ (Malt Extract Broth, MEB) โดยใช้ปริมาตรของหัวเชื้อตั้งต้นประมาณ 1 ใน 10 ของปริมาณอาหารเลี้ยงเชื้อที่เหมาะกับการสร้างสาร การหมักบ่มเชื้อทำในสภาวะเขย่า (shake condition) เป็นเวลา 20 วัน หลังจากนั้นทำการสกัดด้วยตัวทำละลายอินทรีย์ ผลิตภัณฑ์จากการสกัดจะถูกนำมาแยกเพื่อให้ได้สารบริสุทธิ์ที่ออกฤทธิ์ทางชีวภาพต่อไป

2. การแยกสารประกอบเฟนเลอรัล (I)

สารประกอบเฟนเลอรัล (**I**) ได้จากการหมักเชื้อรา *Hypoxylon fendleri* สายพันธุ์ BCC32408 โดยการสกัดแยกของเซลล์และน้ำเลี้ยงเชื้อที่ได้จากการหมัก ด้วยตัวทำละลายอินทรีย์ คือ เอทธิลอะซิเตท (ethyl acetate) จำนวน 3 ครั้ง การแยกสารประกอบเฟนเลอรัล (**I**) ออกจากสารสกัด และทำให้บริสุทธิ์โดยวิธีโครมาโตรกราฟีมาตรฐานโดยใช้ตัวดูดซับ (adsorbant) คือ เซปฟาเดกซ์ แอล เอช 20 (Sephadex™ LH-20) ก่อนนำไปแยกต่อด้วย เครื่องโครมาโตรกราฟีของเหลวสมรรถนะสูงแบบเก็บแยกส่วน (preparative HPLC) ด้วยวิธีดังกล่าวทำให้ได้ผลิตภัณฑ์ที่บริสุทธิ์ (substantially purified) การแยกด้วยเซปฟาเดกซ์ แอล เอช 20 ทำโดยใช้เมทธานอล (methanol) เป็นตัวชะล้าง ทำให้ได้สารออกมาเป็นส่วนๆ (fractions) นำส่วน (fraction) ที่มีสารประกอบเฟนเลอรัล (**I**) อยู่ไปแยกต่อให้บริสุทธิ์ด้วยเครื่องเอชพีแอลซี (High Performance Liquid Chromatography; HPLC) โดยใช้คอลัมน์แบบเก็บแยกส่วน (preparative column) และใช้น้ำกับอะซิโตไนไตรล์ (CH_3CN) เป็นตัวชะล้าง จากนั้นนำสารประกอบเฟนเลอรัล (**I**) ตามการประดิษฐ์นี้ไปทดสอบการออกฤทธิ์ยับยั้งเซลล์มะเร็งและเชื้อก่อโรคมาลาเรียตามวิธีมาตรฐาน

3. การเตรียมสารประกอบเฟนเลอรัล (I) ตามการประดิษฐ์นี้เพื่อใช้ในทางเภสัชกรรม

การประดิษฐ์ได้ทดสอบใช้สารประกอบเฟนเลอรัล (**I**) เพียงอย่างเดียวหรือใช้ร่วมกับสารอื่นที่ออกฤทธิ์ยับยั้งเซลล์มะเร็งและยับยั้งเชื้อมาลาเรีย หรือใช้สารประกอบเฟนเลอรัล (**I**) นี้กับตัวนำพาหรือตัวทำละลายที่เข้ากันได้ในทางเภสัชกรรมหรือเลือกประกอบกับองค์ประกอบเสริม (adjuvant) ซึ่งขึ้นอยู่กับวิธีมาตรฐานในทางเภสัชกรรม สารประกอบนี้อาจจัดให้เข้าสู่ร่างกายโดยการกิน (orally) การฉีด (parentally) เข้าสู่หลอดเลือดดำ (intravenous) เข้ากล้ามเนื้อ (intramuscular) ช่องท้อง (intraperitineal) เข้าผิวหนัง (subcutaneous) หรือทางทวาร (rectal)

ตัวอย่างที่ 1

การเตรียมสารประกอบเฟนเลอรัล (I)
โดยการหมักบ่มเชื้อ *Hypoxylon fendleri* สายพันธุ์ BCC32408

<u>แหล่งมวลชีวภาพ</u>

เชื้อราที่ผลิตสารประกอบเฟนเลอรัล (**I**) ถูกคัดแยกมาจากไม้ (ไม่ระบุชื่อ) ที่เก็บจากพื้นที่เขตรักษาพันธุ์สัตว์ป่าภูสีฐาน อ.กุฉินารายณ์ จังหวัดกาฬสินธุ์ ประเทศไทย เมื่อเดือน กันยายน พ.ศ. 2551 รา *Hypoxylon fendleri* สายพันธุ์ BCC32408 นี้ถูกฝากเก็บไว้ เมื่อวันที่ 23 กันยายน พ.ศ. 2551 ที่ห้อง ปฏิบัติการเก็บรวบรวมสายพันธุ์จุลินทรีย์ (BIOTEC Culture Collection หรือ BCC; http://www1a.biotec.or.th /TNCC/dbstore/BCC_search.asp) ศูนย์พันธุวิศวกรรมและเทคโนโลยีชีวภาพแห่งชาติ (ไบโอเทค) สำนักงานพัฒนาวิทยาศาสตร์และเทคโนโลยีแห่งชาติ (สวทช) จังหวัดปทุมธานี ประเทศไทย ด้วยรหัสเลขที่ BCC32408 โดยข้อมูลลักษณะสัณฐานวิทยาสายพันธุ์ BCC32408 ถูกบ่งชี้จากฐานข้อมูลสากล ชื่อว่า อินเด็กฟันโกรัม (Indexfungorum) และ ไมโคแบงค์ (Mycobank) ว่าชื่อ *Hypoxylon fendleri* อยู่ในไฟลัมแอสโคไมโคตา (Ascomycota) ซับไฟลัมเพซิโซไมโคตินา (Pezizomycotina) คลาสซอดาริโอมัยซีส (Sordariomycetes) ซับ

คลาสไซลาเรียมัยซีสติดี (Xylariamycetidae) ออเดอร์ไซลาเรียลีส (Xylariales) แฟมิลี่ไซลาเรียซีอี (Xylariaceae) และ จีนัสหรือสกุลราไฮปอกซิลอน (*Hypoxylon*) ทั้งนี้ได้มีการยืนยันข้อมูลลักษณะสัณฐานวิทยาด้วยข้อมูลลำดับพันธุกรรมของดีเอ็นเอ ประกอบด้วย ไรโบโซมอลดีเอ็นเอ ชนิด 28เอส (LSU rDNA) ไรโบโซมอลดีเอ็นเอชนิด 5.8เอสต่อกับดีเด็นเอชนิดไอทีเอส (5.8S-ITS rDNA) และ ยีนเบต้า-ทิวบูลิน (β-tubulin) และโดยการวิเคราะห์ข้อมูลดังกล่าวด้วยโปรแกรมที่ทำหน้าที่ในการค้นหาความเหมือนหรือความแตกต่างของข้อมูลลำดับทางพันธุกรรมของดีเอ็นเอเปรียบเทียบกับฐานข้อมูลที่เก็บรวบรวมข้อมูลทางพันธุกรรมของสิ่งมีชีวิตต่างๆของเอ็นซีบีไอ (NCBI) ฐานข้อมูลของราของไมโคแบงค์ (Mycobank) และฐานข้อมูลของราของศูนย์เก็บรวบรวมข้อมูลของเชื้อจุลินทรีย์ CBS-KNAW Fungal Biodiversity Centre

<u>ขั้นตอนการทดลอง</u>

เลี้ยงเชื้อรา *Hypoxylon fendleri* สายพันธุ์ BCC32408 บนอาหารวุ้น PDA อุณหภูมิ 25 องศาเซลเซียส ส่วนของวุ้นจะถูกตัดเป็นชิ้นเล็กๆ ขนาด 1 เซนติเมตร × 1 เซนติเมตร แล้วใส่ลงในขวดรูปชมพู่ (Erlenmeyer flask) ขนาด 250 มิลลิลิตร ที่มีอาหารเลี้ยงเชื้อ PDB ปริมาตร 25 มิลลิลิตร (อาหาร PDB มีส่วนประกอบคือ 1. แป้งมันฝรั่ง (potato starch) 4 กรัมต่อลิตร 2. เด็กโทรส (dextrose) 20 กรัมต่อลิตร ละลายในน้ำกลั่น) หลังจากบ่มที่ 25 องศาเซลเซียส เป็นเวลา 5 วัน แบบเขย่า 200 รอบต่อนาที (rpm) หัวเชื้อแต่ละขวดจะถูกถ่ายไปยังขวดขนาด 1,000 มิลลิลิตร ที่มีอาหารเลี้ยงเชื้อ PDB ปริมาตร 250 มิลลิลิตร แล้วนำไปบ่มที่ 25 องศาเซลเซียส เป็นเวลา 5 วัน โดยเขย่า 200 รอบต่อนาที (rpm) จากนั้นนำหัวเชื้อที่ได้ปริมาณ 25 มิลลิลิตร ใส่ลงในขวด 1,000 มิลลิลิตร ที่มีอาหารเลี้ยงเชื้อ MEB (มีส่วนประกอบคือ 1. สารสกัดมอลต์ (Malt extract) 6 กรัมต่อลิตร 2. มอลโทส (Maltose) 1.8 กรัมต่อลิตร 3. เด็กโทรส 6 กรัมต่อลิตร 4. สารสกัดยีสต์ (Yeast extract) 1.2 กรัมต่อลิตร ละลายในน้ำกลั่น) ปริมาตร 250 มิลลิลิตร ให้ได้ปริมาตรทั้งหมด 20 ลิตร และนำไปบ่มต่อที่ 25 องศาเซลเซียส อีก 20 วัน แบบสภาวะเขย่า (shake condition) หลังจากนั้นนำส่วนอาหารเลี้ยงเชื้อมาสกัดด้วยเอทธิลอะซิเตท (3 × 1000 มิลลิลิตร) และนำตัวทำละลายนี้ไปทำให้แห้งภายใต้การลดความดัน ได้สารสกัดหยาบทั้งสิ้น 17.47 กรัม

ในส่วนของเซลล์นำไปแช่ด้วยเมทธานอล 3 วัน แล้วกรองเซลล์ออก จากนั้นนำเซลล์ไปแช่ต่อด้วยไดคลอโรมีเธน อีก 3 วัน แล้วกรองเซลล์ออก นำส่วนเมทธานอลและไดคลอโรมีเธนมารวมกันแล้วกลั่นภายใต้การลดความดันเพื่อให้มีความเข้มข้นสูงขึ้น จากนั้นนำส่วนที่เหลือมาสกัดด้วยเอทธิลอะซิเตท (3 × 1000มิลลิลิตร) นำไปทำให้แห้งภายใต้การลดความดัน จะได้สารสกัดหยาบ 7.15 กรัม

จากนั้นนำสารสกัดที่ได้ไปผ่านคอลัมน์โครมาโตกราฟีเซปฟาเดกซ์ แอล เอช 20 ใช้ตัวทำละลายเมทธานอล รวมส่วนที่ผ่านคอลัมน์ที่มีสารประกอบเฟนเลอรัล (**I**) จากนั้นนำส่วนของสารผสมที่มีส่วนประกอบของสารประกอบสูตร (**I**) (fraction) ที่ได้ทั้งจากส่วนอาหารเลี้ยงเชื้อและเซลล์ มาทำให้บริสุทธิ์ต่อด้วยเอชพีแอลซีโดยใช้คอลัมน์ชนิด ซันไฟร์ ซี18 โอบีดี (SunFire Prep C18 OBD) ขนาด 19 × 250 มิลลิเมตร ขนาดซิลิกาเจล 10 ไมโครเมตร และใช้ตัวทำละลายผสมระหว่างอะซิโตไนไตรล์และน้ำในอัตราส่วนตั้งแต่ 45% จนถึง 95% อะซิโตไนไตรล์ในระยะเวลา 30 นาที เป็นตัวทำละลายชะล้าง มีอัตราไหลของตัวทำละลายเคลื่อนที่ผ่าน

คอลัมน์ 15 มิลลิลิตรต่อนาที จะได้สารประกอบเฟนเลอรัล (**I**) (จำนวน 80.3 มิลลิกรัม เวลาที่สารเคลื่อนที่ผ่านคอลัมน์ 22.4 นาที และ จำนวน 170.8 มิลลิกรัม เวลาที่สารเคลื่อนที่ผ่านคอลัมน์ 22.7 นาที) และพบว่าสารประกอบที่พบนี้เป็นสารประกอบชนิดใหม่ที่ไม่เหมือนกับสารใดที่ปรากฏมาก่อนหน้านี้

ลักษณะเฉพาะทางฟิสิกส์และเคมี (physico-chemical characteristics) ของสารประกอบ (**I**) ดังแสดงต่อไปนี้

1. ลักษณะที่ปรากฏ คือ ผงสีเหลืองอ่อน หรือ เป็นผงสีขาว
2. มวลโมเลกุลความละเอียดสูง (High resolution MS) (ESI-TOF): มวลต่อประจุ (*m/z*) 571.1233 $[M + H]^+$ (calcd for $C_{31}H_{23}O_{11}$, 571.1235) และ *m/z* 593.1059 $[M + Na]^+$ (calcd for $C_{31}H_{22}O_{11}Na$, 593.1054)
3. กราฟช่วงการดูดกลืนแสงยูวี (UV absorption spectrum) ในเมทานอล (MeOH): ความยาวคลื่นสูงสุด (λ_{max}) (log ε) 237 (3.56), 268 (3.64), 390 (3.13) นาโนเมตร (รูปที่ 1).
4. กราฟช่วงการดูดกลืนแสงอินฟาเรด (IR absorption spectrum) เทคนิคเอทีอาร์ (ATR): ความยาวคลื่นสูงสุด ν_{max} 3430 (br), 1728, 1637, 1615, 1568, 1503, 1433, 1332, 1296, 1240, 1211, 1178, 1099, 1078, 1014, 856, 740 ซม.$^{-1}$ (รูปที่ 2).
5. กราฟโปรตอน-เอ็นเอ็มอาร์ (^{1}H-NMR spectrum) ($CDCl_3$, 500 เมกะเฮิร์ต): *เดลต้า* (δ) 10.37 (1H, s), 6.49 (1H, s), 4.22 (1H, dd, *J* = 9.7, 5.8 Hz), 4.22 (3H, s), 4.15 (1H, dd, *J* = 9.7, 4.4 Hz), 3.74 (3H, s), 2.29 (3H, s), 1.95 (1H, dt, *J* = 10.2, 3.1 Hz), 1.90-1.94 (1H, m), 1.78 (2H, dt, *J* = 12.7, 3.0 Hz), 1.72 (1H, dq, *J* = 13.8, 3.0 Hz), 1.59-1.68 (1H, m), 1.56 (1H, dt, *J* = 10.2, 3.4 Hz), 1.49 (1H, dquint, *J* = 13.5, 3.4 Hz), 1.42 (1H, dt, *J* = 13.3, <1 Hz), 1.29 (1H, td, *J* = 13.3, 3.2 Hz), 1.26 (3H, s), 1.18-1.25 (1H, m), 1.05 (1H, dd, *J* = 12.2, 1.9 Hz), 0.91 (3H, s) , 0.85 (3H, s), 0.82 (3H, s) (รูปที่ 3 ก.).
6. กราฟโปรตอน-เอ็นเอ็มอาร์ (^{1}H-NMR spectrum) ($CDCl_3$, 500 เมกะเฮิร์ต): *เดลต้า* (δ) 10.39 (1H, s), 6.50 (1H, s), 4.28 (1H, dd, *J* = 9.7, 5.8 Hz), 4.22 (3H, s), 4.09 (1H, dd, *J* = 9.7, 4.2 Hz), 3.74 (3H, s), 2.28 (3H, s), 1.95 (1H, dt, *J* = 10.5, 3.0 Hz), 1.90-1.94 (1H, m), 1.78 (2H, dt, *J* = 12.6, 3.0 Hz), 1.72 (1H, dq, *J* = 13.7, 3.0 Hz), 1.59-1.68 (1H, m), 1.57 (1H, dt, *J* = 10.5, 2.8 Hz), 1.48 (1H, dquint, *J* = 10.8, 3.3 Hz), 1.42 (1H, dt, *J* = 13.1, <1 Hz), 1.30 (1H, td, *J* = 13.7, 2.9 Hz), 1.26 (3H, s), 1.18-1.25 (1H, m), 1.06 (1H, dd, *J* = 12.1, <1 Hz), 0.91 (3H, s) , 0.84 (3H, s), 0.82 (3H, s) (รูปที่ 3 ข.).
7. กราฟคาร์บอน-เอ็นเอ็มอาร์ (^{13}C-NMR spectrum) ($CDCl_3$, 125 เมกะเฮิร์ต): *เดลต้า* (δ) 188.1 (CH), 166.8 (qC), 165.5 (qC), 162.6 (qC), 146.8 (qC), 128.3 (qC), 120.7 (qC), 113.7 (qC), 102.4 (CH), 75.7 (CH_2), 72.8 (qC), 63.1 (CH_3), 60.9 (CH), 58.4 (CH_3), 55.8 (CH), 44.1 (CH_2), 41.6 (CH_2), 40.4 (CH_2), 38.0 (qC), 33.5 (CH_3), 33.3 (qC), 24.9 (CH_3), 21.6 (CH_3), 20.2 (CH_2), 18.5 (CH_2), 16.2

(CH_3), 10.1 (CH_3) (รูปที่ 4 ก.).

8. กราฟคาร์บอน-เอ็นเอ็มอาร์ (^{13}C-NMR spectrum) ($CDCl_3$, 125 เมกะเฮิร์ต): *เดลต้า* (δ) 188.4 (CH), 166.7 (qC), 165.5 (qC), 162.6 (qC), 146.9 (qC), 128.3 (qC), 120.7 (qC), 113.7 (qC), 102.4 (CH), 75.7 (CH_2), 72.8 (qC), 63.1 (CH_3), 61.0 (CH), 58.5 (CH_3), 55.8 (CH), 44.0 (CH_2), 41.6 (CH_2), 40.3 (CH_2), 38.0 (qC), 33.5 (CH_3), 33.3 (qC), 25.0 (CH_3), 21.6 (CH_3), 20.2 (CH_2), 18.5 (CH_2), 16.2 (CH_3), 10.1 (CH_3) (รูปที่ 4 ข.).

ตัวอย่างที่ 2

การตรวจสอบฤทธิ์ยับยั้งเซลล์มะเร็งของสารประกอบเฟนเลอรัล (I)

วิธีการตรวจวิเคราะห์ใช้วิธีการ รีซาซูรินไมโครเพลท (resazurin microplate) (O'Brien และคณะ, 2000) เซลล์มะเร็ง 3 ชนิดของมนุษย์ที่นำมาใช้ทดสอบมีดังนี้ เซลล์ไลน์ KB (อีพิเดอมอยด์(epidermoid) เซลล์มะเร็งของช่องปาก, ATCC CCl-17) เซลล์ไลน์ MCF-7 (เซลล์มะเร็งของต่อมเต้านม, ATCC HTB-22) และเซลล์ไลน์ NCI-H187 (เซลล์มะเร็งปอดขนาดเล็ก, ATCC CRL-5804) ใช้เซลล์ในระยะที่มีการเจริญเติบโตคงที่ระยะล็อก (logarithmic phase) สำหรับ KB เตรียมเซลล์เข้มข้นในอาหารเหลวจำนวน 2.2×10^4 เซลล์ต่อมิลลิลิตร และ MCF-7, NCI-H187 จำนวน 3.3×10^4 เซลล์ต่อมิลลิลิตร ตามลำดับ ดูดสารตัวอย่างปริมาตร 5 ไมโครลิตรที่ละลายด้วย 5% DMSO และ เซลล์ปริมาตร 45 ไมโครลิตร ใส่ลงในถาดขนาด 384 หลุม เก็บในตู้บ่มเชื้อที่อุณหภูมิ 37 องศาเซลเซียส มีความเข้มข้นก๊าซคาร์บอนไดออกไซด์ 5% (บ่ม 3 วัน สำหรับ KB, MCF-7 และ 5 วันสำหรับ NCI-H187) หลังจากนั้นเติมสารละลายรีซาซูรินเข้มข้น 62.5 ไมโครกรัมต่อมิลลิลิตร จำนวน 12.5 ไมโครลิตร ลงไปในแต่ละหลุม นำไปเก็บในตู้บ่มเชื้อต่ออีก 4 ชั่วโมง แล้วนำมาวัดแสงฟลูออเรสเซนต์ ที่ความยาวคลื่น 530, 590 นาโนเมตร ด้วยเครื่องสเปคตราแมกซ์ เอ็ม 5 (SpectraMax M5 muti-detection microplate reader) คำนวณเปอร์เซนต์การยับยั้งการเจริญเติบโตด้วยสมการ

$$\text{เปอร์เซนต์การยับยั้งการเจริญเติบโต} = [1-(FU_T/FU_C)] \times 100$$

FU_T และ FU_C คือจำนวนเซลล์ที่ดูดกลืนแสงฟลูออเรสเซนต์และไม่ดูดกลืนแสง ตามลำดับ จากนั้นนำค่าที่ได้ไปสร้างกราฟ ใช้สารเจือจาง 6 ความเข้มข้น ทำซ้ำ 3 หลุม สามารถคำนวณหาความเข้มข้นสารที่สามารถยับยั้งการเจริญเติบโตเซลล์ที่ 50% (IC_{50}) โดยใช้โปรแกรม SOFTMax Pro สารมาตรฐานเชิงบวกที่ใช้คือ ด็อกโซรูบิซินไฮโดรคลอไรค์ และใช้น้ำ 0.5 เปอร์เซนต์ DMSO เป็นสารเทียบเชิงลบ ค่า IC_{50} ของสารนี้ต่อการต้าน KB, MCF-7 และ NCI-H187 เท่ากับ 0.612, 9.22 และ 0.090 ไมโครกรัมต่อมิลลิลิตร ตามลำดับ สารประกอบ (I) แสดงค่า IC_{50} ต่อการต้านเซลล์มะเร็งทั้ง 3 ชนิดนี้ เท่ากับ 2.27–2.58, 2.71–5.18 และ 2.93–4.24 ไมโครกรัมต่อมิลลิลิตร ตามลำดับ ดังนั้น สารนี้อาจจะมีประโยชน์สำหรับการรักษาหรือยับยั้งเซลล์มะเร็งได้

ตัวอย่างที่ 3

การตรวจสอบความเป็นพิษต่อเซลล์สัตว์ปกติ (Vero cell) ของสารประกอบเฟนเลอรัล (I)

การตรวจสอบความเป็นพิษต่อเซลล์สัตว์ปกติชนิดวีโร่ (Vero, African green monkey kidney fibroblasts) ของสารประกอบ (**I**) โดยใช้วิธีการวัดปริมาณจีเอฟพี (GFP) ในไมโครเพลท (microplate) ซึ่งดัดแปลงมาจากวิธีของ Hunt และคณะ, 1999 โดยใช้ เซลล์ชนิดวีโร่ที่สร้างจีเอฟพีซึ่งพัฒนามาจากเซลล์ไลน์ชนิดวีโร่ (ATCC CCL-81) โดยห้องปฏิบัติการทดสอบฤทธิ์ทางชีวภาพ ศูนย์พันธุวิศวกรรมและเทคโนโลยีชีวภาพแห่งชาติ เซลล์จะถูกเลี้ยงในอาหารเหลวที่ประกอบด้วย 10% ซีรัมตัวอ่อนของลูกวัวที่ทำให้หมดฤทธิ์ด้วยความร้อน (heat-inactivated fetal bovine serum), 2 มิลลิโมลาร์ แอล-กลูตามีน (L-glutamine), 1 มิลลิโมลาร์ โซเดียม ไพรูเวท (sodium pyruvate), 1.5 กรัมต่อลิตร โซเดียม ไบคาร์บอเนต (sodium bicarbonate) และ 0.8 มิลลิกรัมต่อมิลลิลิตร เจเนทิซิน (geneticin) ในตู้บ่มเชื้อที่มีก๊าซคาร์บอนไดออกไซด์ 5% ที่อุณหภูมิ 37 องศาเซลเซียส ในการทดสอบจะเติมเซลล์แขวนลอยปริมาตร 45 ไมโครลิตร ที่หนาแน่น 3.3×10^4 เซลล์ต่อมิลลิลิตร ลงในแต่ละถาดหลุมชนิด 384 หลุมต่อถาด จากนั้นจึงเติมสารที่ละลายด้วย 0.5% DMSO ปริมาตร 5 ไมโครลิตร และนำไปบ่มในตู้บ่มเป็นเวลา 4 วัน ที่อุณหภูมิ 37 องศาเซลเซียส มีความเข้มข้นของก๊าซคาร์บอนไดออกไซด์ 5% จากนั้นนำไปวัดแสงฟลูออเรสเซนต์ด้วยเครื่องสเปคตราแมกซ์ เอ็ม 5 (SpectraMax M5 multi-detection microplate reader) ที่ความยาวคลื่น 485 และ 535 นาโนเมตร และคำนวนหาค่าเปอร์เซ็นต์ความเป็นพิษของเซลล์ด้วยสมการ

$$\% \text{ ความเป็นพิษของเซลล์} = [1-(FU_T/FU_C)] \times 100$$

เมื่อ FU_T และ FU_C คือความเข้มของแสงฟลูออเรสเซนต์จากเซลล์ที่บ่มกับยา และเซลล์ที่บ่มโดยไม่มียาตามลำดับ จากนั้นนำค่าที่ได้ไปสร้างกราฟ โดยใช้ผลทดสอบสารที่ 6 ความเข้มข้น โดยทำซ้ำ 3 ครั้ง ในแต่ละความเข้มข้น และหาค่า IC_{50} โดยใช้โปรแกรม SOFTMax Pro ในการทดสอบแต่ละครั้งใช้ เอลลิปทิซีน (Ellipticine) และ 0.5% DMSO เป็นตัวอย่างควบคุมผลบวกและลบ ตามลำดับ ค่าเฉลี่ยปกติของค่า IC_{50} ของเอลลิปทิซีน เท่ากับ 0.56 ไมโครกรัมต่อมิลลิลิตร ส่วนสารประกอบ (**I**) แสดงผลความเป็นพิษต่อเซลล์ปกติโดยมีค่า IC_{50} เท่ากับ 3.03–3.42 ไมโครกรัมต่อมิลลิลิตร

จากผลการทดลองดังตัวอย่างที่ 2 และ 3 แสดงให้เห็นว่า สารตามการประดิษฐ์นี้มีความเป็นพิษต่อเซลล์ปกติต่ำ แต่มีฤทธิ์ในการยับยั้งเซลล์มะเร็งได้ดี ดังนั้น สารนี้น่าจะมีศักยภาพสูงในการนำไปใช้ในการยับยั้งเซลล์มะเร็ง นอกจากตัวอย่างในการยับยั้งเซลล์มะเร็งดังกล่าว ยังพบว่าสารตามการประดิษฐ์นี้มีฤทธิ์ในการยับยั้งเชื้อก่อโรคมาลาเรียดังแสดงในตัวอย่างที่ 4

ตัวอย่างที่ 4
การตรวจสอบฤทธิ์ยับยั้งเชื้อก่อโรคมาลาเรียของสารประกอบเฟนเลอรัล (I)

<u>การเตรียมเชื้อก่อโรคมาลาเรีย</u>

การเลี้ยงเชื้อพลาสโมเดียม ฟาลซิพารัม (K1, multidrug resistant strain) เพื่อเป็นตัวแทนเชื้อก่อโรคมาลาเรียในหลอดทดลอง (Trager&Jensen, 1976) ใช้อาหารเลี้ยงเชื้อ RPMI 1640 ที่มีเฮช-อี-พี-อี-เอส (เอ็น-(สอง-ไฮดรอกซีเอทิล)พิเพอราซีน-เอ็นไพร์ม-(สองอีเทนซัลโฟนิก แอซิด)) [HEPES, (*N*-(2-hydroxyethyl)

piperazine-*N*' -(2-ethanesulfonic acid))] 20 มิลลิโมลาร์ โซเดียมไฮโดรเจนคาร์บอเนต ($NaHCO_3$) 32 มิลลิโมลาร์ 10% ซีรั่มมนุษย์ (human serum) และ 3% เม็ดเลือดแดงมนุษย์กรุ๊ปโอ (human group O erythrocyte) โดยนำเชื้อไปไว้ในตู้บ่มเพาะที่มีความชื้น ที่อุณหภูมิ 37 องศาเซลเซียส และมีความเข้มข้นของก๊าซคาร์บอนไดออกไซด์ 3% ทำการเปลี่ยนถ่ายอาหารเลี้ยงเชื้อทุกวันเพื่อให้ปรสิตเจริญเติบโตมีคุณภาพพร้อมใช้ทดสอบในระดับหลอดทดลองโดยใช้เทคนิคไมโครคัลเจอร์ เรดิโอไอโซโทป (microculture radioisotope) ในการประเมินผล (Desjardins และคณะ, 1979) เมื่อจะทำการทดสอบ นำเชื้อที่เลี้ยงไว้มาเตรียมให้เป็นเซลล์แขวนลอยมีความหนาแน่นของเม็ดเลือดแดงมนุษย์กรุ๊ปโอ (human group O erythrocyte) 1.5% และเชื้อในระยะรูปวงแหวน (ring stage) 1.0% จากนั้นจึงนำเซลล์แขวนลอยปริมาตร 200 ไมโครลิตร มาเติมในถาดหลุมเลี้ยงเซลล์ชนิด 96 หลุมต่อถาด ตามด้วยสารตัวอย่างที่ละลายอยู่ใน 1% DMSO ปริมาตร 25 ไมโครลิตร และนำไปเลี้ยงในตู้บ่มเชื้อเป็นเวลา 24 ชั่วโมง จากนั้นจึงเติมสารตริเตียมไฮโพแซนทีน ([^{3}H] hypoxanthin) ที่ละลายอยู่ในอาหารเลี้ยงเชื้อที่ความเข้มข้น 0.5 μCi ปริมาตร 25 ไมโครลิตรต่อหลุม จากนั้นนำไปเก็บในตู้บ่มต่ออีก 24 ชั่วโมง เมื่อครบเวลาแล้วจึงนำเซลล์แขวนลอยไปวัดปริมาณสารรังสี โดยใช้ เครื่องวัดกัมมันตรังสีในถาดหลุม (Top Count microplate scintillation counter) และนำค่าสัญญาณรังสีต่อนาทีของปรสิตที่เลี้ยงในภาวะที่มียา (CPM_T) และปรสิตที่เลี้ยงโดยไม่มียา (CPM_U) มาหาอัตราการเจริญเติบโตของเชื้อพลาสโมเดียม ดังสูตรนี้

$$\% \text{ การเจริญเติบโตของปรสิต} = CPM_T/CPM_U \times 100$$

ประสิทธิภาพในการยับยั้งเชื้อพลาสโมเดียมของสารทดสอบ วัดได้จากความเข้มข้นของสารที่สามารถยับยั้งการเจริญเติบโตของปรสิตได้ 50% (IC_{50}) เมื่อเทียบกับเซลล์ปรสิตที่เลี้ยงโดยไม่มียา ในแต่ละครั้งที่ทำการทดสอบจะใช้สารไดไฮโดรอาทิมิซินิน ซึ่งเป็นยารักษาโรคมาลาเรียสายพันธุ์พลาสโมเดียม ฟาลซิฟารัม ที่ดีที่สุดตัวหนึ่งในปัจจุบันเป็นสารตัวอย่างควบคุมผลบวก โดยสารชนิดนี้มีค่า IC_{50} ในการยับยั้งเชื้อพันธุ์พลาสโมเดียม ฟาลซิฟารัม โดยเฉลี่ยเท่ากับ 0.00075 ไมโครกรัมต่อมิลลิลิตร ส่วนสารประกอบ (**I**) มีค่าการยับยั้งการเจริญเติบโตในระดับหลอดทดลองด้วยค่า IC_{50} เท่ากับ 2.12 – 2.22 ไมโครกรัมต่อมิลลิลิตร ค่า IC_{50} ของสารประกอบ (**I**) นี้แม้จะไม่เทียบเท่ากับยามาตรฐานที่ใช้อ้างอิง แต่เมื่อพิจารณาค่า IC_{50} ดังกล่าวพบว่าอยู่ในระดับที่ยอมรับได้ สรุปได้ว่าสารชนิดนี้มีฤทธิ์ยับยั้งเชื้อก่อโรคมาลาเรียมีประโยชน์สำหรับการรักษาหรือป้องกันโรคมาลาเรียที่เกิดจากเชื้อพลาสโมเดียม ฟาลซิฟารัม ได้ และมีศักยภาพในการพัฒนาต่อ และอาจกล่าวได้ว่า โครงสร้างสารประกอบเฟนเลอรัลโครงสร้าง (I) ตามการประดิษฐ์นี้มีทั้งฤทธิ์ในการยับยั้งเซลล์มะเร็งและยับยั้งเชื้อก่อโรคมาลาเรีย ซึ่งไม่เคยมีรายงานโครงสร้างสารประกอบใกล้เคียงกันที่มีฤทธิ์ในลักษณะนี้มาก่อน

วิธีการในการประดิษฐ์ที่ดีที่สุด

เหมือนกับที่ได้บรรยายไว้ในหัวข้อการเปิดเผยการประดิษฐ์โดยสมบูรณ์

ข้อถือสิทธิ

1. สารประกอบเฟนเลอรัล ที่มีสูตรโครงสร้าง (I) ดังนี้

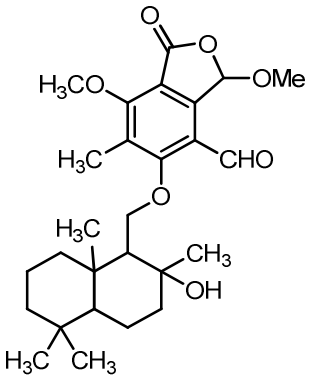

(I)

2. เกลือของสารประกอบเฟนเลอรัลที่มีสูตรโครงสร้าง (I) ตามข้อถือสิทธิ 1
3. องค์ประกอบทางเภสัชกรรม ที่ออกฤทธิ์ ยับยั้งเซลล์มะเร็ง หรือ ยับยั้งเชื้อมาลาเรีย ที่ประกอบด้วย
   ก. สารออกฤทธิ์ ที่เลือกได้จากกลุ่มที่ประกอบด้วย สารประกอบเฟนเลอรัลที่มีสูตรโครงสร้าง (I), เกลือของสารประกอบเฟนเลอรัลที่มีสูตรโครงสร้าง (I) หรือ สารผสมของสารดังกล่าว
   ข. สารตัวพาที่ยอมรับได้ทางเภสัชกรรม
4. กรรมวิธีการผลิตสารประกอบเฟนเลอรัลที่มีสูตรโครงสร้าง (I) ในข้อถือสิทธิ 1 ที่ซึ่ง กรรมวิธีดังกล่าวประกอบด้วยขั้นตอนดังนี้ การเลี้ยงเชื้อรา *Hypoxylon fendleri* สายพันธุ์ BCC32408 ที่เริ่มจากการปลูกถ่ายเส้นใยเชื้อราหรือสปอร์ของเชื้อรา การบ่มเพาะเชื้อรา การสกัดสารประกอบออกจากส่วนของอาหารเลี้ยงเชื้อและตัวเซลล์ การแยกสารประกอบออกจากสารสกัด และการทำให้บริสุทธิ์

บทสรุปการประดิษฐ์

การประดิษฐ์นี้เกี่ยวกับการพัฒนาสารประกอบเฟนเลอรัลซึ่งเป็นสารประกอบชนิดใหม่ที่มีฤทธิ์ยับยั้งเซลล์มะเร็งได้ดี โดยที่มีความเป็นพิษต่อเซลล์ปกติต่ำ ซึ่งผลิตได้จากกรรมวิธีการเลี้ยงเชื้อราไฮปอกซิลอน เฟน-เลอรี (*Hypoxylon fendleri*) สายพันธุ์ BCC32408 ที่พัฒนาขึ้น ประกอบกับวิธีการแยกสารประกอบออกจากสารสกัดหยาบและการทำให้สารบริสุทธิ์ นอกจากนี้ ยังพบว่าสารประกอบเฟนเลอรัลยังมีฤทธิ์ในการยับยั้งเชื้อมาลาเรียอีกด้วย ดังนั้น จึงสามารถใช้สารประกอบตามการประดิษฐ์นี้เป็นสารออกฤทธิ์ในองค์ประกอบทางเภสัชกรรมที่ออกฤทธิ์ ยับยั้งเซลล์มะเร็ง หรือ ยับยั้งเชื้อมาลาเรียได้ ทั้งนี้ สารประกอบเฟนเลอรัลตามการประดิษฐ์นี้ มีสูตรโครงสร้าง (**I**) ดังนี้

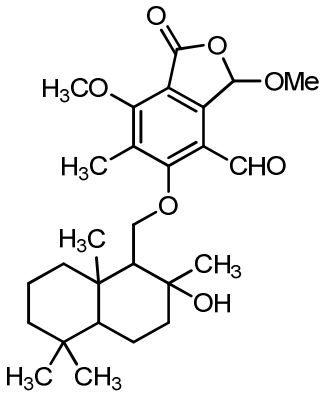

(**I**)

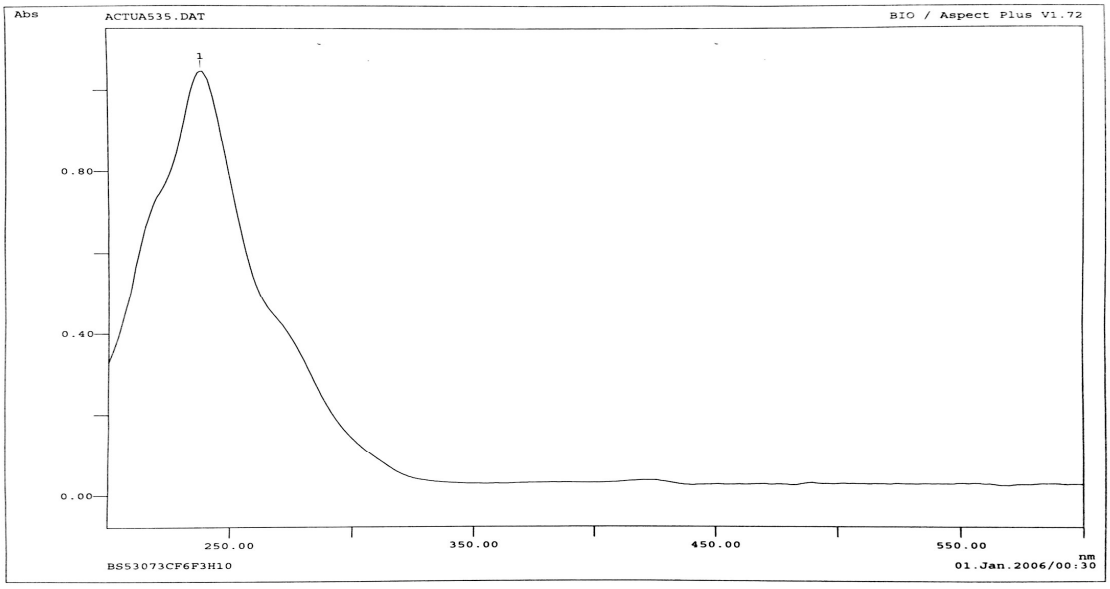
Abs
ACTUA535.DAT
BIO / Aspect Plus V1.72
1
0.80
0.40
0.00
250.00
350.00
450.00
550.00
nm
BS53073CF6F3H10
01.Jan.2006/00:30

รูปที่ 1

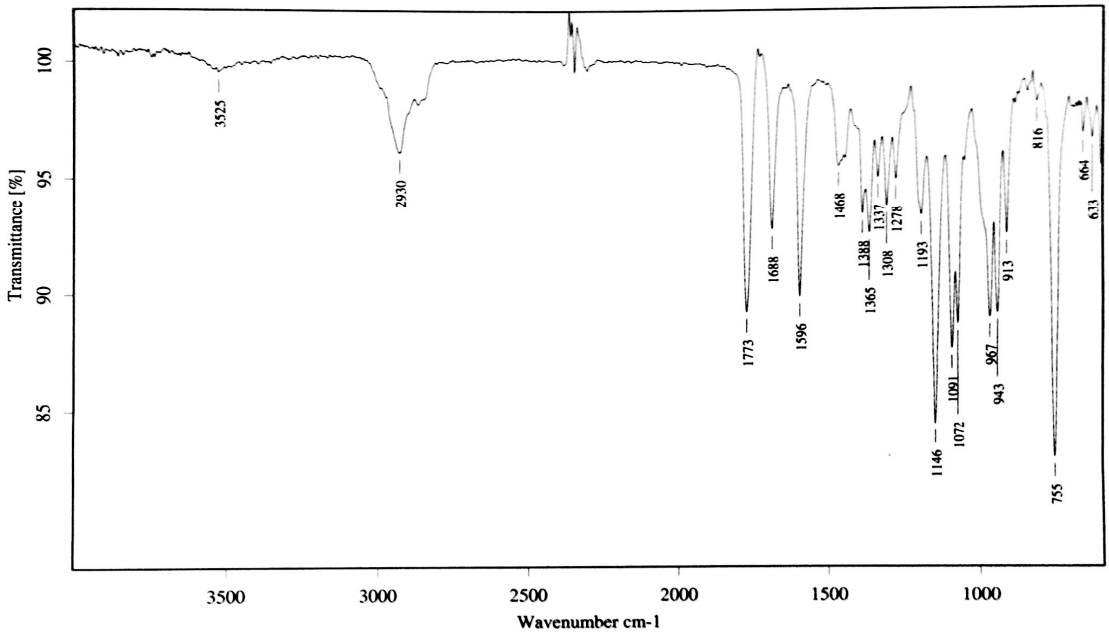
Transmittance [%]
100
95
90
85
3525
2930
1773
1688
1596
1468
1388
1337
1308
1278
1365
1193
1146
1091
1072
967
943
913
816
755
664
633
3500
3000
2500
2000
1500
1000
Wavenumber cm-1

รูปที่ 2

ก.

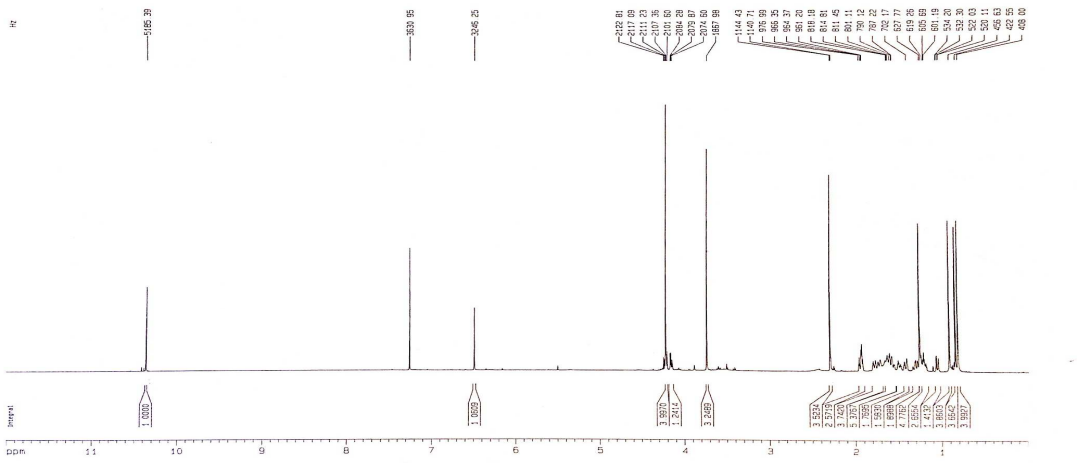

ข.

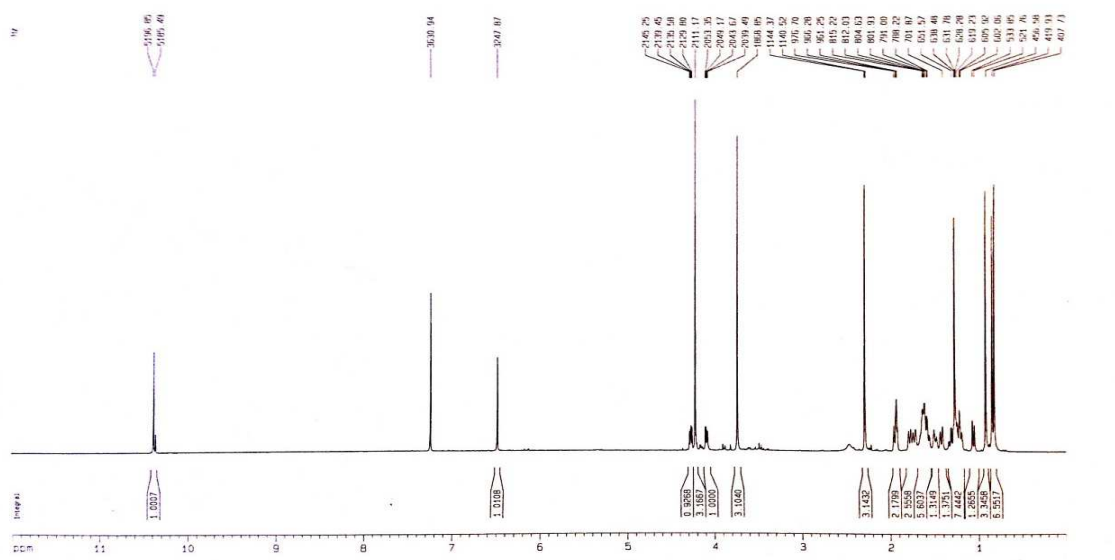

รูปที่ 3

ก.

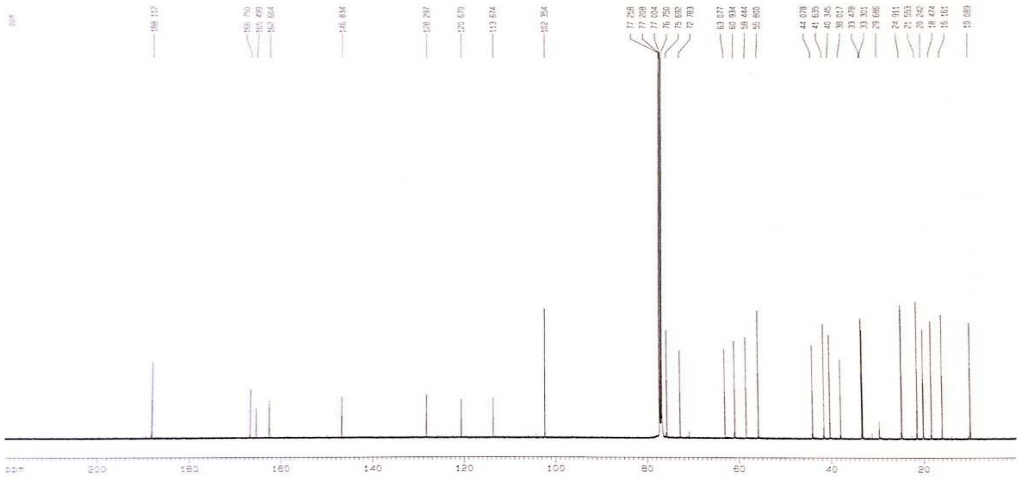

ข.

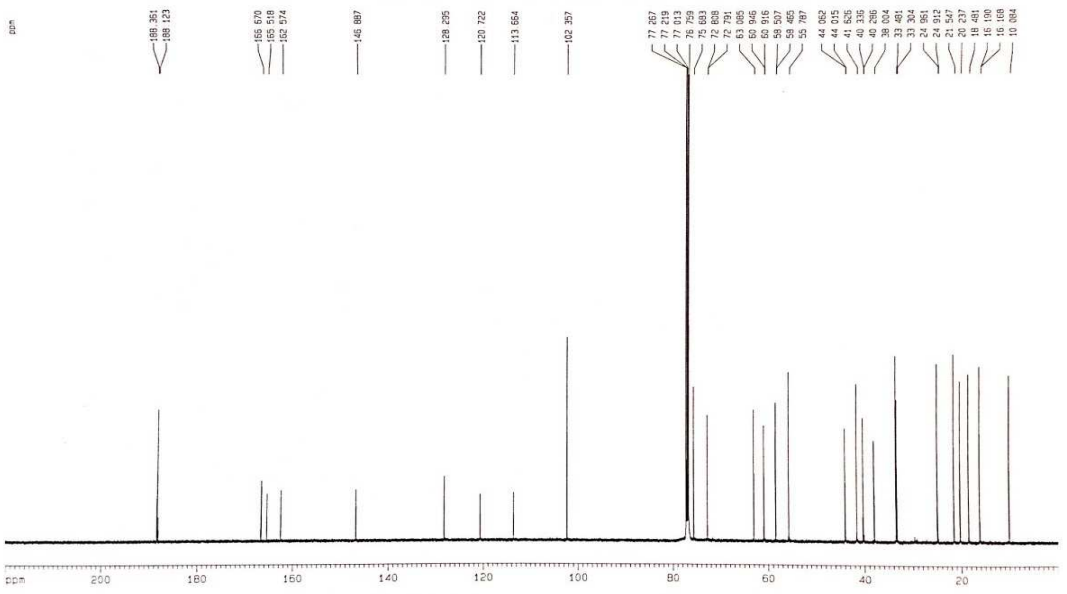

รูปที่ 4